THE DETERMINATION OF ACTIVITY COEFFICIENTS AT INFINITE DILUTION

THESIS

Submitted in fulfilment of the requirements for the Degree of
DOCTOR OF PHILOSOPHY
of NATAL UNIVERSITY-DURBAN

by

Warren Charles Moollan

DECLARATION

I hereby certify that the work presented in this thesis is the result of my own investigation under the supervision of professor T. M. Letcher, and has never been submitted in candidature for a degree in any other university.

Warren Charles Moollan

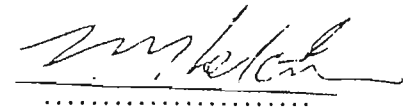

Professor T. M. Letcher

ACKNOWLEDGEMENTS

The author gratefully makes the following acknowledgements:

To Professor T. M. Letcher, under whose supervision this thesis was conducted, for his guidance and encouragements during the course of this study.

A special thank to Professor Urszula M. Domańska, for providing me with her moral support, her constant guidance, for the interest she has shown in my research, and for instilling in me the enthusiasm to conduct this work. Also for giving me the opportunity to work with her at the Technical University of Warsaw, where part of this research was conducted.

To the Technical staff of the Chemistry Department at the University of Natal for their valuable assistance especially, Mr. D. Jajevian Mr. K. Singh.

To the staff at the Technical University of Warsaw, especially Dr. A. Goldon, for the hours of stimulating discussion.

To my friends and colleagues in the department, most especially, Mr. H. Mohammed, Mr. Nesan Naidoo, Miss. P. Govender, Mr. A. Nevines and Mr. Paul Whitehead, for making research such fun.

ABSTRACT

The aim of this work was to extend the theory of Everett and Cruickshank, for the determination of activity coefficients at infinite dilution, γ^{∞}_{13} (where 1 refers to the solute and 3 to the solvent), to accommodate solvents of moderate volatility, using the gas liquid chromatography (GLC) method. A novel data treatment procedure is introduced to account for the loss of solvent off the column, during the experiment. The method also allows us to determine the vapour pressure of the solvent. No auxiliary equipment is required, and the method does not employ the use of a presaturator.

Further, the effect of a polar involatile solute is examined using various types of solutes. The activity coefficient was found to be independent of column packing and flowrate.

Considering the volatile solvent, the systems investigated by the GLC method were straight chain hydrocarbons, (n-pentane, n-hexane and n-heptane), cyclic hydrocarbons (cyclopentane, and cyclohexane) and an aromatic compound, benzene. The systems were investigated at 2 temperatures, 280.15 K and 298.15 K. The results indicate a clear dependence of the activity coefficient on temperature.

For the polar nonvolatile solvent, sulfolane (tetrahydrothiophene, 1,1 dioxane) was used. The systems studied were sulfolane + n-pentane, n-hexane, n-heptane, cyclopentane, cyclohexane, benzene, tetrahydrofuran, and tetrahydropyran. The systems were studied at one temperature, 303.15 K, due to the low melting point of sulfolane i.e. 301.60 K.

Part of this study into the thermodynamics of solutions was conducted at the Technical University of Warsaw, where the equilibria of sulfolane was studied using two techniques, a dynamic solid-liquid equilibrium method (SLE), and an ebulliometric, vapor-liquid method (VLE).

The main purpose of this was to apply solution theories to this data in order to predict the activity coefficient at infinite dilution for the sulfolane mixtures.
The systems measured using solid liquid equilibrium are sulfolane + tetrahydrofuran, or, 1,4-dioxane, or, 1-heptyne, or, 1,1,1,-trichloroethane, or, benzene, and cyclohexane. The results of these measurements were then described using various solution theories, and new interaction parameters obtained.

The vapour liquid equilibrium systems measured were sulfolane + 1-heptyne, or, tetrahyrdofuran, or, 1,1,1-trichloroethane, and tetrachloromethane. Here as in SLE the results were described using solution theories.

The results of both the VLE and SLE measurements were used in a multiple optimization procedure to produce new parameters for the interaction of sulfolane with various groups, using two group contribution method, DISQUAC and modified UNIFAC.
The predicted activity coefficients compare well with the measured values using GLC.

CHAPTER 1
INTRODUCTION

The first aspect of this work was to develop and test a theory that allowed for the determination of activity coefficients at infinite dilution (γ_{13}^{∞}), from gas liquid chromatography measurements using volatile solutes and *moderately volatile solvents* (liquid stationary phase). In the original theory developed by Cruickshank[1] and Everett[2] the γ_{13}^{∞} can only be measured for systems with volatile solutes and *involatile solvents*. The aim was to test the new method using mixtures for which parameters were either known or could be calculated.

The Everett[2] and Cruickshank[1] equation is:

$$\ln\gamma_{13}^{\infty} = \ln\frac{n_3RT}{V_N P_1^*} - \left[\frac{(B_{11} - V_1^*)}{RT}\right] P_1^* + \left[\frac{(2B_{12} - V_1^{\infty})}{RT}\right] J_3^2 P_O \qquad (1.1)$$

where V_N is the net retention volume, P_O the outlet pressure, $J_3^2P_O$ the mean column pressure, n_3 is the amount of liquid solvent on the column, T the column temperature, P_1^* the saturated vapour pressure of the solute at temperature T, B_{11} the second virial coefficient of the pure solute, V_1^* the molar volume of the solute as a liquid, V_1^{∞} the partial molar volume of the solute at infinite dilution in the solvent, and B_{12} the mixed second virial coefficient of the solute and carrier gas. In this thesis the subscripts 1, 2 and 3 refer to the solute, carrier gas and solvent respectively.

The theory developed here involves a modification of the above equation and takes into account the loss of solvent on the column during the experiment. Simple physico-chemical considerations result in a new equation that relates the amount of solvent lost to its partial pressure (P_3') (see chapter 3):

$$\frac{V_N}{n_3 e^C} = \frac{RT}{\gamma_{13}^{\infty} P_1^*} - \frac{U_o t}{n_3}\left[\frac{P_3^l}{\gamma_{13}^{\infty} P_1^*}\right] \qquad (1.2)$$

where

$$C = -\left[\frac{B_{11} - V_1^*}{RT}\right] P_1^* + \left[\frac{2B_{12} - V_1^{\infty}}{RT}\right] P_o J_3^2 \qquad (1.3)$$

U_o is the volumetric flow and t is the time of the injection of the solute on to the column.

The activity coefficient at infinite dilution was determined at two temperatures, 283.15 K and 298.15 K for solutes n-pentane, cyclopentane, n-hexane, cyclohexane, benzene and n-heptane using n-dodecane as the solvent.

In order to calculate γ_{13}^{∞}, a gas liquid chromatograph was built along the lines of that described by the Bristol group[1-3]. A detailed theory of gas liquid chromatography and the modifications to accommodate moderately volatile solvents is given in chapter 3. The apparatus used, the experimental procedure and the measurements obtained are presented in chapter 4.

An investigation into the thermodynamic mixing properties of tetrahydrothiophene-1,1-dioxane (sulfolane) and various solvents form the second aspect of this work. The aim was to determine γ_{13}^{∞} under different conditions and for a variety of mixtures using different experimental techniques. The parameters were obtained using these different techniques and were used to predict thermodynamic properties of various solvents in sulfolane. Sulfolane was the focus of attention because it is an important solvent in extraction processes used by the Shell Chemical Company[4] and it could also be of great importance to organizations involved in the

separation of organic compounds, such as SASOL.

The work involved exposure to a large number of experimental techniques viz. G.L.C., excess molar volume determination, excess molar enthalpy determination, solid liquid equilibrium, and vapour liquid equilibrium. The work also concentrates on many of the most important theories relating to liquid mixtures and solution. eg. WILSON[5], NRTL[6], UNIQUAC[7], UNIFAC[8] and DISQUAC[9].

Chapters 5 and 6 discuss the methods used to measure the excess molar volumes and enthalpy respectively. The systems studied are: an alkyne + sulfolane at 303.15 K. The results obtained are discussed in relation to the significant interactions between sulfolane and the alkynes.

In chapter 7, the vapour liquid equilibria method employed in this work is discussed. The Rogalski[10] modified Świętoslawski[11] dynamic ebulliometer still was used to obtain binary vapour-liquid equilibria for the following systems at 338.15 K or 353.15 K: 1-heptyne, or tetrahydrofuran, or 1,4-dioxane, or tetrachloromethane or 1,1,1-trichloroethane + sulfolane, over the whole concentration range. The data is described using the Margules[12], van Laar[13], WILSON, NRTL and UNIQUAC equations.

The solid liquid equilibria measurements are discussed in chapter 8. The systems studied here are: 1-heptyne, or tetrahydrofuran, or 1,4-dioxane, or tetrachloromethane or trichloroethane + sulfolane. The results of the correlation of solubility for sulfolane in the solvents with respect to the solid-solid phase transition in sulfolane is given in terms of the WILSON, NRTL and UNIQUAC equations, utilizing parameters taken from solid-liquid equilibria for the simple eutectic mixtures only. The correlations have been done using the data reported here as well as data published earlier.[14-17]

Chapter 9 concentrates on examining the well-established theories of

correlations and predicting activity coefficients at finite and infinite dilution. A detailed discussion of two group contribution methods (modified UNIFAC and DISQUAC) is also given. These two methods are used to predict the activity coefficients of sulfolane in a variety of mixtures at different temperatures using the excess enthalpy, VLE, and SLE data presented here, as well as data published earlier. New parameters for the interactions of various groups (CH_3, CH_2, Cl, A-CH_2, C_6H_6 etc.) with sulfolane (as a single group) are obtained for both modified UNIFAC and DISQUAC.

CHAPTER 2.
METHODS OF MEASURING ACTIVITY COEFFICIENTS AT INFINITE DILUTION OTHER THAN G.L.C.

Activity coefficients permit the specific measurements of unlike pair interactions in solution without any dependence on composition functionality or mixing rules.[18] *Activity coefficients at infinite dilution (γ^{∞}_{13}), where 1 refers to the solute and 3 to the solvent) are of great interest to the practising chemist and chemical engineer from both a theoretical and a practical point of view. This activity coefficient characterizes the behaviour of an infinitely dilute material (the solute) which is completely surrounded by solvent molecules. A knowledge of activity coefficients at infinite dilution is important not only for the development of new thermodynamic models but they are also important for the adjustment of reliable model parameters*[18] *and in the choice of solvents for processes such as extractive rectification, extraction, or absorption*[19]. *Infinite dilution activity coefficients have found numerous applications in characterizing solution behaviour. They can be used to generate accurate binary parameters for solution models*[20-21], *to predict the existence of azeotropes*[22] *and to estimate mutual solubilities.*[23] *In addition they can be used to calculate kinetic solvent effects with relationships such as the Brönsted-Bjerrum relationship*[24]. *One can accurately construct an entire binary vapour liquid equilibrium curve from the two activity coefficients at infinite dilution* [25-27] *using liquid mixing models based on two parameters.*

This chapter deals with the determination of determining γ^{∞}_{13} from experimental methods other than Gas Liquid Chromatography[28]. *This method is the subject of Chapters 3-4. The methods discussed are: Differential Ebulliometry*[20], *the Inert Gas Stripping Method*[29], *a modification of the Inert Gas Stripping Method*[30], *the Differential Static Cell Method*[31], *and the Dew Point Technique*[32]. *The experimental methods are discussed in order to give a brief insight into the complexities of each*

method and the equipment required. These methods are also compared to the method employed in this work (gas liquid chromatography, Chapter 3 and 4). This chapter puts into perspective the work carried out and described in Chapters 3 and 4.

2.1. Activity Coefficients at Infinite Dilution from Binary Vapour Liquid Equilibrium

Activity coefficients at infinite dilution are often determined from the extrapolation of VLE data[27]. If a vapour composition method, (rather than a total pressure technique) is used, one may calculate activity coefficients from each data point and extrapolate graphically. Unless the data are particularly accurate and plentiful in the dilute region, their extrapolation to infinite dilution is very imprecise[20]. Chapter 7 gives a detailed account of the equipment and theory of binary vapour liquid equilibrium measurements. This method is not discussed in this chapter, as it is not a method relating to infinite dilution.

2.2. The Ebulliometric Method for the Measurements of Activity Coefficients at Infinite Dilution.

Eckert *et al.*[20] proposed the Differential Ebulliometric Technique for the measurement of γ_{13}^{∞}. The differential ebulliometer used is similar in some respects to that described previously by Null[33]. It involves boiling a solution in an ebulliometer connected, through condensers to a common manifold, with a second ebulliometer containing pure boiling solvent. In this way the vapour pressure of the two boiling liquids are maintained at the same pressure. The system used by Eckert *et al.*[20] is depicted in figure 2.1. The data is analyzed using equation 2.1 following the method developed by Gautreaux and Coates [34] with additional terms (the fugacity coefficients) included to account for vapour-phase nonideality:

$$\gamma_{13}^{\infty} = \frac{\phi_1^{(P_3^*)} P_3^* [P_3^* - (1 - P_3^* \frac{V_3}{RT} + \frac{P_3^*}{\phi_3^*}(\frac{\partial \phi_3^*}{\partial P})_T)](\frac{dP_3^*}{dT})(\frac{\partial T}{\partial x_1})_P^{\infty}}{P_1^* \phi_1^* \exp[(P_3^* - P_1^*)V_1/RT} \qquad (2.1)$$

where P_1^* and P_3^* are vapour pressures of component 1 (the solute) and 3 (the solvent) respectively. $\phi_1^{(P)}$ is the fugacity coefficient of component 1 at the vapour pressure of component 3, ϕ_1^* and ϕ_3^* are the fugacity coefficients of components 1 and 3 at their vapour pressures, respectively. V_1 and V_3 are the molar volumes of components 1 and 3 respectively, and x_1 the mole fraction of component 1 in the liquid phase.

2.2.1. Description of Equipment used and Principles of the Method

The boiling temperature of the pure solute in one ebulliometer (A) is compared with that in the second ebulliometer (B) containing the solution (figure 2.1).

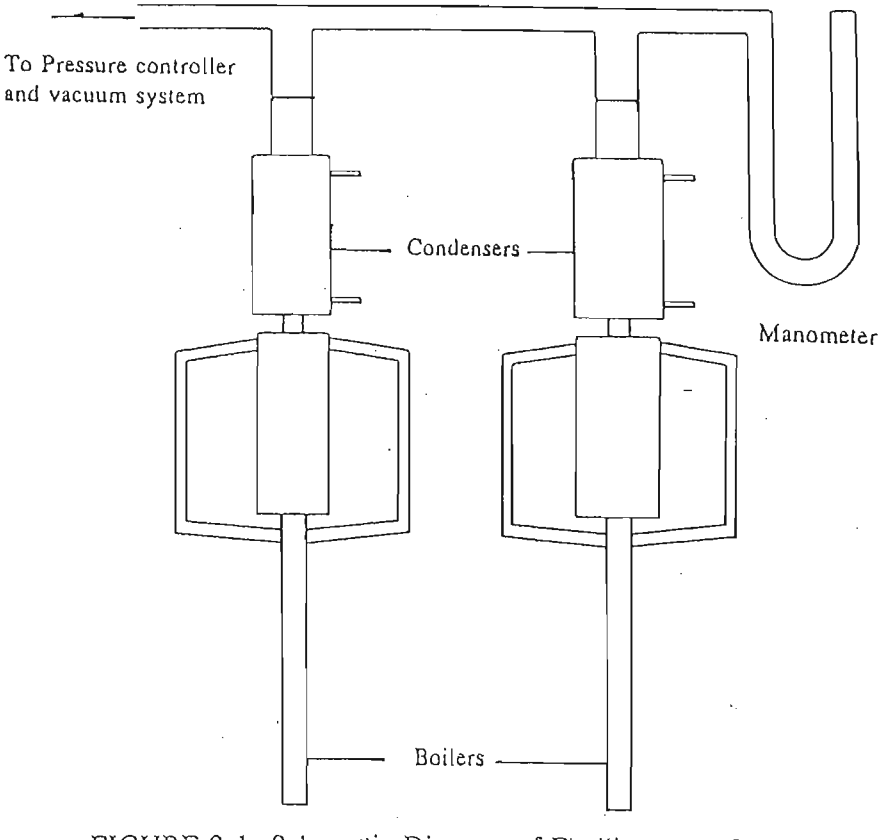

FIGURE 2.1. Schematic Diagram of Ebulliometers Connected to a Vacuum System

Small fluctuations in pressure have minimal effect on the γ_{13}^{∞}. In addition, the pressure, and in consequence the temperature, at which γ_{13}^{∞} is determined, can be readily set and controlled. A vacuum pump is connected through a solenoid valve to the manifold, which includes a 15-L ballast tank.[20] The tank is controlled through a relay, by a differential sulphuric acid manostat, and dry air is continuously bled into the system. Control of better than $\pm$ 0.2 mmHg is usually achieved and the pressure was read to better than $\pm$ 0.1 mm from a mercury manometer using a cathetometer. The boiling point elevation is often measured with a quartz crystal thermometer with matching sensing probes capable of resolution to 0.001 K.[20] The ebulliometer used by

Eckert *et al*[20] is shown in detail in Figure 2.2. Like most ebulliometers, it is based on a Cottrell pump (see Chapter 7), in this case, consisting of two concentric cylinders, separated by a seal at the top, between which the liquid is boiling. The outer cylinder is heated by nichome wire connected to a variable resistor. Superheated liquid is pumped up through the side tubes and onto the thermometer well, where some of the

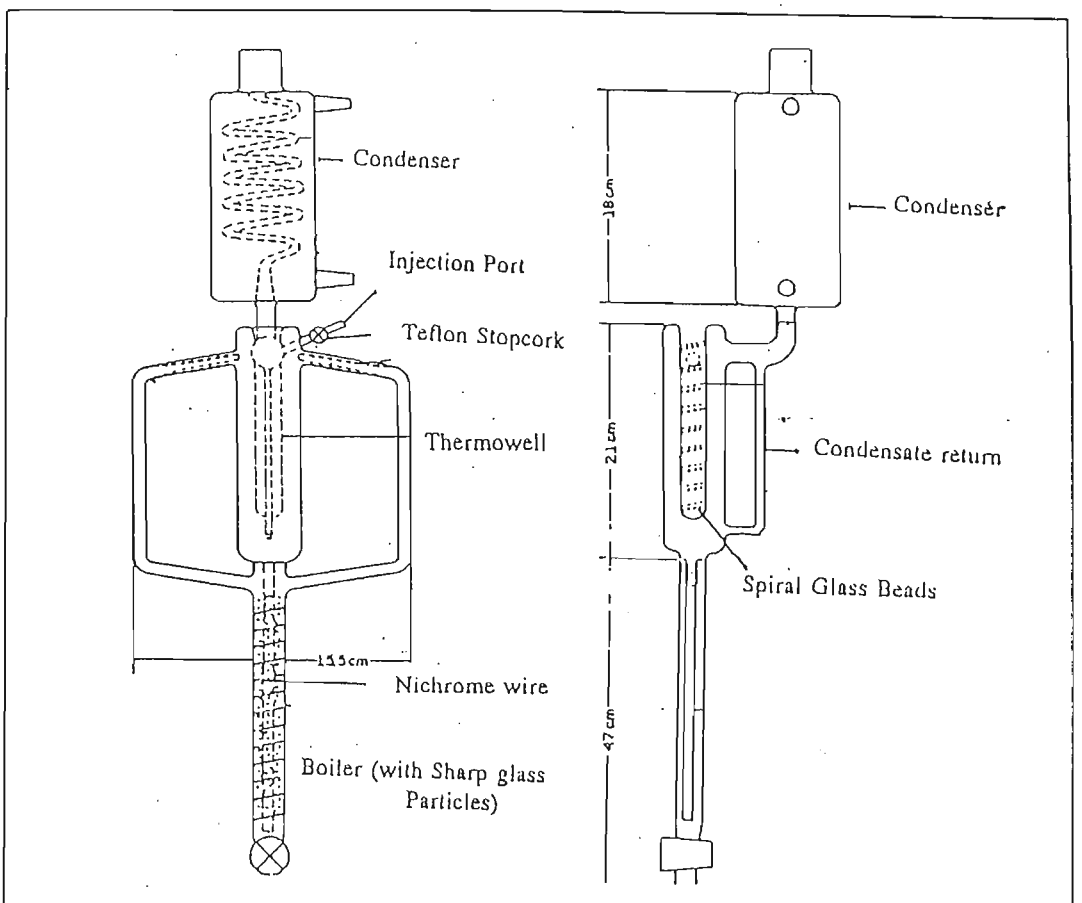

FIGURE 2.2. Front View and Side View of an Ebulliometer

liquid is taken up by evaporation. The remaining liquid passes down the outsides of the thermowell, slowed by helical beads, returns via the inner cylinder, and is joined by the cooled condensate. The whole ebulliometer is thoroughly insulated.

Using too small a volume of solute (1) is impractical, since the original liquid composition would be drastically affected by the enrichment of vapour with the more volatile component. It is in fact, this complication that has led to questions about the applicability of ebulliometry to mixtures[35].

2.2.2. Procedure

Initially, both ebulliometers (A and B) are filled gravimetrically with pure solvent to a level about 25 mm from the side tube. The pressure control is set, the liquid heated to boiling, and the system allowed to come to equilibrium (usually about 30 minutes). With both ebulliometers containing pure solvent only, the optimum heating rate and any systematic offset in the measured temperature difference is determined. Either pure solute or a gravimetrically prepared mixture is injected into the ebulliometer through a septum stopper with a syringe. The syringe is weighed before and after each injection to obtain an injected mass in the order of 1 g, to a precision of $\pm$ 0.1 mg. When equilibrium is again reached, (5 - 15 minutes) the pressure and the temperature differences are recorded. The procedure can be repeated a number of times.

2.2.3. Data Analysis

The ebulliometric data are analyzed following the method development by Gautreaux and Coates [34] with additional fugacity terms included for the vapour-phase non-idealities. A rigorous expression for the activity coefficient at infinite dilution can

be readily derived in terms of pure component properties and the limiting slope of the temperature versus composition curve ie. $(\partial T/\partial x_i)_P^\infty$:

$$\gamma_{13}^{\infty} = \frac{\phi_1^{(P_3^*)} P_3^* [P_3^* - (1 - P_3^* \frac{V_3}{RT} + \frac{P_3^*}{\phi_3^*}(\frac{\partial \phi_3^*}{\partial P})_T)](\frac{dP_3^*}{dT})(\frac{\partial T}{\partial x_1})_P^\infty}{P_1^* \phi_1^* \exp[(P_3^* - P_1^*)V_1/RT} \qquad (2.1)$$

Equation 2.1, is based on liquid-phase nonideality. The fugacity coefficients terms, are obtained by Eckert[20] from virial coefficients estimated using the method of Hayden and O'Connell.[36]

The quantity determined experimentally is $(\partial T/\partial x_i)_P^\infty$ which is the limiting composition derivative of the temperature. The advantage of using the equation is that no functional dependence of the activity coefficient on composition is assumed. Instead of extrapolating finite activity coefficients to the infinite value, an inherently uncertain process, the limiting slopes of nearly linear x-T curves whose end points are always fixed, are measured.

Equation 2.1 can be used to examine the sensitivity of γ_{13}^{∞} to errors in the measured limiting slope and thus provide a criterion for the applicability of the ebulliometric method to a given binary system. If we disregard the fugacity coefficient term and the Poynting correction all of which have minor significance anyway, the equation becomes[20]

$$\gamma_{13}^{\infty} = \frac{P_3^* - \frac{dP_3^*}{dT}(\frac{\partial T}{\partial x})_P^\infty}{P_1^*} \qquad (2.2)$$

The γ_{13}^{∞} is essentially the algebraic sum of the two terms. Since it may become

the difference between two much larger numbers, extremely high accuracy is needed in the data. To measure the sensitivity Eckert[20] considered the fractional change in γ_{13}^{∞} with the equivalent change of the limiting slope;

$$\frac{(\frac{\partial T}{\partial x_1})_P^{\infty}}{\gamma_{13}^{\infty}} \frac{d\gamma_{13}^{\infty}}{d(\frac{\partial T}{\partial x_1})_P^{\infty}} = 1 - \frac{P_3^*}{P_1^* \gamma_{13}^{\infty}} \qquad (2.3)$$

Since the activity coefficient of the solvent is unity at this limit and the total pressure is the vapour pressure of the solvent, the second term on the right hand side is essentially the relative volatility at infinite dilution.

The ebulliometric method is thus best suited to *solvents of similar volatility.* If the solute is much less volatile than the solvent, γ_{13}^{∞} determination will be difficult unless its value is very high. If the solute is more volatile than the solvent, the liquid composition correction becomes important. While this causes no instability in the data reduction, heavy reliance must be set on the estimated values of the vapour space and the liquid holdup. There is also an increased risk of losing some solute through the condenser during a run.

2.3. Measurement of the Activity Coefficients at Infinite dilution by means of the Inert Gas Stripping Method.

The inert gas stripping method presented by Leori *et al.*[29] is a fast and accurate method for the determination of γ_{13}^{∞} of a solute dissolved in a liquid mixture. It is based on the study of the solute elution with time and the solute is stripped from the solution by a constant flow of gas. The basis of the method of Leori[29] is a measurement of the desorption of a solute from a solution as a function of time. The solute is present in the solution at a very low concentration and is desorbed by the

passage of an inert gas at a constant flow rate. During the desorption, samples of the vapour phase are withdrawn and their compositions are determined. It is important to ensure a large gas-liquid interface, a sufficiently long time contact between the two phases, and good dispersion of bubbles in the liquid. Under such conditions, the gas leaving the saturation vessel may be expected to be very close to equilibrium with the liquid mixture. The variation of solute concentration in the gaseous phase is measured only by gas-liquid chromatography. The gas stripping method uses the following equations for the calculation of γ_{13}^{∞}: [29]

$$\frac{dn}{dt} = \frac{n}{N}\gamma_{13}^{\infty} P_1^* \frac{1}{1 - \frac{n}{N}\gamma_{13}^{\infty}\frac{P_1^*}{P} - \frac{P_3^*}{P}} \frac{D}{RT} \qquad (2.4)$$

and

$$\frac{dN}{dt} = P_1^* \frac{1}{1 - \frac{n}{N}\gamma_{13}^{\infty}\frac{P_1^*}{P} - \frac{P_3^*}{P}} \frac{D}{RT} \qquad (2.5)$$

Where n and N are respectively the total number of moles of solute and solvent in the dilution still at time t, D_2 is the total volumetric rate of gas flow, and D is pure carrier gas flow rate measured at temperature T and pressure P. The other terms have been previously defined. Equation 2.4 is used for non-volatile solvents while equation 2.5 is used in the case when the solvent is volatile.[29]

2.3.1. Principles of the Method

A binary solute-solvent systems is kept in an equilibrium still placed in a constant temperature bath. A constant carrier gas flow GF_1 is introduced into the still and strips the components into the vapour phase (Figure 2.3). The outlet gas flow, in

equilibrium conditions with the liquid phase placed in the still, is periodically injected into a chromatograph by means of a gas sampling valve maintained at a higher temperature to avoid any condensation. The total pressure at equilibrium, the carrier gas flow rate, and the total amount of solvent in the still are measured. For a non-volatile solvent whose concentration is in the range of the detector, the variation of time with the peak area is exponential and the limiting activity coefficient of the solute can be simply derived from these measurements. No calibration is necessary; there is no need a knowledge of the initial concentration of the solute in the liquid phase. The method can be extended to multicomponent systems, the only conditions required being a good chromatographic separation. The use of an electronic integrator to determine the peak areas yield accurate and reliable values of γ_{13}^{∞}[29].

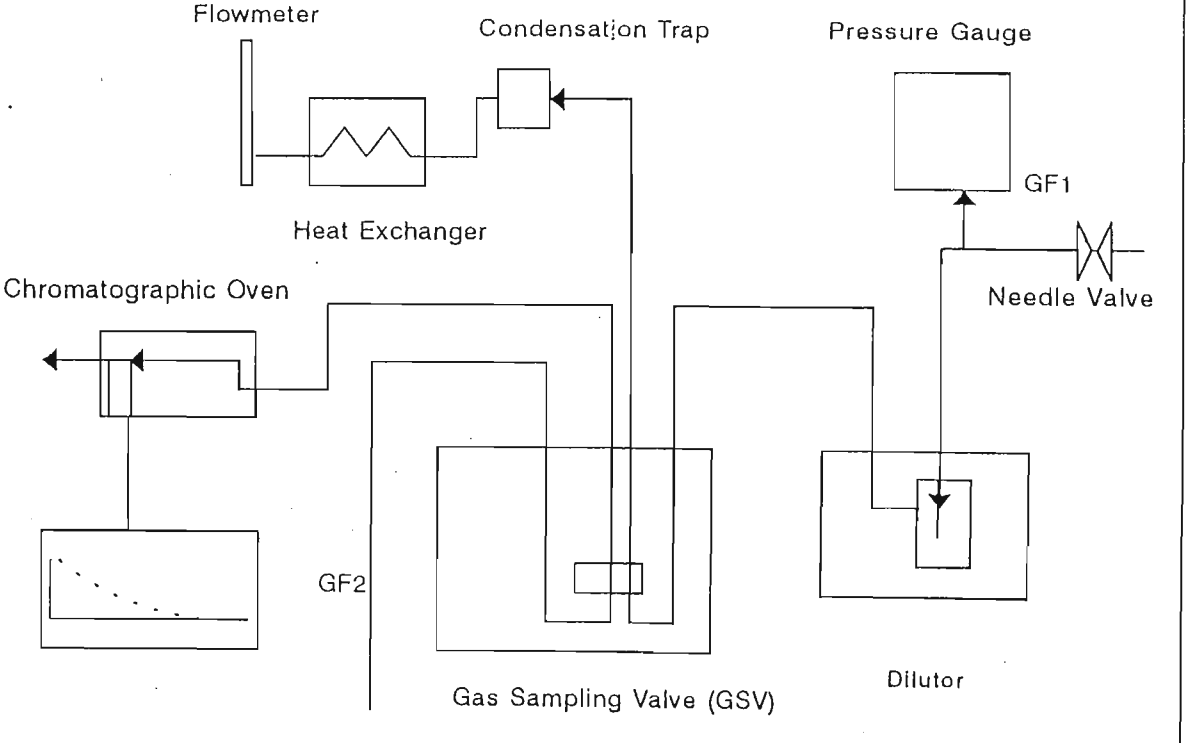

FIGURE 2.3 Flow Diagram of the Gas Stripping Equipment

2.3.2. Equipment and Procedure

The constant carrier gas flow (GF_1) (see figure 2.3) is introduced into the equilibrium still and its flow rate is controlled by a needle valve. The pressure drop between the needle valve and the still is measured by a pressure gauge. The equilibrium still (figure 2.4) contains about 25 cm^3 of solvent.

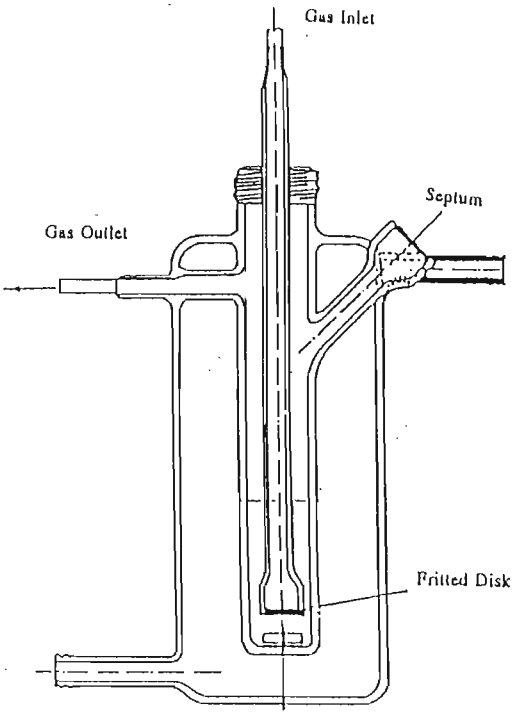

Figure 2.4. Dilution Flask used in the Gas Stripping Technique

The liquid solute is introduced by means of a syringe, through the septum before starting the experiment. This mole fraction of solute is small enough to observe no significant deviation of the activity coefficient from its value at infinity. The carrier gas passes through a fine porosity fritted glass disk and is dispersed into small bubbles. The standard gas flow range is 1-2 $cm^3 \cdot s^{-1}$. A large transfer area, a sufficiently long contact time and good dispersion of the bubbles in the liquid are important conditions to fulfil in the dilution still. It can then be expected that the gas

leaving the device is very nearly in thermodynamic equilibrium with the liquid phase. Liquid droplet entrainment is limited by keeping the dead space for the gas phase small enough to obtain steady state conditions in a short time. The gas outlet is wrapped with a heating tape to avoid any condensation of organic vapours which are diluted in the carrier gas stream. The outlet is connected to a gas sampling valve immersed in a thermostatic bath filled with silicon oil and maintained at 323.15 K. All the metal connections used are swagelock connectors with inox ferrules. The gas flows through the sampling loop, and is evacuated after passing through the precision soap film flow meter. A trap condenses the organic vapours before measurements of the carrier gas flow rate. The heat exchanger is a 40 m copper coil placed in a thermostatic water bath; its purpose is to keep gas flow rate at ambient temperature for a precise measurement of the flow rate GF_1. The gas sampling valve (GSV) allows the introduction of a sample of a constant number of moles of GF_1 into GF_2. Gas stream GF_2 then enters the chromatographic column placed in the oven.[29]

2.3.3. Data Analysis

If it is assumed that the gas phase is in equilibrium with the liquid phase, it is possible to write the equilibrium equations (neglecting gas phase corrections):

$$x_1 \gamma_{13}^{\infty} P_1^* = y_1 P \qquad (2.6)$$

where y_1 is the mole fraction of component 1 in the vapour phase.

If n and N are respectively the total number of moles of solute and solvent in the dilution still at time t, the quantities (-dn) and (-dN) withdrawn from the solution during a change of time, dt, by the carrier gas flow are given by:

$$dn = -y_1 P \frac{D_2 dt}{RT} \tag{2.7}$$

$$dN = -y_3 P \frac{D_2 dt}{RT} \tag{2.8}$$

where D_2 is the total volumetric rate of gas flowing out of the still converted to the pressure P and temperature T.

From the above equations it can be deduced that

$$\frac{dn}{dt} = -x_1 \gamma_{13}^{\infty} P_1^* \frac{D_2}{RT} \tag{2.9}$$

and

$$\frac{dN}{dt} = -P_3^* \frac{D_2}{RT} \tag{2.10}$$

An overall mass balance around the dilution still gives

$$D_2 = D - \frac{RT}{P}\left(\frac{dn}{dt} + \frac{dN}{dt}\right) \tag{2.11}$$

where D is the pure carrier gas flow rate at the measured T and P.

Combining the equations and replacing x_1 by

$$x_1 = \frac{n}{n+N} \simeq \frac{n}{N} \quad (\textit{at infinite dilution conditions}) \tag{2.12}$$

the results are

$$\frac{dn}{dt} = \frac{n}{N}\gamma_{13}^{\infty} P_1^* \frac{1}{1 - \frac{n}{N}\gamma_{13}^{\infty}\frac{P_1^*}{P} - \frac{P_1^*}{P}} \frac{D}{RT} \tag{2.4}$$

and

$$\frac{dN}{dt} = P_3^* \frac{1}{1 - \frac{n}{N}\gamma^{\infty}\frac{P_1^*}{P} - \frac{P_3^*}{P}} \frac{D}{RT} \tag{2.5}$$

Equations 2.4 and 2.5 are the basic differential equations relating the variations of the amounts of solute and solvent with time. Integrating equation 2.4 and assuming that in the case of a non volatile solvent, N is considered constant, the resulting equation is,

$$\ln \frac{n}{n_o} = \frac{D}{RT}\frac{P_1^*}{N}\gamma_{13}^{\infty} t \tag{2.13}$$

where n_0 is the initial value of n at t = 0.

Since the sampling loop of the gas sampling valve is maintained at a constant temperature, the amount of solute injected into the column is proportional to the solute partial pressure over the solution. It can therefore be deduced that,

$$S_1 \propto y_1 P \tag{2.14}$$

where S_1 is the solute peak area. Therefore

$$\ln\frac{S_1}{S_{1(t=0)}} = -\frac{D}{RT}\frac{P_1^*}{N}\gamma_{13}^{\infty}t \qquad (2.15)$$

Equation 2.14 indicates an exponential variation of solute peak area with time.
In the case of a volatile solvent integration of the differential system formed by equations 2.4 and 2.5 yield

$$\ln\frac{S_1}{(S_1)_{t=0}} = (\frac{\gamma_{13}^{\infty}P_1^*}{P_1^*} - 1)\ln(1 - \frac{P}{P-P_1^*}\frac{DP_1^*}{N_oRT}t) \qquad (2.16)$$

2.4. Modification of the Inert Gas Stripping Method for Measuring Activity Coefficients at Infinite Dilution

Surovy et al[30] proposed a modification to Leori's [29] gas stripping method (section 2.3) for the measurement of the limiting activity coefficient. Compared to the previous method, the modification consists of a change in the apparatus and measurement of the decrease in solute concentration in the liquid phase only. In the original apparatus of Leori and co workers[29] the inert stripping gas is fed to the liquid phase through a tube terminated with a frit. In order to prevent the vapour or organic substance from condensing in the gas stream, whilst leaving the saturation vessel, both the outlet and the sampling valve are heated. The positioning and shape of the outlet vessel should help ensure gas phase homogeneity, and hence reproducibility of the results. The gas phase homogeneity and the absence of vapour condensation in the

stream of the stripping gas before entry to the chromatographic column are important features which require special attention.

Modifications by Surovy[30] and co workers, include the measurement of the decrease in solute concentration in the liquid phase which.

2.4.1 Experimental

2.4.1.1. Apparatus

A scheme of the modified apparatus is given in figure 2.5. An inert gas (usually nitrogen) is introduced from pressure vessel 1 through magnetic valve 3 controlled by manostat 4 into buffer vessel 5 of about 20 dm^3 volume.

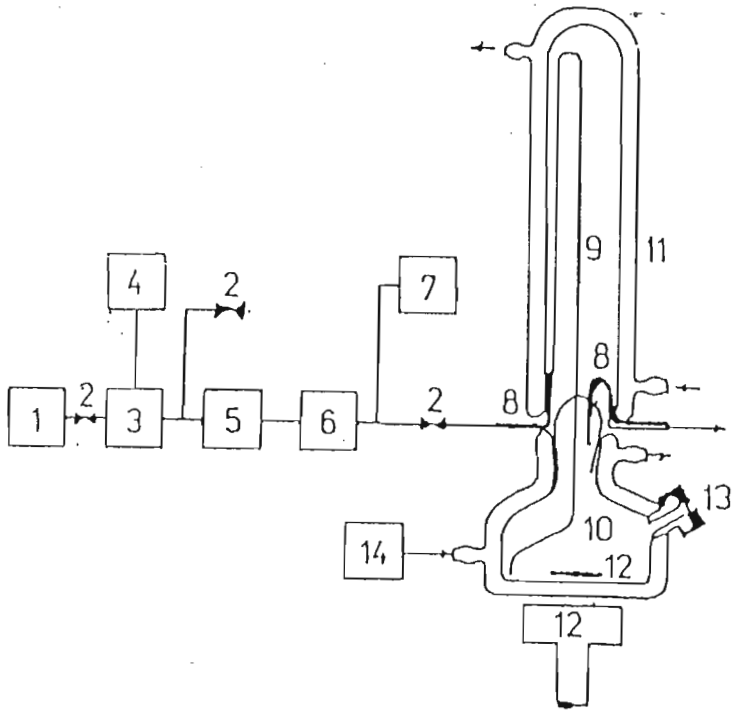

FIGURE 2.5 Modified Apparatus by Surovy *et al.*[30]

The nitrogen (after drying) then flows through valve 2 and capillary restrictor 9 into saturation vessel 10. The capillary is placed in constant-temperature jacket 11 and is sized so that the nitrogen flow rate at an over-pressure between 7 and 20 kPa, ranges from 0.04 and 0.12 $cm^3 \cdot s^{-1}$. Before the measurements, the calibration of the volumetric flow rate of nitrogen versus its "over-pressure" relative to atmospheric pressure is determined experimentally. Magnetic stirrer 12 provides for good mixing of the liquid. Simultaneous agitation of the gas bubbles increase the time of contact between the two phases. Moreover, the liquid keeps the gas above the surface in angular motion, so extending further the contact time. In this way, the gas-liquid contact time is increased several times as compared to the bubble passage without agitation. The gas then exits from the saturation vessel into the atmosphere through metal tube 8. Samples are taken with a microsyringe through seal 13 which is a rubber septum.

2.4.1.2. Procedure

Prior to measurements, the whole apparatus is flushed with an inert gas. An amount of solvent with a volume of 10 to 11 cm^3 is weighed into the saturation vessel. After turning on the magnetic stirrer the vessel (10) and the jacket (11) with the capillary restrictor are thermostatted at the working temperature. The inert gas is then admitted and the required amount of solute is injected with a microsyringe. At time intervals, which depend on the rate of solute stripping from the solution, the liquid samples are withdrawn for chromatographic analysis.

A prerequisite for the success of the work is that the carrier gas must be saturated with the vapour of the component being stripped. This is usually done by measuring the solute content of the carrier gas after bubbling it thorough the solute at a fixed temperature. Nitrogen saturated with the solute is led through a U-tube filled with active carbon. The mass gain of the active carbon after bubbling, is used to calculate the partial pressure of the solute in the carrier gas and this value is compared

with the saturated vapour pressure at the temperature of the saturation vessel. All chemicals used, have to be of a high purity which in most cases means vacuum fractional distillation on a column.

2.5. Infinite Dilution Activity Coefficients using a Differential Static Cell Method

Sandler et al.[31], have developed a new static cell apparatus (Figure 2.6) to measure the activity coefficients at infinite dilution for binary systems. Here the direct measurements of γ_{13}^{∞} is determined by measuring the equilibrium total pressure at a temperature T above a liquid of known composition.[37]. The static cell is particularly suited for the measurements of equilibrium pressures of systems with large relative volatilities or with partial miscibility. An important aspect of the static cell is that measurements are made at equilibrium conditions in contrast to a dynamic apparatus, such as a vapour-liquid still or an ebulliometer, which operate at steady state with temperature gradients and with liquid and condensed vapour holdups. However the solvents and the solutes used here, must be totally free of any impurities, especially dissolved gases or volatile components which, even at low concentrations, would significantly affect the measured pressure. Therefore all chemicals must be degassed before operation.

The differential static cell was developed by Sandler *et al.*[31] to overcome problems associated with the measurement of γ_{13}^{∞} with dynamic equipment[38]. In particular, since there is no condensed vapour holdup to alter the composition of gravimetrically prepared mixtures, static cells can be used to measure γ_{13}^{∞} of systems with a higher solute volatility than is possible with ebulliometers. Static cells can also be used for solvents with poor boiling properties, such as water[29] over large temperature ranges. Data treatment for the calculation of γ_{13}^{∞} is similar to that of the ebulliometric method using Equation 2.1.

2.5.1. Theory

From the equilibrium relationship:

$$f_1^L = f_1^V \tag{2.17}$$

where f_i is the fugacity of species i, Gautreaux and Coates[34] derived the equation for the determination of γ_{13}^{∞} from isothermal pressure-composition measurements. Their equation for binary activity coefficients at infinite dilution is:

$$\gamma_{13}^{\infty} = \frac{\phi_1^{(P_3^*)} P_3^* [P_3^* - (1 - P_3^* \frac{V_3}{RT} + \frac{P_3^*}{\phi_3^*}(\frac{\partial \phi_3^*}{\partial P})_T)](\frac{dP_3^*}{dT})(\frac{\partial P}{\partial x_1})_T^{\infty}}{P_1^* \phi_1^* \exp[(P_3^* - P_1^*)V_1/RT} \tag{2.18}$$

The terms have been previously described (section 2.2 page 3)
At low pressures and at moderate temperatures, so that the virial coefficients can be neglected after the second term, equation 2.18 becomes:

$$\gamma_{13}^{\infty} = \epsilon_1^{\infty} \frac{P_3^*}{P_1^*}(1 + \beta_3 \frac{1}{P_3^*}(\frac{\partial P}{\partial x_1})_T^{x_1 \to 0}) \tag{2.19}$$

where

$$\epsilon_1^{\infty} = \exp\left[\frac{(B_{11} - V_1)(P_3^* - P_1^*) + \delta_{13}P_3^*}{RT}\right] \tag{2.20}$$

$$\beta_3 = 1 + P_3^*\left(\frac{B_{33} - V_3}{RT}\right) \tag{2.21}$$

$$\delta_{13} = (2B_{13} - B_{11} - B_{33}) \tag{2.22}$$

where B_{11} and B_{33} are the second virial coefficients of pure components 1 and 3, respectively. The other terms have been previously defined.

The static cell is used to measure the limiting slope at infinite dilution (see equation 2.2). Virial coefficients are calculated using the Hayden and O'Connell[36] correlation. Vapour pressures are either measured or calculated from the Antoine constants. From this information γ_{13}^{∞} can be computed.

2.5.2. Equipment and Procedure.

Static cells are typically used to measure the equilibrium vapour pressure of mixtures of known composition. Sandler's static cell was designed and constructed specifically to measure the equilibrium total pressure of dilute gravimetrically prepared binary mixtures at constant temperatures. By using two static cells, a reference cell containing the pure solvent, and a cell containing the solvent and the solute mixture, pressure differences can be measured directly. This reduces the error in measuring the pressure difference. Furthermore, the effect of small temperature fluctuations is minimized.

A schematic diagram of the apparatus is shown in figure 2.6. The static cell apparatus consists of two glass cells each having an injection port, sealed with double septum, for the addition of solvent and solute. Additional equipment used for the static cell measurements consists of a temperature bath that can be manouvered so that the static cells can be removed or placed on the static cell manifold.

Before each series of measurements is started, all the septa are replaced, and the glass wear washed and dried in an oven. The cell to which the solute injections are made together with the septa and the stirring bar, are weighed before being attached to the degassing manifold. Once attached, the solvent is added, the cells are capped, and a vacuum is applied to one cell at a time.

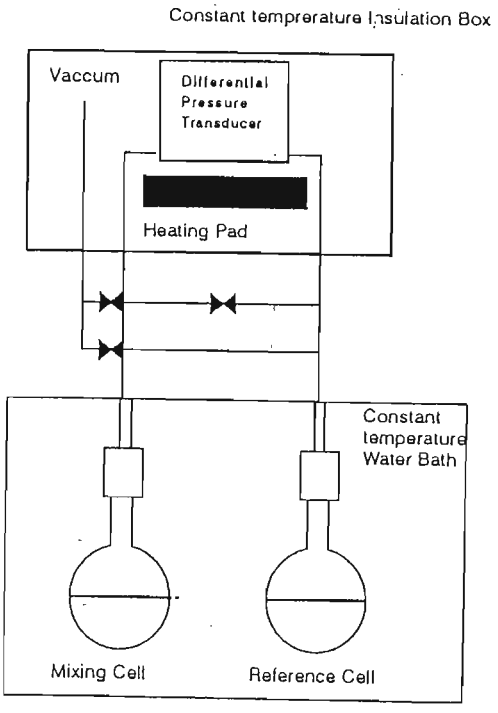

FIGURE 2.6 Schematic Diagram of the Differential Static Cell Equilibrium Apparatus

Once the solvents have been boiled, the cells are placed in an ultrasonic bath for further degassing. A vacuum is again applied to one cell at a time for approximately 3-5 minutes, and the cycle is repeated 4-6 times. If the solvent is moderately volatile, the procedure is similar except that degassing cycles are shorter. Alternatively, freeze-thaw cycles using liquid nitrogen are used for very volatile solvents.

The cells are then attached to the manifold containing the pressure transducer. A vacuum is then applied to the transducer, and the zero point of the pressure transducer is then recorded. By opening and closing certain valves, the transducer is isolated from the vacuum pump and is exposed to the vapour of the solvent. After the vapour pressure measurements, the mixing cell is prepared for the solute injection, by disconnecting the cell, and placing it in a hot water bath for about 10 minutes, so that the vapour pressure in the cell is slightly greater than 1 atm. This prevents air from entering the cell during injection. The degassed solute is then injected in to the cell, using a syringe of known weight. The cell is cooled to the water bath temperature. The pressure is then recorded every 5 minutes for 30-45 minutes until a constant value is obtained. The injection procedure is repeated about five times, doubling the solute volumes with each injection. Solute quantities are usually 10 μl for the first injection.

2.5.3. Chemicals

The purity of the solutes is crucial to the determination of γ_{13}^{∞} from static cell measurements. The highest purity solvents available are used in all experiments.

2.5.4. Data Analysis

The measurements made are total pressure and mole fraction. The change in pressure is expressed as a function of the liquid mole fraction. A second degree polynomial is fitted to the data:

$$\Delta P = a + bx_i + cx_i^2 \qquad (2.23)$$

By using this polynomial an accurate value of the limiting slope $(\partial P/\partial x_i)_T$ can be obtained which is equal to the parameter b. The limiting slope is used in equation 2.18 to calculate γ_{13}^{∞}.

2.6. The Dew Point Technique for Determining γ_{13}^{∞}

Trampe and Eckert[32] have developed the a Dew Point Technique for the determination of γ_{13}^{∞} of a very dilute vapour phase. This method is especially applicable to systems of low solute volatility, precisely where other methods such as ebulliometry and headspace gas chromatography become less precise. The technique is analogous to the differential ebulliometer and involves the change of temperature of the dew point of a vapour solvent when a dilute amount of solute is added.

The expression relating γ_{13}^{∞} of a solute in a solvent to a change in the dew point temperature $(\partial T/\partial y_1)_P^{\infty}$ at constant pressure is derived in a similar fashion to that of the ebulliometer technique, ie. equation 2.1.

2.6.1. Theory of the Dew Point Technique

Once again, disregarding the fugacity coefficient terms and the Poynting correction, all of which are generally of little significance at low pressure, and expressing the relative volatility of a solute infinitely dilute in a solvent can be expressed by:

$$\alpha = \frac{P_1^* \gamma_1^\infty}{P_3^*} \tag{2.24}$$

By substituting Equation 2.24 into Equation 2.1 an expression relating the measured dew point temperature to the relative volatility of the pure solute in the solvent is obtained,

$$(\frac{\partial T}{\partial y_1})_P^\infty = \frac{P_3^*}{(\frac{\partial P_3^*}{\partial T})} \frac{(1-\alpha)}{\alpha} \tag{2.25}$$

The quantities have been previously defined.

From equation 2.25 it can be noted that the expression depends only on the properties of the solvent and the temperature.

2.6.2. Apparatus

The experiment revolves around a General Eastern model D2 chilled mirror[32] dew point sensor, a commercial device used primarily to measure humidity of gas samples. It is shown in figure 2.7. The sensor works by flowing a vapour sample over a thermoelectrically cooled platinum mirror. A high-intensity, solid-state, light emitting diode is reflected off the mirror surface, and the intensity of the reflected light is monitored. As the mirror is cooled, dew begins to form on the mirror surface, scattering the light and reducing the reflected intensity. The mirror's temperature is kept at the dew point of the sample and is measured with a platinum resistance

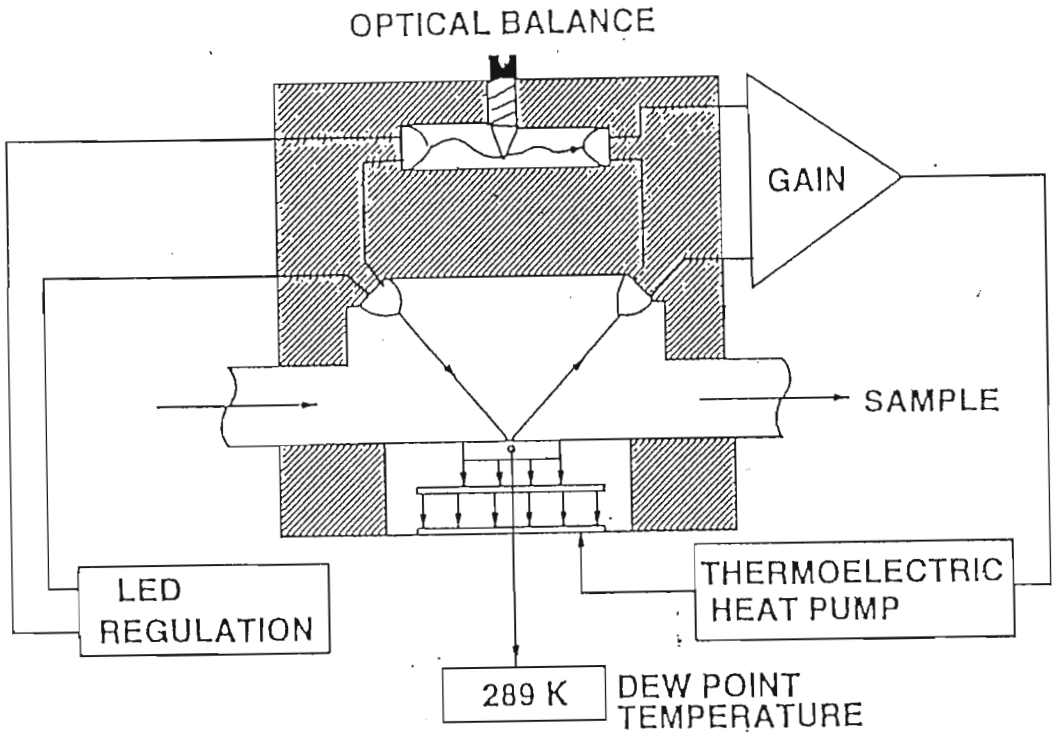

FIGURE 2.7. Dew Point Sensor[32]

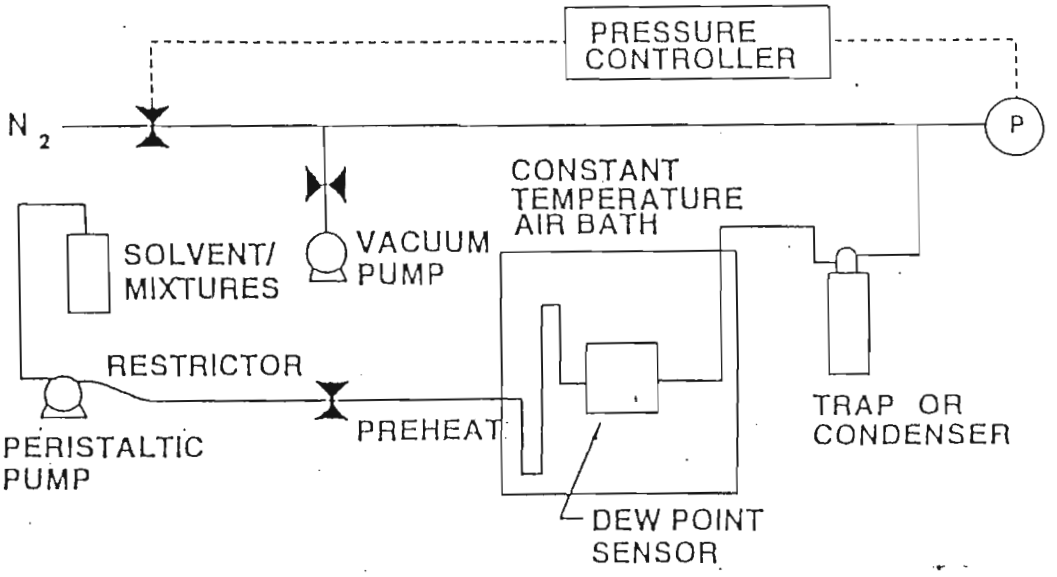

FIGURE 2.8. Overall design of the system used to measure the Activity coefficient at infinite dilution by dew point measurements.[32]

thermometer embedded just below the mirror surface.

The sensor is used in the experimental setup as shown in figure 2.8. Pure solvent or a solution of known composition is pumped through silica tubing. The liquid is "pumped" and not "pulled" into the system as a result of the pressure drop, thus ensuring a relatively constant flow rate. The vapour then flows through the sensor, exits from the oven and is cooled and collected in a water-cooled condenser or an ice trap.

2.6.3. Materials

High purity solvents are required, and the water content in the solvents has to be kept as low as is possible.

2.6.4. Procedure

The solutions are made up gravimetrically and are stirred for 30 minutes with a magnetic stirrer. The oven temperature is set so that the sensor is maintained at approximately 5 K above the expected dew point and held fairly constant. The preheat section is heated to 40 - 60 K higher than the dew point temperature. Although this is not critical, it must be hot enough to totally vaporise the solution. The mirror surface is cleaned with acetone before the pressure is set to give the desired temperature. At each temperature a liquid flow rate must be determined. The vapour flow rate was found not to affect the dew point measurements.

Pure solvent is pumped through the system for approximately 10 minutes. The cooling current in the sensor mirror is switched on, and the mirror is cooled to the dew point temperature. When the sensor signals that it has control of the dew layer on the mirror surface, the temperature of the mirror and the system pressure are recorded for approximately 10 minutes. The cooling current is then disabled and the pure solvent is replaced with a solution. The procedure is repeated four or five times with increasing solute concentrations.

2.6.4. Data Reduction

The temperature values are all found by taking the difference between each corrected solution dew point temperature and the first pure solvent dew point measurement. The experimental ΔT - y data are fitted to various empirical equations:

$$\Delta T = Ay_1 + By_1^2 \qquad (quadratic) \tag{2.26}$$

or

$$\Delta T = Ay_1 + By_1^2 + Cy_1^3 \qquad (cubic) \tag{2.27}$$

or

$$\frac{1}{\Delta T} = \frac{A}{y_1} + \frac{B}{y_1 y_3} \qquad (van\ Laar) \tag{2.28}$$

In the first two expressions $(\partial T/\partial y_1)_P^\infty$ = A, and in the third expression $(\partial T/\partial y_1)_P^\infty$ is equal to 1/B.[32] The fits are generally close to linear. The value for the limiting slope is taken from the expression that has the smallest standard deviation of fit given by:

$$\sigma = \left[\frac{\Sigma(\Delta T_{calc} - \Delta T_{exp})^2}{(n-N)}\right]^{\frac{1}{2}} \tag{2.29}$$

where n is the number of experimental points and N is the number of adjustable

parameters in the equation. This value of $(\partial T/\partial y_1)_P^\infty$ is used in equation 2.1 to obtain γ_{13}^∞. Since the experiment relies on difference in temperatures there is no need for temperature calibration. Also, since this is a vapour phase and flow experiment, there is no need to make corrections in the vapour phase composition.

2.7. Other methods

Other less well-establish methods for the determination of activity coefficients at infinite dilution have been reported in the literature.[40-41] One such method is a variation of headspace Gas Liquid Chromatography that minimizes the difficulties of calibration found in direct headspace chromatography[40]. In this method the liquid space consists of two (virtually immiscible) solvents. Small amounts of solute are first added to one of the solvents, and then increments of the second solute are added, along with continual sampling and analysis of the equilibrium vapour space. The changes in solute concentration in the vapour can be related to a partition coefficient, which in turn can be related to an infinite dilution activity coefficient. This indirect headspace chromatography is especially applicable to systems of higher relative volatility.

A relatively new method developed by Ray[41] is the determination of Binary Activity Coefficients from Microdroplet Evaporation. Although this method does not measure the activity coefficient at infinite dilution it is of some importance as it can be used to measure both γ_1 and γ_3. The method is based on the evaporation of a constant-composition droplet containing two components that differ markedly in volatility. The method accurately estimates activity coefficients of both components. This new technique was developed to simultaneously determine the evaporation rate and composition of a droplet from intensity peaks observed in the light scattered by the droplet. It has no upper or lower limits on the relatively volatility of the system and is particularly suitable for systems containing one relatively nonvolatile component.

2.8. Use of Activity Coefficients at Infinite Dilution

Thermodynamic models of liquid mixtures for G^E are generally constructed is such a way that a given number of empirical parameters must be determined on the basis of experimental data. The equations developed thus far generally require two or three parameters per binary system. However the activity coefficient at infinite dilution can be used to predict finite activity coefficients only if a one parameter model is used eg. Margules[12] or Van Laar[13]. If both γ_{13}^{∞} and γ_{31}^{∞} were obtainable experimentally then there are many two parameter models available, eg. Wilson[5] and UNIQUAC[7], that can be used to predict finite concentration activity coefficients. A detailed discussion of these models, among others, is given in Chapter 9.

Table 2.1. Comparison of the Advantages and Disadvantages of the Different Methods of Calculating Activity Coefficients at Infinite Dilution

Technique	Advantages	Disadvantages
Gas Liquid Chromatography	Gas chromatography is a relatively rapid experiment. Such speed is possible since the stationary phase is highly dispersed and has a large area interface with the gas. Also several solutes can be studied at the same time. The amount of solute injected onto the column is such a small quantity that it is effectively at infinite dilution. A chromatographic column can separate and purify components of a mixed sample at the same time as it measures it properties. Hence only moderately pure material need be used. Since the column is normally made into a compact shape, such as a coil, and housed in a thermostatted enclosure, it is a simple matter	It is characteristic of chromatography that the column may contain more components or phases than those being studied. Measurements may therefore reflect equilibrium interactions in more than one phase. A major disadvantage of G.L.C. is the solvent volatility. Liquid phases are usually limited to those with vapour pressures of less than 0.01 torr ie. 1 Pa, if one is to ensure that the amount of stationary phase in the column remains virtually constant over a reasonable period. In this work (chapter 4) the volatility problem is addressed.

	to operate it at any temperature within the capacity of the equipment. Chromatographic methods are often preferred for reactive solutes since quantities are small and the contact time is short.	
The Ebulliometric Method	No functional dependence of the Activity Coefficients on composition is assumed. The limiting slopes (ie. slope of the x vs T curve at infinite dilution or, x vs p) are measured.	If the solute volume is too small liquid composition is affected by enrichment of vapour with the more volatile component. Is best suited to solvents of similar volatility. If the solute is much less volatile that the solvent, determination of γ_{13}^{∞} is difficult.
Gas Stripping	No calibration is necessary. Can be extended to multicomponent systems. Developed to measure activity coefficients at infinite dilution of solvents with relatively high volatility.	Important to ensure large gas-liquid interface, long contact time between two phases, good dispersion of bubbles. Reproducibility of results due to difficulty in obtaining gas liquid equilibrium. Gas phase homogeneity and the absence of vapour condensation in the stream of the stripping gas before entry to the chromatographic column require special attention. Perfect gas saturation is required.

		Chemical used must be of the highest purity
Differential Static Method	Suited for measurements of equilibrium pressures of systems with large volatilities or the possibilities of partial miscibility. Possibility to measure γ_{13}^{∞} of solvents with low boiling points, such as water over over large temperatures. Partial pressures are measured directly, thereby reducing errors. Minimization of temperature fluctuations due to experimental conditions.	Solvents used must be totally free of any impurities, especially dissolved gases or volatile components even at low concentrations
Dew Point Technique	Applicable to systems of low volatility.	High purity solvents required. Water especially must be kept to a minimum

CHAPTER 3
THEORY OF GAS LIQUID CHROMATOGRAPHY

3.1. Gas Chromatography Principles

The chromatographic process involves the distribution of a solute component (1) between two phases, a mobile phase (2) and a solvent stationary phase (3). The two phases are mutually well dispersed with a large area of contact. In Gas Liquid Chromatography (G.L.C.) the liquid stationary phase (eg. dodecane or sulfolane) is dispersed on an inert solid support, such as celite, which is packed into a column. The liquid is held on the surface and in the pores of the support, while a stream of inert gas, the mobile phase, flows continuously through the spaces between the particles.[42]

In the elution process a small quantity of solute is introduced into the column at the inlet. The solute zone or peak is carried through the column by the mobile phase and its emergence at the other end is observed by a suitable detector (in this work two types of thermal conductivity detectors were used). The velocity with which the peak travels through the column is less than that of the mobile phase and depends on the distribution coefficient of the solute between the two phases.[43]

When the solute reaches the column, an equilibrium is set up between the liquid phase and the carrier gas phase so that a proportion of the sample always remains in the gas phase. This portion moves a little further along the column in the carrier gas stream, where it again equilibrates with the stationary phase. At the same time, material already dissolved in the stationary phase re-enters the gas phase so as to restore equilibrium with the clean carrier gas, which follows the zone of vapour.[24] This process in which carrier gas containing the vapour is stripped by the solvent in front of the zone, while vapour enters carrier gas at the rear of the zone, goes on

continuously with the result that the zone of vapour moves along the column more or less compactly. The speed at which the zone moves depends mainly on two factors, the rate of flow of the carrier gas and the partition coefficient of the solute between carrier gas and liquid phase. The faster the flow of carrier gas the faster the zone moves, and the more strongly the vapour is retained on to the solvent, the more slowly the zone moves. When two or more components are present in the sample, each usually behaves independently of the other, so that for a given carrier gas flow rate, the speed of the zone of each component will depend on the extent to which it is retained. Since different substances differ in their retention, they may therefore be separated by making use of their different speeds of progress through the column. When eluted the solutes will appear one after the other in the gas stream, the fastest first and the slowest last. The gas liquid chromatographic process is one of equilibrium between a vapour and a liquid, and the retention is a function of the solutes vapour pressure and the interaction between the solute and solvent (this process involves the dissolution of the vapour in the solvent).

3.1.1. Assumptions

One of the theories related to the determination of activity coefficients at infinite dilution is the plate theory and rests on the following assumptions.[43]

(i) The column can be divided into a large number of theoretical plates.

(ii) The partition coefficient is constant throughout the range of concentration encountered, that is, Henry's Law is obeyed. This is only true for very low solute concentrations.

(iii) The solute volume upon introduction into the column occupies only a small portion of the column length.

(iv) There is negligible resistance to mass transfer from gas to solvent i.e. the rate at which equilibrium is reached is very much greater than the rate of travel of

solute down the column. Equilibrium exists at each stage in the process ie. theoretical plate.

3.2. Summary of the G.L.C. Theory Involving γ_{13}^{∞}

In 1941 Martin and Purnell[44] related the equilibrium partition coefficient, K_R, to retardation properties using the plate theory, whereby they related the apparent retention volume of the solute, V_N', to the apparent gas hold up volume, V_G', and the solvent volume, V_3 (for zero pressure difference across the column).

$$V_R' = V_G' + K_R V_3 \tag{3.1}$$

In 1952 James and Martin[45] extended the theory and took into account the compressibility of the mobile phase by using a correction factor which according to Everett's notation can be generalized as

$$J_n^m = \frac{n}{m} \frac{(P_i / P_o)^m - 1}{(P_i / P_o)^n - 1} \tag{3.2}$$

where P_i is the inlet pressure and P_o the outlet pressure.

In 1956 Porter [46] related the net retention volume, V_N, to the activity coefficient of the solute at infinite dilution, γ_{13}^{∞}, (where 1 refers to the solute and 3 to the solvent) by

$$V_N = \frac{n_3 RT}{\gamma_{13}^{\infty} P_1^*} \tag{3.3}$$

where n_3 is the amount of solvent on the column and P_1^* the vapour pressure of the solute. The net retention volume is obtained from the corrected outlet flow rate U_O using

$$\begin{aligned} V_N &= J_3^2 U_O (t_R - t_G) \\ &= J_3^2 U_O t_R - V_G \end{aligned} \tag{3.4}$$

where t_R and t_G are the retention times for the solute and an unretained gas respectively, and V_G is the gas hold up volume.

Everett and Stoddard[47] took into into account solute vapour and the solute + carrier gas imperfections. Desty[48] applied these ideas to the determination of B_{12} values and used an extrapolation procedure based on the equation:

$$\ln V_N = \ln V_N^0 + \beta P_O J_3^2 \tag{3.5}$$

where V_N^O is the extrapolated retention volume at zero column pressure and can be calculated by extrapolating $ln\ V_N$ to $P_o = 0$.

β is given by

$$\beta = \frac{2B_{12} - V_1^{\infty}}{RT} \tag{3.6}$$

in which B_{12} is the mixed second virial coefficient of the solute vapour in the carrier gas and V_1^{∞} is the partial molar volume of the solute at infinite dilution in the solvent.

Alternatively, (as was done in this work) V_N^o can be calculated from known values of B_{12}. γ_{13}^{∞} is related to V_N^0 by the equation[1]

$$\ln V_N^0 = \ln \frac{n_3 RT}{\gamma_{13}^{\infty} P_1^*} - [\frac{B_{11} - V_1^*}{RT}]P_1^* \qquad (3.7)$$

where V_1^* is the molar volume of the pure solute, and B_{11} is the second virial coefficient of the pure solute vapour.

The Bristol group[1-3] took into account carrier gas imperfection and suggested a different extrapolation technique other than equation 3.5 for ideal gases

$$\ln V_N = \ln V_N^O + \beta P_1^* J_3^4 \qquad (3.8)$$

In this work however the following equation was used,

$$\ln V_N = \ln V_N^O + \beta P_1^* J_3^2 \qquad (3.9)$$

since, for a pressure drop across the column of less than 1 atm. $J_3^4 = J_3^2$.

3.3. Detailed Theory of G.L.C.

3.3.1. The Theoretical Plate Concept

In the theoretical plate model, the column is regarded as being divided into a large number of theoretical plates small enough so that the concentration of sample in both mobile and stationary phases can be regarded as uniform. Each plate consists of two volumes, ie. the volume of free gas (ΔV_{GAS}) and of liquid (ΔV_L); the sum of the volumes being the total plate volume Δx, thus

$$\Delta x = \Delta V_{GAS} + \Delta V_L \tag{3.10}$$

The solute sample in the first theoretical plate is distributed between the stationary and mobile phases according to a partition coefficient, such that at equilibrium a fraction z of solute exists in the gas phase and a fraction y in the liquid phase.[42]
If r volumes of carrier gas is passed through the column and we designate the number of any plate by N, the quantity of solute in the $(N + 1)^{th}$ plate can be shown to be[43]:

$$Q_{N+1} = \frac{r!\ (y)^{r-N}\ (z)^N}{N!\ (r-N)!} \tag{3.11}$$

In order to have some measure of the rate of movement of a solute through a column, the maximum of the distribution curve is chosen as a reference point. Assuming that the $(N + 1)^{th}$ plate contains more solute than any other plate after r volumes of ΔV_{GAS} have passed, this would mean that this plate contains more solute than when $(r\text{-}1)$ or $(r+1)$ volumes have passed.[43]
Thus we require

$$Q(r) > Q(r - 1) \tag{3.12}$$

and

$$Q(r) > Q(r + 1) \tag{3.13}$$

simultaneously. If $Q(r) > Q(r\text{-}1)$ then

$$\frac{r!\ y^{(r-N)}\ z^N}{N!\ (r-N)!} > \frac{(r-1)!\ y^{(r-N-1)} z^N}{N!\ (r-N-1)!} \tag{3.14}$$

This implies that

$$\frac{ry}{r - N} > y^{-1} \tag{3.15}$$

However since

$$y = 1 - z \tag{3.16}$$

equation 3.14 therefore becomes

$$r\ (1 - z) > r - N \tag{3.17}$$

This implies that

$$N > rz \tag{3.18}$$

Similarly

$$Q(r) > Q(r+1) \quad \Rightarrow \quad N < (r + 1)z \tag{3.19}$$

Therefore to all intents and purposes for Q_{max}

$$N = rz \tag{3.20}$$

The solute fraction is given by

$$z = \frac{C_{GAS}\Delta V_{GAS}}{C_{GAS}\Delta V_{GAS} + C_L\Delta V_L} \tag{3.21}$$

the liquid. If the solute partition coefficient K_R is given by,

$$K_R = \frac{C_L}{C_{GAS}} \tag{3.22}$$

the faction of solute (1) in the gas phase at any plate is given by

$$z = \frac{\Delta V_{GAS}}{\Delta V_{GAS} + K_R\,\Delta V_L}. \tag{3.23}$$

3.3.2. Relation of the Net Retention Volume and the Activity Coefficient to the Partition Coefficient

The distribution of a solute between a stationary liquid phase (3) and a mobile phase, at constant temperature and pressure, corresponds to equilibrium when the solute free energy is a minimum.[49] Its chemical potential in one phase is then equal to that in the other phase.

Thus

$$\mu_L = \mu_G \tag{3.24}$$

where

$$\mu_i = \mu_i^0 + RT \ln a_i \tag{3.25}$$

a_i being the solute activity in the i^{th} phase and μ_i^0 is the solute chemical potential at some unit activity.

Approximating for the moment that activities can be replaced by concentration

$$\mu_i^0 + RT \ln C_L = \mu_G^0 + RT \ln C_{GAS} \tag{3.26}$$

$$\frac{C_L}{C_{GAS}} = \exp(\frac{\Delta\mu^0}{RT}) = K_R \tag{3.27}$$

K_R being the solute partition coefficient.

When the solute is dissolved in, ie. retained, on the solvent stationary phase (liquid), it is assumed at any instant to be immobile; movement occurs only when the solute vaporizes and is carried down the column by the mobile gas phase. [49]

The linear rate of travel is therefore equal to the average carrier velocity $\bar{u}$ multiplied by the fraction of time the solute spends in the mobile phase.

$$rate\ of\ travel = \bar{u}\ [\frac{C_{GAS}V_{GAS}}{C_{GAS}V_{GAS} + C_LV_3}] \tag{3.28}$$

V_G being the mobile phase volume (or gas hold up) and V_3 being the stationary phase volume.

$$rate\ of\ travel = \bar{u}\ [1 + \frac{C_LV_3}{C_{GAS}V_G}]^{-1} \tag{3.29}$$

since $C_L/C_{GAS} = K_R$. Alternatively

$$= \bar{u}\ [1 + K_R \frac{V_L}{V_G}]^{-1} \tag{3.30}$$

$$rate\ \ of\ \ travel = \frac{column\ length\ (L)}{retention\ time\ (t_R)} \tag{3.31}$$

Therefore the retention time is given by

$$t_R = \frac{L}{\bar{u}} [1 + K_R \frac{V_3}{V_G}] \tag{3.32}$$

The quantity $L/\bar{u}$ is identical to t_G, the time a non-retained solute ($K_R = 0$) requires to pass through the column.

$$t_R = t_G (1 + K_R \frac{V_3}{V_G}) \tag{3.33}$$

To convert retention times to gas volumes the flow rate of the mobile phase generally measured at the column outlet, must be known. The measured flow rate (U_C) must therefore be corrected to the conditions prevailing in the column; that is

$$U_O = U_C (\frac{T}{T_{fm}})(\frac{P_{fm} - P_w}{P_{fm}}) \tag{3.34}$$

where T is the column temperature, T_{fm} is the flowmeter temperature, P_{fm} is the flowmeter vapour pressure at T_{fm}, P_w is the water vapour pressure at T_{fm}. The apparent gas hold up (V_G) and retention (V_R') volumes are now given by

$$V_G' = t_G U_O \tag{3.35}$$

$$V_R^{/} = t_R U_O \tag{3.36}$$

by substituting equation 3.35 and 3.36 into eq.3.33

$$V_R^{/} = V_G^{/} (1 + K_R \frac{V_3}{V_G}) \tag{3.37}$$

From equation 3.1

$$V_R = V_R^{/} - V_G^{/} = U_O(t_R - t_G) \tag{3.38}$$

In order for a mobile phase to flow through a column a pressure gradient must exist. This necessitates the introduction of a gas compression factor, as first recognized by James and Martin [45] in 1952.

Consider a carrier gas flowing through a packed column of uniform cross section A at a pressure P, and velocity u. The volume throughout must be constant within the column so that by Boyles law, [43]

$$Pu = P_O u_O = \bar{P}\,\bar{u} \tag{3.39}$$

where $\bar{P}$ is the average pressure, P_O the outlet pressure, $\bar{u}$ the average velocity and u_O the outlet velocity. The velocity at any given point is given by

$$u = \frac{P_O u_O}{P} \tag{3.40}$$

The velocity can also be related to the pressure gradient ***dp*** within a length ***dx*** along the column, the column specific permeability coefficient ***K***, porosity ***e*** and gas viscosity, through Darcy's law[43]

$$u = -\frac{K\ dP}{\eta\ dx} \tag{3.41}$$

Substituting for ***u*** in equation 3.40

$$\frac{P_o \mu_o}{P} = -\frac{KdP}{e\eta dx} \tag{3.42}$$

Therefore

$$dx = [-\frac{K}{e\eta u_o P_o}]\ PdP \tag{3.43}$$

Multiplying by P we obtain

$$Pdx = [\frac{K}{e\eta u_o P_o}]\ P^2 dP \tag{3.44}$$

The average value of a continuous function $\overline{F(x)}$ is

$$\overline{F}(x) = \frac{\int F(x)dx}{\int dx} \tag{3.45}$$

$$\bar{P} = \frac{\int (-\frac{K}{e\eta u_O P_O}) P^2 dP}{\int (-\frac{K}{e\eta u_O P_O}) P dP} \tag{3.46}$$

$\bar{P}$ being the average pressure over the column. Integrating over the column pressure gradient, which is bounded by the inlet (P_i) and outlet (P_o) pressure

$$\bar{P} = \frac{2}{3} [\frac{(P_i^3 - P_O^3)}{(P_i^2 - P_O^2)}] \tag{3.47}$$

$$\frac{\bar{P}}{P_O} = \frac{2}{3} [\frac{(P_i/P_O)^3 - 1}{(P_i/P_O)^2 - 1}] \tag{3.48}$$

Since $\bar{P}/P_o = \bar{V}/V_o$, then

$$\bar{V} = \frac{3}{2} V_O [\frac{(P_i/P_O)^2 - 1}{(P_i/P_O)^3 - 1}] = JV_O \tag{3.49}$$

where

$$J = \frac{3}{2}\left[\frac{(P_i/P_O)^2 - 1}{(P_i/P_O)^3 - 1}\right] \tag{3.50}$$

Gas volumes measured at the column outlet can therefore be corrected to the average column pressure by multiplying by the fraction $\bar{V}/V_O$ which is given by the symbol J. Everett [2] suggested that the compressibility correction can be represented as

$$J_n^m = \frac{n}{m}\left[\frac{(P_i/P_O)^m - 1}{(P_i/P_O)^n - 1}\right] \tag{3.2}$$

The fully corrected gas hold up volume is given by $V_G = J_3^2\, V_G'$

Therefore from equation 3.37

$$J_3^2 V_R' = V_G\left(1 + K_R\frac{V_3}{V_G}\right) \tag{3.51}$$

The term $J_3^2 V_R'$ is given the symbol V_R^o and is referred to as the corrected retention volume[1].

$$V_R^o = V_G + K_R V_3 \tag{3.52}$$

The product $K_R V_3 = V_N$, the net retention volume.

Therefore

$$V_N = J_3^2 V_R^{'} = V_R^o - V_G = K_R V_3 = U_O J_3^2 (t_R - t_G) \tag{3.53}$$

The solute partial pressure over its infinitely dilute solution (Henry law region) in the liquid phase is

$$P_1 = \gamma_{13}^{\infty} x_1 P_1^* \tag{3.54}$$

where γ_{13}^{∞} is the activity coefficient at infinite dilution and P_1^* is the vapour pressure of the pure solute.

Recognizing that $x_1 = n_1^L/n_3$[44] where x_1 is the solute mole fraction in the liquid phase, n_1^L is the solute molar amount in the liquid, and n_3 is the liquid phase molar amount.

$$P_1 = \gamma_{13}^{\infty} P_1^* \frac{n_1^L}{n_3} \tag{3.55}$$

Dividing by V_3

$$\frac{P_1}{V_3} = \frac{\gamma_{13}^{\infty} P_1^* n_1^L/n_3}{V_3} \tag{3.56}$$

Therefore

$$\frac{n_1^L}{V_3} = \frac{n_3 P_1}{\gamma_{13}^{\infty} P_1^* V_3} \tag{3.57}$$

where P_1 is the solute partial vapour pressure and P_1^* is the solute saturation vapour pressure.

For ideal gases

$$\frac{n_1^G}{V_3} = \frac{P_1}{RT} \tag{3.58}$$

and

$$K_R = \frac{(n_1^L V_G)}{(n_1^G V_3)} \tag{3.59}$$

From equation 3.56

$$\frac{n_1^L}{V_3} = \frac{n_3 P_1}{\gamma_{13}^{\infty} P_1^* V_3} \tag{3.60}$$

and from equation 3.57

$$\frac{n_1^G}{V_G} = \frac{P_1}{RT} \tag{3.61}$$

Substituting equation 3.57 and 3.58 into equation 3.59

$$K_R = \left[\frac{n_3\ P_1}{\gamma_{13}^{\infty}\ P_1^*}\ V_G\right] / \left[\frac{P_1 V_G}{RT}\ V_3\right] \tag{3.62}$$

$$K_R = \frac{n_3\ P_1\ V_G}{\gamma_{13}^{\infty}\ P_1^*} \cdot \frac{RT}{P_1\ V_G\ V_3} \tag{3.63}$$

$$\therefore \quad K_R = \frac{RT}{\gamma_{13}^{\infty}\ P_1^*\ \overline{V_L}} \qquad since \frac{V_3}{n_3} = \overline{V_L} \tag{3.64}$$

where $\bar{V}_L$ is the molar volume of the liquid stationary phase

$$n_3 = \frac{Mass\ of\ stationary\ phase\ (W_L)}{Molar\ mass\ of\ stationary\ phase\ (M_3)} \tag{3.65}$$

The partition coefficient is then given by

$$K_R = \frac{n_3\ RT}{V_L\ \gamma_{13}^{\infty}\ P_1^*} \tag{3.66}$$

$$K_R\ V_3 = \frac{n_3\ RT}{\gamma_{13}^{\infty}\ P_1^*} \tag{3.67}$$

But

$$K_R\ V_3 = V_N \tag{3.68}$$

Therefore

$$V_N = \frac{n_3\ RT}{\gamma_{13}^{\infty}\ P_1^*} \tag{3.3}$$

3.3.3. The Pressure Dependence of the Partition Coefficient[42]

The partition coefficient at infinite dilution, K_R, in a static system can be defined as

$$K_R = \lim_{x_i \to 0} \frac{n_1^{\,L}\ V_G}{V_L\ n_1^{\,G}} \tag{3.69}$$

where n_1^L is the number of mole of 1 in volume V_3 of liquid and n_1^G is the number of

mole of 1 in volume V_G of gas. $n_1^G = y_1 n^G$ and $n_1^L = x_1 n^L$ where n^G is the total number of mole of gas (solute + carrier gas) in volume, V_G, of carrier gas, n^L is the total number of mole of liquid (solute + solvent) in V_L, y_1 is the mole fraction of solute 1 in the gas, and x_1 is the mole fraction of solute 1 in liquid.

$$K_R = \lim_{x \to 0} \frac{x_1 n^L}{V_3} \cdot \frac{V_G}{y_1 n^G} \tag{3.70}$$

$$K_R = \lim_{x \to 0} \frac{x_1 n^L}{V_3 y_1} \bar{V}_G \tag{3.71}$$

where $\bar{V}_G$ is the molar volume in the gas phase.

In the limit of infinite dilution of the solute (1) in gas phase (2)[42]

$$\bar{V}_G = \frac{RT}{P} + B_{22} + \frac{(C_{222} - B_{22}^2)}{RT} P \tag{3.72}$$

where P is the carrier gas pressure, B_{22} is the second virial coefficient of carrier gas and C_{222} is the third virial coefficient of the carrier gas.

$$K_R = \lim_{x \to 0} \frac{x_1 n_3}{V_3 y_1} \frac{RT}{P} \left[1 + \frac{B_{22} P}{RT} + \frac{(C_{222} - B_{22}^2}{(RT)^2} P^2 + \ldots\right] \tag{3.73}$$

where $n_3 = n^L$

Now since $y_1 P = P_1$ (partial pressure of solute),

$$K_R = \lim_{x\to 0} \frac{x_1 n_3 RT}{V_3 P_1} \left[1 + \frac{B_{22}P}{RT} + \frac{(C_{222} + B_{22}^2)}{(RT)^2}P^2 + \ldots\right] \qquad (3.74)$$

$$\lim_{x\to 0} \frac{P_1}{x_1} = \frac{n_3 RT}{V_3 K_R} \left[1 + B_{22}\frac{P}{RT} + \frac{C_{222} - B_{22}^2}{(RT)^2}P^2 + \ldots\right] \qquad (3.75)$$

multiplying by $1/P_1^*$

$$\lim_{x\to 0} \frac{P_1}{x_1 P_1^*} = \frac{n_3 RT}{V_3 K_R P_L^*} \left[1 + \frac{B_{22}P}{RT} + \frac{(C_{222} - B_{22}^2)}{(RT)^2}P^2 + \ldots.\right] \qquad (3.76)$$

But

$$\gamma_{13}^{\infty}(T,P) = \lim_{x_1\to 0} \frac{P_1}{P_1^* x_1} \qquad (3.77)$$

$$\therefore \quad \gamma_{13}^{\infty}(T,P) = \frac{n_3 RT}{V_3 K_R P_1^*} \left[1 + \frac{B_{22}P}{RT}\right] + \frac{(C_{222} - B_{22}^2)}{(RT)^2}P^2 + \ldots.\right] \qquad 3,78$$

It can be shown that $\gamma_{13}^{\infty}(T,P)$ is related to the activity coefficient at zero pressure and infinite dilution $\gamma_{13}^{\infty}(T,0)$ by

$$\ln\gamma_{13}^{\infty}(T,0) = \ln\gamma_{13}^{\infty}(T,P) - \frac{B_{11} - V_1^{\infty}}{RT}P + [\frac{2C_{222} - 3B_{11}^2}{2RT}]P_1^{*2} + \frac{2B_{12} - B_{22} - V_1^*}{RT}P + \frac{(2C_{222} - 3C_{122} - 3B_{22}^2 + 4B_{12}B_{22})}{2(RT)}P^2 \quad (3.79)$$

Substituting into the equation for $\gamma_{13}^{\infty}(T,P)$

$$\ln\gamma_{13}^{\infty}(T,0) = \ln\frac{n_3RT}{V_3K_RP_1^*} - \frac{(2B_{12}-V_1^o)}{RT}P_1^* + \frac{(2B_{12} - V_1^{\infty})}{RT} + (3C_{122} - 4B_{12}B_{22})\frac{P^2}{2RT} \quad (3.80)$$

where

$$\ln\,[1 + \frac{B_{22}P}{RT} + \frac{B_{22}^2P^2}{(RT)^2} + \frac{C_{222}P^2}{(RT)^2} + ...]$$

has been approximated by

$$[\frac{B_{22}P}{RT} - \frac{3}{2}\frac{B_{22}^2P^2}{(RT)^2} + \frac{C_{222}P^2}{(RT)^2} + ...]$$

Solving for K_R in equation 3.80

Therefore

$$\ln K_R = \ln \frac{n_3 RT}{P_1^* V_3 \gamma_{13}^{\infty}(T,0)} - \frac{(B_{11} - V_1^*)}{RT} P_1^* + \frac{(2B_{12} - V_1^{\infty})}{RT} P + (3C_{122} - 4B_{12}B_{22}) \frac{P^2}{2RT} \tag{3.81}$$

$$K_R = \ln K_R(0) + \beta P + \zeta P^2 \tag{3.82}$$

where

$$\ln K_R(0) = \ln \left[\frac{n_3 RT}{\gamma_{13}^{\infty}(T,0)\ P_1^*\ V_3}\right] - \left[\frac{B_{11} - V_1^*}{RT}\right] P_1^* \tag{3.83}$$

$$\beta = \frac{(2B_{12} - V_1^{\infty})}{RT} \tag{3.6}$$

$$\zeta = \frac{(3C_{122} - 4B_{12}B_{22})}{2(RT)^2} \tag{8.84}$$

The term P^2 is negligible at pressures below 15 atms. From equation 3.83

$$\ln[K_R(0)V_3] = \ln \left[\frac{n_3 RT}{\gamma_{13}^{\infty}(T,0)P_1^*}\right] - \left[\frac{B_{11} - V_1^*}{RT}\right] P_1^* \tag{8.85}$$

From equation 3.53

$$K_R V_3 = V_N \quad \Rightarrow \quad K_R(0)V_3 = V_N^o \tag{3.86}$$

where V_N^o is the retention volume at zero mean column pressure

$$\ln V_N^o = \ln \left[\frac{n_3 RT}{\gamma_{13}^{\infty}(T,0)P_1^*}\right] - \left[\frac{B_{11} - V_1^*}{RT}\right] P_1^* \qquad (3.7)$$

Equation 3.85 expresses the pressure dependence of the partition coefficient K_R.

3.3.4. The Elution Process

When the distribution coefficient is defined as[42]

$$K_R = \lim_{x \to 0} \frac{n_1^L V_G}{V_3 n_1^G} \qquad (3.69)$$

the peak velocity W is given by

$$W = \frac{\bar{u} V_G}{V_G + K_R V_3} \qquad (3.87)$$

equation 3.87 can be written as

$$\frac{l}{W} = \frac{V_G + K_R V_3}{\bar{u} V_G} \qquad (3.88)$$

where l is the distance from the column inlet.

Also

$$\frac{l}{w} = \frac{dt}{dl} = \frac{V_G + K_R V_3}{\bar{u} V_G} \qquad (3.89)$$

where t is the retention time ie. the time taken for the peak to travel a distance l. Now $\bar{u}$ is the volumetric flow rate of the carrier gas therefore $\bar{u}V_G$ can be replaced by U

$$Udt = (K_R V_3 + V_G)dl \qquad (3.90)$$

Since U varies along the column in proportion to the carrier gas molar flow, it is convenient to express this variation in terms of local pressure, using the approximate equation of state.

$$PV_2 = RT + B_{22}P \qquad (3.91)$$

$$\Rightarrow \quad U = \frac{P_o(1 + bP)}{P(1 + bP_o)} U_o \qquad (3.92)$$

where $b = B_{22}/RT$

U_o is the corrected carrier gas flowrate at the column outlet and P_o is the pressure at the column outlet.

Equation 3.92 is derived as follows

$$\frac{PV_2}{RT} = 1 + \frac{B_{22}P}{RT} \tag{3.91}$$

Dividing equation 3.92 by RT

since $b = B_{22}/RT$

$$V_2 = \frac{1 + (B_{22}/RT)P}{P/RT} \tag{3.93}$$

$$V_2 = \frac{1 + bP}{P/RT} \tag{3.94}$$

At the outlet of the column

$$V_2^o = \frac{1 + bP_o}{P_o/RT} \tag{3.95}$$

Dividing equation 3.93 by 3.94

$$\frac{V_2}{V_2^o} = \frac{[\frac{1 + bP}{P}]\ RT}{[\frac{1 + bP_o}{P_o}]\ RT} \tag{3.96}$$

Therefore

$$\frac{V_2}{V_2^o} = \frac{P_o(1 + bP)}{P(1 + bP_O)} \tag{3.97}$$

but V_2/V_2^0 = ratio of molar volumes = U/U_o = ratio of volumetric flow rates

$$U = \frac{P_o(1 + bP)}{P(1 + bP_o)} U_o \tag{3.92}$$

substituting for U in equation 3.90

$$U_o dt = \frac{(K_R V_3 + V_G)(1 + bP_o)}{P_o(1 + bP)} P dl \tag{3.98}$$

$U_o\ dt$ is the volume of gas leaving the column outlet as the elution peak advances a distance dl. Because of the difficulty of defining V_G accurately it is more convenient to consider instead $U_o dt$, the volume of carrier gas measured at the column outlet which passes the elution peak during its progress from l to $l + dl$.

This is obtained by allowing $V_3 = 0$ (value corresponding to no liquid phase). This is simply

$$dV_R = K_R V_3 \frac{1 + bP_o}{P_o} \frac{P}{1 + bP} dl \tag{3.99}$$

The retention volume V_R is the same given in equation 3.38 ie. the observed retention volume minus the gas holdup at the column outlet. Since K_R is a function of pressure, the most direct way to integrate the equation is to change the variable from l to P by means of Darcy's law.[43]

$$\frac{dP}{dl} = \frac{-ue\eta}{K} \tag{3.100}$$

$$dl = dx \quad \Rightarrow \quad \frac{dP}{dx} = -\frac{u}{A} \tag{1.101}$$

where A takes into account the column packing permeability. If the pressure < 50 atms the Chapman-Enskog[2] relation in approximation form can be used ie.
where

$$a = 0.175 \frac{B_{22}}{RT} \tag{3.102}$$

Combining with Darcy's law

$$dl = -\frac{a}{u_o(1 + aP0)\eta} dP \tag{3.103}$$

But carrier gas pressure varies according to

$$U = \frac{P_O(1 + bP)}{P(1 + P_O b)} U_O \tag{3.92}$$

$$U_O = \frac{UP(1 + bP_O)}{P_O(1 + bP)} \tag{3.104}$$

but

$$U_O = \frac{dP}{dl} \frac{A}{\eta} \tag{3.105}$$

also

$$\eta = \eta_o(1 + aP) \tag{3.106}$$

substituting equations 3.92 and 3.106 into equation 3.105

$$\frac{UP(1 + bP_O)}{P_O(1 + bP)} = \frac{dP}{dL}\frac{A}{\eta_o(1 + aP)} \tag{3.107}$$

$$dl = \frac{AP(1 + bP_O)dP}{P_O(1 + bP)U\eta_o(1 + aP)} \tag{3.108}$$

Integrating

$$L = \frac{A(1 + bP)}{U(\eta_o)P}\int_{P_O}^{P_l}\frac{P}{(1 + bP_o)(1 + aP)}\,dP \tag{3.109}$$

Dividing equation 3.103 by equation 3.109

$$\frac{dl}{L} = \frac{\dfrac{AP(1+bP_O)dP}{P_O(1+bP)\ U\eta_o(1+aP_O)}}{\dfrac{A(1+bP)}{U(\eta_o)P}\displaystyle\int_{P_O}^{P_l}\frac{P}{(1+bP_O)(1+aP_OdP)}} \tag{3.110}$$

$$dl = \frac{\dfrac{LPdP}{(1 + aP)(1 + bP)}}{\displaystyle\int_{P_o}^{P_l}\frac{PdP}{(1 + aP)(1 + bP)}} \tag{3.111}$$

$$\ln K_R = \ln K_R(0) + \beta P + \zeta P^2 \tag{3.82}$$

$$K_R = K_R(0) + e^{\beta P} + e^{\zeta P^2} \tag{3.112}$$

equation 3.108 states that

$$dV_R = K_R V_3 \frac{1 + bP_O}{P_O} \frac{P}{1 + bP} dl \tag{3.113}$$

Substituting equation 3.111 and 3.112 into equation 3.99

$$dV_R = \frac{K_R + e^{\beta P} + e^{\zeta P^2} . V_3(1+bP_O)}{P_O} \cdot \frac{P}{(1+bP)} \cdot \frac{\frac{LPdP}{(1+aP)(1+bP)}}{\int_{P_o}^{P_i} \frac{PdP}{(1+aP)(1+bP)}} \tag{3.114}$$

Also by substituting equations 3.112 and 3.108 into equation 3.99

$$dV_R = [K_R(0) + e^{\beta P} + e^{\zeta P^2}][V_3 \frac{1+bP_O}{P_O} \cdot \frac{P}{1+bP}][\frac{AP(1+bP_O)bP}{P_O(1+bP)U\eta_O(1+aP)}] \tag{3.115}$$

By integration

$$V_R = K_R(0) V_3 \left[\frac{1 + bP_O}{P_O}\right] \frac{\int_{P_o}^{P_i} \frac{P^2 e^{\beta P} e^{\zeta P^2}}{(1 + aP)(1 + bP)^2} dP}{\int_{P_o}^{P_i} \frac{P}{(1 + aP)(1 + bP)} dP} \tag{3.116}$$

The above equation gives the required relationship between the retention volume V_R and the partition coefficient.

3.3.5. The Net Retention Volume of an Ideal Carrier Gas

In the case of an ideal carrier gas a and b in equation 3.116 and B_{22} (second viral coefficient of the carrier gas) are all zero. Therefore

$$V_R = \frac{K_R(0)V_3 \int_{P_o}^{P_i} P^2 \, e^{\beta P} \, e^{\zeta P^2} \, dP}{P_o \int_{P_o}^{P_i} P \, dP} \qquad (3.117)$$

By integration

$$\ln \left(\frac{V_R}{J_3^2}\right) = \ln V_N = \ln V_N^0 + \beta P_O J_3^4 + \zeta (P_O J_3^4)^2 \qquad (3.118)$$

where

$$V_N^0 = K_R(0) \; V_3 \qquad (3.119)$$

since $\zeta(P_o \, J_3^4)^2$ is negligible at pressures below 15 atm equation 3.118 approximates to

$$\ln V_N = \ln V_N^O + \beta P_o J_3^4 \qquad (3.8)$$

But

$$\ln V_N^O = \ln \left[\frac{n_3 RT}{\gamma_{13}^{\infty}(T,0)P_1^*}\right] - \left[\frac{B_{11} - V_1^*}{RT}\right] P_1^* \qquad (3.7)$$

Therefore substituting for $\ln V_N^O(T)$ and β

$$\ln V_N = \ln\left[\frac{n_3 RT}{\gamma_{13}^{\infty}(T,0)P_1^*}\right] - \left[\frac{B_{11} - V_1^*}{RT}\right]P_1^* + \left[\frac{2B_{12} - V_1^{\infty}}{RT}\right]P_o J_3^4 \quad (3.120)$$

This is identical to equation 1.1 since for pressures a pressure drop across the column of less than 1 atm $J_3^4 \approx J_2^3$ and $\gamma_{13}^{\infty}(T,0) = \gamma_{13}^{\infty}$.

The above equation was developed by Everett[2] and Cruickshank[1] for the determination of activity coefficients at infinite dilution.

In this work the following equation was used,

$$\ln V_N = \ln\left[\frac{n_3 RT}{\gamma_{13}^{\infty}P_1^*}\right] - \left[\frac{B_{11} - V_1^*}{RT}\right]P_1^* + \left[\frac{2B_{12} - V_1^{\infty}}{RT}\right]P_o J_2^3 \qquad (3.121)$$

where $J_3^4 \approx J_2^3$

3.3.6. Treatment of a Volatile Solvent

The usual method (using equation 3.120) for determining activity coefficients at infinite dilution developed by Cruickshank[1] and Everett[2] is restricted to volatile solutes (eg. n-pentane, n-hexane and n-heptane) and involatile solvents (eg. dotricontane,squalane, and dinonylphthlate).

3.3.6.1. Review of Work Using Volatile Stationary Phases

Some workers (employing the G.L.C method) have taken the volatility of the solvent into account by using a presaturator.[42] Evaporation off the column by the stationary phase is avoided by pre-saturating the carrier gas with vapour of the volatile phase before it enters the column. The presaturator involved bubbling the carrier gas through the liquid or passing the carrier gas through a short precolumn which, like the main column, contained a stationary phase coated on a solid support. This technique was introduced by Kwantes and Rijnders.[50] However, even though the carrier gas is saturated with vapour it still removes the stationary phase as it expands along the column. Since a smaller pressure drop led to less evaporation of the stationary phase, a coarse packing was used which reduced the pressure drop considerably. While the use of a precolumn and coarse packing kept the bleed rate very low, the loss cannot be eliminated completely.

Another method was introduced by Kurkchi and Iogansen[51]. They proposed weighing the column before and after use, assuming that the solvent loss was constant with time. This then gave them the amount of solvent lost during the course of the experiment.

Langer et al[52] monitored the loss of solvent by measuring the retention time of a solute at intervals, taking the first reading as soon as the column reached its operating temperature. A graph of retention time against elapsed time of operation was plotted. The graph was then extrapolated to zero time and the correct retention time obtained. Letcher[53] successfully used this method for the determination of the activity of various hydrocarbons with decahydronaphthalene as the volatile stationary phase.

Yet another method employed successfully by Letcher, was the use of an "internal standard". This method uses a solute of known activity coefficient. Throughtout the experiment, the solute is injected and its γ_{13}^{∞} monitored with the loss

of solvent of the column. The change of the γ_{13}^{∞} value with time, gives an indication of the rate of solvent loss of the column. An extension of this work is to measure, at the same flowrate, the retention times of a solute of known γ_{13}^{∞} (a standard) and a solute of an unknown γ_{13}^{∞}. Using equations 3.3 and 3.4 the following ratio can be established:

$$\frac{t_{R\,(standard)}}{t_R} = \frac{\gamma_{13}^{\infty} P_1^*}{\gamma_{13\,(standard)}^{\infty} P_{1\,(standard}^*} \qquad (3.122)$$

Therefore γ_{13}^{∞} can be simply an quickly calculated from the retention times of the two solutes only.

3.3.6.2. A Novel Method for taking Volatile Solvents into Account

In the present work, Everett's[2] and Cruickshank's[1] method (for solvents of low volatility) has been extended to accommodate a solvent of low volatility by assuming equilibrium along the entire column, and taking into account the vapour pressure of the solute P_3'. During its passage through the column the carrier gas becomes charged with solvent vapour. The total amount of solvent lost from the column, n_3', may be expressed in terms of the total volume of gas which has passed through the column, the partial pressure, P_3', of the solvent in the gas at the column outlet and the time t elapsed from the start of the carrier gas passing through the column. The corrected gas flow rate, U_O, measured at the outlet is maintained constant during the whole experiment. The expression for n_3' is given by

$$n_3' = \frac{U_O t P_3'}{RT} \qquad (3.123)$$

In this work the partial pressure of the solvent in the carrier gas was very much less than 1 per cent of the total gas pressure. It is probably further reduced in the flowmeter. Therefore no correction was applied to the flowrate for the presence of the solvent. Equation 3.120 becomes

$$\ln V_N = \ln \left[\frac{n_3 RT - P_3' U_O t}{\gamma_{13}^{\infty} P_1^*}\right] + C \qquad (3.124)$$

where

$$C = -\left[\frac{B_{11} - V_1^*}{RT}\right] P_1^* + \left[\frac{2B_{12} - V_1^{\infty}}{RT}\right] P_O J_2^3 \qquad (3.125)$$

Hence

$$\frac{V_N}{e^C n_3} = \frac{RT}{\gamma_{13}^{\infty} P_1^*} - \left[\frac{U_O t}{n_3}\right] \frac{P_3'}{\gamma_{13}^{\infty} P_1^*} = a + b \left[\frac{U_O t}{n_3}\right] \qquad (3.126)$$

By plotting $V_N/n_3 e^C$ against $U_O t/n_3$ a straight line should be obtained, giving an intercept of $RT/\gamma_{13}^{\infty} P_1^*$ (a) and a slope of P_3'/RT (b). The values of γ_{13}^{∞} and P_3' are obtained graphically from this linear relationship.

CHAPTER 4

APPARATUS AND EXPERIMENTAL PROCEDURE FOR THE DETERMINATION OF γ_{13}^{∞} BY GAS LIQUID CHROMATOGRAPHY

The gas-liquid chromatograph used for the determination of the activity coefficients at infinite dilutions was similar to that used by Cruickshank[1] and also by Marsicano[54] (where V_N was determined as a function of P_1^* and hence B_{12} was obtained together with γ_{13}^{∞} (see equation 3.130). The chromatograph used in this work, was identical to that used by Letcher[53]. The mixed virial coefficients, B_{12}, were calculated (using equation 4.1) from McGlashan and Potter's equation[55] and Hudson and McCoubrey's combining rules[56,57] following Letcher et al.,[58] and γ_{13}^{∞} was determined from retention times.

4.1 The Design of the Gas-Liquid Chromatograph

The basic plan of the gas chromatograph is shown in figure 4.1. This type of chromatograph is suitable for physico-chemical measurements. The scheme is similar to that of a commercial analytical chromatograph except for the addition of a manometer to register the column inlet pressure, an accurate flowmeter to measure the flowrate (0.01 s) and an accurate temperature controller to regulate the temperature of the column ($\pm$ 0.01 K). Two types of thermal conductivity detectors (T.C.D) were used in this work, differing only in the make and design of the detector. The advantage of using a thermal conductivity detector or a katharometer is that the flow-meter can be placed downstream of the column exit. The flow and pressure control unit was constructed mainly of 6.35 mm o.d. (1/4 inch) copper tubing and Swagelock couplings. The flow-meter and manometer were constructed of thick-walled glass tubing.

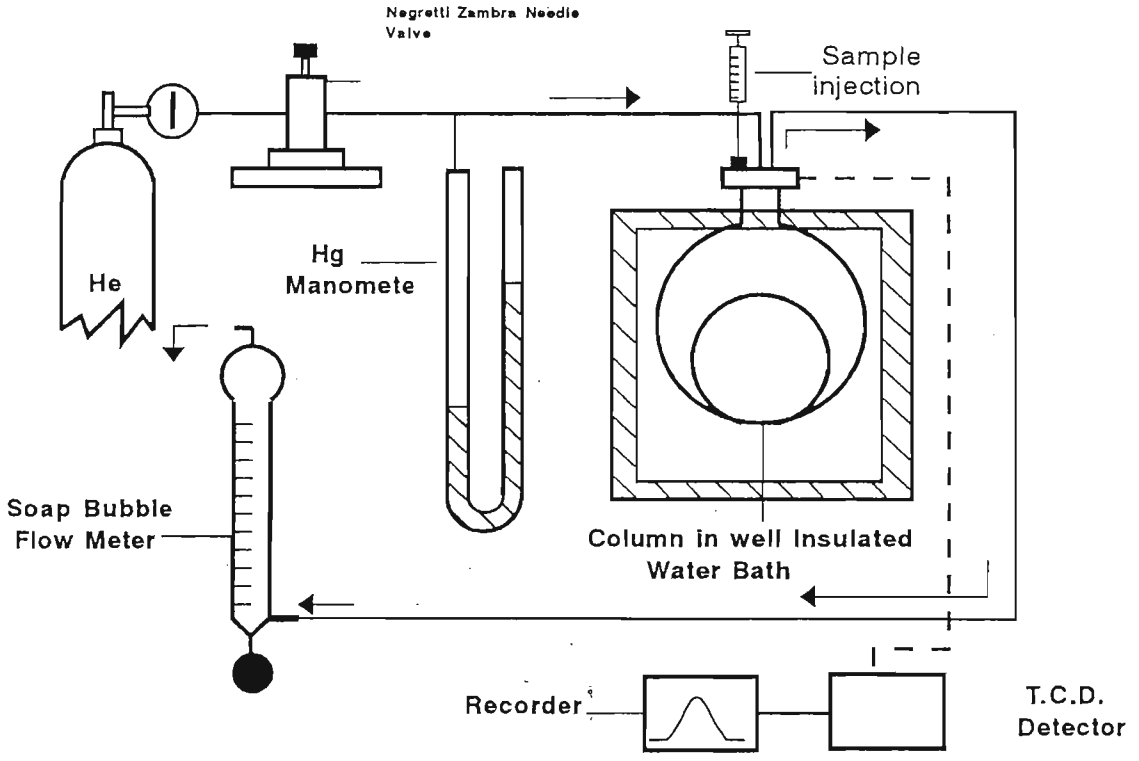

FIGURE 4.1. FLOW DIAGRAM OF G.L.C.

4.1.1. Flow Control

Good flow control was achieved by using a two-stage pressure regulator, attached to a pressure cylinder, in conjunction with a Negretti and Zambra precision pressure regulating valve which controlled the pressure to better than 0.1 torr.[1] The column outlet in the experiment was connected to the flow-meter which was open to the atmosphere. It not was necessary to monitor the outlet pressure since variations in atmospheric pressure would have small effects on the flow-rate only if the column impedance was unusually high.[43] A buffer vessel was placed at the column outlet to minimise the effect of pressure changes due to slight disturbances in the laboratory atmosphere.

4.1.2. Pressure Measurement

The outlet pressure was considered to be atmospheric and was measured on a normal Fortin barometer. The column inlet pressure was measured with a mercury manometer using a kathetometer capable of measuring to within $\pm$ 0.01 mm Hg. A trap was attached to one end of the manometer to retain mercury in case of an accidental pressure surge.

4.1.3. Flow Rate Measurements

The measurement of the gas flow-rate was carried out with a soap bubble meter (figure 4.2), constructed from a graduated 100 ml burette, which was situated downstream of the column. Since helium was used as the carrier gas, it was necessary to ensure that air did not enter the burette during flow measurements since light gases, such as helium, diffuse more rapidly through soap films than air which would cause the actual flow-rate to be different from the rate of film movement. To prevent back diffusion of air a rubber bung with a tiny hole was placed at the flowmeter outlet. The hole was large enough not to cause a significant pressure rise in the flow tubes.

---

[1] 1 torr = 1 mmHg

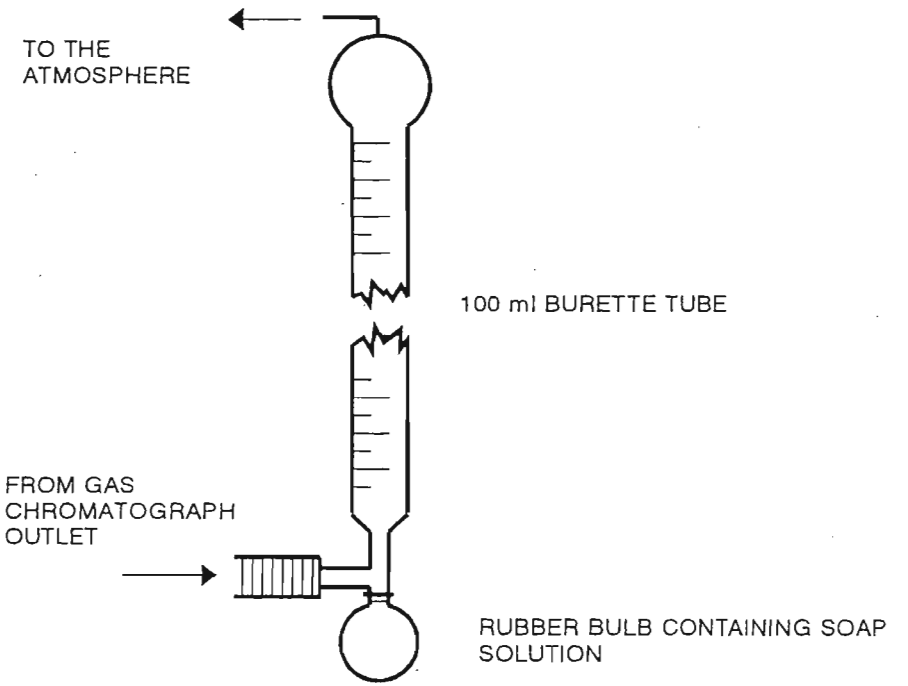

FIGURE 4.2. THE SOAP BUBBLE FLOW METER

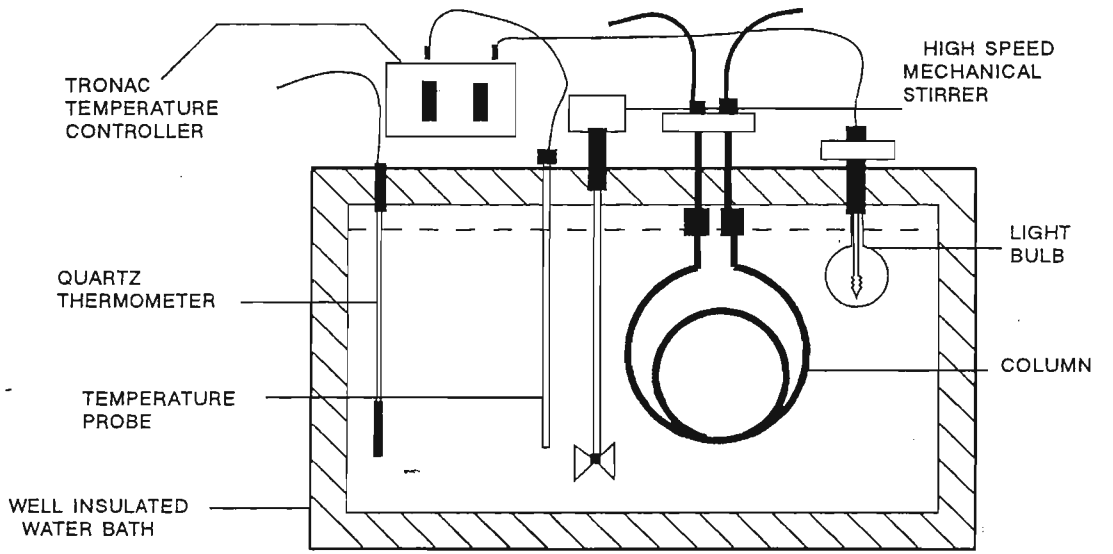

FIGURE 4.3. WATER BATH FOR TEMPERATURE CONTROL AT 298.15 K

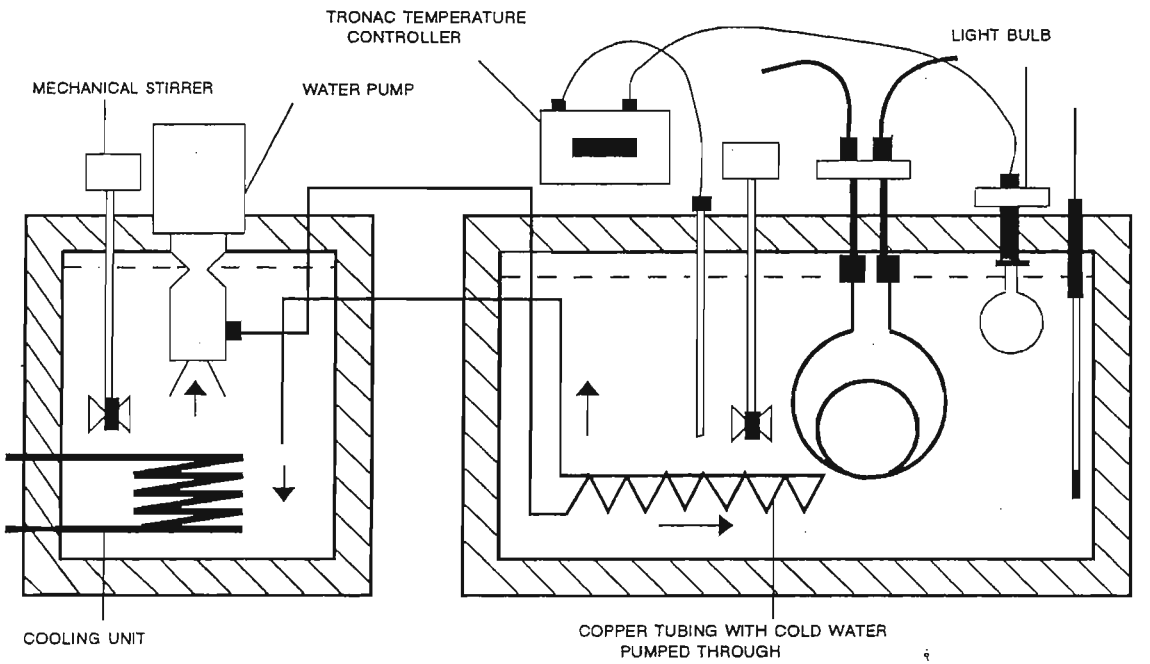

FIGURE 4.4. TWO WATER BATH SYSTEM FOR TEMPERATURE CONTOL AT 283.15 K

4.1.4. Column Temperature Control

Good temperature control was essential since the vapour pressure (of the solute and the solvent) is temperature dependent. This was achieved by immersing the column in a well-stirred water bath. The temperature at 298.15 K (using a single waterbath) was controlled by a Tronac temperature controller in conjunction with a light bulb as the low thermal capacity heater (figure 4.3).

The temperature was measured using an accurate quartz thermometer. The bath temperature was always known to an accuracy of better than 0.01 K. For the control of the temperature at 283.15 K two water baths were used (figure 4.4). The temperature of one bath (not used for accurate temperature control) was kept at approximately 280 K using a large cooling unit and an immersion heater. The bath was kept well stirred using two high speed mechanical stirrers. The temperature in the second bath (containing the column) was maintained at 283.15 K by pumping water from the first bath through a 6 m coil of copper tubing placed on the floor of the second bath. As with temperature control at 298.15 K the temperature in the second bath was controlled by a Tronac temperature controller and a light bulb as the heater element. The temperature was monitored using a quartz thermometer calibrated using a platinum resistance thermometer (SA Bureau of Standards). (See Appendix 1)

4.1.5 Sample Injection and the Injection System

The solutes used were usually of the purest grade available although this was not necessary since the nature of the chromatographic column separates impurities from the solute being studied, thereby not affecting the retention times of the solutes. Samples were injected using a microsyringe and sample sizes varied from 0.1 μl to 1.0 μl. The injection system for both the Gow-Mac and Shandon detectors was the same and was specially designed to minimise back diffusion, gas hold up, multiple septum perforation and damage to the syringe. It consisted of an inner tube located concentrically inside an outer tube (figure 4.5). Carrier gas entering at the one end of

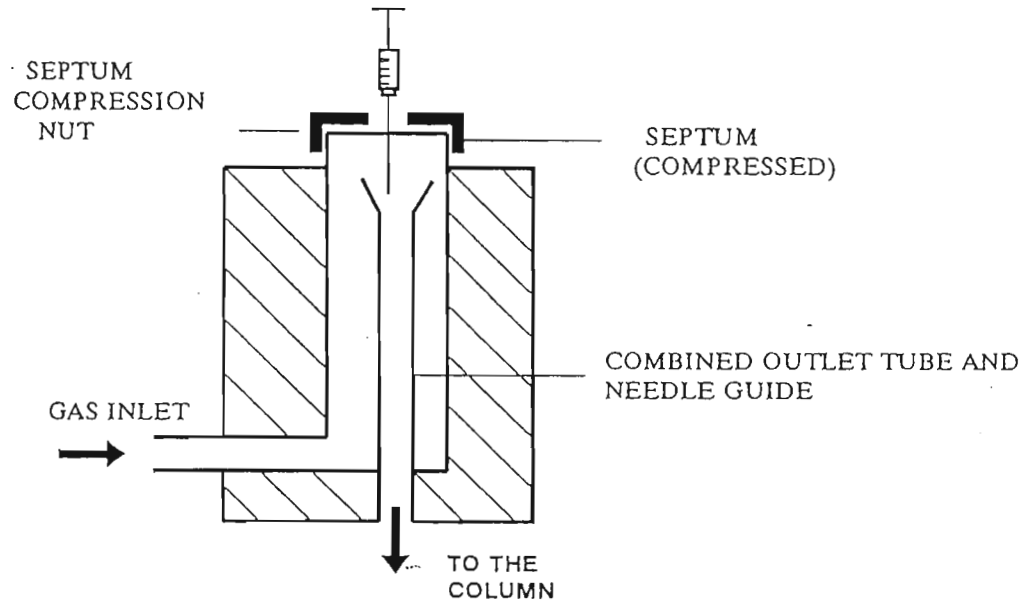

FIGURE 4.5. THE INJECTION SYSTEM

the annulus between the tubes is deflected into the inner tube by the septum at the other end. The entry of the gas at the one end of the narrow annulus in conjunction with the high velocity purge of the gas through it, ensured that there was no upswept carrier gas, back diffusion of the sample, or the retention of the solute on the underside of the septum. The diaphragm injection system was mounted in a tapered bore. It was retained under compression by a funnel shaped needle guide, which was screwed down on its upper surface. This needle guide ensures that the needle penetration was always at the same spot in the septum.

4.1.6. G.L.C. Columns

The packed columns used were made from stainless steel which was inert to the solutes used. The stainless steel columns were also assumed to be inert to solute adsorption. The columns were all 6.35 mm o.d. (1/4 inch) and 1 to 1.5m in length.

4.1.7. Detectors

Two types of thermal conductivity detectors were used, a Shandon U.K.3 detector and a Gow-Mac 40-200 detector.

The Shandon U.K.3 Detector.- A circuit diagram of the detector system is shown in figure 4.6. The detector consists of two matched, electrically heated, helically coiled, tungsten filaments. These are mounted in the brass detector body by means of mechanical seal tube-nuts. In this way the two filaments are inserted directly into the gas stream, one (reference) in the pure carrier gas before it enters the column, and the other (measuring) in the column effluent. The geometrical configuration of each filament was identical. The filament forms two arms of an electrical Wheatstone bridge circuit. This bridge resistance is unbalanced by a change in the temperature of the filament in the effluent, which is caused by a change in the composition of the gas stream as a component is eluted. The signals were recorded on a Phillips recorder.

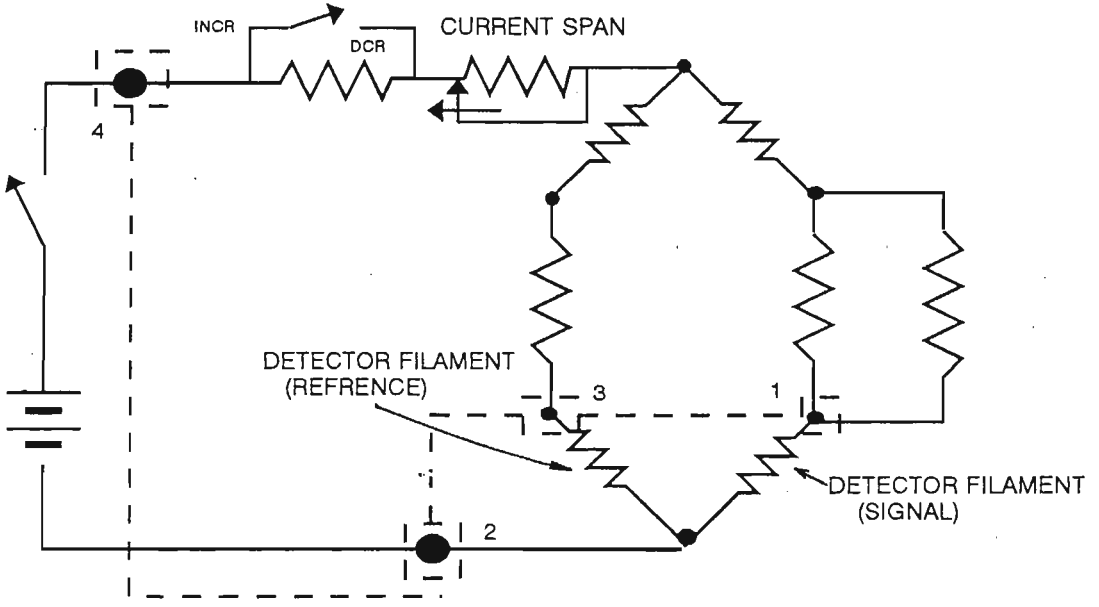

FIGURE 4.6. CIRCUIT DIAGRAM OF THE SHANNDON UK3 T.C.D. DETECTOR

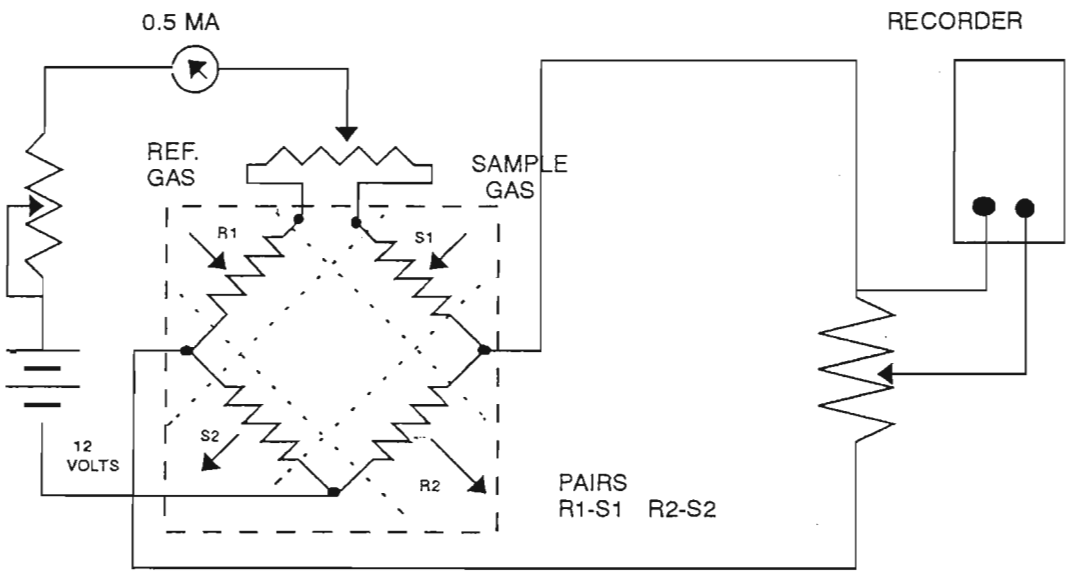

FIGURE 4.7. CIRCUIT DIAGRAM OF GOW-MAC T.C.D. DETECTOR

The Gow-Mac 40-200 Detector.- A circuit diagram of the four filament Gow-Mac detector cell is shown in figure 4.7. In this detector four tungsten filaments lie in the gas path. It is a semi-diffusion cell of a flow-through design with a response time less than 1.0 second. The stream of pure gas is split so that half of the pure gas enters the reference chamber and passes over the two reference filaments and the other half of the gas enters the column. The gas emerging from the column flows over the measuring filaments. The filaments used are of the same design as those used in the Shandon detector.

4.2. Experimental Procedure

4.2.1. Preparation of the Stationary Phase

The stationary phase was prepared following the procedure used by Marsicano.[54] The columns were cleaned with hot soap solution followed by acetone, rinsed with distilled water, and dried with nitrogen. Celite was used as the solid support for the stationary phase. The column loading (mass solute/total mass coated solid support) ranged between 3 to 15 mass per cent. The packing was prepared by adding a known mass of solvent to a known mass of celite. The combined mass was noted. A solvent in which the stationary phase is soluble (diethyl ether) was added (approx. 50 ml) and the contents were swirled gently in order to dissolve the stationary phase and distribute it throughout the celite. The ether was slowly removed by the application of a vacuum using a Buchi rotary evaporator without heating. The flask was rotated slowly to minimise disintegration of the fragile celite. The last trace of ether was removed by allowing the flask to stand in a fume hood. The coated celite was weighed and reweighed on completion to check that all the ether had been removed and that no stationary phase had been lost. An uncoiled stainless steel column was packed using a plastic funnel and rubber tubing of known mass. The funnel was attached to the column by the tubing and the coated celite was poured into the funnel. The other end of the column was plugged with glass wool. A rubber stopper was attached to this end which was lightly tapped on the floor during packing. The column

was also lightly tapped with a rubber-covered metal rod. On completion the funnel and tubing were weighed and the amount of stationary phase added was determined by difference. The column was plugged with glass wool at the open end and coiled. We believe that the small amount of compression produced on coiling does not significantly change the properties of the packing, nor its adsorptive properties.

4.2.2. Measurement Procedure

4.2.2.1. Treatment of a Volatile Solvent (n-Dodecane)

Measurements of the flow-rate (which was kept constant), retention times of solute and unretained gas (nitrogen), and temperature were made for each column. The flowrate was set, depending on the length of the column and the amount of solvent on the column, so that the column would have a life of about 3-4 hours. The system was allowed to equilibrate for about 10-15 min before the first injection was made. When several solutes are studied on a single column, the solutes are injected simultaneously as a mixture. Solutes chosen for such measurements must have significantly different retention times to allow each component to be fully resolved at the detector. Incorporation of air to determine the gas holdup was accomplished by first taking up the desired volume of solute into the syringe and withdrawing the plunger further to admit a suitable volume of air before making an injection.

Retention times were calculated from distance measurements on the chart from the point of injection to the point at which the tangents to the peak intersect (figure 4.8). These are then converted to retention times using the chart speed which was accurately measured using a stopwatch.

The carrier gas flow-rate was measured regularly throughout each run using an accurate stopwatch. Prior to measuring the flow-rate a stream of bubbles was sent through the flowmeter to allow the interior walls of the burette to be thoroughly wetted by the soap solution to avoid errors arising from uneven movement of the

bubble film due to surface tension effects and the possibility that the burette was not fully saturated with water vapour.

4.2.2.2. Treatment of a Polar Solvent (n-Sulfolane)

In the case of a polar solute (Sulfolane) no modification of the data treatment procedure is required. Measurements of the flow-rate (which was varied), retention times of solute and unretained gas (nitrogen), and temperature were made for each column. The flowrate was changed throughout the experiment. The system was allowed to equilibrate for about 10-15 min after changing the flowrate to allow equilibrium to be established. As with n-dodecane, when several solutes are studied on a single column, the solutes are injected simultaneously as a mixture. Solutes chosen for such measurements must have significantly different retention times to allow each component to be fully resolved at the detector. The determination of the gas hold up, (using nitrogen),was conducted in the same manner as was done in the case of a volatile solvent. Measurement of retention times was done using the tangent method as explained earlier.

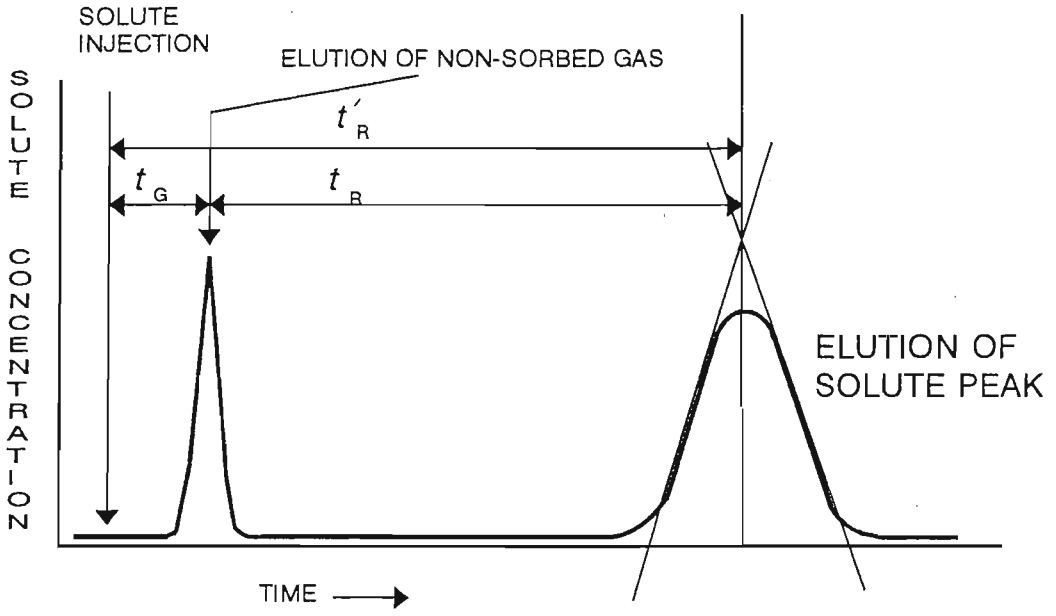

FIGURE 4.8. A Typical Chromatogram Showing the Determination of the Retention Time of a Solute Using the Tangents to The Peak Method

4.3. The Determination of γ_{13}^{∞} of Solutes in a Moderately Volatile Solvent (n-Dodecane)

The method used is described in chapter 3, section 3.3.6 5. The systems involving moderately volatile solvents, is used to determine γ_{13}^{∞} for the investigated in this work were: n-pentane, n-hexane, n-heptane, cyclopentane, cyclohexane, and benzene in the solvent n-dodecane, at the temperatures 280.15 K and 298.15 K.

The flow rate of the helium was maintained constant for each set of measurements on a particular column. Each column was used for a time (t) which ranged from 3 to 4 hours. The helium flow rate ranged from 1.2×10^{-6} $m^3 \cdot s^{-1}$ to 2.8×10^{-6} $m^3 \cdot s^{-1}$ and was measured using a calibrated bubble meter and the results were corrected for water vapour pressure. The injection volume used was about 0.1 mm^3. The column temperature was controlled to within 0.01 K.

The solvent, dodecane, was supplied by BDH. The suppliers quoted a mole-fraction purity of 0.99. The solvent was used without further purification at a column loading of (3 to 10) mass per cent. The solutes used were n-pentane, n-hexane, n-heptane, cyclopentane, cyclohexane, and benzene, and were supplied by Aldrich. It was not necessary to purify the solutes further as the chromatographic column separated impurities from the major solute component.

Results were collected from seven columns loaded with dodecane. The gas holdup volume was determined by injecting nitrogen into the carrier gas. Table 4.1 summarizes all the operating conditions.

The mixed virial coefficients, B_{12}, were calculated (using equation 4.1) from McGlashan and Potter's equation[55] and Hudson and McCoubrey's combining rules[56,57] following Letcher *et al.*,[58] using $n_1 = 5$ (pentane and cyclopentane), $n_1 = 6$ (hexane, cyclohexane, and benzene), $n_1 = 7$ (heptane) and $n_2 = 1$ (helium).

$$B_{12}/V_{C,12} = 0.43 - 0.886(T_{C,12}/T) - 0.694(T_{C,12}/T)^2 - 0.0375(n_{12} - 1)(T_{C,12}/T)^{4.5} \quad (4.1)$$

where

$$T_{C,12} = 128\cdot(T_{C,11}T_{C,22})^{1/2}\cdot(I_{C,11}I_{C,22})^{1/2}\cdot V_{C,11}\cdot V_{C,22}/I_{C,12} \quad (4.2)$$

$$V_{C,12} = (V_{C,11}^{1/3} + V_{C,22}^{1/3})^3/8 \quad (4.3)$$

$$I_{C,12} = (I_{11} + I_{22})\cdot(V_{C,11}^{1/3} + V_{C,22}^{1/3})^6 \quad (4.4)$$

and

$$n_{12} = (n_1 + n_2)/2 \quad (4.5)$$

The second virial coefficients for the pure compounds were calculated from Deiters equation of state, following Baonza et al.[59] The vapour pressures for the solutes were obtained from the literature.[60] The molar volumes were determined from density values, which were obtained from the literature.[61] The values of the properties used in the calculation of γ_{13}^{∞} are given in Table 4.2.

4.3.1. Calculation of γ_{13}^{∞}

The calculation γ_{13}^{∞} for a volatile solvent is explained in Chapter 3 (3.3.6). From the experimental readings, values of V_N were calculated using the programme GAMMA (see Appendix 2) which uses the following equations,

$$V_N = J_3^2\, U_0\, (t_R - t_G) \quad (3.4)$$

and

$$\frac{V_N}{n_3 e^C} = \frac{RT}{\gamma_{13}^{\infty} P_1^*} - \frac{U_O t}{n_3}\left[\frac{P_3'}{\gamma_{13}^{\infty} P_1^*}\right] \qquad (3.126)$$

The linear equation (3.126) is fitted to each set of results (usually involving about 15 injections for each solute, collected from each of the seven columns as done previously[62,63]) using a method of least squares analysis. From the intercept of that line $RT/\gamma_{13}^{\infty}P_1^*$ was obtained and the activity coefficient at infinite dilution (γ_{13}^{∞}) was calculated. From the ratio of the slope to the intercept the quantity (RT/P_3') was obtained and consequently, P_3', the partial pressure of the solvent at the temperature of the experiment was calculated. All the plots were linear.

4.3.2. Discussion

Activity coefficients at infinite dilution have been reported for the volatile hydrocarbon solutes, n-pentane [$CH_3(CH_2)_3CH_3$], n-hexane [$CH_3(CH_2)_4CH_3$], n-heptane [$CH_3(CH_2)_5CH_3$], cyclopentane [c-C_5H_{10}], cyclohexane [c-C_6H_{12}] and benzene [c-C_6H_6] in involatile alkane solvents n-pentadecane [$CH_3(CH_2)_{13}CH_3$] to n-hexatricontane [$CH_3(CH_2)_{34}CH_3$],[64-68] as well as in the volatile alkane solvents n-octane [$CH_3(CH_2)_6CH_3$] and n-decane [$CH_3(CH_2)_8CH_3$].[67] All these values have been determined using the G.L.C. method. Where γ_{13}^{∞} values at 298.15 K were not available, the literature data at other temperatures were extrapolated to 298.15 K. Finite concentration activity coefficients have been determined for many of the above solutes in volatile alkane solvents n-pentane [$CH_3(CH_2)_3CH_3$] to n-octane [$CH_3(CH_2)_6CH_3$],[63-68] but very few measurements have been made on mixtures of the above solutes and the alkanes ranging from n-nonane [$CH_3(CH_2)_7CH_3$] to $CH_3(CH_2)_{12}CH_3$. Of the systems presented in this work, the only finite concentration

activity coefficient results found in the literature was for [x{$CH_3(CH_2)_4CH_3$ or c-C_6H_{12} or c-C_6H_6} + (1-x) $CH_3(CH_2)_{10}CH_3$].[79-84] We have used these data to predict activity coefficients at infinite dilution and have compared the predicted values with the experimentally determined values reported here.

In order to put the new experimental results reported here in context with the results obtained from the literature, all the results have been graphed in figures 4.9 and 4.10.

The results obtained in reference (67) by Kwantes and Rjinders did not take into account the solute vapour and solute + carrier gas imperfections. Furthermore in order to prevent loss of the stationary liquid during the experiment Kwantes and Rjinders presaturated the carrier gas with the solvent before introducing the gas into the g.l.c. column. To reduce loss of solvent to a minimum a coarse-graded support was used. Our experience with presaturated columns has not been very successful.

The activity coefficients at infinite dilution for the solutes in the solvents $CH_3(CH_2)_3CH_3$ to $CH_3(CH_2)_6CH_3$ was calculated from finite concentration data,[79-84] by the use of the Guggenheim-Miller-Flory-Huggins (G-M-F-H) equation,[57,58]

$$\ln \gamma_{13} = \ln (1-\phi_1)/x_3 + (1-1/r)\phi_1 + \chi\phi_1^2 \qquad (4.7)$$

which becomes at $x_1 = 0$,

$$\ln \gamma_{13}^{\infty} = \ln (1/r) + (1 - 1/r) + \chi \qquad (4.8)$$

The calculated values are given in Table 4.4. The G-M-F-H equation is also used to predict the activity coefficient at infinite dilution from finite concentration data obtained from the literature for the solutes n-hexane [$CH_3(CH_2)_4CH_3$][85], cyclohexane [c-C_6H_{12}][86] and benzene [c-C_6H_6][87] in the solvent n-dodecane [$CH_3(CH_2)_{10}CH_3$]. The calculated γ_{13}^{∞} are given in Table 4.3. The average standard deviations of γ_{13}^{∞} is $\pm$ 0.005 and an estimate of the accuracy is < 0.01. The quasi-lattice theory[73] has been used here to predict γ_{13}^{∞} for an alkane (1) + dodecane (3). The value of ω_{ab} used in this work, $\omega_{ab}/kT = 0.1733$, was obtained from the literature[57], where Cruickshank et al. used a mean value of ω_{ab} for a system of simple hydrocarbons in octadecane.

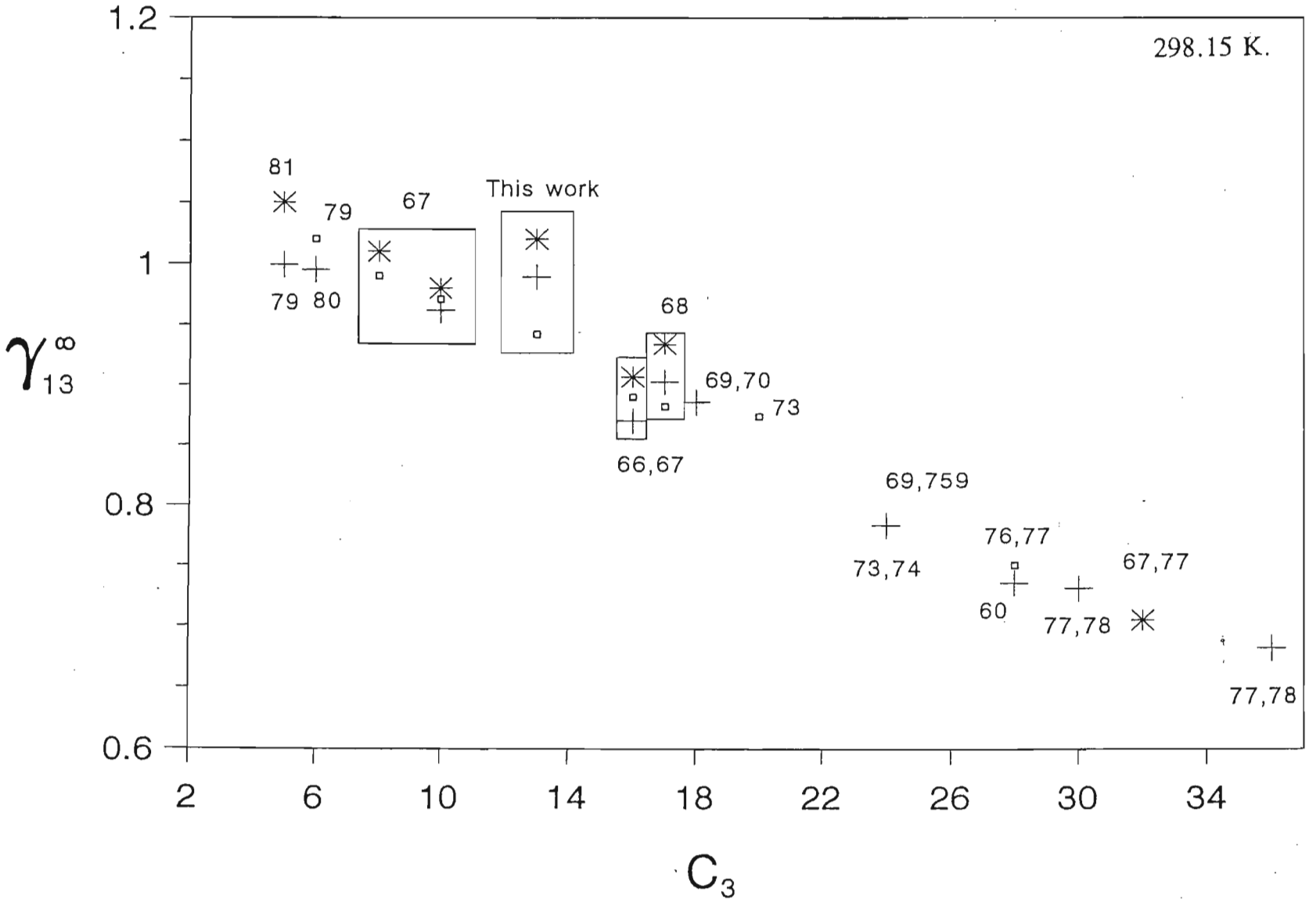

FIGURE 4.9. Diagram of Carbon Number of the Solvent (C_3) where, □ represents pentane, + represents hexane and * represents heptane

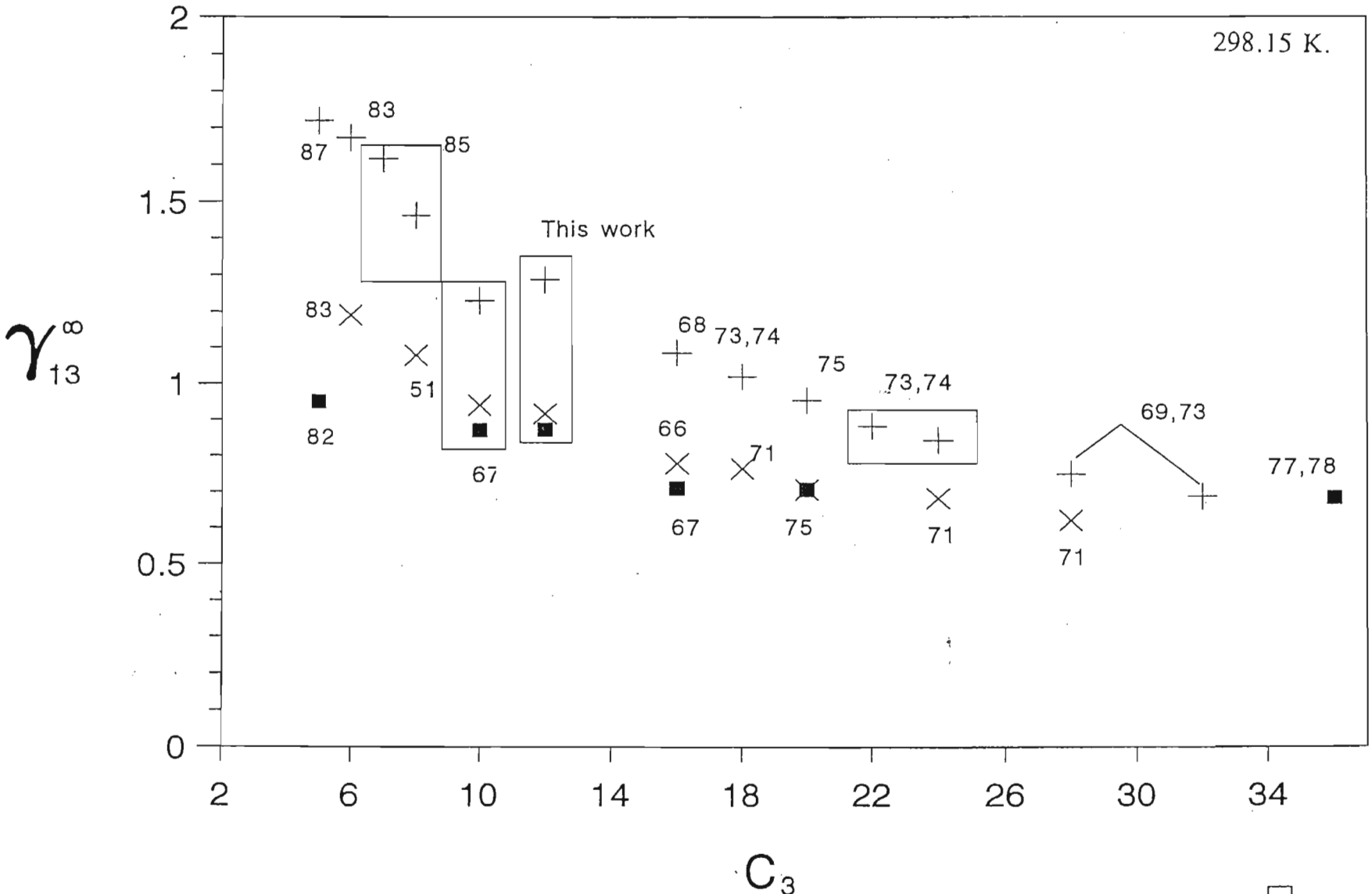

FIGURE 4.10. Diagram of Carbon Number of the Solvent (C_3) where, □ represents Cyclopentane, x represents Cyclohexane and + represents Benzene

The predictions are compared with our experimental results in Table 4.3.

The γ_{13}^{∞} values obtained from the literature and from this work can be summarized using a simple polynomial

$$\gamma_{13}^{\infty} = k + l \cdot C_3 + m \cdot C_3^2 \qquad (4.9)$$

where C_3 is the carbon number of the solvent. The coefficients of the polynomial b1, b2 and b3 are given in Table 4.5.

As discussed previously[62,63] (and in chapter 3, section 3.3.6), this method is capable of predicting the vapour pressure, p_3', of the solvent. Using the results from the slope of equation 3.125, the vapour pressures obtained here are, 4.2 $\pm$ 3.0 Pa, and 21.2 $\pm$ 4.1 Pa at 280.15 K, and 298.15 K respectively. The standard deviations are calculated from at least 18 measurements. The vapour pressure of dodecane at these temperatures have not been reported in the literature. Keistler and Winkel[88] have however measured the vapour pressure of dodecane in the range 90.1 K to 213.3 K. Extrapolation of their results, fitted to an Antoine equation, gives values for the saturated vapour pressure of 2.7 Pa and 15.5 Pa at the temperatures 280.15 K, and 298.15 K respectively.

4.4. The Determination of γ_{13}^{∞} of Solutes in a Polar Solvent (Sulfolane)

Sulfolane is a highly polar compound and has found extensive use in petroleum refining for the recovery by liquid extraction, of aromatic compounds, including benzene, from catalytic reformats.[14]

The activity coefficient at infinite dilution for a series of n-alkane solutes (C_5-C_7), cycloalkanes (C_5 and C_6), benzene, tetrahydrofuran, and tetrahydropyran have been measured in a polar solvent, tetrahydrothiophene-1,1-dioxane (sulfolane) at 303.15 K. The effect of the size of the injection volumes of the solute and the solvent loading on the column was investigated in order to ensure infinite dilution and non-

adsorption conditions respectively. The mixed second virial coefficients used in this work were calculated in the same manner as in section 4.3 The γ_{13}^{∞} results obtained here highlights the polar nature of sulfolane. Despite the obvious importance of the activity coefficients at finite concentrations or at infinite dilution for these mixtures, activity coefficients have been reported for only three of the mixtures reported here (hexane, cyclohexane and benzene). The reason for this could lie with the experimental difficulties in measuring the mixing properties of a volatile component at low concentrations in a viscous and involatile solvent. Furthermore most of the solutes discussed here do not dissolve in sulfolane over the whole composition range. However some of these properties are particularly well suited for the G.L.C. method we have chosen. All measurements were carried out at 303.15 K.

The solvent, tetrahydrothiophene-1,1-dioxane, was supplied by Janssen Chimica. The suppliers quoted a mole-fraction purity of 0.99. The solvent was used without further purification at a column loading of (4 to 25) mass percent. The solutes used were pentane, hexane, heptane, cyclopentane, cyclohexane, benzene, tetrahydrofuran, and tetrahydropyran and were supplied by Aldrich. It was not necessary to purify the solutes further as the chromatographic column separated impurities from the major solute component.

The flow rate of the helium was kept constant for each measurement on a particular column. About 15 to 20 minutes was allowed between each measurements to ensure equilibrium. The helium flow rate was measured using a calibrated bubble meter and the results were corrected for water vapour. The injection volume used was about between 0.1 to 1 mm^3. The column temperature was controlled in a well insulated water bath to within 0.01 K.

Data was collected for three columns loaded with sulfolane with helium used as the carrier gas. Table 4.6 gives the column preparation conditions. The retention time t_G was determined using nitrogen. To check the g.l.c. technique used, a test

system of hexane and hexadecane was run. The results compared well with the results in the literature[1]. To ensure that equilibrium conditions prevailed, the effect of varying flow rate on the calculated activity coefficient was monitored and found to be independent of flow rate. Also the symmetrical peaks obtained confirmed that equilibrium had been established. To ensure that infinite dilution conditions were satisfied, the injection volume was varied and the effect on the calculated γ_{13}^{∞} was monitored over a range of 0.1 mm^3 to 1.0 mm^3. The results showed that the injection volume did not influence the calculated γ_{13}^{∞}. No loss of solvent from the column was experienced, so there was no need to make allowances as was done in previous studies.[62,63]

Varying the solvent loading on the column from (4 to 25) mass percent, had no measurable effect on the calculated γ_{13}^{∞} and hence solute-solvent adsorption was considered to be negligible.

The critical data and ionization energies used in the calculation of B_{12} are given in table 2 using $n_1 = 4$ (tetrahydrofuran), $n_1 = 5$ (pentane, cyclopentane and tetrahydropyran), $n_1 = 6$ (hexane, cyclohexane, and benzene), $n_1 = 7$ (heptane) and $n_2 = 1$ (helium). The vapour pressures for the solutes were obtained from the literature.[60,61] These values as well as the calculated virial coefficients are all listed in table 4.7. Table 4.8 gives the operating conditions as well as the calculated γ_{13}^{∞}.

4.4.1. Calculation of γ_{13}^{∞}

No modification of the theory is required for a polar solvent. The retention time of both the solute and the unretained gas, along with the flow-rate and the inlet and outlet pressures is all the experimental data that is required to calculate γ_{13}^{∞}.

Using equation 3.121 γ_{13}^{∞} is calculated. The virial coefficients are calculated separately, along with the pure component vapour pressures.

$$\ln\gamma_{13}^{\infty} = \ln\frac{n_3 RT}{V_N P_1^*} - \left[\frac{(B_{11} - V_1^*)}{RT}\right] P_1^* + \left[\frac{(2B_{12} - V_1^{\infty})}{RT}\right] J_2^3 P_o \quad (3.121)$$

4.4.2. Discussion

The values of γ_{13}^{∞} obtained for pentane, hexane, heptane, cyclopentane, and cyclohexane in sulfolane range between 32 and 100. These high values can be attributed to the disparity in the chemical nature of the compounds. The γ_{13}^{∞} for benzene, tetrahydrofuran, and tetrahydropyran in sulfolane are very much closer to unity and reflect the compatibility in chemical nature between the solvent and the solutes.

Gajle *et al.*[90] measured γ_{13}^{∞} for hexane, cyclohexane and benzene, but did not take into account solute non-idealities. However the values obtained by Gajle *et al.*[90], 72.0, 33.8, 2.4, for hexane cyclohexane, and benzene respectively are reasonably similar to that obtained in this work namely 75.0, 34.2 and 2.16. Karvo[91] has measured G_m^E $\{x_1C_6H_6 + (1\text{-}x_1)C_4H_8O_2S\}$ at 303.15 K between the composition range 0.1 to 0.9 mole fraction. Using his results at finite concentrations and applying it to a modified NRTL equation[6] (see Chapter 9) for infinite dilution conditions:

$$\ln\gamma_{13}^{\infty} = \tau_{31}\cdot\exp(-2\alpha_{13}\tau_{31})/[\exp(-\alpha_{13}\tau_{31})]^2 + \tau_{13}\cdot\exp(-\alpha_{13}\tau_{13}), \qquad (4.10)$$

we obtained $\gamma_{13}^{\infty} = 2.4$ for benzene in sulfolane. This value was also obtained from a manual extrapolation of the finite concentration results given by Karvo[91]. The value is higher than our reported results of 2.16 ± 0.01.

TABLE 4.1. Summary of operating conditions for dodecane at the temperatures 280.15 K and 298.15 K for 7 different columns, U_0 is the flow rate[§], n_3 the amount of substance of dodecane initially on the column, m_3 the mass of dodecane and m_4 the mass of celite in each column

Column number	$10^6 \cdot U^0$ / $m^3 \cdot s^{-1}$	n_3 / mmol	$10^2 \cdot m_3$ / $m_3 + m_4$	Column number	$10^6 \cdot U_0$ / $m^3 \cdot s^{-1}$	n_3 / mmol	$10^2 \cdot m_3$ / m_3+m_4
	T = 298.15 K				T = 280.15 K		
1	1.564	1.969	5.13	4	1.292	2.139	4.88
2	2.724	3.727	8.28	5	1.234	1.949	4.43
3	2.698	3.700	9.31	6	1.994	1.949	3.74
				7	2.507	2.761	6.48

[§] The precision of the flow rate is estimated to be 0.003×10^{-6} $m^3 \cdot s^{-1}$

TABLE 4.2. The critical constants[60] (V_c and T_c), and ionization energies[61], I, used in the calculation of mixed second virial coefficients B_{12}, and the virial coefficients, B_{11}, together with the vapour pressures, p_1^*[60], and the molar volumes, V_1^* of the solutes

V_c	T_c	I	Temperature	p_1^*	V_1^*	B_{12}	$-B_{11}$
$cm^3 \cdot mol^{-1}$	K	$kJ \cdot mol^{-1}$	K	Pa	$cm^3 \cdot mol^{-1}$	$cm^3 \cdot mol^{-1}$	$cm^3 \cdot mol^{-1}$
				$CH_3(CH_2)_3CH_3$			
311.0	469.7	0.9937	298.15	68326	116.2	24	1120
			280.15	33312	113.1	24	1290
				$CH_3(CH_2)_4CH_3$			
370.0	507.3	0.9822	298.15	20166	131.7	29	1640
			280.15	8692	128.5	28	1900
				$CH_3(CH_2)_5CH_3$			
432.6	540.1	0.9533	298.15	6095	147.5	31	2250
			280.15	2309	144.3	31	2630
				$c\text{-}C_5H_{10}$			
262.2	511.6	1.0139	298.15	42324	94.7	18	1110
			280.15	19744	92.5	18	1300

TABLE 4.2 continued

V_c	T_c	I	Temperature	p_1^*	V_1^*	B_{12}	$-B_{11}$
$cm^3 \cdot mol^{-1}$	K	$kJ \cdot mol^{-1}$	K	Pa	$cm^3 \cdot mol^{-1}$	$cm^3 \cdot mol^{-1}$	$cm^3 \cdot mol^{-1}$
				$c\text{-}C_6H_{12}$			
308.3	553.4	0.9431	298.15	12813	108.8	21	1500
			280.15	5325	106.4	22	1740
				$c\text{-}C_6H_6$			
259.4	562.1	0.9242	298.15	12690	89.4	17	1370
			280.15	5177	87.4	18	1590

TABLE 4.3. Experimental values for γ_{13}^{∞} for a solute, C_xH_y in $CH_3(CH_2)_{10}CH_3$ at the temperature T. The estimated standard deviation σ for the experimental γ_{13}^{∞} determined in this work, is of the order 0.01. The results for the n-alkane solutes are compared with predictions by the quasi-lattice theory

Column number	T K	γ_{13}^{∞} Experimental	Predictions	Column number	T K	γ_{13}^{∞} Experimental	Predictions
	$CH_3(CH_2)_3CH_3$				$c\text{-}C_5H_{10}$		
1	298.15	0.942	0.949§	1	298.15	0.872	
2	298.15	0.940		2	298.15	0.875	
3	298.15	0.942		3	298.15	0.873	
4	280.15	0.970	0.967§	4	280.15	0.902	
5	280.15	0.971		5	280.15	0.901	
6	280.15	0.970		6	280.15	0.899	
	$CH_3(CH_2)_4CH_3$				$c\text{-}C_6H_{12}$		
1	298.15	0.989	0.972§	1	298.15	0.916	0.901*
2	298.15	0.989	1.013*	2	298.15	0.915	
3	298.15	0.987		3	298.15	0.915	
4	280.15	0.994	0.980§	5	280.15	0.922	
5	280.15	0.994		6	280.15	0.924	
6	280.15	0.996		7	280.15	0.925	
	$CH_3(CH_2)_5CH_3$				$c\text{-}C_6H_6$		
1	298.15	1.020	1.104§	1	298.15	1.287	1.275*
2	298.15	1.022		2	298.15	1.290	
3	298.15	1.023		3	298.15	1.288	
5	280.15	1.077	1.152§	5	280.15	1.332	
5	280.15	1.079		6	280.15	1.334	
6	280.15	1.079		7	280.15	1.334	

* Predicted by the (G-M-F-H) equation.

§ Predicted by the simple lattice theory

TABLE 4.4. Summary of the values of γ_{13}^{∞} obtained from this work and from the literature. C_3 represents the carbon number of the solute and $\delta\gamma_{13}^{\infty}$ is the difference between the experimental and calculated value of γ_{13}^{∞} by equation 4.7

Solute	γ_{13}^{∞}	C_3	$\delta\gamma_{13}^{\infty}\cdot 10^{-2}$	Literature
$CH_3(CH_2)_3CH_3$	0.992	6	-1.05	79
	0.990	8	0.73	67
	0.971	10	0.89	67
	0.890	16	0.14	66,67
	0.872	17	-0.53	68
	0,870	20	-1.15	73
	0.773	24	2.30	73,74
	0.750	28	0.92	73,74
$CH_3(CH_2)_4CH_3$	0.984	5	-2.11	79
	0.976	7	-0.29	80
	0.962	10	-0.39	67
	0.870	16	4.71	66
	0.903	17	-2.66	68
	0.886	18	1.78	69,70
	0.877	20	1.22	75
	0.804	22	2.62	70,71
	0.783	24	-2.38	69,75
	0.738	28	-2.16	75
	0.731	30	-0.35	77,78
	0.682	36	1.86	77,78
$CH_3(CH_2)_5CH_3$	1.050	5	-0.29	81
	0.980	10	-2.01	67
	0.907	16	-2.26	66
	0.934	17	1.69	68
	0.889	18	-1.54	69,72
	0.705	32	0.18	69,75
c-C_5H_{10}	0.950	5	-1.27	81
	0.750	10	2.11	67
	0.710	16	-4.57	66
	0.707	20	0.69	68
	0.583	36	0.15	69,72

TABLE 4.4 continued

Solute	γ_{13}^{∞}	C_3	$\delta\gamma_{13}^{\infty} \cdot 10^{-2}$	Literature
	1.190	6	3.08	82
	0.940	10	-0.44	67
	0.778	16	-1.04	66
$c\text{-}C_6H_{12}$	0.764	18	2.26	71
	0.706	20	0.25	75
	0.682	24	2.71	77
	0.621	28	-2.16	71
	1.720	5	-0.13	83
	1.673	6	2.16	84
	1.617	7	3.31	84
	1.585	8	6.60	84
	1.230	10	-1.16	67
C_6H_6	1.086	16	-0.37	68
	1.020	18	1.30	73,74
	0.954	20	1.94	73
	0.882	22	0.98	71,72
	0.843	24	2.23	71,72
	0.750	28	0.51	69,74
	0.687	32	-2.30	74,75

TABLE 4.5. Summary of the coefficients obtained (b1, b2, b3) from equation 4.9 and $\sigma\gamma^{\infty}_{13}$ which is the standard deviation calculated by a method of least squares.

Solute	b1	$b2 \cdot 10^{-2}$	$b3 \cdot 10^{-3}$	$\sigma\gamma^{\infty}_{13} \cdot 10^{-2}$
$CH_3(CH_2)_3CH_3$	1.057	-0.857	-0.979	1.596
$CH_3(CH_2)_4CH_3$	1.075	-1.094	-0.014	2.296
$CH_3(CH_2)_5CH_3$	1.100	-0.892	-1.008	2.329
c-C_5H_{10}	1.083	-2.565	0.325	3.470
c-C_6H_{12}	1.490	-6.201	1.333	2.601
C_6H_6	2.108	-8.368	1.249	5.407

TABLE 4.6. Summary of conditions for the preparation of the 3 columns, where n_3 is the amount of sulfolane in mmol, m_3 the mass of sulfolane, and m_4 is the mass of celite in each column

Column number	n_3 mmol	$10^2 \cdot m_3 / (m_3 + m_4)$	Column number	n_3 mmol	$10^2 \cdot m_3 / (m_3 + m_4)$
1	2.016	24.6	2	1.260	15.4
3	0.388	4.7			

TABLE 4.7. The critical constants[60] (V_c and T_c), and ionization energies[61], I, used in the calculation of mixed second virial coefficients B_{12}, and the virial coefficients, B_{11}, together with the vapour pressures, p_1^*[60], and the molar volumes, V_1^* of the solutes at 303.15 K

V_c / $cm^3 \cdot mol^{-1}$	T_c / K	I / $kJ \cdot mol^{-1}$	p_1^* / Pa	V_1^* / $cm^3 \cdot mol^{-1}$	B_{12} / $cm^3 \cdot mol^{-1}$	$-B_{11}$ / $cm^3 \cdot mol^{-1}$
				$CH_3(CH_2)_3CH_3$		
304.0	469.7	0.9937	46438	117.0	24	1120
				$CH_3(CH_2)_4CH_3$		
370.0	507.3	0.9822	12834	132.5	29	1810
				$CH_3(CH_2)_5CH_3$		
432.6	540.1	0.9533	3621	148.4	33	2760
				$c\text{-}C_5H_{10}$		
260.2	511.6	1.0139	28093	95.6	20	1210

TABLE 4.7 continued

V_c / $cm^3 \cdot mol^{-1}$	T_c / K	I / $kJ \cdot mol^{-1}$	p_i^* / Pa	V_i^* / $cm^3 \cdot mol^{-1}$	B_{12} / $cm^3 \cdot mol^{-1}$	$-B_{11}$ / $cm^3 \cdot mol^{-1}$
				c-C_6H_{12}		
308.3	553.4	0.9431	7998	109.5	24	1946
				c-C_6H_6		
259.4	562.1	0.9242	7843	89.9	20	1720
				c-$(CH_2)_5O$		
263.0	572.2	0.8733	43392	60.6	20	1660
				c-$(CH_2)_4O$		
224.0	540.2	0.8625	26736	51.2	17	1090
				He		
5.2	57.7	5.2487				

TABLE 4.8. Summary of operating conditions for sulfolane at the temperature 303.15 K for 3 different columns, where γ_{13}^{∞} is the activity coefficient at infinite dilution and U_0 is the flow rate

Column Number	$10^6 \cdot U_0$ $m^3 \cdot sec^{-1}$	γ_{13}^{∞}	Column Number	$10^6 \cdot U_0$ $m^3 \cdot sec^{-1}$	γ_{13}^{∞}
	$CH_3(CH_2)CH_3$			c-C_6H_{12}	
1	4.49	61.9	1	2.24	35.3
1	3.64	56.9	1	3.63	36.0
1	3.38	58.2	1	6.23	32.0
1	6.22	61.9	2	2.35	34.6
2	2.35	57.6	2	2.69	35.2
2	2.69	55.2	2	5.85	32.6
2	5.37	56.2	2	6.67	33.5
2	5.13	58.1			
2	5.93	57.5			
	c-C_5H_{10}			$CH_3(CH_2)_5CH_3$	
1	4.49	41.6	1	2.24	96.5
1	3.38	43.2	1	3.63	95.6
1	3.83	47.2	1	4.49	98.3
1	6.22	47.0	1	6.23	99.4
2	2.35	43.3	2	2.34	98.7
2	2.69	44.7	2	2.69	97.4
2	5.85	42.0	2	5.85	96.9
2	6.67	43.6	2	6.67	100.9
			2	5.89	98.5
	$CH_3(CH_2)_4CH_3$			c-C_6H_6	
1	4.49	73.0	2	7.46	2.16
1	2.24	77.8	2	5.36	2.16
1	3.38	72.3	2	1.39	2.16
1	6.22	72.7	2	1.23	2.15
2	2.35	74.4	2	1.14	2.16
2	2.69	75.9	3	2.48	2.16
2	5.37	76.2	3	1.47	2.16
2	5.13	75.0	3	0.81	2.15
2	5.89	77.5	3	1.17	2.16
			3	0.95	2.16

TABLE 4.8 continued

Column Number	$10^6 \cdot U_0$ $m^3 \cdot sec^{-1}$	γ_{13}^{∞}	Column Number	$10^6 \cdot U_0$ $m^3 \cdot sec^{-1}$	γ_{13}^{∞}
	c-$(CH_2)_4O$			c-$(CH_2)_5O$	
2	7.46	2.24	2	7.46	1.11
2	5.36	2.24	2	5.36	1.12
2	1.39	2.23	2	1.39	1.11
2	1.23	2.23	2	1.23	1.11
2	1.14	2.24	2	1.14	1.11
3	2.48	2.23	3	2.48	1.12
3	1.47	2.24	3	1.47	1.11
3	0.81	2.24	3	0.81	1.11
3	1.17	2.24	3	1.17	1.11
3	0.95	2.24	3	0.95	1.12

CHAPTER 5

EXCESS MOLAR VOLUMES OF MIXING

Excess functions are thermodynamic properties of solution which are in excess of an ideal (or ideally dilute) solution at the same conditions of temperature, pressure and composition. For an ideal solution all excess functions are zero. For example an excess molar function of mixing, X_m^E, for a binary mixture is given by[72]

$$X_m^E = X_{(actual\ solution\ at\ T,P,x)} - X^i_{(ideal\ solution\ at\ the\ same\ T,P,x)} \qquad (5.1)$$

where X is a thermodynamic property such as enthalpy, volumes or Gibbs energy. In this work the excess molar volumes, V_m^E of mixing for the following systems were measured: sulfolane + an unsaturated hydrocarbon (1-hexyne or 1-heptyne or 1-octyne) at 303.15 K.

5.1. Excess Molar Volumes of Mixing

The excess molar volume, V_m^E, of component 1, at a concentration x_1 is defined as[92]

$$V_m^E = V_{(mixture)}(T,P,x) - [x_1 V_1^O(T,P,) + x_3 V_3^O(T,P,] \qquad (5.2)$$

where V_1^O and V_3^O are the molar volumes of pure solute and solvent, respectively, and $x_1 + x_3 = 1$. The last term is the ideal molar volume of the mixture. The volume changes for the binary mixture can be determined experimentally in one of two ways, namely directly from density measurements (densitometer or pycnometric) or from a more direct dilatometric method, ie. by measuring the resultant volume change upon mixing of the two components. Both these methods have been extensively reviewed by

Battino[93], Letcher[94], Handa and Benson[95] and by Stokes and Marsh.[96-98]

5.1.1. Density Measurements

5.1.1.1. Pycnometric Measurements

Scatchard, *et al.*[99] were the first to describe the use of a pycnometer to obtain the density of binary mixtures. The pycnometer consists of a bulb with a capacity of about 10 cm^3, and arms with an internal diameter of 1 mm. During measurements, the bulb is filled using a hypodermic syringe. Potentially serious errors could arise due to inadequate mixing, evaporation and vapour space composition. However careful measurements with excellent accuracy and reproducibility have been reported using this method.[100]

5.1.1.2. The Mechanical Oscillator Densitometer

Remote or external measuring cells (as used in the densitometer) were developed to eliminate the inherent sources of error in the pycnometer technique and to achieve the highest possible accuracy and precision of the density[101]. The introduction of the remote cell offers a method for liquid measurements according to the oscillating sample tube method[102]. The density determination is based, in principle, on measuring the period of oscillation of a vibrating U-shaped sample tube which is either filled with sample or through which the sample is continuously flowing. The accuracy of the method is limited to some extent by four factors[103]: the calibration procedure, the viscosity of the sample, the pressure of the system and the temperature control. The density of the sample is related to the resonance frequency of an electronically excited mechanical oscillator and the period of oscillation of the sample contained in the oscillator[104]. The effective mass (M) of the oscillator is composed of its own unknown mass (M_o) as well as the unknown mass of the sample, and the density ρ contained in volume V, and is given by

$$M = M_o - V\rho \tag{5.3}$$

The resonance frequency is given by[93]

$$2\pi V = (c/M)^{\frac{1}{2}} = [\frac{c}{(M_o + V\rho)}]^{\frac{1}{2}} \tag{5.4}$$

where the mass M is attached to a spring of constant elasticity c, under the condition that the oscillator performs an undamped oscillation[95]. Rearranging and making ρ the subject of the formulae

$$\rho = -\frac{M_o}{V+(\frac{c}{4\pi^2 V})(\frac{1}{V^2})} = A + B\tau^2 \tag{5.5}$$

where τ = 1/V, ie. the period of oscillation, and A and B are constants characteristic of the oscillator.

Densities are measured relative to a reference material:

$$\rho - \rho_o = B(\tau^2 - \tau_o^2) \tag{5.6}$$

where ρ_o is the density of the reference material (usually the pure solvent, distilled water, or air) and τ_o is its corresponding period of oscillation.

5.1.2. Direct Dilatometric Measurements

Highly accurate measurements are obtainable by direct measurements using dilatometry.[95] The method eliminates the need for time consuming procedures such as filling and weighing the pycnometer, and reduces errors arising from weight,

composition and temperature determination of the sample.

There have been fundamentally two types of dilatometric apparatus designed for the direct measurement of volume changes[95]: batch dilatometry and continuous dilatometry.

5.1.2.1. Batch Dilatometry

One of the earliest designs for a single loading dilatometer was the apparatus by Keyes and Hildebrand[95]. It consisted of a U-tube with mercury filling the bottom of the vessel in order to separate the two sample components. Graduated capillaries on the two arms of the dilatometer provide the means by which volumes before and after were determined. The entire mixing vessel is immersed in a thermostatted bath and mixing was achieved by rocking the apparatus to and fro.

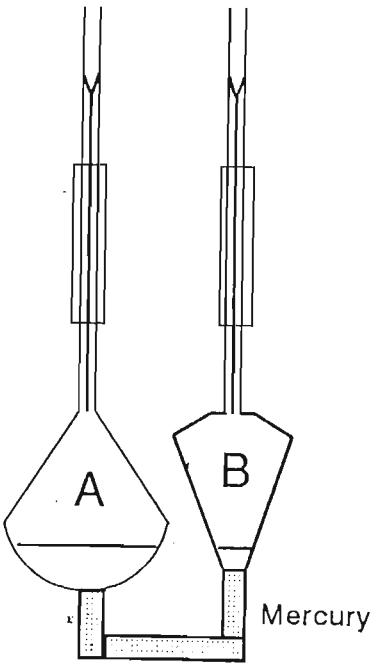

FIGURE 5.1. The Keyes and Hildebrand Dilatometer

5.1.2.2. Continuous Dilution Dilatometry

The fundamental disadvantage of batch dilatometry (ie. speed) was overcome by the introduction of the many composition per loading dilatometer, ie. continuous dilatometry. The original design of the dilution dilatometer was that of Geffcken, Kruis, and Solana[105] The dilatometer consists of a mixing chamber containing mercury, into which pure solvent is loaded. The solute is added to the solvent and the change in the mercury level is read directly from a calibrated and graduated burette. The entire apparatus is kept in a thermostatted vessel.

5.2. The Anton Paar DMA 601 Vibrating Tube Densitometer

5.2.1. Design of the System

In this work an Anton Paar DMA 601 Vibrating Tube Densitometer was used o determine the excess volumes. The laboratory arrangement for the densitometer is shown in figure 5.2. The measuring cell is contained in its own separate housing. The oscillator or sample tube is made out of borosilicate glass and is fused into a duel wall glass cylinder. The space between the U-shaped sample tube and the inner wall of the dual wall is filled with a gas of high thermal conductivity to facilitate a rapid temperature equilibrium of the sample inside the oscillator with a thermostat liquid which flows through the duel wall cylinder around the sample tube. An additional shorter capillary tube inside the inner space of the duel wall cylinder is for the accurate determination of the measuring cell temperature by means of a temperature sensor. In operation the sample tube is filled with $\pm$ 0.7 ml of sample, then electronically excited and density measurements are determined precisely by measurements of the period of oscillation of the sample tube.

From equation 5.5, the following relationship between the period, τ and the density ρ[106] exists:

$$\rho = A + B\tau^2 \tag{5.5}$$

where A and B are instrument constants that are determined through calibration measurements with substances of known density. The constants A and B contain the spring constants of the oscillator as well as the empty oscillator's mass and that volume of the sample involved in the oscillation. An unknown sample density, ρ_x, with a period value τ_x, can thus be calculated from equation 5.6 as,

$$\rho_x - \rho_{H_2O} = B(\tau_x^2 - \tau_{H_2O}^2) \tag{5.6}$$

where water is the calibrating substance.

A prerequisite for the measurement of densities to a high level of accuracy is good temperature control of the sample tube[106]. In the instrument used in this work the temperature was monitored using a thermistor inserted inside the inner space of the duel wall cylinder of the sample tube. The achievable accuracy in density depends on the achievable operating temperature. A good external thermostat with a temperature stability of ± 0.01 K can yield an uncertainty in the density measurement of approximately $\pm$ 6 x 10^{-6} g.cm^3. For this reason the stability was controlled to within 0.002 K in this work.

Errors may occur during the injection of the mixture into the sample cell. If the mixture is introduced too fast, tiny air bubbles may be generated, which results in an errorous τ value. Precaution was taken during sample introduction to ensure no trapment of air. In this work the pure solvents were degassed by boiling before the making up of the mixtures.

Uniform temperature control was achieved through the use of two variable speed mechanical stirrers. An auxiliary cooling system comprising a 50 litre water bath cooled by a Grants refrigeration coil, was incorporated to assist with the temperature control of the main water bath. Water from this auxiliary bath was pumped via a Haake immersion thermostat unit at a rate of 2.8 litre/min through a

four meter coiled copper tube placed inside the main water bath. The auxiliary bath was maintained at a temperature of approximately 1 K below the operating temperature of the main water bath. The thermostat liquid used for both the auxiliary and the main water bath was distilled water, treated with a commercially available corrosion algae inhibitor.

The thermostat system within the main water bath consisted of a permanent rheostatted immersion heater, delivering up to 4 W, and a 100 W light bulb connected to a Tronac temperature controller. Water from the main bath was pumped through the water jacket by a submersible pump. All rubber tubing to and from the densitometer was insulated to reduce heat loss. A Hewlett Packard 2801A quartz thermometer calibrated as discussed in APPENDIX 1, was employed to monitor the temperature within the main bath. A Paar digital thermometer, linked to a thermocouple was used to monitor the temperature of the cell.

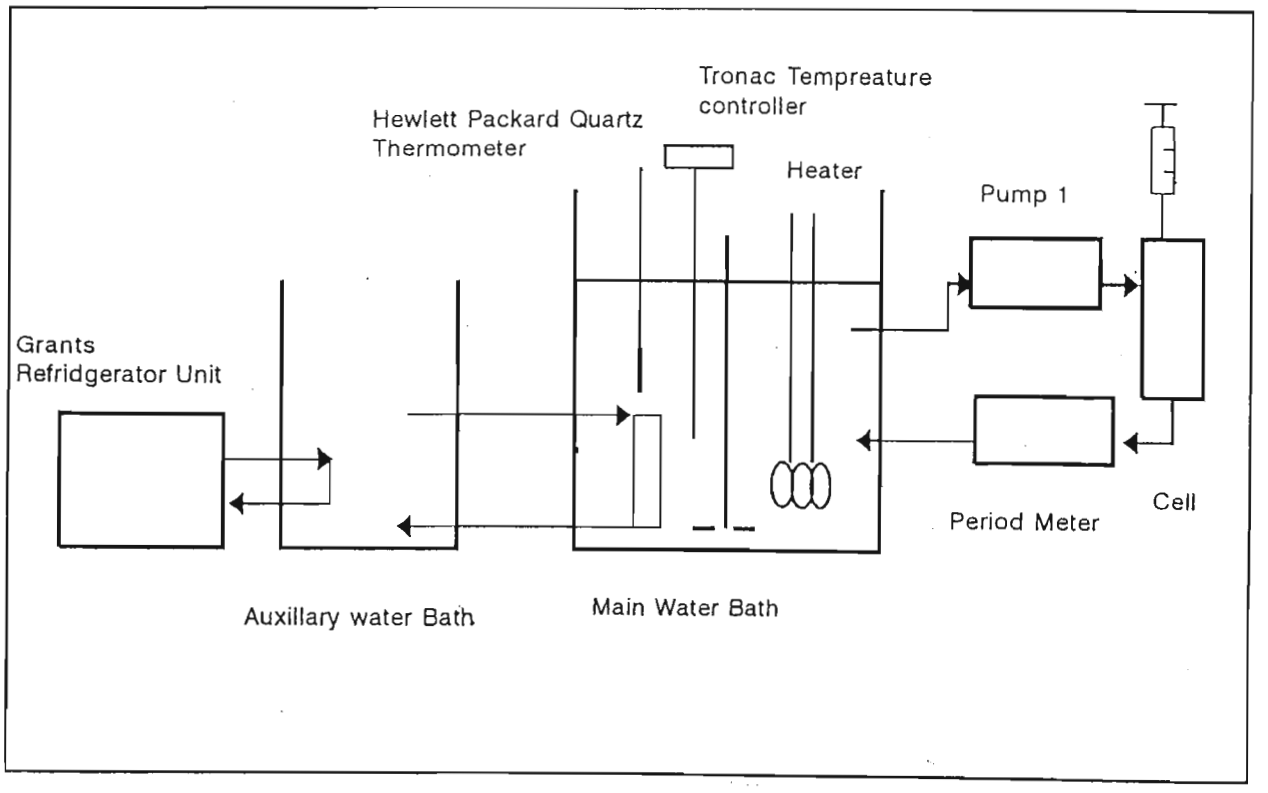

Figure 5.2 Laboratory arrangement for the glc apparatus

5.2.2. Operation Procedure

Prior to each experimental run, the cell was flushed thoroughly with warm methanol, and then acetone. After flushing, compressed air was blown through the cell. A constant period value, τ, for the sample tube filled with air was obtained before the sample is introduced. Double distilled pre-boiled water (used as the calibrated standard sample) was then introduced into the cell by means of a glass syringe, equipped with a teflon nozzle, ensuring a leak proof fit at the sample cell-syringe junction. The injection process was carried out slowly and carefully, enabling the liquid to properly wet the walls of the cell, and thus reducing the risk of trapping air bubbles in the U-tube. The sample was always filled past its nodal points and the syringe was left in place at the inlet point during each measurement. The outlet of the cell was sealed with a teflon plug to reduce evaporation. The solutions were introduced in to the sample cell in exactly the same manner as the distilled water.

With the cell illumination light off, the photoelectric portion of the excitation system was automatically activated. Each measuring cycle was allowed to continue until a constant period value was obtained. Period values for water (reference substance), pure solvents and air were determined between each solution injection. These valves were not only required for the density calculations, but also permitted a continuous check on both the purity of samples and the densitometer operation. The precision of τ, judged by repeated measurements for the same solution at different times, was estimated to be better than 2×10^{-6} Hz.

5.2.3. Preparation of Mixtures

The pure solvents were degassed before sample solutions were made up by immersing the sample into a sonic bath for 30 minutes. The mixtures were then made up in five cm^3 flasks with ground glass stoppers.Care was taken to first add the least volatile component into the flask, and that the completed mixture left a small vapour-

just large enough to aid mixing. The mixtures were made up shortly before injection into the densitometer, and were shaken vigorously to ensure complete mixing.

5.3. Results

The excess molar volumes of the following systems were measured at 303.15 K: sulfolane + 1-hexyne, or 1-heptyne or 1-octyne. The excess volumes were measured as part of an investigation into the thermodynamic mixing properties of the binary mixtures formed with sulfolane. Although the measurements of excess volumes is not a good indicator of the interactions involved in binary mixtures it can provide evidence of specific interactions. Various theories of solution, have been proposed to describe excess volumes of mixing ie., the Flory-Patterson Theory[107], the Extended Real Associated Solution Theory (ERAS)[108] and the Patterson-Treszczanowicz[109] theory. Due to the strong dipole-dipole interaction between sulfolane and the alkynes, the simple Flory Patterson[107] equation fails to describe the mixing curve. In the absence of any hydrogen bonding (as in the case of sulfolane and the alkynes) the theories of ERAS[108] and Patterson-Treszczanowicz[109] are also unable to describe the mixing curve accurately. In this work, all attempts at fitting theses theories to the V^E data have been excluded as the results were very poor.

The Redlich-Kister equation,[110] (equation 5.7) has been fitted to the excess volumes data. The results together with the Redlich-Kister parameters are given in Table 5.1.

$$V_m^E = (x_1 - 1)x_1 \Sigma_{i=1}^{n} A_i(1 - 2x_1)^{i-1} \qquad (5.7)$$

The partial molar excess volumes (V_1^E and V_3^E) are calculated using equation 5.8. and are listed in Table 5.1. The partial molar volumes at infinite dilution for both the solute (1) and the solvent (3) are calculated using equations 5.9. and 5.10. The calculated values are listed in Table 5.1.

$$V_i^E=[\frac{\partial V_m^E(x_i,A)}{\partial x_i}] = \Sigma_{i=1}^{n} A_i[(1-2x_i)(2x_i-1)^{i-1}+2(x_i-1)(2x_i-1)^{i-1}(x_i-x_i^2)] \qquad (5.8)$$

At infinite dilution the equation is simplified and the partial molar excess volume is:

$$V_1^{E\infty} = \Sigma_{i=1}^{n}(x_i-1)^{i-1}A_i \qquad (5.9)$$

and

$$V_3^{E\infty} = \Sigma_{i=1}^{n} A_i \qquad (5.10)$$

The standard deviation of the excess molar volume, $\sigma(V_m^E)$, is obtained using the following equation,

$$\sigma(V_m^E) = [\Sigma_{i=1}^{n}\frac{(V_{m(cal)}^E - V_m^E)^2}{(n-2)}]^{\frac{1}{2}} \qquad (3.11)$$

Graphs of excess molar volumes and the partial molar volumes at 303.15 K for all systems studied are given in figures 5.3 - 5.8.

The very large negative excess volumes quoted in Table 5.1 indicate a strong interaction between sulfolane + alkynes. This supports the evidence obtained from the VLE (Chapter 7) and SLE (Chapter 8) results.

TABLE 5.1. Results of the Excess Molar Volume Determination of an Alkyne (1) + Sulfolane (3) at 303.15 K, where V_m^E is the measured excess molar volume, $V_{m(cal)}^E$ is the excess molar volume calculated by the Redlich-Kister equation (equation 5.7), V_1^E and V_3^E are the partial molar volumes of the alkyne and sulfolane respectively, and $V_{m1}^{E\infty}$ and $V_{m3}^{E\infty}$ are the partial molar volumes at infinite dilution of the alkyne and sulfolane respectively

x_1	$-V_m^E$	$-V_{m(cal)}^E$	$-V_1^E$	$-V_3^E$
	$cm^3 \cdot mol^{-1}$			
1-Hexyne + Sulfolane at T= 303.15 K				
0.1072	0.6532	0.6606	5.7737	0.0466
0.1739	1.0554	1.0219	5.2297	0.1362
0.2171	1.4546	1.5156	4.2804	0.4206
0.2837	1.9177	1.8557	3.3325	0.9065
0.3913	1.9918	2.0180	2.5297	1.5353
0.4954	2.0007	2.0417	1.8408	2.3104
0.5722	1.9989	2.0249	1.6590	2.5662
0.5967	1.8911	1.8180	0.9435	3.9070
0.7146	1.7615	1.6229	0.6406	4.7335
0.7600	1.5604	1.5684	0.5773	4.9413
0.7729	1.4444	1.5237	0.5302	5.1063
0.7829	1.1555	1.2662	0.3207	5.9893
0.8928	1.0731	1.0366	0.1955	6.7105

Redlich-Kister Coefficients $A_1 = -8.1230$, $A_2 = 1.5153$ and $A_3 = 0.0499$

Partial Molar Excess Volumes at Infinite Dilution

$V_{m1}^{E\infty} = -6.56\ cm^3 \cdot mol^{-1}$ $V_{m3}^{E\infty} = -9.56\ cm^3 \cdot mol^{-1}$

Correlation coefficient $R^2 = 0.9765$
Residual variance $S^2 = 0.0055$
Standard deviation $\sigma(V_m^E) = 0.0743$

Minimum Value of the Excess Molar Volumes

x_1	V_m^E
0.5452	-2.0480

TABLE 5.1 continued

x_1	$-V_m^E$	$-V_{m(cal)}^E$	$-V_1^E$	$-V_3^E$
	$cm^3 \cdot mol^{-1}$			
1-Heptyne + Sulfolane at T = 303.15 K				
0.0308	0.2241	0.3517	5.0310	0.0151
0.1154	0.3357	0.4271	4.9299	0.0233
0.1574	0.4398	0.4912	4.8407	0.0320
0.1831	1.1840	1.0721	3.8632	0.2275
0.2051	1.4068	1.3306	3.2708	0.4500
0.2672	1.4035	1.3377	3.2523	0.4584
0.3262	1.5812	1.5970	2.3484	1.0088
0.3594	1.6008	1.6119	2.2657	1.0751
0.3692	1.5995	1.6513	1.9695	1.3406
0.4449	1.5874	1.6645	1.5728	1.7789
0.5059	1.5851	1.6076	1.1244	2.4332
0.5491	1.5571	1.5940	1.0704	2.5273
0.5609	1.5371	1.5372	0.8956	2.8626
0.6853	1.4531	1.3937	0.6171	3.5235
0.6878	1.1929	1.1813	0.3733	4.3129
0.7677	1.0993	1.0905	0.3002	4.6164
0.9045	1.0219	0.9739	0.2242	4.9871
0.9177	0.8132	0.7582	0.1225	5.6314
0.9329	0.0391	0.2267	0.0090	7.0779

Redlich-Kister Coefficients $A_1 = -6.6192$, $A_2 = 1.1005$ and $A_3 = 0.0643$

Partial Molar Excess Volumes at Infinite Dilution

$V_{m1}^{E\infty} = -5.45\ cm^3 \cdot mol^{-1}$ $V_{m3}^{E\infty} = -7.66\ cm^3 \cdot mol^{-1}$

Correlation coefficient $R^2 = 0.9786$
Residual variance $S^2 = 0.0066$
Standard deviation $\sigma(V_m^E) = 0.0810$

Minimum Value of the Excess Molar Volumes

x_1	$V_m^E/cm^3 \cdot mol^{-1}$
0.4596	-1.6660

TABLE 5.1 continued

x_1	$-V_m^E$	$-V_{m(cal)}^E$	$-V_1^E$	$-V_3^E$
	$cm^3 \cdot mol^{-1}$			
	1-Octyne + Sulfolane at T = 303.15 K			
0.0734	0.2079	0.2262	5.9734	0.0159
0.1400	0.6154	0.6026	4.4642	0.1307
0.2116	0.6754	0.6253	4.3726	0.1422
0.3744	0.8556	0.8721	3.3652	0.3159
0.4220	1.0532	1.0533	2.5957	0.5288
0.4771	1.1891	1.2596	1.4783	1.0932
0.5677	1.2632	1.2651	1.1420	1.3999
0.7462	1.2673	1.2402	0.9675	1.6138
0.8176	1.2589	1.2011	0.8250	1.8294
0.8858	0.9159	0.9166	0.3623	4.3726
0.8911	0.6513	0.6939	0.1840	4.4642
0.9647	0.4083	0.4130	0.0580	5.9734

Redlich-Kister Coefficients $A_1 = -5.0766$, $A_2 = -0.1980$ and $A_3 = -1.5998$

Partial Molar Excess Volumes at Infinite Dilution

$V_{m1}^{E\infty} = -6.87\ cm^3 \cdot mol^{-1}$ $V_{m3}^{E\infty} = -6.48\ cm^3 \cdot mol^{-1}$

Correlation coefficient $R^2 = 0.9899$
Residual variance $S^2 = 0.0016$
Standard deviation $\sigma(V_m^E) = 0.0397$

Minimum Value of the Excess Molar Volumes

x_1	$V_m^E/cm^3 \cdot mol^{-1}$
0.5142	-1.2698

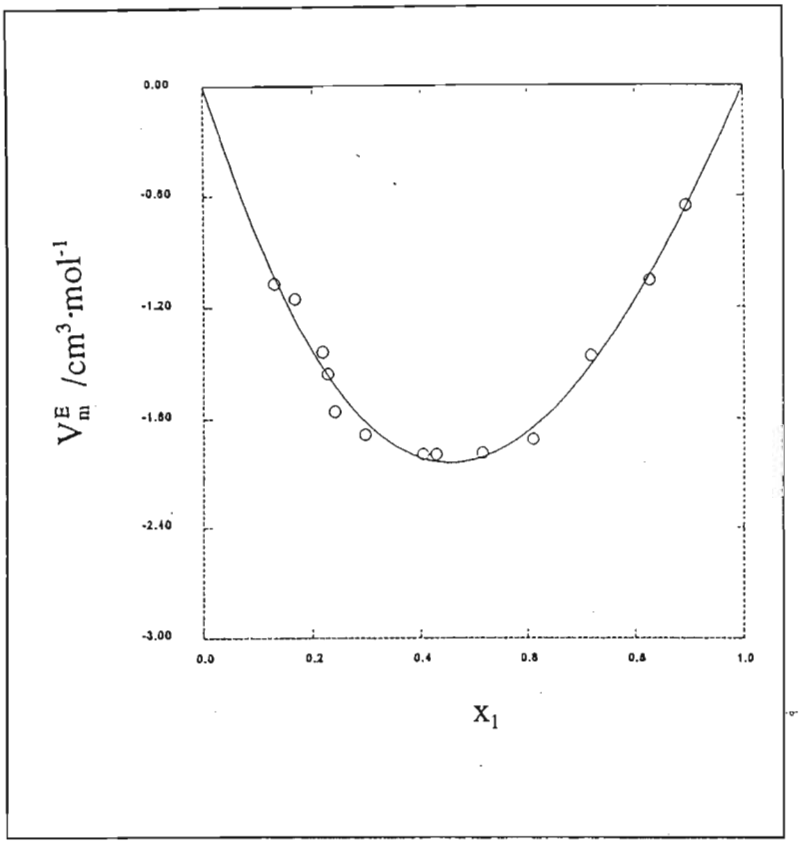

FIGURE 5.3. Excess Molar Volumes of 1-Hexyne(1) + Sulfolane (3) at 303.15 K

FIGURE 5.4. Partial Molar Volumes of 1-Hexyne (1) and Sulfolane (3) at 303.15 K

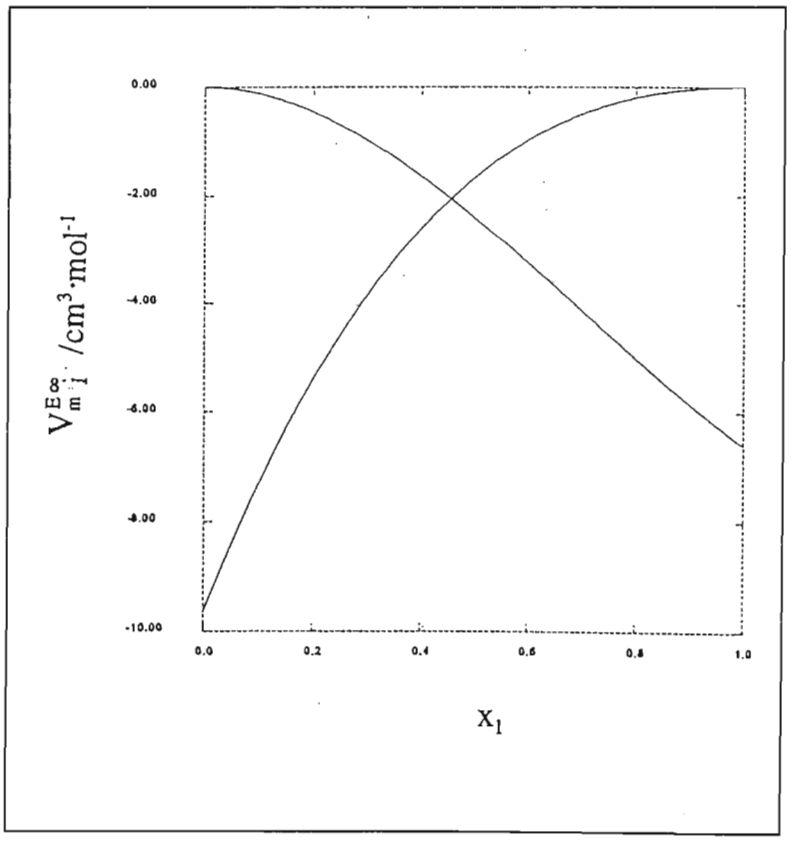

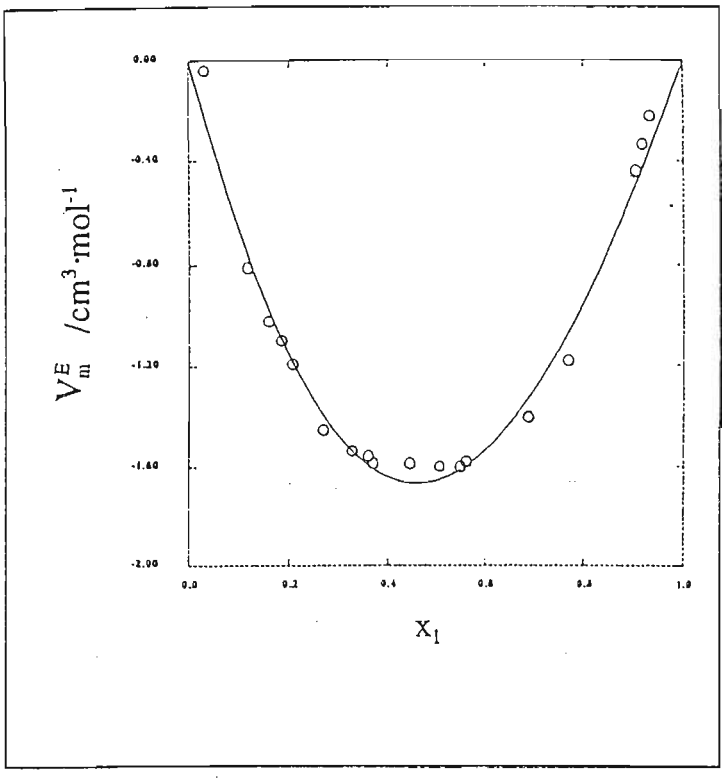

FIGURE 5.5. Excess Molar Volumes of 1-Heptyne versus Sulfolane at 303.15 K

FIGURE 5.6. Partial Molar Volumes of 1-Heptyne and Sulfolane at 303.15 K

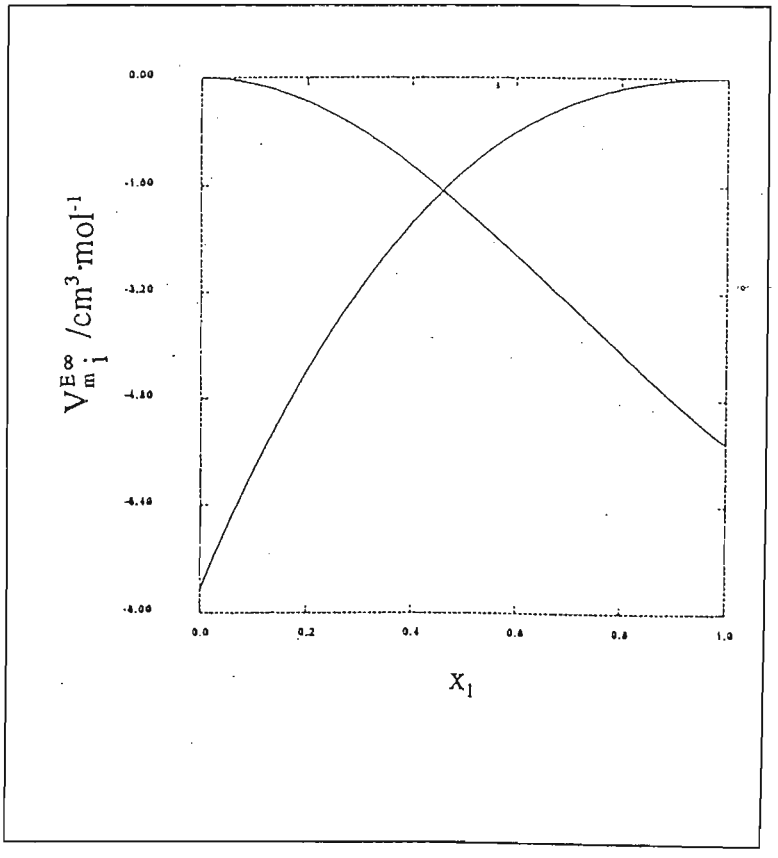

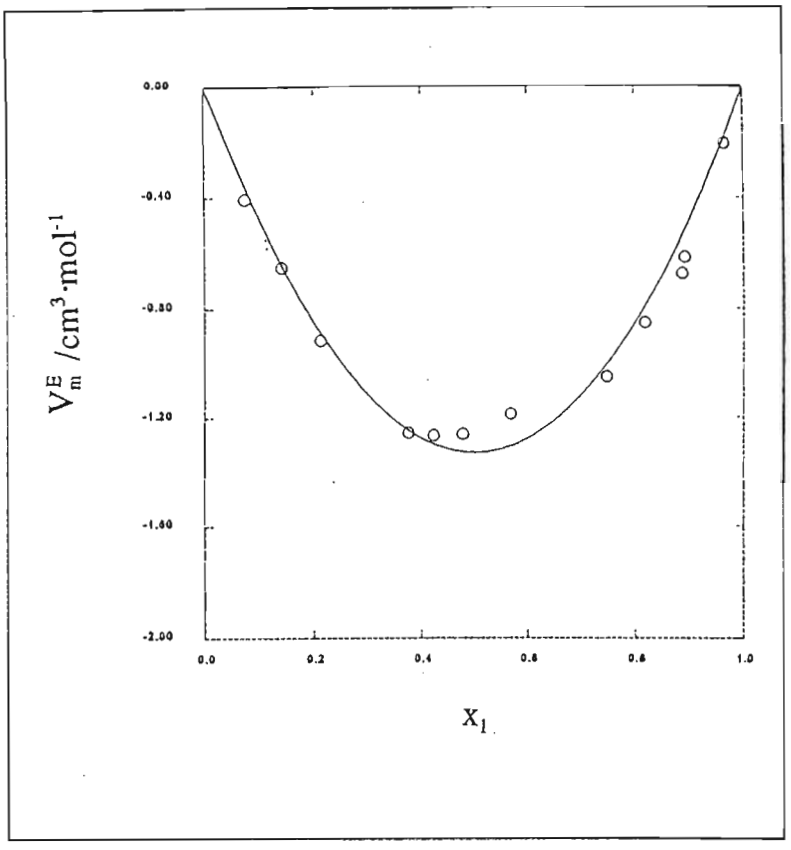

FIGURE 5.7. Excess Molar Volumes of 1-Octyne + Sulfolane at 303.15 K

FIGURE 5.8. Partial Molar Volumes of 1-Octyne and Sulfolane at 303.15 K

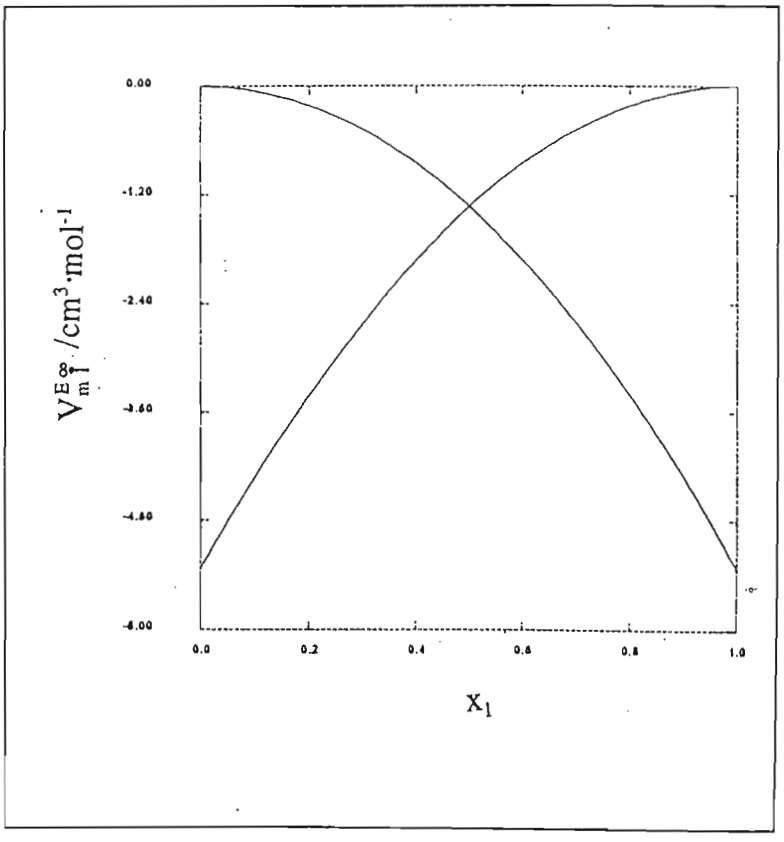

CHAPTER 6
EXCESS MOLAR ENTHALPIES OF MIXING

All chemical and physical reactions have a nett heat evolution which gives basic information on the mechanism and extent of reactions, a process which often only calorimeters can detect and measure[111]. *In an ideal solution there is no enthalpy change on mixing. In real solution however, interactions between liquids result in a change on enthalpy. A means of investigating these interactions between component molecules in the liquid state is achieved by a study of excess molar enthalpy of binary mixtures. The excess enthalpy* H_m^E, *can be represented by*

$$H^E = H_{(mixture)} - H_{(ideal\ mixture)} \tag{6.1}$$

If we consider the value of $H_{(ideal\ mixture)}$ *to be zero, the excess molar enthalpy,* H_m^E *is given by*

$$H_m^E = \frac{H_{(mixture)}}{n_1 + n_3} \tag{6.2}$$

where n_1 *and* n_3 *are the number of moles of solute and solvent, respectively.*

In principle, the direct measurements of heats of mixing is quite simple. The basic design involves a cell in which the two liquids are initially separated[93]. *All that is required is an apparatus in which known quantities of two liquids can be brought to a constant temperature, mixed, and the change in temperature noted, a thermometer to measure the temperature change and an electric heater in which measured amounts of energy can be dissipated in order to calibrate the apparatus*[93,111,112].

6.1. H_m^E Measurements

Two types of calorimeters were used in this work, the commercially available LKB 2107-101 microcalorimeter, and the Thermometric 2277 Thermal Activity flow-mix microcalorimeter.

6.2. The LKB 2107 Microcalorimeter

6.2.1. Principle of Operation

The isothermal flow mix measuring cylinder for the LKB calorimeter used in this work is discussed in great detail in the literature.[113] The mixing vessel has a separate inlet and comprises a spiral-wound 24 carat gold tube of 1 mm i.d. and with a volume of 0.5 cm^3. The design is such that adequate mixing is achieved with no vapour space. The mixing vessel is in thermal contact with a pair of matched thermocouples in the thermopiles and an aluminium heat-sink assembly, with the heat sink compound covering all the surfaces of these items. An exothermic reaction results in heat flow to the heat sink assembly, while the opposite effect is observed for the endothermic reactions. In each case the resultant temperature difference is detected by the thermopiles positioned between the vessel and the heat sink. The output from the thermopiles is amplified and fed to a digital readout system and a Perkin-Elmer 561 chart recorder.

The aluminium block heat sink assembly is contained within an insulated housing. A heater and a temperature sensor are mounted within the heat sink. The entire arrangement is contained within an LKB thermostat which consists of a thermostatically controlled air bath to maintain the temperature required for this investigation. Water, cooled to 287 K by a Labcon Thermostat unit is pumped through at a rate of 8 $cm^3 \cdot s^{-1}$.

The LKB was used in conjunction with a LKB control unit. This incorporates a power supply capable of providing an adjustable current to the calibration heaters

within the insulated mixing vessel assembly, and a facility for heating and monitoring the temperature of the calorimeter heat sink assembly. This heating facility helps to reduce the equilibrium time of the apparatus during "startup" or when raising the operating temperature. It was always switched off when measurements with the instrument were made.

Since liquids entering the microcalorimeter are required to be within 0.05 K of the experimental temperature, they were first routed through an external heat exchange fitted into a recess in the bottom of the air bath of the thermostat unit and then through the internal heat exchangers, situated inside the housing containing the mixing vessel assembly. Samples were introduced using two Jubilee peristaltic pumps, capable of stable flow rates ranging from 0.03 - 0.2 $cm^3 . min^{-1}$. Viton tubing, 1.5 mm i.d., and teflon tubing, 1.2 mm i.d. were used in the pumps and flows lines respectively. The temperature inside the microcalorimeter was monitored using a Hewlett Packard 2804 A quartz thermometer and was found to be constant to better than 0.01 K.

6.3. The 2277 Thermal Activity Monitor (TAM)

6.3.1. Principles of Operation

The 2277 Thermal Activity Monitor circulator equipped with an external thermostatic water circulator (Thermometric 2219 Multi-temp II) and a pair of Eldex variable speed piston pumps capable of stable flow rates from 0.05 to 3 $ml \cdot min^{-1}$ was also employed in this work. The TAM utilizes the heat flow or heat leakage principle where heat produced in a thermally defined vessel flows away in an effort to establish thermal equilibrium with its surroundings. The calorimetric mixing device used in the TAM has a 24 carat gold flow-mix cell where two different liquids can be mixed. The flow mix cell has a small bore T-piece at the base of the measuring cup where the two incoming flows are mixed. After mixing the reaction takes place as the mixed flow passes the spiral around the measuring cup and out to waste. The measuring cup is

sandwiches between a pair of Peltier thermopile heat sensors. These sensors are in contact with a heat sink. The system is designed so that the main path for the flow of heat to or from the measuring cup is through the Peltier elements. The Peltier elements act as a thermoelectric generators capable of responding to temperature gradients of less than one millionth of a degree celsius. These highly sensitive detectors convert the heat energy into a voltage signal proportional to the heat flow. Results are presented as a measure of the thermal energy produced by a sample per unit of time.

Results are quantified where known power values are passed through built in precision resistors. Precision wire wound resistors are located within each measuring cup to represent a reaction during electric calibration. The calibration resistors is integral with the measuring cup, to simulate as near as possible, the position of the reaction. This ensures that the output from the detector will be, as near as possible, identical to the output when the power is dissipated from the resistor as from the sample. During the calibration, a know current is passed through the appropriate channel heater resistor, and because the resistors value is know, a specific thermal power gives a calibration level that may then be used to determine experimental results.[114]

The entire assembly is located in a stainless steel cylinder. Each cylinder has two measuring cup assemblies just described; the Peltier elements in each measuring cup are connected in series but in opposition so that the resultant signal represents the difference in the heat flow from the two measuring cups. This design allows one measurement cup assembly to be used for the sample and the other to be used as the blank.

This instrument is suitable for the solvents used in this investigation as outside the calorimeter unit the liquids are in contact with Teflon and glass only. Inside contacts are the gold tube of the heat exchanger and the mixing cell and the teflon

tubes. Samples were introduced into the cell using two Eltron piston pumps capable of producing flow rates from 0.5 to 3.0 cm^3min^{-1}.

The sensitivity and high level of precision of the TAM is largely due to the stability of the infinite heat sink which surrounds the measuring cylinders. This heat sink is formed by a closed 25 litre thermostatted water bath to $\pm$ 2 x 10^{-3} K within the experimental range. Water is continuously circulated by being pumped upwards into a cylindrical stainless steel tank, where it overflows into a similar but larger outer tank. The pump then re-circulates the water from the outer tank back into the inner tank. Several inactive controlling systems work together to maintain the water temperature whose signals are fed to an electronic temperature regulator unit. The 25 litre thermostat is filled with deionised water and a corrosion inhibitor containing sodium nitrate, sodium metasilicate and benzotriazole.

6.4. Operation Procedure and Actual Sample Measurement

The solvent used, sulpholane has a melting point of 301.60 K, therefore the pumps and the tubing that are normally at room temperature had to be insulted above the sulpholane melting point to allow it to be pumped into the calorimeters. This was done by designing a housing for the pumps and tubing using a well insulated glove box with a Goldair heater, which circulated warm air within the housing.

For both instruments, an initial equilibrium time of at least three days was required. Power to the equipment was left on continuously for the duration of the experimental determination to ensure that thermal equilibrium was maintained in the temperature control units. The flow lines were filled with water overnight. In the morning warm methanol was pumped through each flow line at a rate of 0.8 $cm^3 \cdot s^{-1}$ for 15 minutes before introduction of the component liquids.

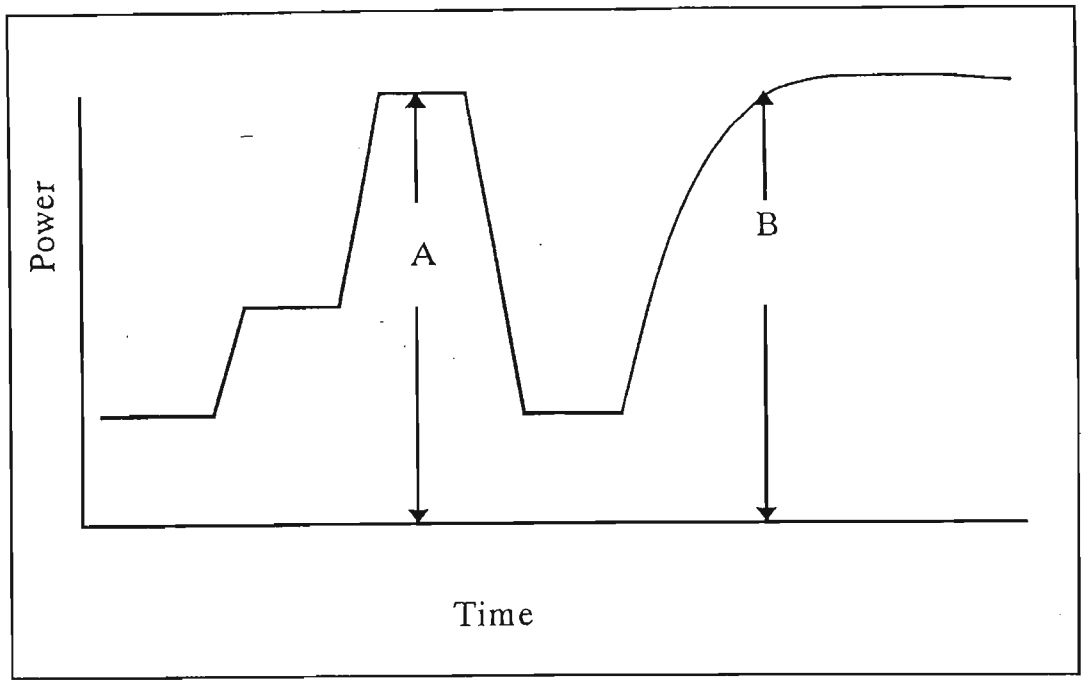

FIGURE 6.1 A typical calibration and experimental recorder output for the TAM

For the LKB microcalorimeter, the two inlets were separately flushed and primed with the two degassed sample components. A typical recorder output as a function of time for a steady state H_m^E measurement is represented in figure 6.1. Section A represents the steady state baseline obtained without any fluid flowing through the mixing vessel. This was always recorded before commencing a set of experimental measurements. Since accurate time elapse values were required for the determination of sample flow rates, the pumps and the stopwatch were activated simultaneously. Pumping of the sample was continued until a new steady state was reached, depicted by the baseline deflection, B, figure 6.1. Thereafter a calibration current to the calibration heater was applied in order to nullify this deflection, in the case of an endothermic reaction restoring the original baseline. In the case of an exothermic reaction, enough current was applied to reproduce this baseline deflection, B. In practise, noise and non-uniform flow rates resulting from the peristaltic pumps operating at low speed produced regular baseline deflections on the recorder. The current was thus always adjusted to a point where the spread about the mean value on

the deflected baseline was reproduced about the zero flow-baseline.

Once the regular baseline had been regained, both pumps were switched off. The molar flow rates, f_1 and f_2 were determined by weighing the two component flasks before and after each experimental run. From these masses and the time elapsed for the experiment, the molar flow rates were determined. A Mettler AE240 electronic balance, accurate to 0.0001 g was used for the mass determinations.

For the TAM, due to sensitivity of the instrument and the absence of a control unit containing an inbuilt current supply, calibration at the individual flow rates was necessary. This involves flushing one of the component solvents through both the inlet tubes at a flow rate similar to that for the actual experimental determination. A know current, I, from an external power source is simultaneously passed through the inbuilt resistor and since R for the resistor is known, the expected thermal power, P, can be obtained from the equation,

$$R = \frac{P}{I^2} \qquad (6.3)$$

and the calorimeter power reading is adjusted accordingly. Both the pumps, and the external power supply were switched off, the baseline was allowed to return to zero and flow of the second sample component in one of the lines was initiated for sufficient time to coat the tubing. Experiments were carried out according to a method similar to that of the LKB microcalorimeter with the flow rates exactly like those used in the calibration.

6.5. Preparation of Mixtures

The samples liquids were degassed in 25 cm^3 Quickfit conical flasks fitted with a modified b14 stopper, which had one 1.8 mm i.d. inlet connected by teflon tubing to the pump. This design reduced evaporation of the component samples and was efficient in reducing bubble formation. The mass of the effluent collected after each run was compared to the mass of pure components consumed, thus serving as a constant check against leaks in the system. For each run, a new pumping rate was set and the process carried out as described.

The sulpholane was kept in a water bath set about 303 K.

6.6. Friction Effects and Flow Rate Determination

The friction effects due to flow of the solvent and the characteristics of the sample components had to be corrected for, in the LKB 2107 microcalorimeter. This correction was not necessary for the TAM as the calibration takes these factors into account. For an experimental run done on the LKB microcalorimeter, the values of the baseline deflections, B, and the corresponding current, I, required to nullify these deflections were plotted for each system. (figure 6.2). In each case the resulting graph together with the graph for the mixture from each run was employed to adjust the experimental readings for the frictional effects.

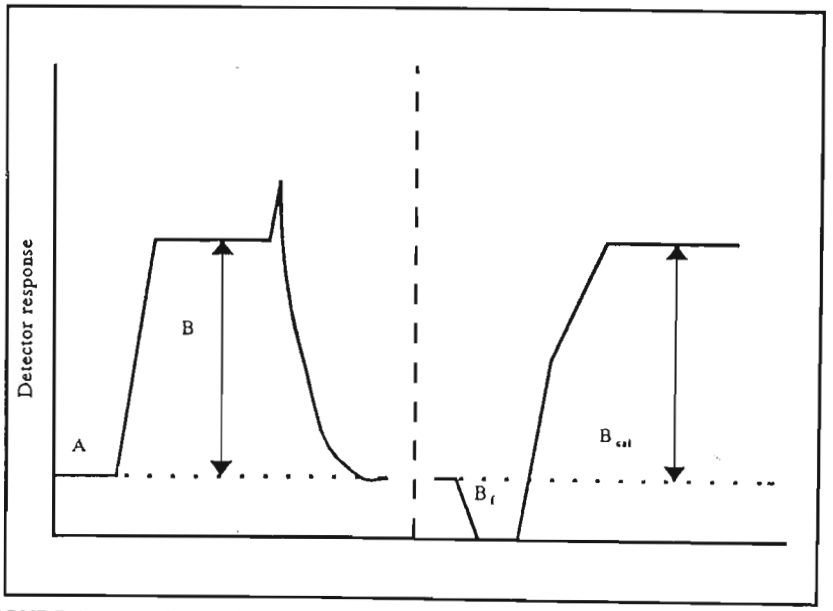

FIGURE 6.2. A typical Calibration and Experimental recorder output for the LKB microcalorimeter

These calibrations were carried out collectively at the end of a series of experimental runs for a system. Each calibration involved purging the mixing vessel with the effluent from a particular run. With the same pumping parameters as were employed for that particular run, any heating effect due to friction exhibited a deflection, B_f in figure 6.2. The experimental detector voltage shift was thus corrected to

$$B_o = B - B_f \tag{6.4}$$

The indicated calibration current, I_{cal}, corresponds to B_o, was then interpolated from the experimentally determined graph and was passed through the calorimeter heater, thereby producing a baseline deflection to B_{cal} in figure 6.2. The excess molar enthalpy was thus calculated from [23]

$$H_m^E = \frac{[(B_o(I_{cal})^2 R/B_{cal}]}{(f_1 + f_2)} \tag{6.5}$$

were R is the resistance heater. It is however, observed that $B_o \approx B_{cal}$ for flow rates less than 0.80 $cm^3\ min^{-1}$. Since the majority of the experimental runs were carried out at flows rate less than this, the above calibration procedure became unnecessary in many cases and H_m^E was then determined by

$$H_m^E = \frac{I_{cal}^2 R}{(f_1 + f_2)} \tag{6.6}$$

For exothermic reactions, the steady state deflection, B, was noted and a current, I, was applied to double this deflection. Heating due to frictional effects would once again produce a deflection, B_f, and hence equation 6.4 becomes

$$B_o = B + B_f \tag{6.7}$$

The TAM was, however, found to give more precise results for small endothermic and exothermic reactions. The calorimeters were tested using the data of Stokes and Marsh[96] to confirm technique and procedure. The test system was (benzene + cyclohexane) and the results obtained were always within 10 $J \cdot mol^{-1}$ of the smooth curve obtained by Stokes and Marsh.[96]

6.7. Results

The excess enthalpies for the following systems were measured at 303.15 K: sulfolane + 1-hexyne, 1-heptyne and 1-octyne. The results are given in Table 6.1.

The Redlich-Kister equation,[97](equation 6.8) is fitted to the excess enthalpy data. The results together with the Redlich-Kister parameters are given in Table 6.1.

$$H_m^E = (x_1 - 1)x_1 \Sigma_{i=1}^{n} A_i(1 - 2x_1)^{i-1} \tag{6.8}$$

The partial molar excess enthalpies are calculated using equation 6.9 and are listed in Table 6.1. The partial molar enthalpies at infinite dilution for both the solute (1) and the solvent (3) are calculated using equations 6.10. and 6.11. The calculated values are listed in Table 6.1.

$$H_i^E = [\frac{\partial H_m^E(x_i A)}{\partial x_i}] = \Sigma_{i=1}^{n} A_i[(1-2x_i)(2x_i-1)^{i-1} + 2(x_i-1)(2x_i-1)^{i-1}(x_i - x_i^2)] \tag{6.9}$$

At infinite dilution the equation simplifies to

$$H_1^{E\infty} = \Sigma_{i=1}^{n}(x_i - 1)^{i-1}A_i \qquad (6.10)$$

and

$$H_3^{E\infty} = \Sigma_{i=1}^{n}A_i \qquad (6.11)$$

The standard deviation of the excess molar enthalpy, $\sigma(H_m^E)$, is obtained using the following equation,

$$\sigma(H_m^E) = [\Sigma_{i=1}^{n}\frac{(H_{m(cal)}^E - H_m^E)^2}{(n-2)}]^{\frac{1}{2}} \qquad (6.12)$$

where n is the number of parameters.

Excess molar enthalpies and the partial molar enthalpies at 303.15 K for all systems studied are given in Table 6.1.

The H^E data is positive over the whole range of concentration. This is most likely a result of the dissociation of the sulfolane and also the alkynes which mask the any association between sulfolane and the alkynes. The association between sulfolane and the alkynes appear to be small. The oxygens on the sulfolane molecule appear to be shielded.

TABLE 6.1. Results of the Excess Molar Enthalpy Determination of an Alkyne (1) + Sulfolane (3) at 303.15 K, where H_m^E is the measured excess molar enthalpy, $H_{m(cal)}^E$ is the excess molar enthalpy calculated by the Redlich-Kister equation (equation 6.8), H_1^E and H_3^E are the partial molar enthalpies of the alkyne and sulfolane respectively, and $H_{m\,1}^{E\,\infty}$ and $H_{m\,3}^{E\,\infty}$ are the partial molar enthalpies at infinite dilution of the alkyne and sulfolane respectively

x_1	H_m^E	$H_{m(cal)}^E$	H_1^E	H_3^E
		$J \cdot mol^{-1}$		
		1-Heptyne + Sulfolane at T= 303.15 K		
0.0191	22.94	10.81	613.15	-0.91
0.1482	122.78	117.95	634.70	-24.15
0.2551	200.36	219.68	890.65	-10.09
0.3445	303.25	291.30	737.17	56.98
0.3652	310.69	304.69	693.57	80.97
0.3745	323.53	310.24	673.40	92.81
0.4205	337.51	333.09	570.51	160.82
0.5021	342.92	352.94	388.62	316.96
0.5026	342.92	352.98	387.55	318.04
0.5501	339.12	351.42	290.59	425.79
0.5623	343.66	349.45	267.38	454.88
0.5842	334.24	344.32	227.73	508.13
0.5864	338.24	343.69	223.90	513.53
0.6174	324.00	332.72	173.06	590.37
0.6841	314.14	296.29	85.07	753.71
0.7112	298.58	276.94	58.05	815.98
0.7211	294.88	269.29	49.45	837.69
0.7222	280.21	268.42	48.53	840.06
0.7668	220.69	230.37	18.20	928.00
0.8510	121.74	147.44	-7.01	1029.61
0.9119	72.48	84.03	-6.70	1023.37

Redlich-Kister Coefficients $A_1 = 1411.14$, $A_2 = 161.33$ and $A_3 = -733.78$

Partial Molar Excess Enthalpy at Infinite Dilution

$H_{m\,1}^{E\infty} = 516.03\ J \cdot mol^{-1}$ $H_{m\,3}^{E\infty} = 838.70\ J \cdot mol^{-1}$

Correlation coefficient	$R^2 = 0.9798$
Residual variance	$S^2 = 221.1372$
Standard deviation	$\sigma = 14.8707$

Maximum Value of the Excess Molar Enthalpy	x_1	$H_m^E/J \cdot mol^{-1}$
	0.5187	353.54

TABLE 6.1.continued

x_1	H_m^E	$H_{m(cal)}^E$	H_1^E	H_3^E
		$J \cdot mol^{-1}$		
		1-Octyne (1) + sulfolane (3)		
0.2060	274.26	275.12	804.30	137.82
0.2130	283.50	279.66	777.77	144.85
0.2430	291.59	296.62	675.19	175.09
0.3050	323.30	320.36	512.41	236.07
0.4090	332.30	334.72	346.98	326.23
0.5640	320.80	318.82	226.99	437.60
0.6040	313.48	309.32	204.55	469.13
0.6790	280.13	285.24	162.38	545.12
0.7430	258.66	256.66	123.80	640.78
0.7920	220.98	228.18	92.77	743.75
0.8530	188.79	182.18	54.69	921.97

Redlich Kister Coefficients $A_1 = 1318.3960$ $A_2 = -250.8396$ $A_3 = 625.1818$

Partial molar excess enthalpies

$H_{m\,1}^{E\infty} = 2194.42\ J \cdot mol^{-1}$ $H_{m\,3}^{E\infty} = 1692.74\ J \cdot moll^{-1}$

Correlation coefficient	$R^2 = 0.9898$
Residual variance	$S^2 = 25.2545$
Standard deviation	$\sigma = 5.0254$

Maximum Value of the Excess Molar Enthalpy	x_1	H_m^E/J·mol^{-1}
	0.4201	334.83

CHAPTER 7
VAPOUR LIQUID EQUILIBRIA

Reliable and accurate vapour-liquid equilibrium (VLE) data are always needed for process engineering design and also provide useful information in the understanding of the behaviour of liquid mixtures.

Two broad areas of VLE measurements can be distinguished, viz. low pressure and high pressure. Most of the low pressure VLE measurements are done on two types of equipment, dynamic (circulation) stills and static equilibrium cells. It is stated that the highest accuracy of measurements is obtained by means of a static cell [10], i.e. a method in which the liquid and the vapour phases are in a state of equilibrium and boiling does not occur. The long time necessary for equilibrium, the need for degassing of samples, and the expensive axillary equipment required are the most important drawbacks of this method. The dynamic stills, working in the stationary state of boiling under the pressure of an inert gas, are considerably simpler in operation, but are usually less accurate.[10,11]

In this work, the Rogalski[10,115] modified Święotoslawski dynamic ebulliometer still[11] is used to produce VLE measurements accurately in the low pressure region. Modifications to the ebulliometer include (i) stable hydrodynamic and thermal conditions under pressure from 100 to 300 kPa and from room temperature to 500 K, even in the case when the mixtures investigated consist of substances of widely differing vapour pressures,[10] and (ii) the composition of the liquid and vapour streams leaving the equilibrium chamber are maintained constant until the streams have passed through the sample chambers and until they correspond to the thermodynamically consistent values of pressure and temperature.[10] The ebulliometer produces VLE measurements rapidly and accurately over a wide temperature range. It is also suited

for determinations at very low concentrations.

Binary Vapour-Liquid Equilibria for the following systems at 338.15 K or 353.15 K were measured: 1-heptyne, or tetrahydrofuran or 1,4-dioxane, or tetrachloromethane or trichloroethane + sulfolane, over the whole concentration range. The data are described using the Margules[12], van Laar[13], WILSON[5], NRTL[6] and UNIQUAC[7] equations.

7.1. Vapour Pressure Measurements

7.1.1. The Static Method

When one component is involatile, the vapour phase consists almost entirely of the volatile component; hence it is unnecessary to analyze this phase. Under these conditions the circulating still (dynamic) methods are of little use. The most satisfactory method for these systems is the static method. In the static method, a mixture of known composition is contained in a vessel attached to a manometer, both being immersed in a thermostat. The manometer may be a nulling type, a differential type, or an absolute type.[116] The major difficulty of the static method is the need to completely remove all traces of air from the system and the liquids.

Following the suggestions of Barker,[27] that the vapour-phase composition of a mixture of two volatile liquids can be calculated from a knowledge of T, P, and x over the composition range, the static method has also been used extensively for measuring vapour pressures above mixtures of volatile liquids.

One of the earliest precision static systems was described by Allen, Everett, and Penney.[117] This apparatus is suitable for measurements at room temperature and above. The unknown vapour pressure was balanced against a known pressure of air using a metal-bellows nulling manometer.[117] The null position was determined optically. Baxendale, Enustun, and Stern[118] have described a similar apparatus, where

the bellows were replaced by a mercury "cut-off" nulling manometer. McGlashan and Williamson[119] built a static apparatus that could measure the pressure to $\pm$ 3 Pa and the temperature to $\pm$ 0.003 K. In this case a known mass of degassed involatile material is contained in a cell of known volume. The container contains a "break-seal" which separates the volatile material from the manometer. By suitable manipulation of vacuum taps and the withdrawal of the mercury below the "cut-off", the solute is distilled into the container with the involatile material. The vapour pressure above the mixture is then determined at the required temperature, by making measurements at known temperatures close to the required temperatures and interpolating the result.[116] It was found by McGlashan[119] that unless the surface of the liquid is continuously disturbed by a stirrer, equilibrium can take up to 40 hours. With efficient stirring equilibrium is normally achieved within 1 hour after a major temperature change.[107] Gomez-Ibanez and Shieh[86] described a similar apparatus except that five ampoules containing the volatile material could be loaded simultaneously into the cell containing the involatile material.

7.1.2. The Dynamic Method

It is sometimes suggested that methods of vapour-pressure measurements which depend on boiling are less accurate than static methods, presumably because of the possibility of superheating the liquid.[116] This is the method employed in this work.

The problems with obtaining a sufficiently large sample of the condensate vapour, along with the difficulty of establishing a steady state which differs insignificantly from true equilibrium, has led to a large number of designs of recirculating stills. The stills are based on a common recirculating principle shown in figure 7.1.

A mixture A is boiled and the vapours pass through B. After complete condensation, the condensate is collected in C and returns, in a controlled manner, to A for

reboiling. After starting the still, and when C just fills with condensate, the contents of C will be richer in the volatile components than the vapour phase over the boiling mixture. On further operation the contents of C returns to A, which becomes richer in the more volatile component, while C is depleted. After continued recirculation a steady state is attained when the compositions of both phases remain invariant with time. At this stage the compositions of the liquids in A and C are determined.

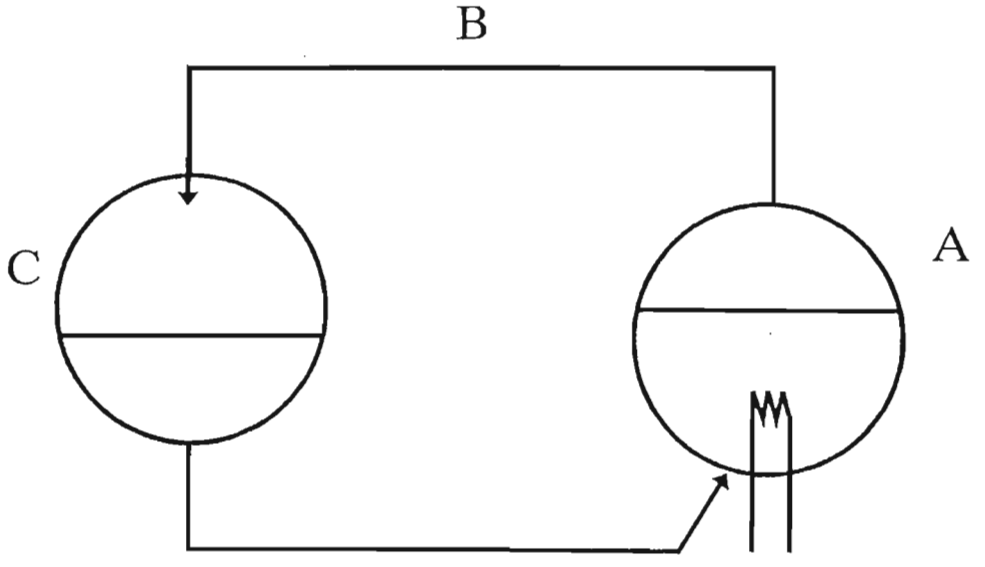

FIGURE 7.1. Principle of recirculating Still. A, Boiler;B, Condensor; C, Receiver

Hala *et al.*[35] has made a comprehensive review of the various recirculating stills described in the literature. One recirculating still that has been found to behave satisfactory over a wide temperature range is the Brown still.[121] Extensive work on ebulliometry was carried out by Świętoslawski[11] who developed ebulliometers in which both the temperature of the boiling liquid, and of the condensing vapour are measured. In the Swietoslawski ebulliometer the differences between the temperatures of the boiling liquid and the condensing vapour may indicate whether impurities are

present, or whether the substance is decomposing under the conditions of the experiment.[107]

7.2. Experimental Procedure

7.2.1. Equipment

In this work the, the Rogalski[10] modified Świętoslawski ebulliometer[11] was used to produce VLE measurements accurately in the low pressure region.The Świętoslawski ebulliometer is well established for the determination of the boiling points of pure substances. Its development and modifications are well described in the literature[11]. The modifications made to the Świętoslawski ebulliometer enabling the determination of VLE is described by Malanowski[121].

When determining VLE data for mixtures, the monitored temperature must remain constant for a given pressure and mean composition of the fluid phases in the ebulliometer, since this will indicate that the stream delivered by the Cotrell pump. Mixing of the liquid stream before entering the Cottrell pump by means of flow turbulence is sufficient for this purpose.

The ebulliometers designed by Świętoslawski and modified by Rogalski[10] (shown in figures 7.2 and 7.3) fulfil these conditions. The apparatus shown in figure 7.2 enables the withdrawal of the sample of both equilibrated phases, i.e. vapour condensate and liquid. The ebulliometer shown in figure 7.3 is adapted for total pressure or boiling temperature measurements. The examined samples are in both cases prepared by introducing a known mass of one substance into the ebulliometer, and adding known masses of the other component. Both pieces of apparatus are of similar proportions and construction and both can be used for the experimental procedure proposed by Rogalski et al.[122]. According to this procedure, the equilibrium composition of the liquid phase already established in the ebulliometer can be calculated from the composition of the introduced sample by means of a material balance equation. For one mole of liquid, L, and vapour, V, streams leaving the equilibrium chamber satisfy the equation

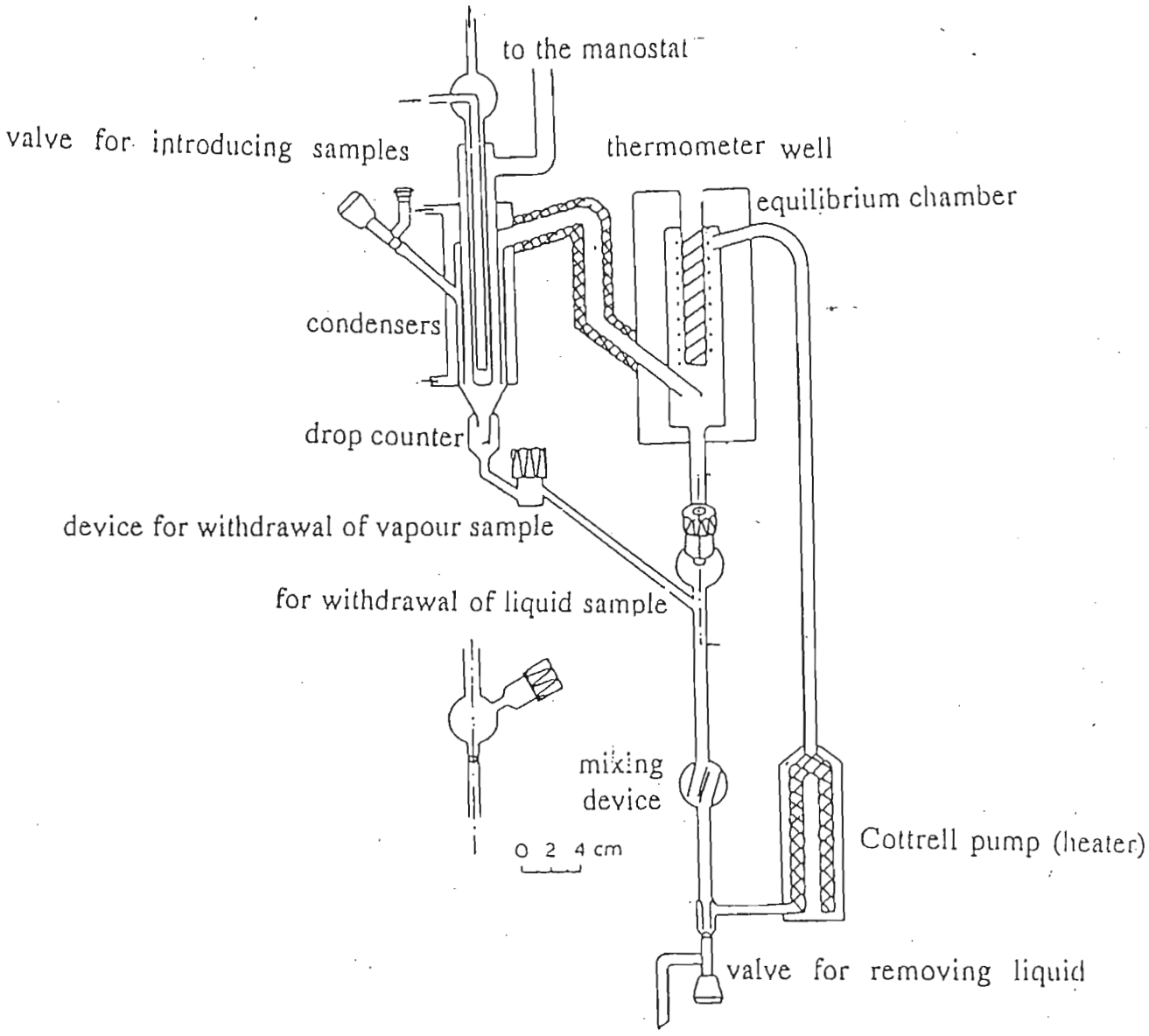

The Ebulliometer allowing the withdrawal of the Samples in Equilibrium

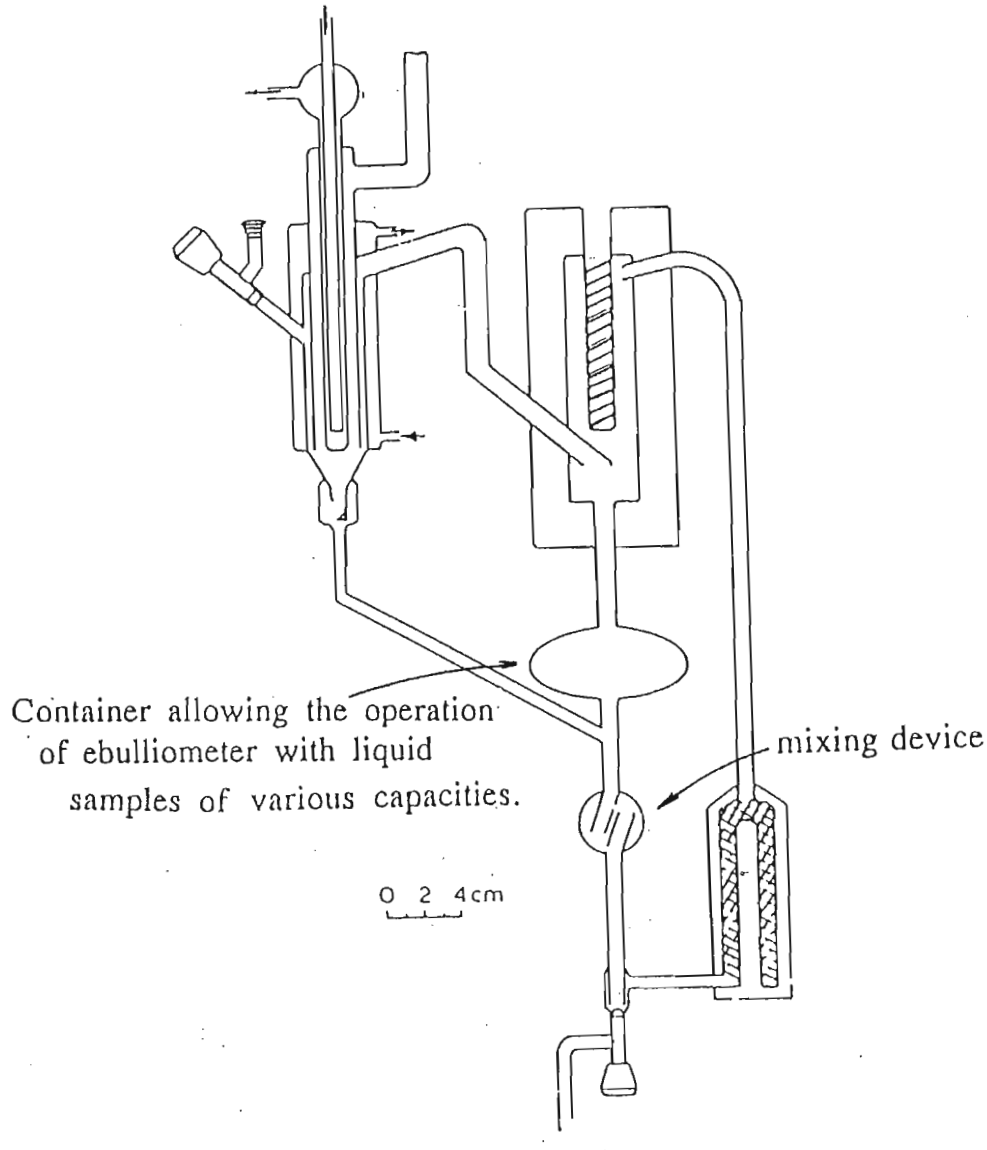

FIGURE 7.3. Ebulliometer for the Determination of Total Pressure against Composition Data

$$V + L = 1 \tag{7.1}$$

The mole fraction of component i in the sample, q_i, is related to the mole fraction of this component in the liquid phase, x_i, and in the vapour phase, y_i by the equation

$$q_i = Vy_i + Lx_i \tag{7.2}$$

Defining the coefficient of evaporation, f, by

$$f = \frac{V}{L} \tag{7.3}$$

and comparing equations 7.1 and 7.2, the relation enabling the calculation of liquid phase composition by an iterative procedure is obtained, viz.[115]

$$x_i = q_i \frac{1 + f}{1 + (y_i/x_i)f} \tag{7.4}$$

For an ebulliometer correctly designed and properly operated, the coefficient f depends little on the system investigated and is fairly constant over the range of temperature and pressure applied in usual ebulliometeric measurements.

The ebulliometers presented earlier offer both the working abilities of an equilibrium still (determination of full VLE data) and an ebulliometer (determination

of total pressure or boiling points of mixture only). In this work, the ebulliometer shown in figure 7.2 (determination of full VLE data) was used. Rogalski[115] suggests that in practice, it is worthwhile to combine these two methods.

7.2.2. Auxiliary Equipment

In the use of ebulliometers, rapid, reliable and accurate methods for determining pressure and temperature are necessary. In this work, a calibrated platinum resistance thermometer (Autotherm2 by Gallenkamp), with a resolution of $\pm$ 0.01 K, and a digital recorder were used for the temperature measurements. Pressure measurements were made with a mercury manometer equipped with a kathetometer with a resolution of 0.01 mm, which gives an accuracy of the vapour pressure measurements to better than 0.03 kPa.

The most important factor in the work is the stabilization of the pressure within the system. The equipment available commercially is seldom better than $\pm$ 10 kPa.[2] In our case, a container of 0.06 m^3, filled with dry gas and kept in a constant temperature air bath was used. Small fluctuations of pressure in the system are immediately followed by changes in the boiling temperature. This fast reaction of the ebulliometer is used for establishing the equilibrium pressure simply by adding or removing small amounts of inert gas from the system.[10]

7.2.3. Methods of Determining Vapour Pressures and Mole Fraction

The ebulliometer measurements can be carried out in the following different ways, determined mainly by the nature of the systems investigated:

(1) Simultaneous determination of pressure, P, temperature, T, and the composition of liquid, x, and vapour, y, phases (P,T,x,y method)

(2) Determination of P, T, and x only (P, T, x method)

(3) Combined determination of P, T, x, with P, T, y (combined method)

In the case of an isobaric determination, steady state is reached within a few minutes of a change of sample composition. When an isothermal determination is performed, the pressure in the system should be adjusted until the temperature in the ebulliometer has reached the desired value. To help achieve this, the measurements of the boiling temperature as a function of pressure for constant composition samples can be determined. In this work, P, T, x and y were measured (ie. method 1).

The introduction or withdrawal of samples in the apparatus used here can be made without interrupting the boiling action in the ebulliometer as the introduction or withdrawal does not disturb the equilibrium. This is a major advance over many circulatory stills.

7.2.4. Determination of P, T, x, and y

The ebulliometer enabling the withdrawal of samples (figure 7.2) is used in this work. After the introduction of the sample, the equilibrium temperature is established after 20 minutes of circulation and the pressure and temperature determined. The samples of both the liquid phase and the condensed vapour phase are collected by means of gas-tight hypodermic syringes. The composition of the liquid and the vapour are determined by a precision refractometer (Carl Zeiss, Jena) at 303.15 K. A calibration curve was made for each mixture, and the mole fractions were determined from

$$n_D(303.15\,K) = Kx_3^2 + Lx_3 + M, \qquad (7.5)$$

where x_3 is the mole fraction of sulfolane and n_D is the refractive index of the mixture. The coefficients of this equation for each of the mixtures are given in Table 7.2. The

accuracy of the composition determination was better than 0.0005 in mole fraction. Within this limit, the measured sulfolane concentration in the vapour phase was close to zero for all the mixtures investigated.

Because the vapour pressures of sulfolane in the temperature range investigated are so low, (close to the accuracy limit of the experimental method), no vapour pressure measurements on pure sulfolane were made and the vapour pressure was obtained from fitted parameters given in Table 7.3.[127,129]

7.2.5. Materials

The solvents were obtained from Aldrich Chemical Co., (with a quoted purity of 99.9 % w/w) and were purified by fractional distillation through a 30 plate distillation column. The compounds were dried using activated type 5A molecular sieves and the water content was found to be less than 100 ppm w/w as determined by GLC analysis. Sulfolane was also supplied by Aldrich Chemical Co., (98 % reagent) and was twice vacuum distilled at a pressure below 20 mmHg to yield a colourless and odourless product. To minimize the contact of this deliquescent reagent with moist air, the product was kept in sealed bottles in a desiccator.

The physical properties of the reagents used in this work are listed in Table 7.1 together with literature values.

7.3. Thermodynamics of Phase Equilibrium

7.3.1. The Vapour Phase

In calculations of vapour-liquid equilibrium, it is necessary to calculate separately the fugacity of each component in each of the two phases. The liquid and vapour phases require different techniques. Here we consider the vapour phase.

At a pressure of a few bars, the vapour phase is at a relatively low density,

i.e., on the average, the molecules interact with one another less strongly than do the molecules in the much denser liquid phase. It is therefore a common simplification to assume that all the nonideality in vapour-liquid systems exist in the liquid phase and that the vapour can be treated as an ideal gas. This leads to the simple result that the fugacity of component i is given by the partial pressure, i.e. the product of y_i, the mole fraction of i in the vapour, and P, the total pressure.[123]

However, the ideal gas assumption can sometimes lead to serious errors. The fugacity coefficients are used to describe nonidealities in the vapour phase. One of the more popular methods of calculating these quantities is the use of a virial equation of state. The virial equation represents the volume of the system in terms of the following power series:

$$z = \frac{PV}{RT} = 1 = \frac{B}{V} + \frac{C}{V^2} + \frac{D}{V^3} + \ldots\ldots \qquad (7.6)$$

where V is the molar volume, z the compressibility factor, B is the second virial coefficient, C, is the third virial coefficient, and D is the forth virial coefficient. The virial equation can also be written in terms of an expansion about the pressure:

$$z = \frac{RV}{RT} = 1 + B'P = C'P^2 + \ldots\ldots\ldots \qquad (7.7)$$

The two forms of the second and the third virial coefficients are related as follows,

$$B' = \frac{B}{RT} \qquad (7.8)$$

$$C' = \frac{C - B^2}{(RT)^2} \tag{7.9}$$

The virial coefficients are functions only of temperature. In the case of mixtures, concentration dependant mixing rules are used to calculate the virial coefficients. For simplicity the equation is truncated after the second virial coefficient. The equation is then accurate only at low to moderate pressures.

One of the advantages of the virial expansion is the relationship between the virial coefficients and the intermolecular forces. For an ideal gas, the intermolecular forces between the molecules are zero, and the virial coefficients are zero. Under such conditions, the corresponding factor z is equal to unity. At conditions other than ideal, expressions for the virial coefficients can be related to the intermolecular forces through the use of statistical mechanics. For mixtures, the second virial coefficient is given by the following theoretically based mixing rule,

$$B_{mix} = \Sigma_{i=1}^{m} \Sigma_{j=1}^{m} y_i y_j B_{ij} \tag{7.10}$$

Here m is the number of components and B_{ij} is the virial coefficients representing the interaction between the components i and j.

The fugacity coefficient is given by,

where ϕ_i is the fugacity coefficient and f_i is the fugacity of component i. Truncating

$$RT\ln\phi_i = RT\ln\frac{f_i}{\gamma_i P} = \int_o^P [v_i - \frac{RT}{P}]dP \qquad (7.11)$$

the virial expression after the second term, and substituting the pressure explicit equation into equation 7.11, we arrive at an expression for the fugacity coefficient after differentiation and integrating

$$\ln\phi_i = [2\Sigma_{j=1}^{m} y_i B_{ij} - B_{mix}]\frac{P}{RT} \qquad (7.12)$$

One of the more successful methods used to calculate second virial coefficients is that of Hayden and O'Connell[36] (used for calculation of G^E shown in Table 7.4). The method is a predictive method, with the virial coefficients being functions of dipole moment, temperature, pressure, critical temperature, critical pressure, and the degree of association between the interacting components. The virial coefficients is assumed to be the sum of two types of interactions:

$$B_{ij} = B_{ij}^F + B_{ij}^D \qquad (7.13)$$

where B_{ij}^F is the contribution due to relatively "free" molecules, those in which physical forces are weak, and B_{ij}^D is the contribution due to bound or dimerized molecules. To use equation 7.12, virial coefficients B_{ij} which depend on temperature are required.

7.3.2. The Liquid Phase

In the liquid mixture the activity coefficients are directly related to the molar excess Gibbs energy G^E defined by,[123]

$$G^E = RT\Sigma_i^m x_i \ln\gamma_i \qquad (7.14)$$

Many functional forms of the excess Gibbs energy have been developed over the years. These mathematical models, based on molecular considerations, provides a convenient method for expressing G^E as a function of x. From this function an individual activity coefficient γ_i for component i can be calculated from G^E using the relationship

$$RT\ln\gamma_i = [\frac{\partial n_t G^E}{\partial n_i}]_{T,P,n_{j\neq i}} \qquad (15)$$

where n_i is the number of moles. Some of the more successful G^E solution models are described in chapter 9 in great detail. These include among others, the WILSON,[5] NRTL,[6] UNIQUAC,[7] and DISQUAC[9] models. Modified UNIFAC[8] model was tested as well. All these theories have been used to describe the VLE data measured in this work.

7.3.3. Vapour Liquid Equilibrium Data for a Solute + Sulfolane

Isothermal vapour-liquid equilibria at 338.15 K or 353.15 K for 1-heptyne, or tetrahydrofuran or 1,4-dioxane, or tetrachloromethane or trichloroethane + sulfolane binary mixtures have been determined using an ebulliometric (P,T,x,y) method. The

excess molar Gibbs energies determined from the vapour-liquid equilibrium data present positive trends for all mixtures, with the maximum varying from 480 $J \cdot mol^{-1}$ to 1550 $J \cdot mol^{-1}$. The data reported have been successfully described using the Margules, van Laar, Wilson, NRTL and UNIQUAC equations, using the program VLE given in APPENDIX 1.

Because of the important industrial applications of sulfolane, several investigators have studied the vapour-liquid phase equilibria (VLE) for binary [124-126] and ternary mixtures containing sulfolane and aromatic hydrocarbons (benzene, toluene, ethylbenzene) or dichloromethane or propan-2-ol. VLE data for mixtures containing sulfolane have not often been the subject of a theoretical interpretation.

For the mixtures studied in this work, no experimental data have been published in the literature. 1-Heptyne was chosen because it contained a triple carbon-carbon bond, tetrahydrofuran and 1,4-dioxane as cyclic ethers containing one or two ether groups respectively, and tetrachloromethane and trichloroethane as examples of compounds containing two different types of Cl atoms.

The experimental data has allowed us to obtain new interaction parameters for the above mentioned groups with sulfolane (as an individual group) in the DISQUAC[9] and Modified UNIFAC models.[8]

The solution models for the molar excess Gibbs energy, were chosen for the reduction of the VLE data as representatives of local composition equations and semi-empirical enthalpic expressions, respectively.

The isothermal VLE data obtained for the mixtures studied are presented in Table 7.4, along with the liquid and the vapour mole fractions. The activity coefficients γ_i were calculated using the following equation:

$$\phi_i P y_i = \gamma_i P_i^0 x_i \phi_{x_i}^0 \exp[V_i(P - P_i^0)/RT] \qquad (7.16)$$

where ϕ_i and ϕ_i^0, the fugacity coefficients of component i in the mixture and pure vapour, respectively, were evaluated by using the second virial coefficients obtained by the Hayden-O'Connell method[36]. The vapour pressures of the pure components, P_i^0, were obtained using fitted parameters from the literature.[127] These are reproduced in Table 7.3. The pure vapour pressures of the solvents P_i^0 measured in this work agree with the literature values[128] within 3 kPa. The liquid molar volumes, V_i were calculated from the densities at 298.15 K[127] and are included in Table 7.1. The critical properties and other parameters required for estimating the second virial coefficients, obtained from the literature [123,129], are listed in Table 7.5 The VLE data are reported in Table 7.4 along with the activity coefficients of both components and the excess molar Gibbs energies, (G^E), calculated from:

$$G^E = RT(x_1 \ln\gamma_1 + x_3 \ln\gamma_3) \qquad (7.17)$$

The activity coefficients and the excess molar Gibbs energies were correlated with the Margules, van Laar, Wilson, nonrandom two-liquid (NRTL) and UNIQUAC eqns. UNIQUAC pure component parameters for the surface area (q) and volume (r) of the molecules were taken from the literature [130] and are listed in Table 7.6.

According to the computer program used[129], the experimental data were shown to be thermodynamically consistent by using the integral or area test described by the DECHEMA group (Gmehling and Onken [131]). The simple area test does not confirm

thermodynamic consistency according to (* Van Ness and Abbot, 1982)[1]. The first test preformed by the DECHEMA group is commonly referred to as the integral or area test. The test uses the following basic equation,

$$\int_{x_1=0}^{x_1=1} \ln[\frac{\gamma_1}{\gamma_3}]dx_1 = 0 \qquad (7.18)$$

Experimental values for the activity coefficients were plotted versus mole fraction in the form of equation 7.18, a polynomial was fit to the data, and the integral from 0 to 1 was calculated. Systems which produced an integral near zero were considered to pass the consistency test. A second test, following the DECHEMA group was also conducted. This involves a numerical method for the prediction of the mole fraction of a component in the vapour phase. The pressure of a mixture can be represented by the following equation,

$$P^* = \frac{x_1\gamma_1^* f_1}{\phi_1} + \frac{x_3\gamma_3^* f_3}{\phi_3} \qquad (7.19)$$

The quantities have been defined previously (Chapter 2, section 2.1). Here the asterisk denotes a calculated or predicted value. An ideal vapour phase was assumed, following the authors of the DECHEMA data base[131], resulting in

$$P^* = x_1\gamma_1^* P_1 + x_3\gamma_3^* P_3 \qquad (7.20)$$

---

[1]*Van Ness,H.C., Abbott,M.M. Clasical Thermodynamics of Nonelectrolyte solutions, Mc Graw-Hill, 1982.

For the purpose of the test, an expression is needed for γ_i^*. The DECHEMA authors used a Legendre polynomial expression. Parameter estimates were obtained through a least squares fit of the following objective function:

$$Q = \Sigma_{i=1}^{n}(P - -P^*)_i^2 \qquad (7.21)$$

After obtaining a set of parameters which best fit the data, the values of y_1 were estimated by

$$y_1^* = \frac{x_1\gamma_1^* P_1}{P^*} \qquad (7.22)$$

and the following quantity was defined:

$$\Delta y = y_1 - y_1^*$$

If the average of Δy was less than 0.01 for a particular system, the data was classified as being thermodynamically consistent.

Calculations done using the van Laar, Margules or Wilson equations were found to be inferior to the NRTL and UNIQUAC equations. The nonrandomness parameter α (in the NRTL equation), listed in Table 7.7, was obtained as a third adjustable parameter and is in the range of 0.3 to 1.4, being especially high for the 1,4-dioxane + sulfolane mixture.

The calculated results using the UNIQUAC equation for the activity coefficients and the excess molar Gibbs energies, are shown by solid lines in figures 7.5 (a-c) and 7.6. All systems studied exhibit zeotropic behaviour. Each of the five mixtures studied in this work, showed significant positive deviations from ideality. The largest deviation was found for the mixture 1-heptyne + sulfolane ($G^E_{max} \approx 1550$ J·mol^{-1}).

The maximum values of G^E for tetrahydrofuran + sulfolane at 353.15 K, and 1,4-dioxane + sulfolane at 353.15 K are $G^E_{max} \approx 1400$ J·mol^{-1} and $G^E_{max} \approx$

500 J·mol^{-1}, respectively, and reflect a stronger AB interaction in the case of the 1,4-dioxane + sulfolane mixture.

A comparison of the excess molar Gibbs energies for the tetrachloromethane + sulfolane mixture ($G^E_{max} \approx 1360$ J·mol^{-1}) and the 1,1,1-trichloroethane + sulfolane mixture ($G^E_{max} \approx 1050$ J·mol^{-1}) with the excess molar Gibbs energy, obtained (1) for the related mixture of dichloromethane + sulfolane, ($G^E_{min} \approx -130$ J·mol^{-1} at 303.15 K), suggests complex-forming interaction between the dichloromethane and sulfolane molecules. This indicates a different type of interaction between tetrachloromethane and sulfolane on the one hand, and between 1,1,1-trichloroethane and sulfolane on the other. The asymmetric molecule 1,1,1-tricholorethane shows weaker interactions with sulfolane than does dichloromethane.

The G^E results obtained in this work are in the same range as the literature data for the propanol + sulfolane system, ($G^E_{max} \approx 1590$ J·mol^{-1} at 303.15 K). For benzene + sulfolane and toluene + sulfolane the results are ($G^E_{max} \approx 670$ J·mol^{-1} at 303.15 K) and ($G^E_{max} \approx 980$ J·mol^{-1} at 303.15 K), respectively.

The experimental values of the excess molar enthalpies H^E for two of the systems studied here have been reported in the literature. H^E_{max} for 1,1,1-tricholoroethane + sulfolane at 303.15 K was found to be 220 J·mol^{-1}. The H^E_{max} versus mole fraction for 1,4-dioxane + sulfolane mixture (also at 303.15 K) was found to be sinusoidal with a H^E_{min} of -40 J·mol^{-1} in the sulfolane rich region, and H^E_{max} of 45 J·mol^{-1} in the 1,4-dioxane rich region. The excess enthalpy of mixing for the 1-heptyne + sulfolane system has also been measured at 303.15 K (see Chapter 6), and shows endothermic deviations from ideality with $H^E_{max} \approx 340$ J·mol^{-1}. These enthalpic results reflect the same interaction as we have interpreted from the Gibbs energy results above.

For the mixtures studied in this work, strong nonideal behaviour is evident from the magnitude of the activity coefficients, given in Table 7.4. The values of γ_i range from 1 to 4 for $x_1 > 0.15$. The 1,4-dioxane + sulfolane mixture (with small values for both G^E_{max} and H^E_{max}) is the least non-ideal mixture with γ_i never exceeding 1.5 for $x_1 > 0.15$.

The activity coefficient at infinite dilution, γ_1^∞, for each of the solvents in sulfolane was calculated using UNIQUAC parameters obtained from (VLE) data. γ_1^∞ for the mixtures tetrahydrofuran at 338.15 K, 1-heptyne + sulfolane at 353.15 K and tetrahydrofuran + sulfolane at 353.15 K are 2.3, 6.2 and 3.8, respectively.[132-133] γ_1^∞ for these two systems were obtained by the G.L.C. technique. The results for the mixtures 1-heptyne + sulfolane at 313.15 K, and 303.15 K (23), and tetrahydrofuran + sulfolane at 303.15 K are 7.78, 8.10, and 2.24, respectively. A further system 1,4-dioxane + sulfolane at 298.15 K has also been measured by the G.L.C. technique and the resulting γ_1^∞ obtained is 3.32 whereas the value obtained in this work, is 1.5 at 353.15 K.

7.4. Parameter Optimization

Methods to regress the constants for the various activity coefficients models and equations of state are discussed here. The recommended method is know as the error-in-variables maximum likelihood technique.[134]

The adjustable parameters, designated as θ_i, are included in the expressions for the activity coefficients, γ_i^*, or the fugacity coefficients, ϕ_i^*.

$$\gamma_i^* = f(x_i, T, \theta_1, \theta_2, \ldots) \tag{7.24}$$

$$\phi_i^* = f(x_i, T, P, \theta_1, \theta_2, \ldots) \tag{7.25}$$

The x_i in equations 7.18 and 7.19 refer to the liquid phase mole fraction. The asterisk indicates a calculated quantity, as opposed to an experimental one. The problem then becomes one of finding the set of parameters θ_1, θ_2,..., which best fit the data set. Two approaches are used in this work, the method of least squares, and the more popular "maximum likelihood method".

7.4.1. The Least Squares Regression

The goal of a least squares method is to choose the set of parameter estimates which minimize the sum of the squares of the error between one or more experimental and calculated quantities. The objective function, then, is the sum of the squares of the errors. Four quantities are often measured experimentally, P, T, x_i,and y_i, meaning that the errors of any of these four, or any combination of the four can be part of the objective function.

7.4.1.2. Least Squares Objective Functions for the Activity Coefficient Models

VLE in a binary system can be described by the following equations

$$y_1 P\phi_1 = x_1 \gamma_1 f_i^o \tag{7.26}$$

$$y_3 P\phi_3 = x_3 \gamma_3 f_3^o \tag{7.27}$$

The quantities have been defined earlier.

These are two equations, with four experimental variables. Therefore, two variables must be considered as independent and the other two as dependent, so as not to *over specify the system.*

In addition to the four experimental quantities P, T, x_i, and y_i, experimental activity coefficients can be defined as

$$\gamma_i = \frac{y_i P\phi_i}{x_i f_i^o} \tag{7.28}$$

Two guideline must be used or the selection of the objective function.

First, information from both constraints, equations 7.18, and 7.19, should be used in the evaluation. For example,

$$Q=\Sigma_{i=1}^{n}[(\gamma_1-\gamma_1^*)_i^2+(\gamma_3-\gamma_3^*)_i^2] \tag{7.29}$$

was used in favour of

$$Q=\Sigma_{i=1}^{n}(\gamma_1-\gamma_1^*)_i^2 \tag{7.30}$$

because equation 7.24 disregards information from the second constraint. Equation 7.23, in which the residual is based on the activity coefficient of both components, was found to give better results.

A second guideline, was to avoid minimization based solely on the error in the vapour mole fractions, y_i. Measurements of this quantity are usually the most inaccurate in comparison to measurements of P, T, and x_i. The large uncertainties associated with y_1 will be propagated into larger uncertainties in the parameter estimates. An objective functions used here, which overcomes this problem is

$$Q=\Sigma_{i=1}^{n}[(y_1-y_1^*)_i^2+(y_3-y_3^*)_i^2+(\frac{P-P^*}{P})_i^2] \tag{7.31}$$

The calculated pressure can be derived from equation 7.27 as

$$P^* = \frac{x_1 \gamma_1 f_1^o}{\phi_1} + \frac{x_2 \gamma_2 f_2^o}{\phi_2} \tag{7.32}$$

Regression using equation 7.31, require the simultaneously solution of the constraints for y_1^* and P^*. The fugacity coefficients, ϕ_i, are functions of pressure and y_i. the standard state fugacity, f_i^o, are functions of pressure through the following approximation

$$f_i^o = \phi_i^{sat} P_i^{sat} \exp[\frac{(P^* - P_i^{sat}) V_i}{RT}] \tag{7.33}$$

where ϕ_i^{sat} is the fugacity coefficient of pure saturated vapour of component i, P_i^{sat} is the vapour pressure of component i at temperature T, and V_i is the molar volume of the pure liquid.

In the calculation of the fugacity coefficient and standard state fugacities, experimental values of P and y_i cannot be used. Therefore, equation 7.26 and the following equation

$$y_1^* + y_3^* = 1 \tag{7.34}$$

must be solved simultaneously for P^* and y_1^*, where

$$y_i^* = \frac{x_i \gamma_i f_i^o}{\phi_i P^*} \tag{7.35}$$

the solution can be best achieved by the iteration sequence found in figure 7.4.

7.4.2. The Maximum Likelihood Regression

Although the least squares approach produces parameter estimates which fit the experimental data well, an alternative approach was used. The criterion for the selection of parameters in the maximum likelihood method is slightly different than the one for the least squares method. In this procedure, parameters are chosen to minimize the deviation in all experimental quantities simultaneously.

An important characteristic is the lack of distinction between dependent and independent variables. In the least squares approach, objective functions and consequently parameter estimates, differ for each designation of dependent and independent variables. Only one objective function exists in the maximum likelihood technique. "Likelihood", in the statistical sense is a measure of the probability of an event to occur. The event in a VLE application is the simultaneous occurrence of the values for the pressure, temperature and liquid and vapour concentrations. The objective function for the maximum likelihood is a measure of this probability. The regressed parameters then are those which maximize the "likelihood" or the probability of the occurrence of the data set. To calculate this probability, the method takes into account all the experimental data, along with estimates of their errors.The method provides information on the degree of accuracy of these parameters. The accuracy of the maximum likelihood parameters are a function of the accuracy of the experimental data, since estimates of the variance of the experimental data are variable of the objective function.

The method employed in this work, follows the error-in-variables method of Patino-Leal and Reilly[135] and Prausnitz et al[123]. Each variable has associated with it an error defined as the difference between the estimate of the true value of the variable and the measured value of the variable. The following symbols are used to distinguish between the quantities:

$$P = \xi_1 + \epsilon_1 \tag{7.36}$$

$$T = \xi_2 + \epsilon_2 \tag{7.37}$$

$$x_1 = \xi_3 + \epsilon_3 \tag{7.38}$$

$$y_1 = \xi_4 + \epsilon_4 \tag{7.39}$$

where ξ_i is the estimate of the true value of the variable i, and ϵ_i is the error of the quantity i. Therefore not only do the parameter estimates need to be regressed, but also the estimates of the true values of the variables. The advantage of this method, is that the calculation of the estimates of the true values of the variables is less time consuming and less complicated than previous methods.

For a system to be in equilibrium in terms of activity coefficients, equations 7.18 and 7.19 must be valid simultaneously. The constraint equations for regressing the parameters θ_1, θ_2,..., are then

$$F_1 = \phi_1 \xi_4 \xi_1 - \xi_3 \gamma_1 f_1^o \tag{7.40}$$

$$F_2 = \phi_2 (1 - \xi_4) \xi_1 - (1 - \xi_3) \gamma_2 f_2^o \tag{7.41}$$

F_1 and F_2 are the constraints. The error-in-variables method is a maximum likelihood method, so the likelihood or probability function for the simultaneous occurrence of

the experimental observations, P, T, x_1, y_1 has to be maximized. The likelihood function can be represented by the proportionality

$$D \propto \exp[-\frac{1}{2}\Sigma_{i=1}^{n}(z_i - \xi_i)^T v_4^{-1}(z_i - \xi_i)] \qquad (7.42)$$

where n is the number of experimental points, z_i a vector of length four containing the measured values of the variables (P, T, x_{1i}, and y_{1i}), ξ_i a vector of length four containing the true values of the variable and v_4 the (4 x 4) error-in-variable matrix. Values for these quantities should be based on the estimated errors of the experimental measurements and could be different for each data point. If such information is not available, the error estimates must be arbitrarily assigned. Superscripts T and -1 refer to the transpose and inverse, respectively.

The "likelihood" function is subject to the constraints equations 7.24 and 7.25, which must be linearized to enable regression. The functions are linearized by a Taylor series expansion about the estimates of the true values of the variables.

$$F_i + B_i(\xi_i - \xi_i') = 0 \qquad (7.43)$$

where F_i is a vector of length two containing the values of the constraints, equations 7.40 and 7.41, B_i is a (2 x 4) matrix containing the derivatives of the constraints with respect to the measured variables $B_{jk} = (\partial F_i/\partial z_k)$ and ξ_i' is a vector of length four containing estimates of the true values of the measured variables.

The ξ_i are integrated out of the distribution function through a series of statistical assumptions. Application of the assumptions reduce the proportionality to

$$D \propto \exp(-\frac{1}{2}\Sigma_{i=1}^{n} Q_i) \tag{7.44}$$

where

$$Q_i=[F_i+B_i(z_i-\xi_i')]^T(B_iVB_i^T)^{-1}[F_i+B_i(z_i-\xi_i')] \tag{7.45}$$

To maximize the likelihood function, one must minimize the summation inside the exponential term. In other words, to obtain the error-in-variable parameter estimates, one must minimize the sum of the Q_i values, where Q_i is a function of the measured data, the estimates of the true values of the measured data, the error-covariance matrix, the constraints, and the derivatives of the constraints. Values for ξ_i' can be obtained through the following algorithm:

$$\xi_i'^{(j+1)}=z_i-VB_i^T(B_iVB_i^T)^{-1}[F_i+B_i(Z_i-\xi_i'^{(j)}] \tag{7.46}$$

where j= 1,2,... . To start the iteration, set $\xi_i'^{(1)} = z$, and continue until the change in Q_i is less than some tolerance.

To simplify the calculation, one can use the experimental data as an estimate of the true values of the variables, $\xi_i' = z_i$. The iterative solution represented by equation 7.46, is eliminated and equation 7.45 reduces to

$$Q_i=F_i^T(B_iVB_i^T)^{-1}F_i \tag{7.47}$$

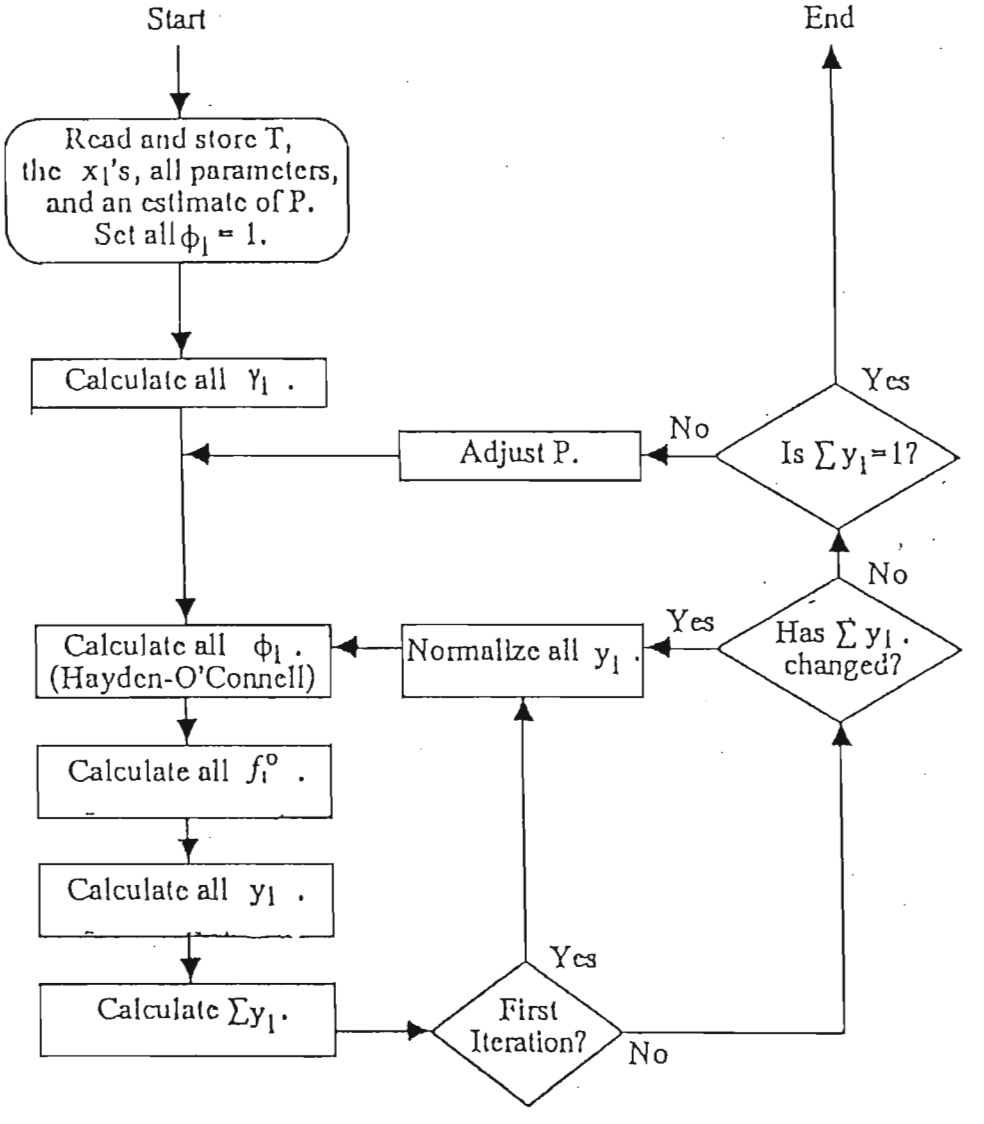

FIGURE 7.4. An Algorithm for the Simultaneous Solution for P and y_i

Because the estimates of the true values of the variables, ξ_i' are not involved in the calculations, parameters found using equation 7.47 are called approximate error-in-variable method. The solution to equation 7.45 is referred to as the exact solution.

TABLE 7.1. Physical Properties of the Pure Components at 298.15 K, Molar Volumes V_i, Refractive Indexes n_D, and Melting Point T_m

component	V_i/cm^3·mol^{-1} [127]	n_D		T_m/K	
		exptl	lit.[127]	exptl	lit.[128]
1-heptyne	138.10	1.40821	1.4080 [a]		
tetrahydrofuran	81.09	1.40512	1.40496		
1,4-dioxane	85.66	1.02786	1.02797		
tetrachloromethane	97.15	1.58435	1.58439		
1,1,1-trichloroethane	100.37	1.43612	1.4359		
sulfolane	95.26	1.48114	1.4810(10)[b]	301.60	301.60

[a] at 293.15 K
[b] at 303.15 K

Table 7.2. Coefficients of Equation 7.5 (n_D) for Mixtures Involving Sulfolane and a Second Component

Second Component	K	L	M
1-heptyne	-0.00199	0.08027	1.40390
tetrahydrofuran	-0.03888	0.11850	1.40286
1,4-dioxane	-0.01407	0.07912	1.41777
tetrachloromethane	-0.03332	0.06196	1.45418
1,1,1-trichloroethane	-0.03182	0.07415	1.43104

TABLE 7.3. Coefficients used in the Determination of the Pure Vapour Pressure of the Component[127,129]

component	A	B	C	$D10^6$	E
1-heptyne[a]	4.0737	1289.55	217		
tetrahydrofuran[a]	6.7537	1146.39	230		
1,4-dioxane[b]	52.2272	-5677.77	-4.364	1.9626	2.0
tetrachloromethane[b]	78.4339	-6128.10	-8.576	6.8461	2.0
1,1,1-trichloroethane[a]	6.9063	1211.31	226		
sulfolane[c]	28.6824	4350.70	6.563		

[a] coefficients of equation $\log (P_i^o/\text{Torr}^*) = A - B/(C + (t/°C))$ [127]
[b] coefficients of equation $\ln (P_i^o/\text{Pa}) = A + B/(T/K) + C \ln (T/K) + [D(T/K)]E$ [129]
[c] coefficients of equation $\log (P_i^o/\text{Torr}^*) = A - B/(T/K) - C \log (T/K)$ [127]
* mmHg

TABLE 7.4. Vapour-Liquid Equilibrium Data for the Solvents (1) + Sulfolane (3) Mixtures at the Temperature T, Experimental Vapour Pressure, P, Liquid Phase, x_1, and Vapour Phase, y_1, Mole Fractions and Activity Coefficient, γ_i, and G^E as Calculated by UNIQUAC

P/kPa	x_1	y_1	γ_1	γ_3	G^E/J·mol^{-1}
		1-heptyne (1) + sulfolane(3) at T = 353.15 K			
0.058	0.0000	0.0000	-	-	0.0
32.509	0.1480	0.9985	4.144	1.033	699.6
35.901	0.1770	0.9986	3.852	1.048	814.8
39.700	0.2170	0.9987	3.487	1.075	961.3
41.349	0.2400	0.9988	3.296	1.093	1038.8
44.143	0.3180	0.9999	2.766	1.176	1263.9
45.488	0.3710	0.9990	2.423	1.254	1382.1
46.741	0.4720	0.9991	1.948	1.474	1524.2
47.446	0.5570	0.9992	1.645	1.766	1552.6
49.217	0.7400	0.9993	1.218	3.114	1293.6
50.070	0.8670	0.9994	1.059	5.580	815.9
54.047	1.0000	1.0000	-	-	0.0
		tetrahydrofuran (1) + sulfolane (3) at T = 338.15 K			
0.022	0.0000	0.0000	-	-	0.0
53.220	0.3520	0.9998	1.868	1.021	625.2
56.840	0.3960	0.9998	1.787	1.037	665.5
62.000	0.4520	0.9998	1.663	1.071	717.2
66.440	0.5100	0.9998	1.558	1.116	748.2
70.610	0.5680	0.9998	1.455	1.176	760.7
72.860	0.6100	0.9998	1.387	1.234	757.0
76.460	0.6560	0.9998	1.318	1.313	739.6
79.720	0.7130	0.9998	1.245	1.442	696.6
82.240	0.7650	0.9998	1.177	1.602	634.5
86.930	0.8300	0.9999	1.108	1.888	522.2
90.970	0.8920	0.9999	1.055	2.304	374.0
98.035	1.0000	1.0000	-	-	0.0

TABLE 7.4 continued...

P/kPa	x_1	y_1	γ_1	γ_3	G^E/J·mol^{-1}
		tetrahydrofuran (1) + sulfolane (3) at T = 353.15 K			
0.058	0.0000	0.0000	-	-	0.0
49.959	0.1700	0.9990	3.822	0.989	623.9
54.233	0.1970	0.9992	3.699	0.991	714.1
65.480	0.2350	0.9993	3.528	0.996	836.2
71.526	0.2670	0.9994	3.387	1.002	934.4
76.907	0.2950	0.9994	3.264	1.010	1016.5
78.453	0.3100	0.9995	3.199	1.015	1058.9
82.374	0.3250	0.9995	3.135	1.021	1100.2
90.694	0.3850	0.9995	2.881	1.052	1253.4
99.827	0.4500	0.9996	2.616	1.104	1394.8
151.55	1.0000	1.0000	-	-	0.0
		1,4-dioxane (1) + sulfolane (3) at T = 353.15 K			
0.058	0.0000	0.0000	-	-	0.0
26.100	0.3960	0.9988	1.391	1.009	385.8
29.212	0.4590	0.9989	1.349	1.023	425.1
31.596	0.5080	0.9990	1.312	1.041	449.0
31.632	0.5110	0.9990	1.310	1.043	450.3
34.260	0.5670	0.9991	1.269	1.071	468.8
36.292	0.6120	0.9992	1.235	1.103	476.1
38.619	0.6720	0.9993	1.190	1.161	473.3
40.868	0.7250	0.9995	1.150	1.735	456.4
42.974	0.7900	0.9996	1.104	1.371	412.9
45.271	0.8500	0.9997	1.064	1.570	344.8
47.562	0.9160	0.9998	1.027	1.941	229.8
49.715	0.9690	0.9999	1.006	2.468	97.8
50.957	1.0000	1.0000	-	-	0.0

TABLE 7.4 continued.

P/kPa	x_1	y_1	γ_1	γ_3	G^E/J·mol^{-1}
	tetrachloromethane (1) + sulfolane (3) at T = 338.15 K				
0.022	0.0000	0.0000	-	-	0.0
55.839	0.3050	0.9997	2.581	1.075	952.3
59.646	0.3790	0.9998	2.323	1.134	1115.1
63.361	0.4430	0.9998	2.113	1.209	1227.3
64.743	0.4910	0.9998	1.965	1.287	1291.5
65.563	0.5480	0.9998	1.799	1.414	1342.4
66.248	0.6100	0.9998	1.631	1.614	1362.0
66.627	0.6680	0.9998	1.487	1.897	1341.0
66.880	0.7370	0.9998	1.334	2.445	1256.7
66.968	0.7860	0.9998	1.238	3.084	1150.2
67.244	0.8470	0.9998	1.168	4.527	951.9
69.956	1.0000	1.0000	-	-	0.0
	1,1,1,-trichloroethane (1) + sulfolane (3) at T = 338.15 K				
0.022	0.0000	0.0000	-	-	0.0
46.670	0.2780	0.9996	2.174	1.047	698.0
51.208	0.3300	0.9997	2.046	1.073	795.5
55.664	0.4060	0.9997	1.868	1.129	914.1
59.375	0.4740	0.9997	1.719	1.203	992.5
61.692	0.5400	0.9998	1.582	1.306	1039.7
64.047	0.6120	0.9998	1.444	1.474	1053.2
65.702	0.6720	0.9998	1.339	1.682	1029.0
67.089	0.7300	0.9998	1.247	1.950	969.6
68.377	0.7800	0.9998	1.176	2.362	885.4
69.545	0.8070	0.9999	1.141	2.642	825.5
78.005	1.0000	1.0000	-	-	0.0

TABLE 7.5. Critical Properties and Parameters Characterising Vapour-Phase Nonideality, Where T_c is the Critical Temperature, P_c is the Critical Pressure, V_c the Critical Volume, ω the Acentric Factor, and RD the Mean Radius of Gyration, and DM the Dipole Moment [123,126,129]

component	T_c/K	P_c/kPa	V_c/cm^3·mol^{-1}	ω	RD/Å	DM/D
1-heptyne	537.30	3210	387.0	0.3580	0.358	0.00
tetrahydrofuran	540.15	5187	224.0	1.9280	2.600	1.63
1,4-dioxane	588.00	5140	238.0	0.2804	3.110	0.00
tetrachloromethane	556.30	4557	276.0	0.1926	3.759	0.00
1,1,1-trichloroethane	533.15	5066	220.0	0.1905	3.759	1.10
sulfolane	776.00	4990	286.9	0.8608	2.910	4.10

Table 7.6. UNIQUAC Pure Component Parameters for Volume (r) and Surface Area (q) of the Compound [129,130]

component	r	q
1-heptyne	4.891	4.096
tetrahydrofuran	2.919	2.722
1,4-dioxane	3.185	2.640
tetrachloromethane	3.390	2.910
1,1,1-trichloroethane	3.541	3.032
sulfolane	4.036	3.206

TABLE 7.7. The Parameters for the NRTL and UNIQUAC Equations Determined from Binary Vapour Liquid Equilibria for the Systems Solvent (1) + Sulfolane (3), as well as the Calculated Standard Deviation for the Total Pressure and the Calculated Gibbs Energy

component	Parameters				
	NRTL			UNIQUAC	
	$g_{12}-g_{22}$	$g_{21}-g_{11}$	α	$u_{12}-u_{22}$	$u_{21}-u_{11}$
	$J \cdot mol^{-1}$			$J \cdot mol^{-1}$	
1-heptyne	5861.27	4055.48	0.47	2532.93	-387.22
tetrahydrofuran (338.15 K)	3536.88	2703.35	0.94	1993.08	-774.27
tetrahydrofuran (358.15 K)	12964.17	418.34	0.31	5813.39	-1295.09
1,4-dioxane	3230.87	1326.03	1.38	2820.19	-1381.27
tetrachloromethane	7306.35	2941.97	0.46	3308.94	-651.30
1,1,1-trichloroethane	5202.51	2820.52	0.61	2758.08	-772.98

	Deviations			
	NRTL		UNIQUAC	
	$\sigma(P)^a$/Pa	$\sigma(G^E)^b$/J·mol^{-1}	$\sigma(P)^a$/Pa	$\sigma(G^E)^b$/J·mol^{-1}
1-heptyne	2.4	67.96	1.1	50.77
tetrahydrofuran (338.15 K)	1.2	54.82	0.4	24.15
tetrahydrofuran (353.15 K)	0.7	45.86	0.6	2.65
1,4-dioxane	0.5	31.51	0.9	21.15
tetrachloromethane	1.2	93.23	2.6	62.09
1,1,1-trichloroethane	1.4	67.80	3.4	52.23

[a] $\sigma(P) = [\Sigma_{i=1} (P_i^{exptl} - P_i^{calcd})^2/ (n-2)]^{1/2}$

[b] $\sigma(G^E) = [\Sigma_{i=1} (G^E{}_i^{exptl} - G^E{}_i^{calcd})^2/ (n-2)]^{1/2}$

TABLE 7.8. The Parameters for the MARGULES, van Laar, and WILSON Equations Determined from Binary Vapour Liquid Equilibria for the Systems Solvent (1) + Sulfolane (3), as well as the Calculated Standard Deviation for the Total Pressure

Margules		van Laar		WILSON	
A_{13}	A_{31}	A_{13}	A_{31}	τ_{13}	τ_{31}
		1-heptyne + sulfolane			
2.2796	1.6751	2.3477	1.7125	2477.70	2708.73
$\sigma(P)^a$/Pa	5.942	5.652		1.688	
		tetrahydrofuran + sulfolane			
0.7428	2.8812	1.2381	4.6290	2669.71	5892.00
$\sigma(P)^a$/Pa	2.256	0.823		12.153	
		dioxane + sulfolane			
-0.1453	0.8976	0.3908	1.1620	-915.57	4706.78
$\sigma(P)^a$/Pa	1.608	0.813		0.756	
		tetrahydrofuran + sulfolane (335.15 K)			
0.3843	1.2686	0.6921	1.4095	386.25	3750.47
$\sigma(P)^a$/Pa	2.605	1.783		0.145	
		tetrachloromethane + sulfolane			
0.5840	2.05560	1.3298	2.9193	2506.77	9677.94
$\sigma(P)^a$/Pa	5.661	3.009		2.042	
		1,1,1-tricholoethane + sulfolane			
0.6137	1.9461	1.0748	2.1504	1103.63	5850.59
$\sigma(P)^a$/Pa	5.959	3.572		1.456	

[a] $\sigma(P) = [\Sigma_{i=1} (P_i^{exptl} - P_i^{calcd})^2/ (n-2)]^{1/2}$

TABLE 7.9. Activity coefficients of a solute (1) + sulfolane (3) across the whole mole fraction range determined using the Margules, van Laar, WILSON, NRTL and UNIQUAC equations.

	VanLaar		Margules		WILSON	
x_1	γ_1	γ_3	γ_1	γ_3	γ_1	γ_3
			1-heptyne + sulfolane at T = 353.15 K			
0.1480	2.049	1.057	3.841	1.027	2.545	1.025
0.1770	1.975	1.084	3.594	1.041	2.406	1.036
0.2170	1.878	1.132	3.279	1.064	2.235	1.055
0.2400	1.825	1.167	3.111	1.081	2.145	1.068
0.3180	1.660	1.328	2.606	1.158	1.883	1.124
0.3710	1.561	1.490	2.316	1.232	1.736	1.173
0.4720	1.396	1.988	1.870	1.441	1.507	1.300
0.5570	1.281	2.745	1.585	1.717	1.358	1.453
0.7400	1.101	3.462	1.189	2.933	1.132	2.041
0.8670	1.027	4.333	1.049	4.916	1.038	2.917
	NRTL		UNIQUAC			
0.1480	4.318	1.054	4.141	1.033		
0.1770	3.887	1.076	3.849	1.048		
0.2170	3.405	1.111	3.484	1.075		
0.2400	3.175	1.134	3.293	1.093		
0.3180	2.571	1.231	2.734	1.176		
0.3710	2.271	1.314	2.422	1.254		
0.4720	1.852	1.524	1.946	1.474		
0.5570	1.599	1.781	1.644	1.766		
0.7400	1.231	2.913	1.217	3.111		
0.8670	1.072	5.200	1.058	5.571		

TABLE 7.9 continued

	VanLaar		Margules		WILSON	
x_1	γ_1	γ_3	γ_1	γ_3	γ_1	γ_3
			tetrahydrofuran + sulfolane at 338.15 K			
0.3520	1.110	1.295	1.526	1.015	1.641	1.114
0.3900	1.102	1.395	1.491	1.029	1.568	1.142
0.4520	1.089	1.623	1.426	1.063	1.461	1.205
0.5100	1.076	1.947	1.361	1.110	1.373	1.277
0.5680	1.064	2.451	1.295	1.176	1.295	1.367
0.6100	1.055	3.001	1.249	1.240	1.245	1.447
0.6560	1.045	3.901	1.200	1.328	1.195	1.553
0.7130	1.034	5.794	1.145	1.472	1.147	1.711
0.7650	1.025	9.029	1.100	1.647	1.098	1.913
0.8300	1.014	18.051	1.054	1.942	1.054	2.241
0.8920	1.006	41.920	1.023	2.353	1.023	2.704
	NRTL		UNIQUAC			
0.3520	1.582	1.165	1.867	1.021		
0.3900	1.513	1.196	1.787	1.036		
0.4520	1.418	1.254	1.663	1.071		
0.5100	1.345	1.317	1.556	1.115		
0.5680	1.283	1.392	1.454	1.176		
0.6100	1.242	1.459	1.387	1.233		
0.6560	1.200	1.546	1.318	1.312		
0.7130	1.153	1.687	1.240	1.442		
0.7650	1.114	1.862	1.177	1.602		
0.8300	1.069	2.190	1.108	1.888		
0.8920	1.033	2.719	1.055	2.304		

TABLE 7.9 continued

	VanLaar		Margules		WILSON	
x_1	γ_1	γ_3	γ_1	γ_3	γ_1	γ_3
			tetrahydrofuran + sulfolane at 353.15 K			
0.1700	1.097	1.173	2.752	0.980	2.315	1.016
0.1970	1.094	1.251	2.779	0.978	2.252	1.023
0.2350	1.091	1.404	2.781	0.978	2.166	1.034
0.2670	1.088	1.589	2.752	0.982	2.096	1.045
0.2950	1.086	1.812	2.708	0.988	2.036	1.057
0.3100	1.084	1.963	2.677	0.993	2.005	1.064
0.3250	1.083	2.142	2.642	0.999	1.975	1.072
0.3850	1.077	3.315	2.468	1.037	1.857	1.109
0.4500	1.070	6.470	2.240	1.113	1.738	1.163
	NRTL		UNIQUAC			
0.1700	3.039	1.015	3.822	0.989		
0.1970	2.960	1.021	3.699	0.991		
0.2350	2.852	1.031	3.528	0.996		
0.2670	2.761	1.043	3.386	1.002		
0.2950	2.681	1.054	3.264	1.010		
0.3100	2.639	1.062	3.199	1.015		
0.3250	2.597	1.070	3.134	1.021		
0.3850	2.430	1.110	2.881	1.051		
0.4500	2.250	1.173	2.616	1.104		

TABLE 7.9 continued

x_1	VanLaar γ_1	VanLaar γ_3	Margules γ_1	Margules γ_3	WILSON γ_1	WILSON γ_3
			1,4-dioxane + sulfolane at T = 353.15 K			
0.3960	1.030	1.398	1.281	0.944	1.387	1.070
0.4590	1.027	1.659	1.268	0.952	1.332	1.103
0.5080	1.024	1.978	1.247	0.967	1.290	1.136
0.5110	1.024	2.003	1.246	0.968	1.288	1.139
0.5670	1.021	2.612	1.214	0.998	1.241	1.188
0.6120	1.019	3.435	1.187	1.033	1.203	1.23
0.6720	1.015	5.527	1.144	1.101	1.164	1.328
0.7250	1.012	6.669	1.108	1.185	1.123	1.433
0.7900	1.008	7.655	1.068	1.332	1.080	1.617
0.8500	1.005	8.011	1.037	1.525	1.046	1.873
0.9160	1.002	9.364	1.012	1.833	1.017	2.331
0.9690	1.000	10.57	1.001	2.186	1.002	2.967

	NRTL		UNIQUAC	
0.3960	1.317	1.094	1.391	1.008
0.4590	1.270	1.125	1.347	1.024
0.5080	1.237	1.152	1.312	1.041
0.5110	1.235	1.154	1.309	1.042
0.5670	1.201	1.193	1.268	1.071
0.6120	1.176	1.230	1.235	1.102
0.6720	1.143	1.293	1.189	1.161
0.7250	1.116	1.369	1.150	1.235
0.7900	1.082	1.506	1.103	1.371
0.8500	1.052	1.715	1.063	1.570
0.9160	1.022	2.152	1.026	1.941
0.9690	1.004	2.920	1.006	2.467

TABLE 7.9 continued

	VanLaar		Margules		WILSON	
x_1	γ_1	γ_3	γ_1	γ_3	γ_1	γ_3
			tetrachloromethane + sulfolane at T = 338.15 K			
0.3050	1.211	1.477	2.370	0.982	2.651	1.161
0.3790	1.184	1.945	2.229	1.015	2.280	1.256
0.4430	1.160	2.704	2.061	1.073	2.025	1.364
0.4910	1.142	2.810	1.921	1.141	1.864	1.466
0.5480	1.121	3.934	1.752	1.261	1.701	1.620
0.6100	1.098	4.411	1.575	1.460	1.550	1.841
0.6680	1.078	4.962	1.425	1.744	1.429	2.126
0.7370	1.054	5.382	1.273	2.281	1.306	2.633
0.7860	1.039	7.513	1.183	2.879	1.230	3.192
0.8470	1.022	8.704	1.096	4.058	1.146	4.377
	NRTL		UNIQUAC			
0.3050	2.639	1.158	2.580	1.074		
0.3790	2.282	1.249	2.323	1.133		
0.4430	2.035	1.353	2.113	1.209		
0.4910	1.878	1.451	1.965	1.287		
0.5480	1.716	1.601	1.798	1.414		
0.6100	1.562	1.822	1.631	1.614		
0.6680	1.435	2.118	1.487	1.896		
0.7370	1.302	2.667	1.334	2.445		
0.7860	1.219	3.299	1.238	3.094		
0.8470	1.127	4.675	1.136	4.526		

TABLE 7.9 continued

	VanLaar		Margules		WILSON	
x_1	γ_1	γ_3	γ_1	γ_3	γ_1	γ_3
1,1,1-trichloroethane + sulfolane at T = 338.15 K						
0.2780	1.207	1.251	2.026	1.001	2.157	1.077
0.3300	1.188	1.399	1.954	1.017	2.001	1.113
0.4060	1.160	1.747	1.818	1.061	1.801	1.184
0.4740	1.136	2.293	1.680	1.130	1.646	1.271
0.5400	1.112	3.244	1.543	1.233	1.515	1.384
0.6120	1.087	4.327	1.402	1.407	1.390	1.556
0.6720	1.067	5.055	1.295	1.622	1.299	1.758
0.7300	1.049	6.170	1.205	1.922	1.221	2.035
0.7800	1.035	7.705	1.139	2.287	1.161	2.379
0.8070	1.028	8.310	1.108	2.540	1.131	2.627
0.2780	2.262	1.123	2.174	1.046		
0.3300	2.056	1.171	2.046	1.073		
0.4060	1.818	1.258	1.868	1.129		
0.4740	1.649	1.358	1.718	1.202		
0.5400	1.513	1.483	1.582	1.306		
0.6120	1.388	1.669	1.444	1.474		
0.6720	1.297	1.885	1.339	1.682		
0.7300	1.219	2.181	1.247	1.980		
0.7800	1.158	2.553	1.176	2.362		
0.8070	1.129	2.823	1.141	2.642		

TABLE 7.10 Activity coefficients at infinite dilution calculated by the Margules, Van Laar, WILSON, NRTL, and UNIQUAC models.

Margules		VanLaar		WILSON		NRTL		UNIQUAC	
$\ln \gamma_1^\infty$	$\ln\gamma_3^\infty$	$\ln \gamma_1^\infty$	$\ln\gamma_3^\infty$	$\ln \gamma_1^\infty$	$\ln\gamma_3^\infty$	$\ln \gamma_1^\infty$	$\ln\gamma_3^\infty$	$\ln \gamma_1^\infty$	$\ln\gamma_3^\infty$
				1-heptyne + sulfolane at T = 353.15 K					
1.675	2.279	1.712	2.347	1.254	1.638	2.162	2.717	1.816	2.521
				tetrahydrofuran + sulfolane at 338.15 K					
0.384	1.268	0.695	1.409	0.988	1.431	1.347	1.647	0.8221	1.506
				tetrahydrofuran + sulfolane at 353.15 K					
0.742	2.881	1.238	4.269	1.015	6.159	1.261	4.551	1.334	4.682
				1,4-dioxane + sulfolane at 353.15 K					
0.145	0.897	0.390	1.162	0.570	1.268	0.692	1.342	0.400	1.280

TABLE 7.10 continued

Margules		VanLaar		Wilson		NRTL		UNIQUAC	
$\ln \gamma_1^\infty$	$\ln\gamma_3^\infty$	$\ln \gamma_1^\infty$	$\ln\gamma_3^\infty$	$\ln \gamma_1^\infty$	$\ln\gamma_3^\infty$	$\ln \gamma_1^\infty$	$\ln\gamma_3^\infty$	$\ln \gamma_1^\infty$	$\ln\gamma_3^\infty$
tetrachloromethane + sulfolane at T = 338.15 K									
0.584	2.556	1.329	2.919	1.840	4.043	1.832	3.245	1.319	3.658
1,1,1-trichloromethane + sulfolane at T = 338.15 K									
0.613	1.946	1.074	2.150	1.221	2.421	1.601	2.394	1.049	2.216

TABLE 7.11. Calculated Gibbs energies, from binary equilibrium data, using the Margules, Van Laar, Wilson, NRTL, and UNIQUAC equations.

Margules	VanLaar	WILSON	NRTL	UNIQUAC
		$G^E/J \cdot mol^{-1}$		
		1-heptyne + sulfolane at T = 353.15 K		
653.3	660.5	469.6	768.3	699.6
762.2	769.3	544.1	882.9	814.8
901.1	907.6	637.6	1024.0	961.2
974.8	980.8	686.4	1096.5	1038.8
1189.0	1193.1	825.4	1298.3	1263.9
1301.4	1304.3	896.1	1398.1	1382.1
1434.5	1436.5	976.4	1508.1	1524.1
1457.5	1460.8	986.7	1519.3	1552.6
1198.9	1209.5	814.7	1268.4	1293.6
744.6	757.4	515.2	820.9	815.9
		tetrahydrofuran + sulfolane at 338.15 K		
446.0	542.5	688.4	733.5	625.1
487.7	579.4	725.8	762.3	665.5
545.9	627.8	770.1	793.4	717.2
586.8	658.5	791.8	805.3	748.2
611.6	673.3	793.5	800.4	760.7
617.8	672.9	781.4	786.1	757.0
611.8	660.6	754.8	759.4	739.5
583.8	626.1	701.2	708.9	696.6
536.1	573.8	630.9	643.9	634.5
443.6	475.9	511.5	532.2	522.2
317.7	343.6	361.4	386.5	374.0

TABLE 7.11 continued

Margules	VanLaar	WILSON	NRTL	UNIQUAC
		$G^E/J \cdot mol^{-1}$		
		tetrahydrofuran + sulfolane at 353.15 K		
458.3	583.2	460.1	591.5	623.8
540.6	668.5	524.0	677.1	714.0
657.3	784.3	609.2	793.3	836.2
754.9	877.8	676.6	886.8	934.3
838.7	956.2	732.1	965.2	1016.4
882.8	996.9	760.5	1005.8	1058.9
926.0	1036.6	787.9	1045.4	1100.2
1088.7	1184.4	887.3	1192.7	1253.4
1239.0	1322.0	975.0	1329.9	1394.7
		1,4-dioxane + sulfolane at T = 353.15 K		
187.9	372.2	501.0	481.2	385.8
243.0	409.7	542.7	509.6	425.0
282.1	432.6	565.4	523.4	449.0
284.3	433.8	566.5	524.0	450.2
321.5	451.6	580.4	530.2	468.8
343.6	458.8	581.5	527.7	476.1
359.5	456.5	567.5	513.0	473.2
357.5	440.9	538.2	487.7	456.3
330.5	400.1	477.0	437.1	412.9
277.4	335.6	390.7	365.8	344.8
182.9	225.1	255.0	248.2	229.8
76.3	96.5	106.8	109.0	97.8

TABLE 7.11 continued

Margules	VanLaar	WILSON	NRTL	UNIQUAC
		G^E/J·mol^{-1}		
tetrachloromethane + sulfolane at T = 338.15 K				
706.4	950.2	1128.5	1119.8	952.3
880.9	1108.6	1276.4	1268.1	1115.1
1011.1	1215.7	1365.6	1359.2	1227.3
1090.6	1275.2	1408.5	1404.2	1291.5
1159.2	1319.8	1431.8	1430.5	1342.4
1195.1	1331.7	1421.3	1423.5	1362.0
1185.4	1303.0	1375.1	1379.6	1340.9
1110.2	1210.3	1269,3	1273.4	1256.7
1009.1	1099.3	1155.8	1155.9	1150.2
821.3	899.1	960.6	950.1	951.8
1,1,1-trichloromethane + sulfolane at T = 338.15 K				
555.3	704.4	753.2	874.4	698.0
654.7	800.1	846.8	966.7	795.5
782.8	914.4	954.4	1066.0	914.0
872.8	987.4	1019.3	1119.8	992.5
931.0	1028.3	1052.0	1139.8	1039.7
954.0	1034.0	1050.1	1123.5	1053.2
935.1	1003.2	1015.3	1076.7	1029.0
879.0	938.1	949.4	999.2	969.6
797.4	850.2	863.4	903.2	885.4
739.5	789.1	804.2	838.5	825.5

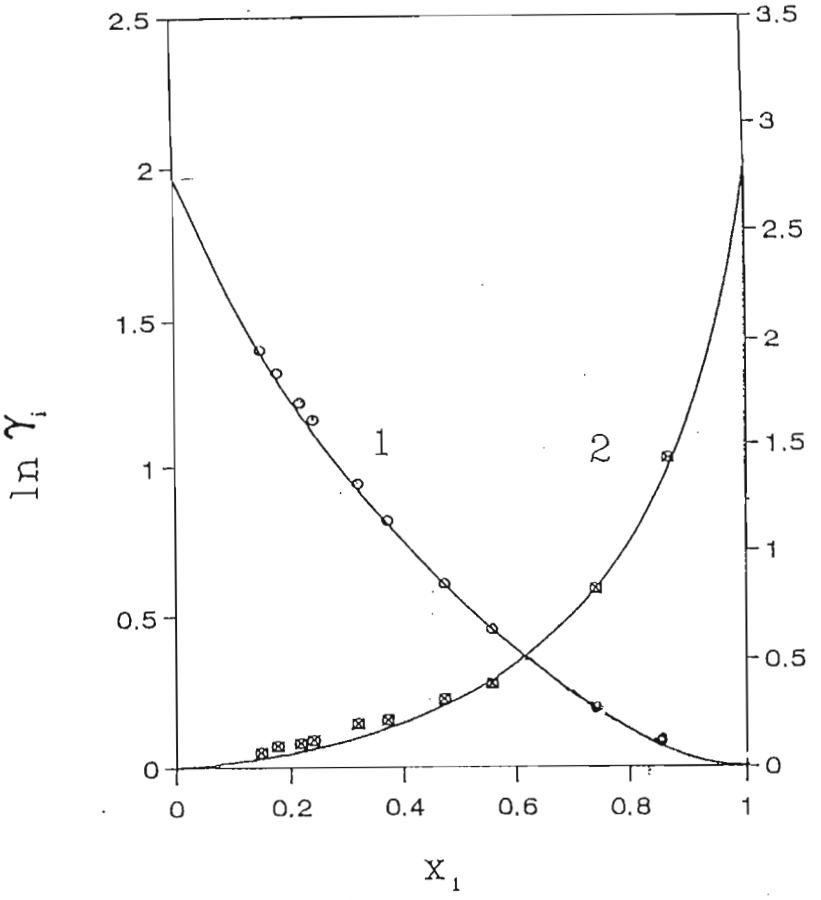

Figure 7.5a. Activity coefficient - liquid composition diagram for 1-heptyne (1) + sulfolane (2) at 353.15 K. Solid lines calculated by the UNIQUAC equation

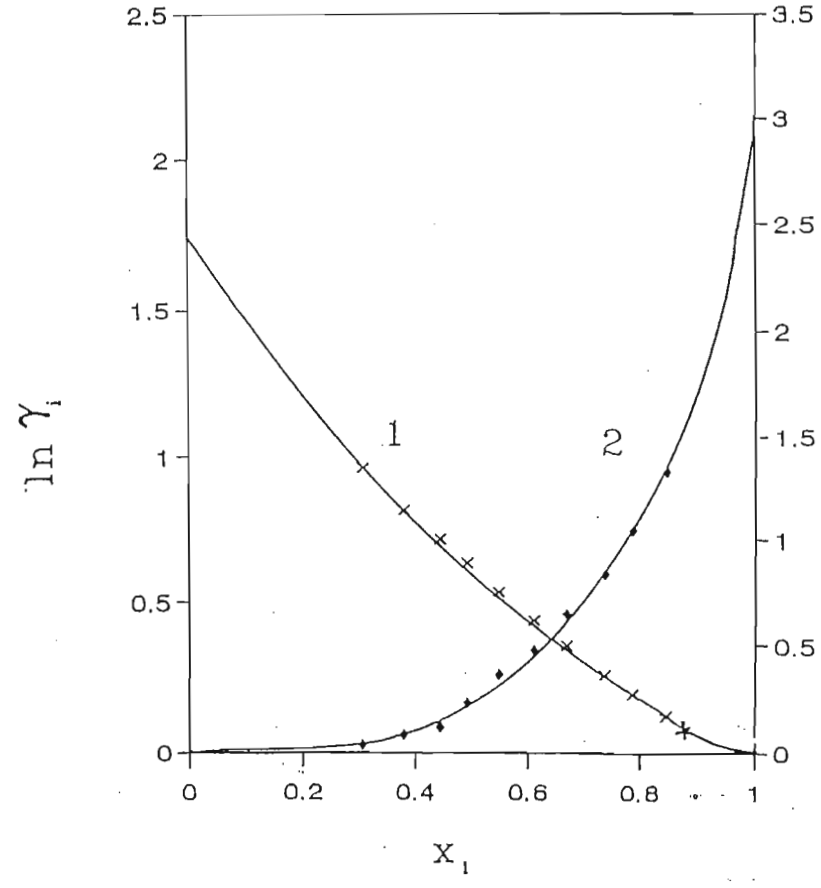

Figure 7.5b. Activity coefficient - liquid composition diagram for tetrachloromethane (1) + sulfolane (2) at 338.15 K. Solid lines calculated by the UNIQUAC

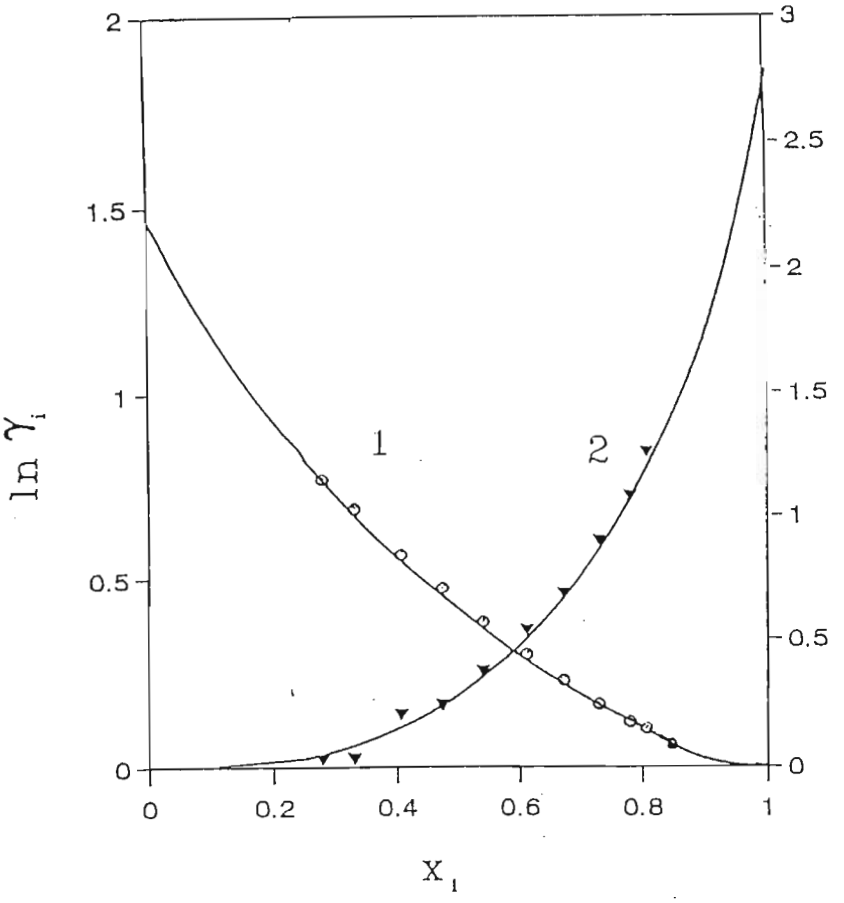

Figure 7.5c. Activity coefficient - liquid composition diagram for 1,1,1-trichloroethane (1) + sulfolane (2) at 338.15 K. Solid lines calculated by the UNIQUAC equation

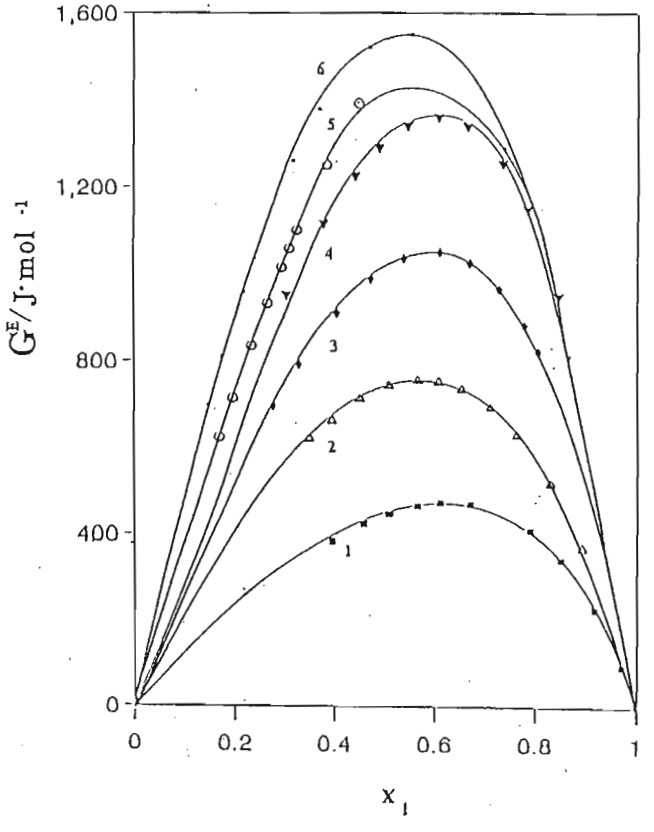

Figure 7.6. Excess molar Gibbs energies, G^E, for the systems: 1) 1,4-dioxane + sulfolane at 358.15 K; 2) tetrahydrofuran + sulfolane at 338.15 K; 3) 1,1,1-trichloroethane + sulfolane at 338.15 K; 4) tetrachloromethane + sulfolane at 338.15 K; 5) tetrahydrofuran + [illegible] at [illegible] K;

CHAPTER 8
SOLID LIQUID EQUILIBRIUM

Two kinds of equilibria between liquids and solids are of particular importance:

1. *Solution equilibrium, which is related to the equilibrium between liquids and solids of different chemical species, and*
2. *Melt equilibrium, which is related to the equilibrium between molten and solid forms of the same chemical species.*

The behaviour related to the two type of mixtures can be quantitatively expressed in terms of the activity coefficient. In principle, liquid-phase activity coefficients that have been deduced from measurements of VLE or LLE are applicable to the liquid phase of solid-liquid equilibrium after temperature compensation. In practise this is reasonably accurate in describing solubilities but less so for melt equilibria.[130]

In this work, as part of a study[132-133] *into the physico-chemical properties of binary mixtures involving sulfolane, the solubility of sulfolane in six solvents 1-heptyne, tetrahydrofuran, 1,4-dioxane, 1,1,1-trichloroethane, benzene and cyclohexane have been measured. Sulfolane has been extensively used in the petroleum industry for the recovery, by liquid extraction, of aromatic compounds and other organic liquids. Its mixtures have been the subject of many experimental investigations over the past 20 years. The cryoscopic behaviour of pure sulfolane and its solutions in some organic compounds have been investigated by M. D. Monica et al.,*[14]*. Their results show that sulfolane solidifies as plastic crystals, (phase I, mesomorphic phase), which undergoes a solid phase transition at 288.60 K forming a new solid phase, (phase II crystalline non rotational). The solid-liquid equilibrium, SLE, phase diagrams for benzene + sulfolane*[15]*, 1,4-dioxane + sulfolane*[16]*, carbon tetrachloride*

+ sulfolane[17], 2-methyl-2-propanol + sulfolane and nitrobenzene + sulfolane[136] have also been reported in the literature. This data is used together with solubility measurements conducted in this work, to fully describe (predict) the mixing properties of sulfolane and various solutes in Chapter 9.

Sulfolane is a dipolar aprotic substance with a low donor number of 14.81 [136] and a large dipole moment in the liquid phase, $\mu = 4.8\ D$ [136]. The steric hinderance resulting from the large globular hydrocarbon moiety is responsible for the weakly structured substance below its melting point (plastic phase I), and also the large enthalpy change of transition which considerably exceeds the melting enthalpy [14].

In the publications cited above, little attention has been paid to the analysis of the (SLE) data using modern theories of mixing. Only for the nitrobenzene + (TMS) (8) mixture was the liquidus curve described together with numerical values of differences between heat capacity of the solute in the solid (plastic phase I) and the heat capacity of the liquid phase (ΔC_{pm2}), at the melting temperature ($\Delta C_{pm2} = 0$). This assumes that there is no loss of rotational freedom of sulfolane molecules on solidification. During the phase transition between plastic phase I and crystalline phase II, which was assumed as an orientational fusion, the ΔC_{ptr2} was calculated to be 45.51 $J \cdot K^{-1} \cdot mol^{-1}$.

In this work, the results of the correlation of solubility for sulfolane in various solvents with respect to the solid-solid phase transition in sulfolane is given in terms of the WILSON[5], NRTL[6], and UNIQUAC[7] equations, utilizing parameters taken from solid-liquid equilibrium for the simple eutectic mixtures only. The correlations have been done using the data reported here as well as the data published earlier [14-17].

8.1. Solubility of Solids in Liquids

When the solvent does not enter the solid phase, the fugacity of the solid remains that of the pure solid, so the condition of equality of partial fugacities at equilibrium becomes[130]

$$f_{3solid} = f_{3(solid)} = \gamma_3 x_3 f_{3(subcooledliquid)} \tag{8.1}$$

Rearranging in simplified notation,

$$x_3 = \frac{f_{3(soild)}}{\gamma_3 f_{3(scl)}} \tag{8.2}$$

where x_3 is the mole fraction of the solute in the solution and $f_{3(scl)}$ represents the fugacity of the pure solid state in a subcooled or hypothetical liquid state below its melting point.

The ratio $f_{3(solid)}/f_{3\,(scl)}$ of the fugacities of the solid and its subcooled liquid can be evaluated in terms of conditions at the triple point. When the fundamental equation,

$$d\ln f = -\frac{\Delta H}{RT^2}dt + \frac{\Delta V}{RT}dP \tag{8.3}$$

is applied to each phase and the results subtracted, the conclusion is[121]

$$d\ln\frac{f_{3(solid)}}{f_{3(scl)}} = \frac{H_L - H_s}{RT^2}dT - \frac{V_L - V_s}{RT}dP \tag{8.4}$$

For practical purposes the difference in specific volumes of condensed phases may be independent of pressure, but the enthalpy of fusion, H_L - H_S, may vary appreciably with temperature. The behaviour is described by

$$\begin{aligned} H_L - H_S &= (H_L - H_S)_{tp} + \int_{T_{tp}}^{T} (C_{pL} - C_{ps} dT \\ &= \Delta H_{tp} + \int_{T_{tp}}^{T} \Delta C_p dT \\ &\simeq \Delta H_{tp} + \Delta C_p (T - T_{tp}) \end{aligned} \tag{8.5}$$

where the subscript tp designates the triple point. The last form of the equation applies when the heat capacity difference is relatively insensitive to temperature.

After equation 8.5 is substituted into equation 8.4 and the result is integrated between (T_{tp}, P_{tp}) and the temperature and the pressure of the system (T, P), the ratio of the fugacities become

$$\ln \frac{f_3}{f_{3(scl)}} = \frac{\Delta H_{tp3}}{R}\left(\frac{1}{T_{tp3}} - \frac{1}{T}\right) - \frac{\Delta C_{p3}}{R}\left(\ln \frac{T_{tp3}}{T} - \frac{T_{tp3}}{T} + 1\right) - \frac{\Delta V}{RT}(P - P_{tp3}) \tag{8.6}$$

Substitution of the relations into equation 8.2 results in the *General Solubility Equation*

$$x_3 = \frac{1}{\gamma_3} \exp\left[\frac{\Delta H_{tp3}}{R}\left(\frac{1}{T_{tp3}} - \frac{1}{T}\right) - \frac{\Delta C_{p3}}{R}\left(\ln \frac{T_{tp3}}{T} - \frac{T_{tp3}}{T} + 1\right) - \frac{\Delta V}{RT}(P - P_{tp3})\right] \tag{8.7}$$

One or more simplifications of the equation are sometime adequate:[130]

1. The pressure may be negligible.
2. Although it is more substantial than the correction for pressure, the contribution of the heat-capacity difference also is often minor (and difficult to find in the literature), and when it is neglected the solubility equation becomes

$$x_3 = \frac{1}{\gamma_3}\exp[\frac{\Delta H_{tp3}}{R}(\frac{1}{T_{tp3}} - \frac{1}{T})] - \frac{1}{\gamma_1}[\frac{\Delta S_{tp3}}{R}(1 - \frac{T_{tp3}}{T})] \tag{8.8}$$

where $\Delta S_{tp} = \Delta H_{tp}/T_{tp}$ is the entropy of fusion at the triple point.

3. Since triple-point temperatures usually are very nearly the same at atmospheric melting points and the latter are more often known, the solubility equation becomes, with this substitution

$$x_3 = \frac{1}{\gamma_3}\exp[\frac{\Delta H_{m3}}{R}(\frac{1}{T_{m3}} - \frac{1}{T})] - \frac{1}{\gamma_1}[\frac{\Delta S_{m3}}{R}(1 - \frac{T_{m3}}{T})] \tag{8.9}$$

where the subscripts *m* identifies conditions at the atmospheric melting point.

4. A compact solubility equation that requires knowledge only of properties of the pure components is obtained in terms of the Scatchard-Hilderbrand[137] equation for the activity coefficient of the solute

$$x_3 = \exp[\frac{\Delta S_{m3}}{R}(1 - \frac{T_{m3}}{T}) - \frac{V_1\phi_1^2(\delta_3 - \delta_1)^2}{RT}] \tag{8.10}$$

where ϕ_1 is the volume fraction of the solvent.

$$\phi_1 = \frac{V_1 x_1}{(V_3 x_3 + V_1 x_1)} \tag{8.11}$$

Sometimes the Flory-Huggins[107] correction can give superior results, but neither

this nor the basic Scatchard-Hilderbrand equation does a particularly well for the non-hydrocarbon mixtures and mixtures containing polar compounds.

5. The version of the solubility equation for the ideal solutions, with unit activity coefficients,

$$x_3 = \exp[\frac{\Delta H_{m3}}{R}(\frac{1}{T_{m3}} - \frac{1}{T})] = \exp[\frac{\Delta S_{m3}}{R}(1 - \frac{T_{m3}}{T})] \qquad (8.12)$$

is based on the Clausius-Clapeyron equation.

The nature of the solvent and the enthalpy and temperature of fusion are the main factors influencing solubility. Even chemically similar compounds may differ substantially in their fusion properties and consequently in their solubilities. The heat capacity term contributes little to the calculated solubility at modest displacements from the fusion temperature[132] and is often neglected.

8.2. Eutectic Compositions

For ideal mixtures, the eutectic temperature and composition can be found when the enthalpy and temperature of fusion are known. When the following solubility equations for each component[130]

$$x_3 = \exp[\frac{\Delta H_{m3}}{R}(\frac{1}{T_{m3}} - \frac{1}{T})] \qquad (8.13)$$

$$x_1 = \exp[\frac{\Delta H_{m1}}{R}(\frac{1}{T_{m1}} - \frac{1}{T})] \tag{8.14}$$

are plotted as T against x, the curves will intersect at the eutectic condition (T_e, x_e). When the two eutectic conditions are required, the two equations are combined into one as

$$\gamma_3 = \exp[\frac{\Delta H_{m3}}{R}(\frac{1}{T_{m3}} - \frac{1}{T_e})] + \exp[\frac{\Delta H_{m1}}{R}(\frac{1}{T_{m1}} - \frac{1}{T_e})] \tag{8.15}$$

from which the T_e can be found by an iterative procedure and substituted in the equation 8.13 or 8.14 to find the composition of x_e.

When the activity coefficients are known as functions of temperature and compositions, the following equations can be solved simultaneously for the eutectic conditions:

$$\gamma_3 x_3 = \exp[\frac{\Delta H_{m3}}{R}(\frac{1}{T_{m3}} - \frac{1}{T_e})] \tag{8.16}$$

$$\gamma_1 x_1 = \exp[\frac{\Delta H_{m1}}{R}(\frac{1}{T_{m1}} - \frac{1}{T_e})] \tag{8.17}$$

In one of the simplest cases the activity coefficients are represented by the equations

$$\ln\gamma_3 = A(1-x_1)^2/T \tag{8.18}$$

$$\ln\gamma_1 = Ax_1^2/T \tag{8.19}$$

and the equations to be solved by trial for the eutectic conditions are

$$\frac{A(1-x_1)^2}{T_e} + \ln x_3 = \frac{\Delta H_{m3}}{R}\left(\frac{1}{T_{m3}} - \frac{1}{T_e}\right) \tag{8.20}$$

$$\frac{Ax_1^2}{T_e} + \ln x_1 = \frac{\Delta H_{m1}}{R}\left(\frac{1}{T_{m1}} - \frac{1}{T_e}\right) \tag{8.21}$$

Since $1/T_e$ occurs linearly in these equations, it can be eliminated readily, and the problem becomes one of a solution of an equation in one unknown, x_1.

Although calculations for ideal mixtures are easily performed, the results should be used with discretion, since many mixtures are significantly non ideal. For instance, the occurrence of partial miscibility of solid phases is not detected by ideal calculations, and they do form occasionally in organic mixtures.

8.3. Activity Coefficients

In Chapter 9 the activity coefficients are shown to be correlated by several different kinds of equations, the van Laar,[13] Margules,[12] WILSON[5], NRTL,[6] and UNIQUAC.[7] Other methods include the NRTL1,[138] NRTL2,[138] and UNIQUAC ASM.[139] The applicability of these theories to various types of mixtures was studied extensively by Domańska.[140-142] It was found that for simple paraffins, in mixtures with hydrocarbons,[140] that the UNIQUAC and NRTL2 equations gave the best correlations. For the more complicated systems of aliphatic alcohols + long chain hydrocarbons[141], UNIQUAC ASM gave the best solubility correlations, using the association constant as an either a adjustable or fixed parameter. The Wilson equation was found to give the best correlation for binary mixtures involving various solvents in about 500 monocarboxylic acids.[142]

The applicability of the above mentioned solution theories as predictive tools can only be used for ternary systems, employing binary solubility and VLE data. For predictions of binary solubility data, the Regular Solution Theory[137], is a model that, with some modifications, has been used frequently in wax formation predictions. In its original form, it cannot predict negative deviations to the ideal solution assumption. In this work, two predictive theories are used to describe the solubility of sulfolane in various mixtures, ie. DISQUAC[9] and Modified UNIFAC[8].

For binary mixtures both activity coefficients can be evaluated from a knowledge of the eutectic conditions by solving:

$$\gamma_i = \frac{1}{x_i}\exp\left[\frac{\Delta H_{mi}}{R}\left(\frac{1}{T_{mi}} - \frac{1}{T_e}\right)\right] \qquad (8.16)$$

γ_1 and γ_3 can then be used to find parameters of a correlating equations such as the

NRTL Wilson and UNIQUAC, so that the complete melting curve can be determined. With the Wilson equation, practical difficulties can arise when the parameters are found from a limited amount of data such as a eutectic condition, since the process can lead to negative values of the parameters. This is unacceptable if the equation is to represent activity coefficients over the whole concentration range.

8.4. Experimental Section

8.4.1. Materials

The solvents were obtained from Aldrich Chemical Co., (with a quoted purity of 99.9 % w/w) and were purified by fractional distillation through a 30 plate distillation column. The compounds were dried using activated type 5A molecular sieves and the water content was found to be less than 100 ppm w/w, as determined by GLC analysis. Sulfolane was also supplied by Aldrich Chemical Co., (98 % reagent) and was twice vacuum distilled at a pressure below 20 mmHg to yield a colourless and odourless product. To minimize the contact of this deliquescent reagent with moist air, the product was kept in sealed bottles in a desiccator. The physical properties of the reagents used in this work are listed in Table 8.1 together with literature values.

8.4.2. Procedure

In this work the solubility of sulfolane in six solvents 1-heptyne, tetrahydrofuran, 1,4-dioxane, 1,1,1-trichloroethane, benzene and cyclohexane have been measured. The solubilities were determined using a dynamic method, described by Domańska [143]. The mixtures of solute and solvent, were prepared by weighing. The mixture was well stirred using a magnetic stirrer and heated very slowly with a heating rate, which did not exceed 2 $K \cdot h^{-1}$ near the equilibrium temperature. The temperature at which the last crystals disappeared (disappearance of solution

cloudiness) was taken as the temperature of the solution-crystal equilibrium. Measurements were performed in a small range of solute concentration from x_3 = 0.16 (1-heptyne, tetrahydrofuran), or 0.6 (1,1,1-trichloroethane), or 0.5 (1,4-dioxane) or 0.9 (cyclohexane) to x_3 = 1 over the temperature range from 250 to 310 K. The temperature was measured using a calibrated platinum resistance thermometer (Autotherm2 by Gallenkamp), with an accuracy of 0.01 K. Reproducibility of measurements was better than 0.1 K, which corresponded to a estimated error in composition of Δx_3 = 0.001. The experimental results are given in Tables 8.2 and 8.3.

8.5.Results and Discussion

The solute, sulfolane is most soluble in tetrahydrofuran and least soluble in 1,4-dioxane. The order of solubility of sulfolane is tetrahydrofuran > 1,4-dioxane > 1,1,1-tertachloroethane > benzene > tetrachloromethane > 2-methyl-2-propanol > 1-heptyne. These results indicate that no hydrogen bonds or other strong interactions exist between sulfolane and 1-heptyne, or 2-methyl-2-propanol. This is supported by work done by M. D. Monica *et al.*[14], that no hydrogen bonds exists between benzoic acid and sulfolane.

In all the solvents used in this work, with the exception of tetrahydrofuran over a small concentration range, the solubility of sulfolane is lower than ideal. The effect of the interactions between (TMS) and the solvents observed in vapour-liquid equilibria measurements[14] , was similar to that observed in this work. The solubility of sulfolane in 1-heptyne is much lower than ideal, and the experimental activity coefficients of the solute (γ_3) for $x_3 > 0.16$, are in the range 4.6 - 1.0.

The solubility of sulfolane in 1,4-dioxane for $x_3 > 0.84$ is close to ideal with experimental activity coefficients $\gamma_3 \approx 1.0$. This corresponds to the liquidus curve related to the sulfolane crystal phases I and II. Evidence for the formation of a solid molecular compound which largely decomposes on melting was observed in the

literature[16] and in our results, presented in Table 8.3. This indicates the possibility of strong interactions between sulfolane and 1,4-dioxane in the concentration range $x_3 < 0.84$. The maximum compound formation was observed at $x_3 = 0.7$ (T = 278.7 K) and also the two eutectic points, $x_3 = 0.36$ (T = 272.1 K) and $x_3 = 0.68$ (T = 258.2 K), respectively. The latter eutectic refers to the metastable crystalline phase II. Although the shape of the phase diagram reported by Jannelli *et al.*[16] is similar to that reported here, the results are not identical. The difference could be a result of the different experimental techniques used - DSC as opposed to our dynamic method as well as the fact that, both cooling and heating curves were used in the DSC method.

Typical examples of shapes of liquidus curves are shown in figures 8.2 and 8.3 for the 1,1,1-trichloroethane + sulfolane and 1-heptyne + sulfolane mixtures.

The solubility of a solid non-electrolyte, 3 in a liquid solvent can be expressed as:

$$-\ln x_3 = \frac{\Delta H_{m3}}{R}\left[\frac{1}{T}-\frac{1}{T_{m3}}\right] - \frac{\Delta C_{pm3}}{R}\left[\ln\left(\frac{T}{T_{m3}}\right)+\frac{T_{m3}}{T}-1\right]+\ln\gamma_3 \qquad (8.22)$$

where x_3, γ_3, ΔH_{m3}, ΔC_{pm3}, T_{m3}, and T are the mole fraction, activity coefficient, enthalpy of fusion, solute heat capacity during the melting process, melting temperature of the solute and equilibrium temperature, respectively. If the solid-solid transition occurs before fusion, an additional term must be added to the right hand side of equation 8.22 [143]:

$$-\ln x_3 = \frac{\Delta H_{m3}}{R}\left[\frac{1}{T}-\frac{1}{T_{m3}}\right] - \frac{\Delta C_{pm3}}{R}\left[\ln\left(\frac{T}{T_{m3}}\right)+\frac{T_{m3}}{T}-1\right]$$
$$+\frac{\Delta H_{tr3}}{R}\left(\frac{1}{T}-\frac{1}{T_{tr3}}\right)-\frac{\Delta C_{ptr3}}{R}\left[\ln\left(\frac{T}{T_{tr3}}\right)+\frac{T_{tr3}}{T}-1\right]+\ln\gamma_3 \qquad (8.23)$$

where ΔH_{tr3} and T_{tr3} and ΔC_{ptr3} are the enthalpy and temperature of the solid-solid transition of the solute and ΔC_{ptr3} is the solute heat capacity during the transition process. Equation 8.22 was used for temperatures above the transition temperature and equation 8.23 at lower temperatures. Equations 8.22 and 8.23 assume the absence of miscibility in the solid phase.

The enthalpy of melting and phase transition of sulfolane were respectively; ΔH_{m3} = 1427.70 J·mol^{-1} and ΔH_{tr3}= 5353.90 J·mol^{-1} (obtained from the cooling curve of pure sulfolane by comparison with the melting area), whereas the differences between heat capacities of the solute in the solid phase and liquid phase are ΔC_{pm3} = 0 and $\Delta C_{p\,tr3}$ = 45.51 J·K^{-1}mol^{-1}, respectively.[136]

In this study, three methods that describe the Gibbs excess free energy of mixing (G^E) were used to represent the solute activity coefficient (γ_3): the WILSON equation[5], the nonrandom two-liquid theory (NRTL)[6] and the UNIQUAC[7] equation. Calculations were performed on the data obtained from this work and also for mixtures of sulfolane in benzene, 1,4-dioxane, 1,1,1-trichlorethane and 2-methyl- 2-propanol, from literature data[14-17] in the sulfolane rich region, for liquidus curves giving simple eutectic points.

The parameters were fitted by the optimization technique. The objective function used was:

$$F(A_1,A_2)=\Sigma_{i=1}^{n} w_i^{-2}[\ln x_{3i}\gamma_{3i}(T,x_{31},A_1,A_2)-\ln a_{3i}(T_i)]^2 \qquad (8.24)$$

where ln a_{3i} denotes an "experimental" value of the logarithm of solute activity, taken as the right side of equations 8.22 or 8.33, w_i is the weight of an experimental point, A_1 and A_2 are the two adjustable parameters of the correlation equations, i denotes the *i*th experimental point and n is the number of experimental data. The weights were calculated by means of the error propagation formula:

$$w_i^2 = \left(\frac{\partial \ln x_3\gamma_3 - \partial \ln a_i}{\partial T}\right)^2_{T=T_i}(\Delta T_i)^2 + \left(\frac{\partial \ln x_3\gamma_3}{\partial x_3}\right)^2_{x_3=x_{3i}}(\Delta x_{3i}) \qquad (8.25)$$

where ΔT and Δx_3 are the estimated errors of T and x_3, respectively.

The objective function is consistent with the maximum likelihood principle, provided that the first order approximation is valid.

The experimental errors of temperature, and solute mole fraction were fixed for all cases at $\Delta T = 0.1$ K and $\Delta x_3 = 0.001$.

The root mean square deviation of temperature given below was used as a measure of the goodness of the fit of the solubility curves - equations 8.22 and 8.23:

$$\sigma_T = \left[\Sigma_{i=1}^{n} \frac{(T_i^{cal} - T_i)^2}{(n-2)}\right]^{\frac{1}{2}} \qquad (8.26)$$

where T_i^{cal} and T_i are, respectively, the calculated and experimental temperatures of the *i*th point and n is the number of experimental points. The calculated values of the parameters and corresponding root mean square deviations are presented in Table 8.4. The pure components structural parameters r (volume parameter) and q (surface parameter) in UNIQUAC were obtained in accordance with the methods suggested by Vera et al.,[144] and relationships (27) and (28);

$$r_i = 0.029281\ V_i \tag{8.27}$$

and

$$q_i = (z-2)r_i/2 + 2(1-l_i)/z \tag{8.28}$$

where V_i is the molar volume of pure component i at 298.15 K, z is the coordination number, further assumed equal to 10, l_i is the bulk factor; it was accepted that $l_i = 0$.

The solubility of sulfolane in cyclohexane was only measured in the sulfolane rich region ($x_3 > 0.94$) as a result the non-miscibility gap in the lower sulfolane concentrations. The NRTL parameters obtained were: $g_{13} - g_{33} = -4151.16$ J·mol^{-1}, and $g_{31} - g_{11} = 11461.16$ J·mol^{-1} with a root mean square deviation of 0.26 K.

For the nine solubility curves, (shown in Table 8.4), the results obtained from the WILSON equation are slightly better than those derived from the NRTL and UNIQUAC equations. The average deviations are 1.56 K, 1.64 K and 1.65 K, for the Wilson, NRTL, and UNIQUAC, respectively.

The experimental data of SLE obtained in this work and the VLE (Chapter 7) have been used to obtain new interaction parameters for the specific solvent groups with sulfolane using the DISQUAC and Modified UNIFAC models.

TABLE 8.1. Physical Properties of the Pure Components at 298.15 K, Molar Volumes V_i, Refractive Indexes n_D, and Melting Point T_{m3}

component	V_i/cm^3·mol^{-1} [127]	n_D		T_{m3}/K	
		exptl	lit.[137]	exptl	lit.[17]
1-heptyne	138.10	1.40821	1.4080 [a]		
tetrahydrofuran	81.09	1.40512	1.40496		
1,4-dioxane	85.66	1.02786	1.02797		
1,1,1-trichloroethane	100.37	1.43612	1.4359		
benzene	89.40	1.49785	1.49792		
cyclohexane	108.70	1.42352	1.42354		
sulfolane	95.26	1.48114	1.4810(*13*)[b]	301.60	301.60

[a] at 293.15 K
[b] at 303.15 K

TABLE 8.2. Solubility Measurements for the Solvent (1) + Sulfolane (3) Mixtures, Liquid Phase Mole Fraction, x_3, Experimental Equilibrium Temperature, T_3^I and T_3^{II} for the Plastic Crystals I and Crystallne Phase II, Activity Coefficient, γ_3

x_3	T_3^{II}/K	γ_3	x_3	T_3^{II}/K	γ_3	T_3^I/K
			1-heptyne (1) + sulfolane (3)			
0.1654	266.09	4.65	0.6696	276.85	1.29	
0.2175	268.82	3.63	0.7005	277.10	1.24	
0.2409	269.32	3.31	0.7035	276.74	1.23	
0.2685	270.45	3.01	0.7395	277.75	1.18	
0.2891	270.90	2.81	0.7697	278.15	1.14	
0.3138	271.43	2.60	0.7889	278.00	1.11	
0.3386	271.82	2.42	0.8217	278.86	1.07	
0.3722	272.44	2.22	0.8361	280.16	1.07	
0.4046	273.00	2.05	0.8499	279.45	1.05	
0.4310	273.35	1.93	0.8800	280.74	1.02	
0.4839	273.80	1.73	0.9062	282.05	1.08	
0.5191	274.15	1.62	0.9294	283.38	1.00	
0.5395	274.50	1.56	0.9259	283.62	1.00	
0.5533	274.57	1.53	0.9467	285.19	1.00	
0.5597	274.90	1.51	0.9718	286.82	1.00	
0.5846	275.30	1.46	0.9872	288.03	1.00	
0.6102	276.00	1.40	0.9959		1.00	293.35
0.6236	275.60	1.37	1.0000		1.00	301.60
0.6421	276.55	1.35				
			tetrahydrofuran (1) + sulfolane (3)			
0.1952	235.46	2.66	0.8509	272.07	0.97	
0.2421	238.94	2.26	0.8968	275.93	0.96	
0.3010	241.50	1.88	0.9278	279.43	0.96	
0.3510	243.94	1.67	0.9437	281.26	0.96	
0.4364	248.35	1.42	0.9599	282.76	0.96	
0.4801	251.14	1.34	0.9644	284.10	0.96	
0.5391	254.25	1.24	0.9728	285.05	0.97	
0.5766	256.05	1.18	0.9773	285.96	0.97	
0.6211	258.79	1.14	0.9787	286.47	0.97	
0.6706	261.00	1.08	0.9811	286.95	0.98	
0.7269	264.75	1.04	0.9830	287.08	0.98	
0.7775	266.85	1.00	0.9910		0.99	292.54
0.8164	269.10	0.97	1.0000		1.00	301.60

TABLE 8.2 continued

x_3	T_3^{II}/K	γ_3	x_3	T_3^{II}/K	γ_3	T_3^{I}/K
			1,1,1-trichloroethane (1) + sulfolane (3)			
0.6630	276.74	1.25	0.9081	281.75	1.02	
0.7100	270.15	1.19	0.9294	283.05	1.01	
0.7610	273.38	1.14	0.9462	284.35	1.00	
0.7869	274.12	1.11	0.9594	285.05	0.99	
0.8081	275.45	1.09	0.9753	287.94	0.99	
0.8201	276.29	1.08	0.9764		1.00	289.55
0.8386	277.45	1.07	0.9837		1.00	292.25
0.8534	278.29	1.06	0.9861		1.00	295.25
0.8689	279.25	1.05	1.0000		1.00	301.60
0.8951	280.74	1.03				
			benzene (1) + sulfolane (3)			
0.4910	257.55	1.41	0.9401	286.72	1.02	
0.5001	257.59	1.39	0.9722	288.32	1.00	
0.5923	264.42	1.27	0.9869		1.00	294.67
0.7003	270.33	1.15	0.9899		1.00	295.80
0.8384	280.12	1.07	1.0000		1.00	301.60
0.8853	283.21	1.04				
			cyclohexane (1) + sulfolane (3)			
0.9398					(LLE)	301.60
0.9412	292.35	1.04	0.9570		1.03	294.00
0.9500	292.71	1.03	0.9662		1.02	294.46
0.9523	293.11	1.03	0.9706		1.01	294.67
			0.9772		1.01	295.01
			0.9856		1.00	296.39
			1.0000		1.00	301.60

TABLE 8.3. Solubility Measurements for the 1,4-Dioxane (1) + Sulfolane (3) Mixture, Liquid Phase Mole Fraction, x_3, Experimental Equilibrium Temperature, T_3^i and Activity Coefficient γ_3

x_3	T_1/K	T_3^{II}/K	x_3	T_3^{II}/K	T_3^I/K	γ_3
0.0000	284.95*		0.6286	277.62(c)		
0.1100	282.88*		0.6610	278.38(c)		
0.1284	282.18*		0.6628	278.21)c)		
0.1530	280.81*		0.7029	278.73(c)		
0.1949	279.49*		0.7426	278.70(c)		
0.2300	278.28*		0.7487	278.66(c)		
0.2581	277.19*		0.7730	267.67(met)		
0.2961	275.80*		0.7737	278.30(c)		
0.3316	274.35*		0.7964	277.86(c)		
0.4020	271.46*(met)	274.24(c)	0.8137	277.28(c)		
0.4152	270.65*(met)	274.44(c)	0.8137	271.29(met)		
0.4252	270.57*(met)	274.62(c)	0.8148	271.32(met)		
0.4860	268.25*(met)	275.70(c)	0.8180	277.29(c)		
0.5200		276.11(c)	0.8361	273.24		1.03
0.5806		276.81(c)	0.9384	274.20		1.03
0.6039		277.44(c)	0.8471	275.33		1.02
0.6089		277.51(c)	0.8732	277.13		1.02
			0.8738	277.65		1.02
			0.9066	280.30		1.02
			0.9372	283.35		1.02
			0.9553	285.15		1.02
			0.9620	286.30		1.02
			0.9665	286.80		1.02
			0.9759	287.65		1.02
			0.9821	293.20		1.02
			0.9860		293.86	1.02
			0.9880		293.93	1.02
			0.9915		297.78	1.02
			0.9950		297.55	1.00
			1.0000		301.60	1.00

*T_1/K = solute (1) liquidus equilibrium temperature
(met) solute (1) or (3) liquidus metastable form
(c) solute (3) compound equilibrium curve

TABLE 8.4. The Parameters for the Wilson, NRTL, and UNIQUAC Equations, Determined from Binary Solid Liquid Equilibria for the Systems Solvent (1) + Sulfolane (3), as well as the Calculated Root Mean Square Deviation, σ_T

	Parameters		
component (1)	Wilson	NRTL	UNIQUAC
	$g_{13} - g_{11}$	$g_{13} - g_{33}$	Δu_{13}
	$g_{13} - g_{33}$	$g_{31} - g_{11}$	Δu_{31}
	$J \cdot mol^{-1}$	$J \cdot mol^{-1}$	$J \cdot mol^{-1}$
1-heptyne	2704.97	4162.25	2152.81
	6092.50	3552.97	44.95
tetrahydrofuran	816.45	3884.61	2209.08
	13096.26	653.30	317.33
1,4-dioxane	899.03	-809.20	-607.47
	-1038.53	645.94	519.93
1,4-dioxane	4076.43	-1326.12	-1325.18
	-1268.74	4042.91	2871.88
tetrachloromethane	4076.43	-3289.31	-2350.03
	-2381.72	7606.35	4896.38
1,1,1-trichloroethane	3227.25	10653.42	-371.82
	1361.98	3688.83	1935.61
benzene	3394.58	-64.86	-663.68
	-56.31	3243.00	2133.11
benzene	3575.91	-207.47	-753.40
	-169.02	3449.04	2284.83
2-methyl-2-propanol	6895.15	-2654.21	-2130.89
	-1621.34	7499.24	4987.72

TABLE 8.4 continued

	Deviations		
	Wilson σ_T^b/K	NRTL σ_T^b/K	UNIQUAC σ_T^b/K
1-heptyne	1.70	1.65	1.99
tertrahydrofuran	3.50	3.49	3.44
1,4-dioxane	2.88	2.88	2.88
1,4-dioxane	0.61	0.66	0.64
tetrachloromethane	2.42	2.04	1.95
1,1,1-trichloroethane	0.91	0.89	0.89
benzene	0.76	0.84	0.82
benzene	1.07	1.14	1.12
2-methyl-2-propanol	3.50	3.04	2.92

[a] calculated with $\alpha = 0.45$

[b] $\sigma_T = \Sigma_{i=1}^{n} (T_i^{cal} - T_i)^2/(n - 2)]^{1/2}$

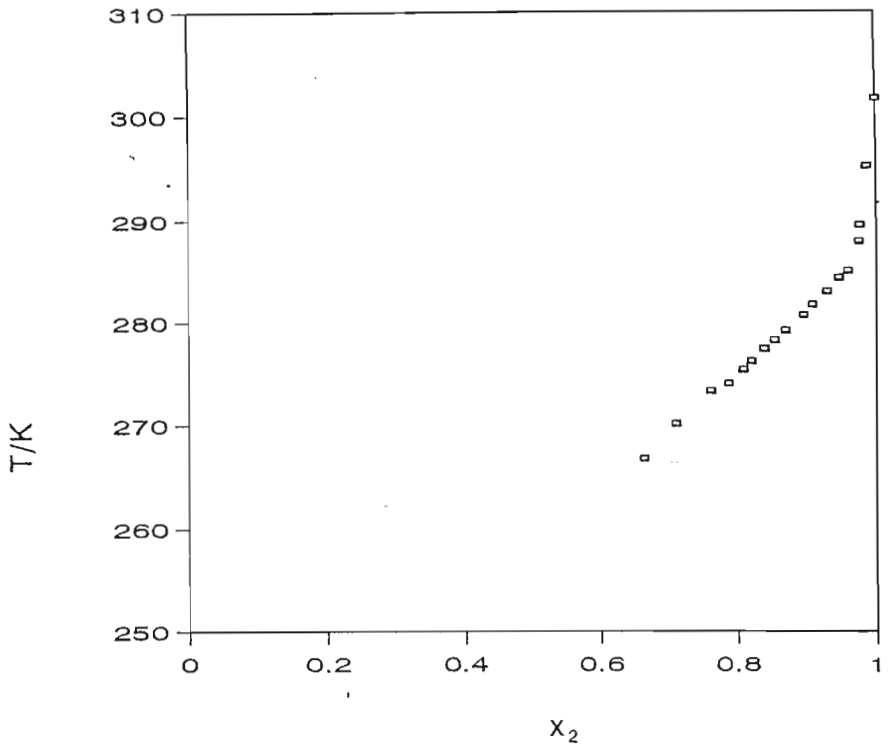

FIGURE 8.1 Solid-Liquid Equilibrium of Sulfolane (3) in 1,1,1-Trichloroethane (1)

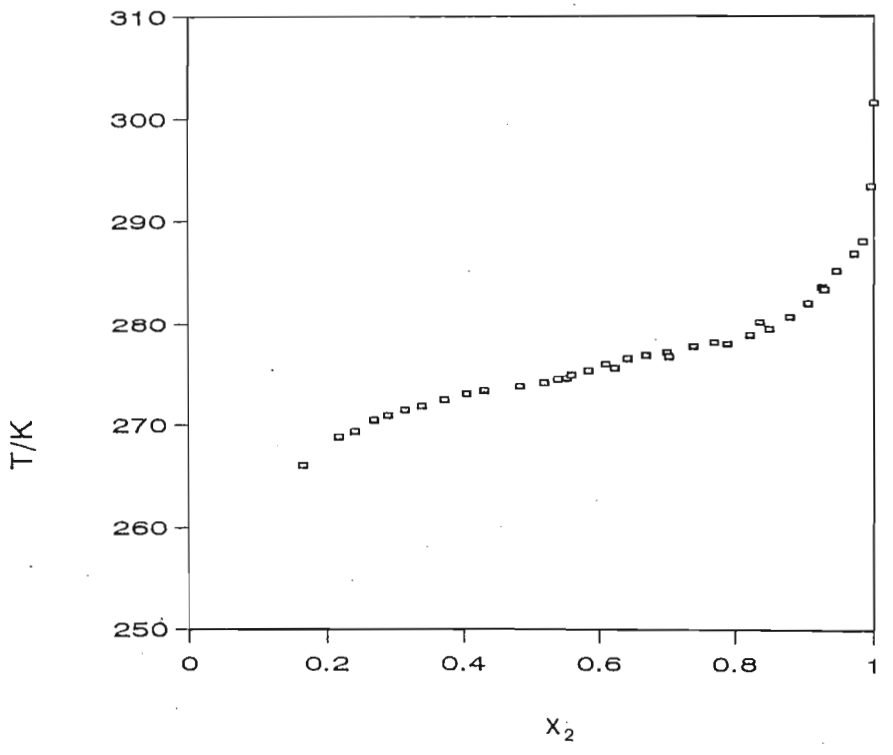

FIGURE 8.2 Solid-Liquid Equilibrium of Sulfolane (3) in 1-Heptyne (1)

CHAPTER 9

ACTIVITY COEFFICIENTS AND EXCESS FUNCTIONS

The aim of this chapter is not to give a detailed and indepth discussion of the activity coefficient and its relation to the excess properties, (there are many excellent reviews of this in the literature[92,130]), rather, the chapter concentrates on examining the well established theories behind the correlation of activities coefficients at finite and infinite dilution γ_{13}^{∞} (where 1 refers to the solute and 3 to the solvent). These solution theories are used to predict and correlate the activity coefficients at infinite dilution as well as the heats of mixing, solid-liquid equilibria and the vapour-liquid equilibrium of some of the systems studied in this work. These theories include among others the ***WILSON*** *equation,[5] Renon's Non Random Two Liquid Theory* ***(NRTL)*** *[6] and the Universal Quasichemical Theory* ***(UNIQUAC).***[7] *Two group contribution methods are also discussed, The* ***UNIQUAC*** *Functional-Group Activity Coefficients* ***(UNIFAC)***[8]*, and the Dispersive Quasichemical Theory* ***(DISQUAC).***[9]

A brief introduction into activity coefficients and the normalization of activity coefficients precedes this discussion.

9.1. The Activity Coefficient

The activity coefficient at infinite dilution characterizes the behavior of a single solute molecule completely surrounded by solvent molecules. It may indicate the maximum non ideality and for this reason offers important information to the theorist.

The constants in the empirical equations used to describe excess functions at finite concentrations and which allows the prediction of thermodynamic properties, are related to the thermodynamic properties at *infinite dilution*. A very important feature of the experimental determination of γ_{13}^{∞} is the possibility of extrapolating

measurements to finite concentrations. Once both γ^{∞}_{13} and γ^{∞}_{31} are known, the binary parameters for any of the two parameter models discussed later, can be determined and hence the prediction of γ_1 and γ_3 at any concentration is possible.

Infinitely dilute solutions are also well suited to the application of statistical mechanical perturbation theory: since solvent-solvent interactions dominate, the solute-solvent interactions can be regarded as perturbation about a pure substance.[130]

The activity coefficient calculated from the experimental work, γ^{∞}_{13}, can be used for making a preliminary prediction of partial miscibility.[130] An attractive application of infinite dilution information is the prediction of solubility in dense gases at supercritical conditions starting from Henry's constants of gases in liquids through extrapolation in respect to pressure and composition.[130]

Measurements of γ^{∞}_{13} are now of increasing interest in chemical technology. These values, which describe highly dilute solutions, can be related to the high-purity requirements in health-related products in pharmacology and biotechnology and to the packaging of foods, medicines and other items for human consumption.[146] γ^{∞}_{13} are also very important in understanding physical separations as used in most processes to obtain a desired product, to recover unreacted material, or to remove byproducts.[146]

Quantitative information on phase equilibria and hence γ^{∞}_{13} data is needed for the design of various separation units involving techniques such as separation distillation, extraction, absorption and stripping.

9.2 Normalization of Activity Coefficients

It is convenient to define activity coefficients in such a way that for an ideal solution, the activity is equal to the mole fraction or, equivalently, that the activity coefficient is equal to unity. Two types of solution ideality (one leading to Raoult's law, and the other to Henry's law), have been defined. It follows that activity coefficients may be normalized (ie. become unity) in two different ways.
If defined on the basis of Raoult's law, then for each component *i* the normalization definition is[92]

$$\gamma_i \to 1 \qquad as \qquad x_i \to 1. \tag{9.1}$$

Since this normalization holds for both the solute and the solvent , eq. (4.9) is called the *symmetric* convention for normalization and applies always to liquid mixtures.

However if activity coefficients are defined with reference to an ideal dilute solution then (Henry's Law)

$$\begin{aligned} \gamma_1 &\to 1 \quad as \quad x_1 \to 1 \ (solvent) \\ \gamma_3 &\to 1 \quad as \quad x_3 \to 0 \ (solute). \end{aligned} \tag{9.2}$$

Since the solute and the solvent are not normalized in the same way, equation 9.2 gives the *unsymmetrical* convention for normalization. To distinguish between symmetrical and unsymmetrical normalization, it is useful to denote with an asterisk

(*) the activity coefficient of a component which approaches unity as its mole fraction goes to zero. Therefore equation 9.2 becomes

$$\begin{aligned} \gamma_1 &\rightarrow 1 \quad as \quad x_1 \rightarrow 1 \ (solvent) \\ \gamma_3^* &\rightarrow 1 \quad as \quad x_3 \rightarrow 0 \ (solute). \end{aligned} \tag{9.3}$$

The two methods of normalization are illustrated below. In the dilute region ($x_2 < 1$), $\gamma_2^* = 1$, and the solution is ideal; however, $\gamma_2 \neq 1$, and therefore, while the dilute solution is ideal in the sense of Henry's law, it is not ideal in the sense of Raoult's law.[92]

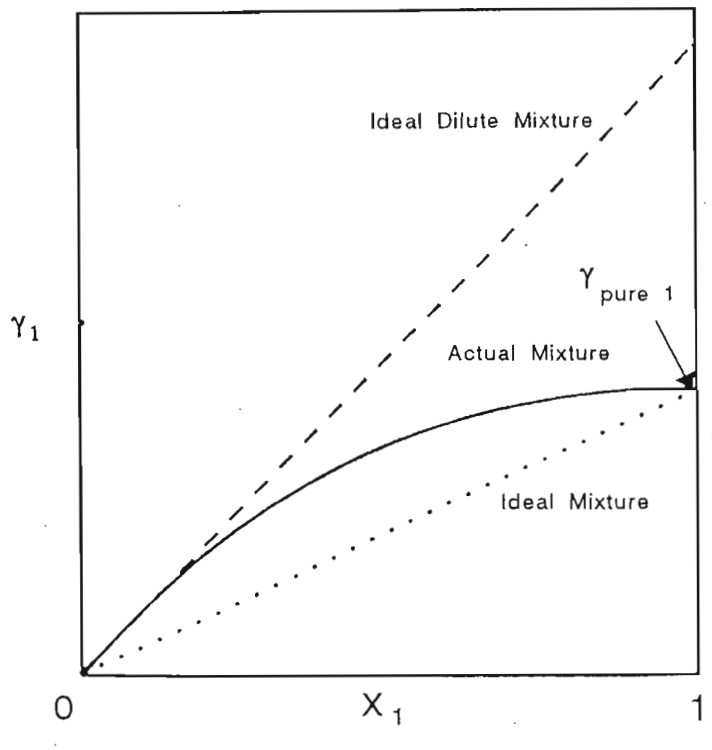

Figure 9.1. Normalization of Activity Coefficients

9.3. The Relationship Between Activity coefficients and Excess Functions in Binary Mixtures

Many equations have been proposed for the correlating of activity coefficients with composition and to a lesser extent with temperature. Some of the have been done on purely empirical grounds, others on more rational grounds. Usually the composition is expressed in mole fractions, x_i, (where i refers to component i in a mixture) but the use of volume fractions or molecular surface fractions may be preferable when the molecules differ substantially in size and chemical nature.

At a fixed temperature, the molar excess Gibbs energy G^E of a liquid mixture depends on the composition of the mixture and, to a smaller extent, on pressure. Considering a binary solution where the excess properties are taken with reference to an ideal solution wherein the standard state for each component is the pure liquid at the temperature and pressure of the mixture. In this case, any expression for the molar excess Gibbs energy must obey the two boundary conditions:

$$\begin{aligned} G^E &= 0 \quad \textit{when} \quad x_1 = 0 \\ G^E &= 0 \quad \textit{when} \quad x_3 = 0. \end{aligned} \tag{9.4}$$

9.3.1. The two suffix MARGULES EQUATION

The oldest of the formulas still in common use is that of Margules[12] (1895) The simplest non-trivial expression which obeys these boundary conditions is

$$G^E = Ax_1x_3 \tag{9.5}$$

where A is an empirical constant with units of energy, characteristic of component 1 and 3, which depend on the temperature but not on composition.
From the relation

$$G_i^E = RT\ln\gamma_i \tag{9.6}$$

we obtain an expression for the activity coefficients

$$RT\ln\gamma_i = G_i^E = \left(\frac{\partial n_T G^E}{\partial n_i}\right)_{T,P,n_j} \tag{9.7}$$

where n_i is the number of moles of i and n_T is the total number of moles.
remembering that $x_1 = n_1/n_T$ and $x_2 = n_2/n_T$, we obtain

$$\ln\gamma_1 = \frac{A}{RT}x_3^2 \tag{9.8}$$

$$\ln\gamma_3 = \frac{A}{RT}x_1^2 \tag{9.9}$$

Equations 9.8 and 9.9 give the two suffix MARGULES EQUATION.[12] These

simple relationship usually give a good representation for many simple liquids ie., for mixtures of molecules which are similar in size, shape and chemical nature. The two equations are symmetrical.

At *infinite dilution* the activity coefficients of both components are equal:

$$\gamma_1^{\infty} \equiv limit_{x_1 \to 0}\ \gamma_1 = \exp(\frac{A}{RT})$$
$$\gamma_3^{\infty} \equiv limit_{x_3 \to 0}\ \gamma_3 = \exp(\frac{A}{RT}). \qquad (9.10)$$

The excess Gibbs energy can be written as

$$G^E/RT = x_1 x_3 (Ax_3 + Bx_1). \qquad (9.11)$$

where A and B are two adjustable parameters.

9.3.2. The Redlich-Kister Expansion

Equation 9.11 is a very simple relation. In the general case, a more complex equation is needed to represent adequately the excess Gibbs energy of a binary solution.

An expansion similar to that of equation 9.11 is that of Ridlich & Kister[110] (1948):

$$G^E/RT = x_1 x_3 [A + B(x_1 + x_3) + C(x_1 + x_3)^2 + D(x_1 + x_3)^3 ....], \qquad (9.12)$$

where the additional parameters B, C, D,... are temperature dependant parameters which must be determined from experimental data. Using equation 9.12 we obtain for the activity coefficients these expressions,

$$RT\ln\gamma_1 = a^{(1)}x_3^2 + b^{(1)}x_3^3 + c^{(1)}x_3^4 + d^{(1)}x_3^5 + ... \tag{9.13}$$

$$RT\ln\gamma_3 = a^{(2)}x_1^2 + b^{(2)}x_1^3 + c^{(2)}x_1^4 + d^{(2)}x_1^5 + ... \tag{9.14}$$

The number of parameters (A, B, C....) which should be used to represent the experimental data depends on the molecular complexity of the solution, on the quality of the data, and on the number of experimental points available.

The Ridlich-Kister expansion provides a flexible algebraic expression for representing the excess Gibbs energy of a liquid mixture.

An equation due to Scathard and Hamer[147] (1935) uses volume fractions as a measure of composition, ie.

The expression for the Gibbs energy is given by

$$\phi_i = \frac{V_i x_i}{\Sigma V_j x_j} \tag{9.15}$$

$$G^E/RT = \phi_1\phi_3(a + b\phi_1 + c\phi_3) \tag{9.16}$$

from which the activity coefficients are obtained as

$$\ln\gamma_1 = [A + 2(\frac{BV_1}{V_3} - A)\phi_1]\phi_3^2, \tag{9.17}$$

$$\ln\gamma_3 = [B + 2(\frac{AV_3}{V_1} - B)\phi_3]\phi_3^2. \tag{9.18}$$

This system takes into account an important difference between molecules and should possibly have a role to play in the representation of data, but because it is slightly more complex than other methods, it does not receive much attention nowadays.

9.3.3. Wohl's Expression for the Excess Gibbs Energy

Wohl's expresses the Gibbs energies[148] of a binary solution as a power series in z_1 and z_3, the effective volume fraction of the two components:

$$\frac{G^E}{RT(x_1q_1 + x_3q_3)} = 2a_{12}z_1z_3 + 3a_{113}z_1^2z_3 + 3a_{133}z_1z_3^2 + 4a_{1113}z_1^3z_3 + 4a_{1333}z_1z_3^3 + \ldots\ldots, \tag{9.19}$$

where

$$z_1 \equiv \frac{x_1 q_1}{x_1 q_1 + x_3 q_3} \qquad z_2 \equiv \frac{x_3 q_3}{x_1 q_1 + x_3 q_3} \tag{9.20}$$

Wohl's equation contains two types of parameters, q's and a's. The q's are the effective volumes, or cross sections, of the molecules: q_i is a measure of the size of the molecule i , or its "sphere of influence "in the solution. A large molecule has a larger q than a smaller one and, in nonpolar molecules of similar shape, it is often a good simplifying and important assumption that the ratio of the q's is the same as the ratio of the pure component liquid molar volumes. The a's are interaction parameters who physical significance is roughly similar to that of the virial coefficients. The parameter a_{13} is a constant characteristic of the interaction between molecule 1 and molecule 3; the parameter a_{113} is a constant characteristic of the interaction between three molecules, two of component 1 and one of component 3 and so on.

One of the main advantages of expressing Gibbs energies as proposed by Wohl[148] is that rough physical significance can be assigned to the parameters which appear in the equation. Wohl's expansion can be extended systematically to multicomponent solutions.

9.3.4. The van Laar Equation

The van Laar equation[13] considers the case of a binary solution of two components which are not strongly dissimilar chemically, but which have different molecular sizes. Making the simplifying assumption that the interaction coefficients a_{13}, a_{113},, ... and higher, from Wohl's expansion , may be neglected; Wohl's equation becomes

$$\frac{G^E}{RT} = \frac{2a_{13}x_1x_3q_1q_3}{x_1q_1+x_3q_3} \tag{9.21}$$

which is the van Laar equation. From this equation the expression for the activity coefficients are given by;

$$\ln\gamma_1 = \frac{A'}{[1+\frac{A'}{B'}\frac{x_1}{x_3}]^2} \tag{9.22}$$

and

$$\ln\gamma_3 = \frac{B'}{[1+\frac{B'}{A'}\frac{x_3}{x_1}]^2} \tag{9.23}$$

where $A' = 2q_1a_{13}$; $B' = 2q_2a_{13}$.

Equations 9.22 and 9.23 are the familiar van Laar equations which are commonly used to represent activity coefficient data. These equations include empirical constants, A', and B'; the ratio of A' to B' is the same as the ratio of ln γ_1 to ln γ_3.

The derivation of van Laar equations suggest that they should be used for

relatively simple, preferably nonpolar liquids but empirically it has been found that these equations are frequently used to represent activity coefficients of more complex mixtures. In the special case when the van Laar constants A' and B' are equal, the van Laar equations are identical to the two-suffix Margules equation.

9.3.5. The WILSON, NRTL, and UNIQUAC Equations

Many equations have been proposed for the relation between activity coefficients and the mole fraction. Some of them can be derived from Wohl's general method. However three of the most useful of these equations cannot be obtained by Wohl's formulation.

9.3.5.1. The WILSON Equation

In the development of this equation Wilson[5] (1964) conceived that interactions between molecules depends primarily on "local concentrations" which he expressed as volume fractions. Wilson considered the case where the components in a mixture differ not only in molecular size but also in intermolecular forces.[5] His modifications are based on a loose semi-theoretical argument's which lack the rigor of the lattice theory of Guggenheim.[145]

Wilson considered a binary solution of 2 components, component 1, and component 3. If the central atom is atom 1, the probability of finding a molecule of type 3, relative to finding a molecule of type 1, around the central molecule 1, is expressed in terms of the overall mole fraction and two Boltzmann factors:

$$\frac{x_{31}}{x_{11}} = \frac{x_3 \exp(-\lambda_{13}/RT)}{x_1 \exp(-\lambda_{11}/RT)} \tag{9.24}$$

The equation implies that the ratio of number of molecules of type 3 to the ratio of molecules of type 1 around the central molecule 1 is equal to the ration of the overall mole fraction of 3 and 1 weighed by the Boltzman's factors exp ($-\lambda_{31}/RT$) and exp ($-\lambda_{11}/RT$). The parameters λ_{31} and λ_{11} are, respectively, related to the potential energies (energies of interactions) of 1-3 and a 1-1 pair of molecules.

Wilson now defines *local volume fractions* using equation 9.24. The local volume of component 1, designated by ξ_1 is defined by

$$\xi_1 \equiv \frac{V_1 x_{11}}{V_1 x_{11} + V_3 x_{31}}, \tag{9.25}$$

where V_1 and V_3 are the molar liquid volumes of components 1 and 3. Substitution gives

$$\xi_1 = \frac{V_1 x_1 \exp(-\lambda_{11}/RT)}{V_1 x_1 \exp(-\lambda_{11}/RT) + V_3 x_3 \exp(-\lambda_{31}/RT)}. \tag{9.26}$$

Similarly, the local volume fraction of component 3 is

$$\xi_3 = \frac{V_3 x_3 \exp(-\lambda_{33}/RT)}{V_3 x_3 \exp(-\lambda_{33}/RT) + V_1 x_1 \exp(-\lambda_{13}/RT)}. \tag{9.27}$$

The molar excess Gibbs energy of a binary system is given by,

$$G^E/RT = x_1 \ln\frac{\xi_1}{x_1} + x_3 \ln\frac{\xi_3}{x_3}. \tag{9.28}$$

In order to introduce simplification Wilson defined two new parameters, Λ_{13} and Λ_{31} in terms of molar volumes V_1 and V_3 and the energies λ_{11}, λ_{33} and λ_{13}. (Assuming that $\lambda_{13} = \lambda_{31}$).

$$\Lambda_{13} \equiv \frac{V_3}{V_1} \exp[\frac{\lambda_{13} - \lambda_{11}}{RT}] \tag{9.29}$$

$$\Lambda_{31} \equiv \frac{V_1}{V_3} \exp[\frac{\lambda_{13} - \lambda_{33}}{RT}] \tag{9.30}$$

Wilson's equation for the excess Gibbs energy now becomes

$$\frac{G^E}{RT} = -x_1 \ln(x_1 + \Lambda_{13}x_3) - x_3 \ln(\Lambda_{31}x_1 + x_3) \tag{9.31}$$

According to Wilson's model $x_{31} + x_{11} = 1$ *and* $x_{13} + x_{33} = 1$. *The sum of* ξ_1 *and* ξ_3 *is not unity except in the limiting case where* $\lambda_{13} = \lambda_{11} = \lambda_{33} = \lambda_{31}$.

The activity coefficients derived from this equation are given by

$$\ln\gamma_1 = -\ln(x_1 + \Lambda_{13}x_3) + x_3\left[\frac{\Lambda_{13}}{x_3 + \Lambda_{13}x_3} - \frac{\Lambda_{31}}{\Lambda_{31}x_1 + x_3}\right] \tag{9.32}$$

$$\ln\gamma_3 = -\ln(x_3 + \Lambda_{31}x_1) + x_1\left[\frac{\Lambda_{13}}{x_1 + \Lambda_{13}x_3} - \frac{\Lambda_{31}}{\Lambda_{31}x_1 + x_3}\right] \tag{9.33}$$

To a fair approximation, the difference in characteristic energies (λ_{13} and λ_{11}) are independent of temperature, at least over modest temperature intervals. As a result, Wilson's equation gives not only an expression for the activity coefficient as a function of composition but also an estimate of the variation of the activity coefficients with temperature.[92]

Wilson's equation provides a good representation of excess Gibbs energies for a variety of miscible mixtures. It is particularly useful for solutions of polar or associating components (eg. alcohols) in nonpolar solvent.
At infinite dilution the Wilson's equations reduce to

$$\ln\gamma_{13}^{\infty} = -\ln\Lambda_{13} + 1 - \Lambda_{31}, \tag{9.34}$$

$$\ln\gamma_{31}^{\infty} = -\ln\Lambda_{31} + 1 - \Lambda_{13}. \tag{9.35}$$

9.3.5.2. Renon's NonRandom Two-Liquid (NRTL) Equation

The NRTL (nonrandom two-liquid) equation[6] is based on the two cell theory.[92] Here it is assumed that the liquid has a structure made up of cells of molecules of type 1 and 3 in a binary mixture, each surrounded by assortments of the same molecule, with each of the surrounding molecules in turn surrounded in a similar manner, and so on. Gibbs energies of interaction between molecules are identified by g_{ij} where the subscript j refers to the central molecule and mol fractions in the surrounding region, x_{ij}, are identified in the same way.

Gibbs energies for the two kinds of cells are

$$G^{(1)} = x_{11}g_{11} + x_{31}g_{31}, \tag{9.36}$$

$$G^{(3)} = x_{13}g_{13} + x_{33}g_{33}, \tag{9.37}$$

where g_{11} and g_{33} are the Gibbs energies of the pure substances and the assumptions is made that $g_{13} = g_{13}$. The excess Gibbs energy for the assemble of cells becomes

$$G^{E} = x_1x_{31}(g_{31} - g_{11}) + x_3x_{13}(g_{13} - g_{33}). \tag{9.38}$$

The local mole fractions, x_{ij}, are given by equations similar to Wilson's Equations

$$\frac{x_{31}}{x_{11}} = \frac{x_3\exp(-\alpha_{13}g_{31}/RT)}{x_1\exp(-\alpha_{13}g_{11}/RT)}, \tag{9.39}$$

$$\frac{x_{13}}{x_{33}} = \frac{x_1 \exp(-\alpha_{13} g_{13}/RT)}{x_3 \exp(-\alpha_{13} g_{33}/RT)}, \tag{9.40}$$

The significance of g_{ij} is similar to that of λ_{ij} in Wilson's equation; g_{ij} is an energy parameter characteristic of an *i-j* interaction. The parameter α_{13} is related to the *nonrandomness* in the mixture. When α_{13} is zero, the mixture is completely random and reduces to the two suffix MARGULES equation.

Since

$$x_{31} + x_{11} = 1 \qquad \sim \qquad x_{13} + x_{33} = 1 \tag{9.41}$$

the local mole fraction may be solved as

$$x_{31} = \frac{x_3 \exp(-\alpha_{13}(g_{13} - g_{33})/RT)}{x_1 + x_3 \exp(-\alpha_{13}(g_{31} - g_{33}/RT)}. \tag{9.42}$$

$$x_{13} = \frac{x_1 \exp(-\alpha_{13}(g_{31} - g_{33})/RT)}{x_3 + x_1 \exp(-\alpha_{13}(g_{13} - g_{33}/RT)}. \tag{9.43}$$

Substituting these into equation 9.38 the final equation for the excess Gibbs energy

becomes

$$G^E/RT = x_1 x_3 \left[\frac{\tau_{31} G_{31}}{x_1 + x_3 G_{31}} + \frac{\tau_{13} G_{13}}{G_{13} x_1 + x_3}\right], \tag{9.44}$$

where

$$\tau_{13} = (g_{13} - g_{33})/RT, \tag{9.45}$$

$$\tau_{31} = (g_{13} - g_{11})/RT, \tag{9.46}$$

$$G_{13} = \exp(-\alpha_{13}\tau_{13}), \tag{9.47}$$

$$G_{31} = \exp(-\alpha_{13}\tau_{31}). \tag{9.48}$$

The activity coefficients are obtained by differentiation as

$$\ln\gamma_1 = x_3^2 \left[\tau_{31}\left(\frac{G_{31}}{x_1 + x_3 G_{31}}\right)^2 + \left(\frac{\tau_{13} G_{13}}{(x_3 + x_1 G_{13})^2}\right)\right], \tag{9.49}$$

$$\ln\gamma_3 = x_3^2[\tau_{13}(\frac{G_{13}}{x_3+x_1G_{13}})^2 + (\frac{\tau_{31}G_{31}}{(x_1+x_3G_{31})^2})]. \qquad (9.50)$$

The NRTL has three parameters, but reduction of experimental data for a large number of binary systems indicates that α_{13} varies from about 0.20 to 0.47.[92] At infinite dilution, when α_{13} can be estimated the equations reduce to

$$\ln\gamma_{13}^{\infty} = \tau_{31}+\tau_{13}\exp(-\alpha_{13}\tau_{13}), \qquad (9.51)$$

and

$$\ln\gamma_{31}^{\infty} = \tau_{13}+\tau_{31}\exp(-\alpha_{31}\tau_{31}). \qquad (9.52)$$

9.3.5.3. The Universal Quasi-chemical (UNIQUAC) Equation

Abrams[7] derived an equation which, in sense, extends the quasichemical theory of Guggenheim[145] for a nonrandom mixture of solutes containing molecules of different size. The extension is called the Universal Quasi-Chemical Theory (UNIQUAC in short). The UNIQUAC equation for the excess Gibbs energy (G^E) consists of two parts, a combinatorial part which attempts to describe the dominant entropic contribution and a residual part which is due primarily to intermolecular forces that are responsible for the enthalpy of mixing. The combinatorial part is determined only by the composition, sizes and shapes of the molecules; it also requires only pure-component data. The residual part, however, depends also on the

intermolecular forces; the two adjustable binary parameters, therefore, appear only in the residual part. The UNIQUAC equation is[7]

$$G^E = G^E(combinatorial) + G^E(residual). \tag{9.61}$$

For a binary mixture,

$$\frac{G^E(combinatorial)}{RT} = x_1 \ln \frac{\Phi_1^*}{x_1} + x_3 \ln \frac{\Phi_3^*}{x_3} + \frac{z}{2}\left(q_1 x_1 \ln \frac{\theta_1}{\Phi_1^*} + q_3 x_3 \ln \frac{\theta_3}{\Phi_3^*}\right) \tag{9.54}$$

$$\frac{G^E(residual)}{RT} = -q_1' \ln(\theta_1' + \theta_3' \tau_{31}) - q_3' x_3 \ln(\theta_3' + \theta_1' \tau_{13}). \tag{9.55}$$

where z is the *coordination number* (considering molecules 1 and 3 the nearest number of touching neighbors is defined as the coordination number). It may have a value between 6 and 12 depending on the type of packing, ie. the way in which the molecules are arranged in three dimensional space; empirically, for typical liquids at ordinary conditions, z is close to 10. Φ^* is the segment fraction and θ and θ' are the area fractions given by[92]

$$\Phi_1^* = \frac{x_1 r_1}{x_1 r_1 + x_3 r_3}, \qquad \Phi_3^* = \frac{x_3 r_3}{x_1 r_1 + x_3 r_3} \tag{9.56}$$

$$\theta_1 = \frac{x_1 q_1}{x_1 q_1 + x_3 q_3}, \qquad \theta_3 = \frac{x_3 q_3}{x_1 q_1 + x_3 q_3} \tag{9.57}$$

$$\theta_1' = \frac{x_1 q_1'}{x_1 q_1' + x_2 q_2'}, \qquad \theta_2' = \frac{x_2 q_2'}{x_1 q_1' + x_2 q_2'}. \tag{9.58}$$

Parameters r, q and q' are pure component molecular structure constants depending on molecular size and external surface areas, where r is the volume of the molecule and q and q' the surface area of the molecule. In the original formulation $q = q'$. To obtain better agreement for the systems containing water or lower alcohols, the q' values for water or alcohols are adjusted empirically by Anderson[149] to give an optimum fit to a variety of systems containing these components. For alcohols, the surface of interaction q' is smaller than the geometrical external surface q, suggesting that intermolecular attraction is dominated by the OH group (ie. hydrogen bonding).

For each binary mixture, there are two adjustable parameters, τ_{13} and τ_{31}. These, in turn are given by the characteristic energies Δu_{13} and Δu_{31} by

$$\tau_{13} = \exp(-\frac{\Delta u_{13}}{RT}) \equiv \exp(-\frac{a_{13}}{T}) \tag{9.59}$$

$$\tau_{21} = \exp(-\frac{\Delta u_{21}}{RT}) \equiv \exp(-\frac{a_{21}}{T}) \ . \tag{9.60}$$

Activity coefficients γ_1 and γ_3 are given by

$$\begin{aligned} \ln\gamma_1 = \ln\frac{\Phi_1^*}{x_1} + \frac{z}{2}q_1\ln\frac{\theta_1}{\Phi_1^*} + \Phi_3^*(l_1 - \frac{r_1}{r_3}l_3) \\ -q_1'\ln(\theta_1' - \theta_3'\tau_{31}) + \theta_3'q_1'(\frac{\tau_{31}}{\theta_1' + \theta_3'\tau_{31}} - \frac{\tau_{13}}{\theta_3' + \theta_1'\tau_{13}}) \end{aligned} \ . \tag{9.61}$$

and

$$\begin{aligned} \ln\gamma_3 = \ln\frac{\Phi_3^*}{x_3} + \frac{z}{2}q_3\ln\frac{\theta_3}{\Phi_3^*} + \Phi_1^*(l_3 - \frac{r_3}{r_1}l_1) \\ -q_3'\ln(\theta_3' - \theta_1'\tau_{13}) + \theta_1'q_3'(\frac{\tau_{13}}{\theta_3' + \theta_1'\tau_{13}} - \frac{\tau_{31}}{\theta_1' + \theta_3'\tau_{31}}) \end{aligned} \ . \tag{9.62}$$

where

$$l_1 = \frac{z}{2}(r_1 - q_1), \ -(r_1 - 1), \tag{9.63}$$

$$l_3 = \frac{z}{2}(r_3 - q_3) - (r_3 - 1). \tag{9.64}$$

The advantages of UNIQUAC is that it is easily applicable to multicomponent mixtures, in terms of binary parameters only. Also it is applicable to liquid-liquid equilibrium. It has a built in temperature dependence valid over at least moderate range, and it form the basis for a group contribution method, from properties of the pure components.

9.4. Group Contribution Methods

Statistical thermodynamics establishes relationship via the partial function, between the equilibrium properties of a system and the energy of its microscopic states. If the system is a mixture, if the property is a thermodynamic excess function, and if the internal degrees of freedom of the molecule are separable from the other degrees of freedom and are the same in the pure components and in the mixture, then the excess properties are related to the energy of intermolecular interactions via the configurational partition function.[150]

Organic molecules which belong to a given homologous series contain varying numbers of the same kind of 'segment' or 'groups'. For physical obvious reasons one may expect that the interaction energy of a given pair of groups will depend less on the nature of the molecules, than on the nature of the groups themselves. The most general definition, or assumption, of the *group contribution method* is that with conveniently defined groups the configurational energy is given by the sum of group

interaction energies. This definitions concerns only the molecular interaction model.[150] If no experimental data are available to fit the required binary pa rameters, group contribution methods can be said to predict the missing equilibrium information. In group contribution methods it is assumed that the mixture does not consist of molecules, but instead, of functional groups. The great advantage of the "solution of groups" concept is that the number of functional groups is much smaller than the number of possible compounds. This means that the behavior of a large number of systems of interest can be predicted with a limited number of group interaction parameters.[151]

There are also obvious theoretical shortcomings of these methods. Most cannot account for induction effects due to neighboring groups (for example a CH_2 -OH interaction is the same whether electron withdrawing or electron supplying groups are attached next to them on the backbone).[152]

9.4.1. Definition of Groups[150]

The application of a group contribution method require, first of all, a clear definition of the ensemble of groups taken into consideration. These methods are useful when the population of 'components' is much larger than the 'groups'. It makes no sense to apply the method to single-group components which have never been investigated in mixtures with poly-segmented molecules. However when a defined group is too large with respect to the average intermolecular distance, then its interaction potential may become so complex, that no existing theory may describe it conveniently.[150]

The two most widely used group contribution methods at the moment are the

UNIFAC (UNIQUAC Function-Group Activity Coefficients) model[8] and DISQUAC (The Dispersive Quasichemical) model.[9] Both these methods are discussed below.

9.4.2. UNIFAC (UNIQUAC Functional-Group Activity Coefficient Model)

UNIFAC is a functional group technique developed from the UNIQUAC (UNiversal QuasiChemical) method for the correlation of excess Gibbs energies. As such, UNIFAC uses the same surface and segment constants for the pure components as the original UNIQUAC model, but uses group-group interactions to model the mixing nonidealities rather than regressed parameters.
UNIFAC implies that the activity coefficient consists of two terms:[150]

$$\ln\gamma_i = \ln\gamma_i^C + \ln\gamma_i^R \tag{9.73}$$

The combinatorial part ($ln\ \gamma_i^C$) takes into account the size and the form of the molecules. In the residual part ($ln\ \gamma_i^R$) the interactions between the various groups are considered. Both parts are based on the UNIQUAC equation. In addition the group interaction parameters a_{nm} and a_{nm}, group volume parameters, R_k, and surface parameters, Q_k, are involved. The configurational part is the same as the UNIQUAC equation (see 9.3.5.3).

In UNIFAC the composition of the system is expressed in terms of the groups and not in terms of the mole fraction of the components, for example, v_{ki} = the number of atoms other than H (hydrogen) of group k in molecule i.[150]
The total number of groups in the mixture is given by

$$S = \Sigma_i(x_i \Sigma_k v_{ki})$$
$$= x_1(v_{11}+v_{21}+v_{31}+.....)+x_2(v_{12}+v_{22}+v_{31}+....)+.....+x_i(v_{1i}+v_{2i}+v_{3i}+...). \quad (9.66)$$

The fraction of group l in the mixture is

$$X_L = \frac{1}{S}\Sigma_i x_1 v_{Li} = \frac{1}{S}(x_{v_{L1}} + x_2 v_{L2} + x_3 v_{L3} + ...). \quad (9.67)$$

Interactions of group k and l in the mixture are represented by the empirical parameters ψ_{kl} which are functions of temperature according to the equation

$$\psi_{kL} = \exp(-a_{kl}/T). \quad (9.68)$$

The group surface-area fraction is given

$$\theta_m = X_m Q_m / \Sigma_n X_n Q_n \quad (9.69)$$

The interaction parameter of group k is

$$E_k = \theta_1 \psi_{1k} + \theta_2 \psi_{2k} + \theta_3 \psi_{3k} \quad (9.70)$$

and an auxiliary function F_k is defined as

$$F_x = \frac{\theta_1\psi_{k1}}{E_1} + \frac{\theta_2\psi_{k2}}{E_2} + \frac{\theta_3\psi_{k3}}{E_3} + \ldots\ldots \qquad (9.71)$$

The quantities θ_k, E_k , and F_k are evaluated for both the mixture and the pure components. For the mixture,

$$\ln\Gamma_k = Q_k(1 - \ln E_k - F_k), \text{ for pure } i, \ln\Gamma_k^{(i)} = Q_k^{(i)}(1 - \ln E_k^{(i)} - F_k^{(i)}) \qquad (9.72)$$

where Γ_k is the group activity coefficient in the mixture and $\Gamma_k^{(i)}$ the group activity coefficient of the pure component *i*.

When there is only one type of group in the molecule, $ln\ \Gamma_k^{(i)} = 0$. The residual part of the activity coefficient becomes

$$\ln\gamma_i^R = \Sigma_k Q_k(\ln\Gamma_k - \ln\Gamma_k^{(i)}). \qquad (9.73)$$

and the complete expression for the activity coefficient of component *i* is,[146]

$$\ln\gamma_1 = \ln\gamma_1^C + \Sigma_k Q_k(\ln\Gamma_k - \Gamma_k^{(i)}). \qquad (9.74)$$

9.5.3. The Dispersive Quasichemical (DISQUAC) Theory

DISQUAC[9] is a simple extension of the quasi-chemical theory. It resembles the theory of non-athermal associated solutions. In this theory the '*chemical*' contribution is supplemented by a random-mixing '*physical*' contribution. In DISQUAC the same random-mixing contribution supplements the known qasi-chemical expression. Each contact, either polar or non-polar, is thus characterized by a dispersive interchange energy, a single parameter, and the polar contacts by two additional parameters, the quasi-chemical interchange energy and the coordination number.

The dispersive and the quasi-chemical are calculated independently and simply added together. Therefore, the contact surfaces are not uniquely defined. There is one set for the dispersive contribution and one set for the quasichemical contribution.

9.4.3.1. Theory of DISQUAC[145]

9.4.3.1.1. The Configurational Partition Function

In a mixture of c components i in which N_i is the molecules of the type i, the total number N molecules in the system is :

$$N = \Sigma_i N_i \qquad (i = 1,2,3,.....,c) \tag{9.75}$$

and the mole fraction of component i is

$$x_i = N_i/N \tag{9.76}$$

Each type of molecule is characterized by a characteristic surface q. The total surface of all the molecules of type i is

$$A_i = q_i N \tag{9.77}$$

and the total surface of all the molecules in the system is

$$A = N \Sigma_i q_i x_i \tag{9.78}$$

Therefore we can express the *surface ratio of component i* in the mixture as [9]

$$\xi_i = q_i x_i / \Sigma_i q_i x_i \tag{9.79}$$

and the total surface of all the molecules of type i as

$$A_i = q_i N_i \tag{9.88}$$

To account for the entropic effect of the mixing process, consider the volume r_i of the molecule i. The volume fraction of the component i is:

Each molecule is composed of different groups, therefore each molecule has

$$\phi_i = \frac{r_i x_i}{\Sigma_j r_j x_j} \qquad (i,j = 1,2,.....c) \tag{9.81}$$

different *types* of surfaces, each being characterized by different *interaction potentials*. If we concider the area of surface type s on a molecule of type i by

$$q_{si} = \alpha_{si} q_i (s = a,b,,....\sigma; i = 1,2,.....c) \tag{9.82}$$

where the total surface of type s on all types of molecules in the system is

$$A_s = A\alpha_s \tag{9.83}$$

where

$$\alpha_s = \Sigma_i \alpha_{si} \xi_i \tag{9.84}$$

is the *surface ratio of surface type s in the system*, and by definition

$$\Sigma_s \alpha_{si} = 1 \qquad \Sigma_s \alpha_s = 1 \tag{9.85}$$

Assuming that the molecules in the mixture are in contact with one another over *ALL* their surface, independent of their relative positions (configuration), then the total surface of contact is one half of the surface of the molecules.[9]

$$\frac{A}{2} = \frac{1}{2} N(\Sigma_i q_i x_i) \tag{9.86}$$

However we have to distinguish between different types of contacts; contacts between surfaces of the same type (*ss*) and between surface of different types (*sl*). We denote the different areas of contact for a particular configuration (c) by A^C_{ss} and A^C_{sl} respectively. Since a surface of type *s* can be in contact with either another surface of type *s* or a different surface of type *l*, the contact must obey the conservation equation

$$2A^c_{ss} + \Sigma_l A^c_{sl} = A\alpha_s \quad (s = a, b, ... \sigma) \tag{9.87}$$

Thus, the total *configurational energy* U^c is the sum of the interactional energies per unit of contact surface for the two types of contact (*ss*) and (*sl*), we now have

$$U^c = \Sigma_s A^c_{ss} \epsilon_{ss} + \frac{1}{2} \Sigma_s \Sigma_l A^c_{sl} \epsilon_{sl} \tag{9.88}$$

where the double sum is take over all contacts between unlike pairs of surfaces (*sl*). After substituting A^c_{ss} by its value from equation 9.86 we get

$$U^c = \frac{1}{2}A\Sigma_s\alpha_s\varepsilon_{ss} + \frac{1}{2}\Sigma_s\Sigma_l A^c_{sl}\Delta\varepsilon_{sl} \tag{9.89}$$

where the quantities

$$\Delta\varepsilon_{sl} = \varepsilon_{sl} - \frac{(\varepsilon_{ss} + \varepsilon_{sl})}{2} \tag{9.90}$$

are by definition the *Interchange Energies*.[9]

In particular homologous molecules, when all the $\Delta\epsilon_{sl} = 0$, the configurational energy no longer depends on the system configuration and at a given composition N_i has a constant value.

$$U^* = \frac{1}{2}A\Sigma_s\alpha_s\varepsilon_{ss} \tag{9.91}$$

The *configurational partition function,* Ω, of the system is given by

$$\Omega = \Sigma_c \exp(-\frac{U^c}{kT}) \tag{9.92}$$

where the sum is taken over all possible configurations of the system, each configuration being characterized by its configurational energy U^c. From equation 9.92 we see that U^c/kt is a function of the contact surface A^c_{sl},

$$\frac{U^c}{kT} = \frac{1}{2}A\Sigma_s\alpha_s(\frac{\varepsilon_{ss}}{kT}) + \frac{1}{2}\Sigma_s\Sigma_l A^c_{sl}(\Delta\frac{\varepsilon_{sl}}{kT}) \tag{9.93}$$

With g^c denoting the *Combinatorial factor* for the system (ie. the number of configurations corresponding to a given value of U^C., equation 9.89 becomes

$$\Omega = \Sigma_{U^c} g^c \exp(-\frac{U}{kT}) \tag{9.94}$$

where the sum is taken over all possible energies U^c.
Assuming that there is one energy (ie. the energy at equilibrium) for which the term $g^c \exp\{-U^c/kt\}$ is large compared to all the other terms and consequently without introducing any appreciable error we can write eq. 9.92 as

$$\Omega = [g^c \exp(-\frac{U^c}{kT})]_{\max} = g\exp(-\frac{U}{kT}) \tag{9.95}$$

The equilibrium values of U and g can be obtained by maximizing the function $g^c\exp\{-U^C/kt\}$. For this we must calculate the partial derivatives of the logarithm of Ω with respect to the variables A^C_{sl}. and the solve the system of equations obtained by putting all the derivatives to zero. However we first have to express the combinatorial factor g^c as a function of A^C_{sl}.. Here the *Quasichemical approximation* of the lattice model used by Guggenheim[145] is applied.[9]

Secondly, assuming that there are a certain number of different ways of having contact between two given elements of surface. Let z be this *coordination number.* It

represents the number of possible orientations that can exist between two surfaces in contact. The total number of orientations is the $zA/2$ and for each type of contact (ss) and (sl) it is equal to zA_{ss} and zA_{sl}. respectively.

If we neglect any interference between different types of orientations of the various types of contacts, the number of configurations of the system, for a given energy would be

$$\frac{(zA/2)!}{\pi_s(zA_{ss}^c)!\,\pi_{sl}(zA_{sl}^c/2)!} \tag{9.96}$$

where the product π_{sl} is extended to all the ordered pairs (sl). But the number is certainly to large because of interferences and therefore we introduce a correction factor, h, assume to be a function of only the N_i

$$g^c = h\frac{(zA/2)!}{\pi_s(zA_{ss}^c)!\,\pi_{sl}(zA_{sl}^c/2)!} \tag{9.97}$$

The value for h is obtained considering the case of mixtures of homologous molecules for which the combinatorial factor g^* can be found. Since all the configurations have the same energy, the energetic factor does not influence the equilibrium values A^*_{sl}. and A^*_{ss}. of the contact surfaces. These values depend only on the composition of the mixture or more exactly on the area of the different types of surfaces (*zero approximation*).[9]

The value of surface A^*_{sl}. and A^*_{ss}. in the zeroth approximation are obtained by maximizing the logarithm of the function $g^c\exp\{-U^*/kt\}$. Using Stirling's formula (eq.

4.98) to approximate the factorials we obtain

$$\ln N! = N\ln N - N \tag{9.98}$$

$$\begin{aligned}\ln g^c - U^*/kT = \ln h + (zA/2)\ln(zA/2) - \Sigma_s(zA^c_{ss})\ln(zA^c_{ss}) \\ -\frac{1}{2}\Sigma_s\Sigma_l(zA^c_{sl}/2) - \frac{1}{2}A\Sigma_s\alpha_s\varepsilon_{ss}/kT\end{aligned} \tag{9.99}$$

To avoid confusion in diffrenciating this relation with respect to the variables A^C_{sl}, the current subscripts in the summation are denoted by $(s'l')$. In the sum $(\Sigma_{s'l'}zA^c_{s's'})ln(zA^c_{s's'})$ only the derivatives of the terms $s'=s$ and $s' = l$ are different from zero and we can write

$$\begin{aligned}\frac{\partial}{\partial A^C_{sl}}[\Sigma(zA^C_{s's'}\ln(zA^C_{s's'}) &= \frac{\partial}{\partial A^c_{sl}}\ln(zA^c_{s's'}) \\ &\quad +(zA^c_{sl})\ln(zA^c_{ss}) \\ &= z[1 + \ln(zA^c_{ss})]\frac{\partial A^c_{ss}}{\partial A^c_{sl}} z[1 + \ln(zA^c_{ss})]\frac{\partial A^c_{ll}}{\partial A^c_{sl}} \\ &= -\frac{z}{2}[2 + \ln(z^2A^c_{ss}A_l{}^c)]\end{aligned} \tag{9.100}$$

where we have used A^c_{ss}/A^c_{sl} = -1/2, obtained from equation 9.88. Furthermore, since the term A^C_{sl} appear twice in the double sum we have

$$\frac{\partial}{\partial A^C_{sl}}[\frac{1}{2}\Sigma_s\Sigma_l(zA^C_{s'l'}\ln(zA^C_{s'l'}/2)] = \frac{\partial}{\partial A^c_{sl}}[(zA^c_{sl})\ln(zA^c_{sl}/2) \\ =z[1 + \ln(zA^c_{ss})/2] \tag{9.101}$$

Thus the required derivatives are

$$\frac{\partial(\ln g^c - U^*/kT)}{\partial A^c_{sl}} = \frac{z}{2}[2 + \ln(z^2A^c_{ss}A^c_{ll})] - z[1 + \ln(zA^c_{sl}/2)] \\ = -\frac{z}{2}\ln\frac{A^{c2}_{sl}}{4A^c_{ss}A^c_{ll}} \tag{9.102}$$

and the equilibrium values in the zero approximation, A^*_{ss}, A^*_{sl}, A^*_{ll} ,are given by the equations[9]

$$A^*_{sl} = 4A^*_{ss}A^*_{sl} \qquad (s,l,=a,b,,.....\sigma) \tag{9.103}$$

For σ different types of surfaces the number of unknowns A^*_{ss} and A^*_{sl} is equal to $\sigma(\sigma + 1)/2$. The $\sigma(\sigma -1)/2$ equations 9.103 and the σ equations 9.88 form a system of $\sigma(\sigma + 1)$ equations from which all the contact surfaces can be calculated. This system of equations can easily be reduced to a system of σ equations by replacing A^*_{sl} by their

values given by equation 9.103.

Let

$$A^*_{ss} = \frac{A}{2}(X^*_s)^2 \tag{9.104}$$

then

$$A^*_{st} = \frac{A}{2}X^*_s X^*_l \tag{9.105}$$

On substituting in equation 9.88 we obtain

$$X^*_s \Sigma_l X^*_l = \alpha_s \quad (s = a, b, ... \sigma) \tag{9.106}$$

Summing all these equations leads to an expression

$$\Sigma_s X^*_s \Sigma_l X^*_l = \Sigma_s \alpha_s \tag{9.107}$$

which become, because of equation 9.86, $(\Sigma_l X^*_l)^2 = 1$, and consequently, from equation 9.106

$$X_s^* = \alpha_s \quad (s = a, b, ... \sigma) \tag{9.108}$$

These are the solution of the system of equations 9.106 in the zeroth approximation.

The contact surfaces are given by

$$A_{ss}^* = \frac{A}{2}\alpha_s^2 \qquad A_{sl}^* = A\alpha_s\alpha_l \tag{9.109}$$

Now with these values we can write

$$g^* = h\frac{(zA/2)!}{\pi_s(zA_{ss}^*)!\,\pi_{sl}(zA_{sl}^*/2)!} \tag{9.110}$$

and replace h in the equation 9.97 by it value from equation 9.110. Therefore

$$g^c = g^*\frac{(zA/2)!\,\pi_{sl}(zA_{sl}^*/2)!}{\pi_s(zA_{ss}^c)!\,\pi_{sl}(zA_{sl}^c/2)!} \tag{9.111}$$

where A^*_{ss}, and A^*_{sl} have the values given by equation 9.117.
To determine the equilibrium values of A^*_{sl}, of the surface A^C_{sl} in the general case

where U^c is given by equation 9.102, we follow the same procedure as before,

$$\frac{\partial(\ln g^c - U^c/kT)}{\partial A_{sl}^c} = -\frac{Z}{2}\ln\frac{A_{st}^{c2}}{4A_{ss}^c A_{sl}^c} \tag{9.112}$$

if we let

$$A_{ss} = \frac{A}{2}(X_s)^2 \tag{9.113}$$

we have at equilibrium

$$A_{sl} = AX_sX_l\eta_{sl} \tag{9.114}$$

where

$$\eta_{sl} = \exp[-\frac{\Delta\varepsilon_{sl}}{zkT}] \tag{9.115}$$

On substituting A_{sl} in equation 9.88 we obtain the system of σ equations with σ unknowns X_s.

$$X_s(X_s + \Sigma_l X_l\eta_{sl}) = \alpha_s \quad (s = a, b, ,.... \sigma) \tag{9.116}$$

We see that for $\Delta\epsilon_{sl} = 0$, or $\eta_{sl} = 1$, the solution of the equation 9.116 is the zeroth approximation A^*_{sl} and A^*_{ss}.

By a process of substitution the equilibrium values A_{ss}, and A_{sl} we obtain in equations 9.88 and 9.111 the configerational energy at equilibrium is obtained

$$\frac{U}{kT} = \frac{1}{2}A\Sigma_s\alpha_s(\varepsilon_{ss}/kT) + \frac{1}{2}\Sigma_s\Sigma_l A_{sl}(\Delta\varepsilon_{sl}/kT) \tag{9.117}$$

and the combinatorial factor at equilibrium

$$g = g^* \frac{\pi_s(zA^*_{ss})!\,\pi_{sl}(zA^*_{sl}/2)!}{\pi_s(zA_{ss})!\,\pi_{sl}(zA_{sl}/2)!} \tag{9.118}$$

These functions, substituted into equation 9.88, completely define the configurational partition function of the system, and will be used for calculating the excess thermodynamic functions.

9.4.3.1.2. Excess Free Energy[9]

The *configurational free energy, F*, of the system is obtained from the configurational partition function Ω according to the relation:

$$F/kT = -\ln\Omega \tag{9.119}$$

For an ensemble of N_i molecules of pure component i;

$$F_i/kT = -\ln\Omega_i \tag{4.120}$$

and the excess free energy F^E is given by:

$$F^E/kT = -\ln\Omega + \Sigma_i \ln\Omega_i - \Sigma_i N_i \ln x_i \tag{9.121}$$

The *excess molar chemical potential* μ^E_i is defined by:

$$\mu_i^E/RT \equiv \frac{\partial(F^E/kT)}{\partial N_i} = -\frac{\partial \ln\Omega}{\partial N_i} + \frac{\ln\Omega_i}{N_i} - \ln x_i \tag{9.122}$$

where $R = N_A k$, N_A being the Avogadro number. From equations.....
we can write

$$\begin{aligned}\ln\Omega &= \ln g - U/kT \\ &= \ln g^{*} + \Sigma_s(zA^{*}_{ss})\ln(zA^{*}_{ss}) \\ &\quad + \frac{1}{2}\Sigma_s\Sigma_l(zA^{*}_{ss})\ln(zA^{*}_{ss}) \\ &\quad - \Sigma_s(zA_{ss})\ln(zA_{ss}) \\ &\quad - \frac{1}{2}\Sigma_s\Sigma_l(zA_{sl})\ln(zA_{sl}/2) \\ &\quad - \frac{1}{2}A\Sigma_s\alpha_s\varepsilon_{ss}/kT - \frac{1}{2}\Sigma_s\Sigma_l A_{sl}\Delta\varepsilon_{sl}/kT\end{aligned} \tag{9.123}$$

Differentiation of *ln* Ω w.r.t N_i can be carried put considering the contact surface A^{*}_{sl} and A^{*}_{ss} to be constant since we know that the partial derivatives w.r.t these variables lead to the equilibrium conditions and are equal to zero. With equations 9.84, 9.88, 9.109, and 9.113 equation 9.123 becomes

$$\begin{aligned}\frac{\partial\ln\Omega}{\partial N_i} &= \frac{\partial\ln g^{*}}{\partial N_i} + \frac{\partial}{\partial N_i}[\Sigma_s(zA^{*}_{ss})\ln(zA^{*}_{ss})] \\ &\quad - \frac{\partial}{\partial N_i}[\Sigma_s(zA_{ss})\ln(zA_{ss})] - \frac{1}{2}\Sigma_s q_i\alpha_{si}\varepsilon_{ss}/kT \\ &= \frac{\partial\ln g^{*}}{\partial N_i} + \frac{zq_i}{2}\Sigma_s\alpha_{si}[1 + \ln(zA^{*}_{ss})] \\ &\quad - \frac{zq_i}{2}\Sigma_i\alpha_i\alpha_{si}[1 + \ln(zA_{ss})] - \frac{q_i}{2}\Sigma_s\alpha_{si}\varepsilon_{ss}/kT \\ &= \frac{\partial\ln g^{*}}{\partial N_i} + \frac{zq_i}{2}\Sigma_s\alpha_{si}\ln(A^{*}_{ss}/A_{sl}) - \frac{q_i}{2}\Sigma_s\alpha_{si}\varepsilon_{ss}/kT \\ &= \frac{\partial\ln g^{*}}{\partial N_i} + zq_i\Sigma_s\alpha_{si}\ln(\alpha_s/X_s) - \frac{q_i}{2}\Sigma_s\alpha_s\alpha_{si}\varepsilon_{ss}/kT\end{aligned} \tag{9.124}$$

For pure components i we will have:

$$\frac{\ln\Omega_i}{N_i} = \frac{\ln g_i^*}{N_i} + zq_i\Sigma_s\alpha_{si}\ln(\alpha_{si}/X_{si}) - \frac{q_i}{2}\Sigma_s\alpha_{si}e_{ss}/kT \tag{9.125}$$

where the X_i are the solutions of the systems of equations 9.116 for $x_i = 1$. Then

$$\frac{\mu_i^E}{RT} = \frac{\mu_i^* E}{RT} + zq_i\Sigma_s\alpha_{si}\ln\frac{X_s\alpha_{si}}{X_{si}\alpha_s} \tag{9.126}$$

where μ_i^{E*} is the *combinatorial molar excess chemical potential. The molar excess free energy, f^E,* is given by:

$$f^E = \Sigma_i x_i\mu_i^E \tag{9.127}$$

If we choose for μ_i^{E*} the simple Flory-Huggins formula

$$\frac{\mu_i^* E}{RT} = \ln\frac{\theta_i}{x_i} - \frac{\theta_i}{x_i} + 1 \tag{9.128}$$

where the volume fraction ϕ_i is given by equation 9.82, the molar excess free energy can be written as

$$\frac{f^E}{RT} = \Sigma_i x_i(\ln\frac{\theta_i}{x_i} + zq_i\Sigma_s\alpha_{si}\ln\frac{X_s\alpha_{si}}{X_{si}\alpha_s}) \tag{9.129}$$

With the Guggenheim combinatorial excess molar chemical potential

$$\frac{\mu_i^{*E}}{RT} = \ln\frac{\phi_i}{x_i} + \frac{zq_i}{2}\ln\frac{\eta_i}{\phi_i} \tag{9.130}$$

the molar excess free energy can be written as

$$\frac{f^E}{RT} = \Sigma_i x_i(\ln\frac{\phi_i}{x_i} + \frac{zq_i}{2}\ln\frac{\xi_i}{\phi_i} + zq_i\Sigma_s\alpha_{si}\ln\frac{X_s\alpha_{si}}{X_{si}\alpha_s}) \tag{9.131}$$

9.4.3.1.3. The Excess Energy[9]

The excess Energy, U^E, which can be equal to the energy of mixing, is deduced from the configurational energy of the system at equilibrium.

$$U = \frac{1}{2}q_iN_i(\Sigma_iq_iN_i)(\Sigma_s\alpha_s\varepsilon_{ss} + \Sigma_s\Sigma_iX_sX_i\eta_{si}\Delta\varepsilon_{si}) \tag{9.132}$$

For N_i molecules of pure component i the configurational energy is

$$U_i = \frac{1}{2} q_i N_i (\Sigma_s \alpha_{si} \varepsilon_{ss} + \Sigma_s \Sigma_l X_{si} X_{li} \eta_{sl} \Delta \varepsilon_{sl}) \tag{9.133}$$

Thus the excess free energy is:

$$\begin{aligned} U^E &= U - \Sigma_l U_l \\ &= \frac{1}{2} (\Sigma_i q_i N_i) \Sigma_s \Sigma_l (X_s X_l - \Sigma_i \xi_i X_{si} X_{li}) \eta_{sl} \Delta \varepsilon_{sl} \end{aligned} \tag{9.134}$$

the *molar excess energy* is $u^E = N_A U^E / N$ and then

$$u^E = \frac{1}{2} (\Sigma_i q_i x_i) \Sigma_s \Sigma_l (X_s X_l (X_s X_l - \Sigma_i \xi_i X_{si} X_{li}) \eta_{sl} N_A \Delta \varepsilon_{sl} \tag{9.135}$$

9.4.3.1.4. Application to Real Mixtures[9]

For each contact, (sl) only one interchange parameter exists, $\Delta\epsilon$ equilibrium remain the same except for the following differences

$$\eta_{sl} = \exp[-\frac{\Delta\omega_{sl}}{zkT}] \tag{9.136}$$

The equilibrium configurational free energy, F, can now be written as

$$\frac{F}{kT} = -\ln g + \frac{F_{inte}}{kT} \tag{9.137}$$

The equilibrium configurational energy, U, is given by the relation,

$$\frac{U}{kT} = -T\frac{\partial(F/kT)}{\partial T} = T\frac{\partial \ln \Omega}{\partial T} \tag{9.138}$$

where Ω is expressed by the equation 9.123 with ω instead of ϵ.

As before, the partial derivatives of *ln* Ω *with respect to* A_{sl} and A^*_{sl} are equal to zero and we can regard the contact surfaces as constants and differentiate only w.r.t. T. It can be seen the result is identical to equation 9.117 if we put

$$\varepsilon_{ss}/kT = -T\frac{d(\omega_{ss}/kT)}{dT} \qquad \Delta\varepsilon_{sl}/kT = -T\frac{d(\Delta\omega_{sl}/kT)}{dT} \tag{9.139}$$

When real mixtures are considered, the parameters $\Delta\omega_{sl}$ and $\Delta\epsilon_{sl}$ are adjusted

according to the experimental values of the molar excess Gibbs free energies (G^E) and the molar excess enthalpies, H^E, respectively. We call these parameters the interchange Gibbs energies and the interchange enthalpy respectively, and each contact (sl) is considered to have two such interchange parameters, g_{sl} and h_{sl}.

The molar interchange Gibbs energies, g_{sl}, in the system of equations 9.116 appear in the exponential factor

$$\eta_{sl} = \exp[-\frac{g_{sl}}{zRT}] \tag{9.140}$$

The solution X_s and X_{si} of this system of equations determine the chemical potential μ_i^E, equation 9.133 and the excess molar Gibbs energy

$$G^E = \Sigma_i x_i \mu_i^E \tag{9.141}$$

The *molar interchange enthalpies, h_{sl},* appear in the expression of the molar excess enthalpy

$$H^E = \frac{1}{2}(\Sigma_i q_i x_i)\Sigma_s \Sigma_l (X_s \Sigma_i (X_s X_l - \Sigma_i \xi_i X_{si} X_{li})\eta_{sl} h_{sl} \tag{9.142}$$

The relation between h_{sl} and g_{sl} is

$$\frac{h_{sl}}{RT} = -T\frac{dg_{sl}/RT}{dT} \tag{9.143}$$

9.4.3.1.4. The Zeroth Approximation[145]

The formula for the excess functions in the zeroth approximation are obtained formally from equation and when z→∞. In that case $X_s = \alpha_s$ and $X_{si} = \alpha_{si}$.

For the molar enthalpy,

$$\begin{aligned} H^{E*} &= \frac{1}{2}(\Sigma_l q_l x_l)\Sigma_s\Sigma_l(\alpha_s\alpha_l - \Sigma_i\xi_i\alpha_{si}\alpha_{li})h_{sl} \\ &= \frac{1}{2}(\Sigma_l q_l x_l)\Sigma_s\Sigma_l[(\Sigma_i\alpha_{si}\xi_i)(\Sigma_i\alpha_{si}\xi_i) - (\Sigma_i\alpha_{si}\alpha_{li}\xi_i)]h_{sl} \end{aligned} \tag{9.144}$$

Since

$$(\Sigma_i\alpha_{si}\xi_i)(\Sigma_i\alpha_{li}\xi_i) = \frac{1}{2}\Sigma_i\Sigma_j(\alpha_{si}\alpha_{lj} + \alpha_{sj}\alpha_{li})\xi_i\xi_j \tag{9.155}$$

and

$$\Sigma_i\alpha_{si}\alpha_{li}\xi_i = \frac{1}{2}(\Sigma_i\alpha_{si}\alpha_{li}\xi_i + \Sigma_j\alpha_{sj}\alpha_{lj}\xi_j) \tag{9.146}$$

or on multiplying by $\Sigma_i\xi_i = \Sigma_j\xi_j = 1$.

$$\Sigma_i \alpha_{si}\alpha_{li}\xi_i = \frac{1}{2}[\Sigma_j \xi_j)(\Sigma_i \alpha_{si}\alpha_{li}\xi_i) + (\Sigma_i \xi_i)(\Sigma_j \alpha_{sj}\alpha_{lj}\xi_j)] = \frac{1}{2}\Sigma_i \Sigma_j (\alpha_{si}\alpha_{li} + \alpha_{sj}\alpha_{lj})\xi_i \xi_j \quad (9.147)$$

Therefore

$$(\Sigma_i \alpha_{si}\xi_i)\Sigma_i \alpha_{li}\xi_i) - \Sigma_j \alpha_{sj}\alpha_{li}\xi_j = \frac{1}{2}\Sigma_i \Sigma_j (\alpha_{sj}\alpha_{ij} + \alpha_{sj}\alpha_{li} - \alpha_{si}\alpha_{li} - \alpha_{sj}\alpha_{ij})\xi_i \xi_j = -\frac{1}{2}\Sigma_i \Sigma_j (\alpha_{si} - \alpha_{sj})(\alpha_{li} - \alpha_{lj})\xi_i \xi_j \quad (9.148)$$

Finally

$$H^{E*} = \frac{1}{2}(\Sigma_t q_t x_t)\Sigma_i \Sigma_j \xi_i \xi_j h_{ij} \quad (9.149)$$

where

$$h_{ij} = -\frac{1}{2}\Sigma_s \Sigma_l (\alpha_{si} - \alpha_{sj})(\alpha_{li} - \alpha_{lj})h_{st} \quad (9.150)$$

The molar excess Gibbs energy, G^{E*}, in the zeroth approximation is the sum of the

two terms

$$G^{E*} = G^{E*}_{comb} + G^{E*}_{inte} \tag{9.151}$$

The combinatorial term, G^{E*}_{comb} is given by Flory's equation.

$$G^{E*}_{comb} = RT\Sigma_i x_i \ln\frac{\phi_i}{x_i} \tag{9.152}$$

It can be seen that the interfactional term, G^{E*}_{int} is given by similar equations.

$$G^{E*}_{inte} = \frac{1}{2}(\Sigma_i q_i x_i)\Sigma_i \Sigma_j \xi_i \xi_j g_{ij} \tag{9.153}$$

where

$$g_{ij} = -\frac{1}{2}\Sigma_s \Sigma_t (\alpha_{si} - \alpha_{sj})(\alpha_{li} - \alpha_{ij}) g_{sl} \tag{9.154}$$

9.5. Mulitiple Optimization Using DISQUAC and Modified UNIFAC

The design of physical processes for liquid mixtures involving the separation of

phases requires the knowledge of equilibrium conditions of the phases separated and the values of the activity coefficients of the components of the mixtures. For this reason the evaluation of a consistent method to predict values of the thermodynamic properties is of great interest. Sulfolane, tetrahydrothiophene-1,1-dioxane, (TMS) represents an industrially important substance. However, owing to its high boiling temperature, mesomorphic phase below the melting point and large hygroscopic nature,experimental data concerning the properties of this compound are scarce in the literature. The application of predictive methods to solvent + (TMS) mixtures is therefore particularly needed. In this work, the liquid - vapour equilibrium, VLE of six mixtures containing sulfolane, the solid - liquid equilibrium, SLE of six organic solvent + sulfolane, the activity coefficients at infinite dilution, γ_i^∞ using a g.l.c of various solutes in sulfolane, as well as the enthalpy of mixing of few systems have been measured. These results are examined on the basis of the surface interaction version of the quasichemical group - contribution theory DISQUAC and Modified UNIFAC (Dortmund).

New DISQUAC and Modified UNIFAC interaction parameters between the aliphatic or triple bond carbons or benzene and toluene or tetrachloromethane or other chlorocarbon groups or cyclic ethers alcohols or nitriles / sulfolane contacts were optimized using the experimental results obtained here as well as from all available literature data. The parameters provided may serve to accurately predict missing thermodynamic data. Sulfolane is taken as one group, as was suggested in UNIFAC model tables[130]. However, we believe that the present group - contribution analysis allows us to evaluate, with wider experimental data, the specific interaction parameters with sulfolane molecule divided for c-CH_2 and sulfolane group, -SO_2 in the future.

9.5.1.Results and Discussion

The DISQUAC model

As part of a systematic study on thermodynamic properties of sulfolane we have applied the DISQUAC[9] model (dispersive - quasichemical group contribution method, to report a complete characterization of the various organic solvents/sulfolane interactions, together with an extensive comparison between the DISQUAC calculations and experimental data.

Usually, the model gives a good representation of the equilibrium data, vapour -liquid, liquid - liquid and solid - liquid[153-155] as well as of the excess molar enthalpy, H^E or C_p^E data[155], the latter quantity being rather difficult to reproduce for any theoretical model[156].

The molecules under study, i.e. different solvents and sulfolane are regarded as possessing few types of surfaces:

- (1) type *a*: (CH_3 or CH_2 or CH) group in 1-heptyne, toluene, 1,1,1-trichloroethane, propan-2-ol and nitriles: propionitrile, butyronitrile, valeronitrile, or (C_6H_6) group in benzene, or (CCl_4) group in CCl_4, or (CCl_3) group in 1,1,1-trichloroethane, or (CH_2=) group in dichloromethane, or (c-CH_2) group in tetrahydrofuran and 1,4-dioxane and cyclic hydrocarbons;
- (2) type *c*:(CH≡C) group in 1-heptyne, or (A-C_6H_5) group in toluene, or (-O-) in tetrahydrofuran and 1,4-dioxane, or (CCl_3) group in 1,1,1-trichloroethane, or (Cl) group in dichloromethane, or (OH) group in alcohols, or (CH_3-C≡N and CH_2-C≡N) group in nitriles;
- (3) type *e*: (C) group in 2-methyl-2-propanol;
-(4) type *t*: sulfolane

The four types of surface generate three pairs of contacts: (*a*,*t*), (*c*,*t*) and (*e*,*t*). The relative group increments for molecular volumes r_G and areas q_G, calculated mainly using Bondi's method[157] and relative volumes r_i, relative total surfaces q_i , and

molecular surface fractions, α_{si}, calculated from the group increments are collected in Tables 9.1 and 9.2. The volume and the surface of methane was taken as unity as usual. The relative molecular volume of an OH group for primary alcohols is $r_{OH}=0.46963$, and the relative area $q_{OH}=0.50345$[155], were changed for a secondary alcohol using the same percentage of change as in UNIFAC.

All the data considered in this work is summarized in Tables 9.3-9.6. The equations used to calculate the excess Gibbs energy, G^E, and enthalpy, H^E, and $\ln\gamma_i^\infty$ are given earlier in Chapter 9. All available experimental data G^E, H^E and SLE data having the same type of surface *a* or *c* were optimized together.

For fitting the required group interaction parameters the Nelder-Mead algorithm has been used in combination with the Rosenbrock method to minimize the following objective functions:

-"weighted relative deviation"

$$F(W) = \Sigma_{nSLE}\Sigma_{i=1}^{N}\left[\frac{(\gamma_i^c(W)-\gamma_i^{exp})G^E(W)}{\gamma_1^{exp}}\right]^2 + \Sigma_{nVLE}\Sigma_{i=1}^{N}\left[\frac{(P_i^c(W)-P_i^{exp})G^E(W)}{P_i^{exp}}\right]^2 + \Sigma_{nGE}\Sigma_{i=1}^{N}\left[\frac{(G_i^{E^c}(W)-G_1^{E^{exp}})G^E(W)}{G_i^{E^{exp}}}\right]^2 + \Sigma_{nHE}\Sigma_{i=1}^{N}\left[\frac{(H_i^{E^c}(W)-H_i^{E^{exp}})G^E(W)}{H_i^{E^{exp}}}\right]^2 \qquad (9.155)$$

-"relative deviation"

$$F(W) = \Sigma_{nSLE}\Sigma_{i=1}^{N}\left[\frac{(\gamma_i^c(W)-\gamma_i^{exp})}{\gamma_1^{exp}}\right]^2 + \Sigma_{nVLE}\Sigma_{i=1}^{N}\left[\frac{(P_i^c(W)-P_i^{exp})}{P_i^{exp}}\right]^2 + \Sigma_{nG^E}\Sigma_{i=1}^{N}\left[\frac{(G_i^{E^c}(W)-G_1^{E^{exp}})}{G^{E^{exp}}}\right]^2 + \Sigma_{nH^E}\Sigma_{i=1}^{N}\left[\frac{(H_i^{E^c}(W)-H_i^{E^{exp}})}{H_i^{E^{exp}}}\right]^2 \quad (9.156)$$

where W represents the set of parameter vectors; nVLE ,nH^E, nSLE, are the number of systems used in the calculation; N is the number of experimental points in each system; G^E is the value of the excess Gibbs free energy calculated for x_i and T_i from VLE measurements with P being the total pressure in the system per isothermal P-x-T measurement.

The root mean square deviation, r.m.s (σ(P)) and relative r.m.s,(σ_r(P)) were calculated for G^E, H^E and SLE according to formulas (for example for VLE data):

$$\sigma(P) = [\Sigma_{i=1}(P_i^c - P_i^{exp})^2/N]^{\frac{1}{2}} \quad (9.157)$$

$$\sigma_r(P) = [\frac{1}{N}\Sigma_{i=1}^{N}(\frac{P_i^c - P_i^{exp}}{P_i^{exp}})^2]^{\frac{1}{2}}.100\% \qquad (9.158)$$

where P_i^c and P_i^{exp} are respectively the calculated and experimental pressures of the *i*th point (or G^E or H^E or T_i in SLE calculations); N is the number of experimental points.

The adjustment of the third interchange coefficients $C_{st,3}^{dis}$ and $C_{st,3}^{quac}$ from the experimental data was impossible because of lack of heat capacity data and H^E data at different temperatures,thus these parameters were optimized. For the "quac" part, the coordination number z=10, was chosen since it represents fairly well the symmetry of the experimental curves. The excess Gibbs energy, G^E and enthalpy, H^E for the n-alkanones + n-alkanes have been also successfully correlated using the quasi-chemical approach with a coordination number z=10[156]. Because of the similarity of the carbonyl and sulphonyl group a similar trend in the description of solvents + sulfolane mixtures was expected. The isothermal P-x and P-x-y data were used without correction for vapour-phase nonideality.

The solid-liquid equilibrium solidus-curve of sulfolane in different solvents was calculated with the following assumptions: phase transition takes place at 288.60 K; the absence of miscibility in the solid phase exists and a simple eutectic binary system is expected. The pure solute temperature and enthalpy of melting and phase transition, as well as molar heat capacities changes during the transition of solute is given in Chapter 8. In the DISQUAC model, the activity coefficient of the solute is as follows:

$$\ln\gamma_i = \ln\gamma_i^{comb} + \ln\gamma_i^{dis} + \ln\gamma_i^{quac} \qquad (9.159)$$

where $\ln\gamma_i^{comb}$ is the combinatorial term represented by the Flory-Huggins equation, while $\ln\gamma_i^{dis}$ and $\ln\gamma_i^{quac}$ are the dispersive and quasichemical contributions, respectively. Final interaction parameters are listed in Table 9.7. The alkane/sulfolane interactions (type *a*) existing in 1-heptyne, toluene, 1,1,1-trichloroethane, propan-2-ol, and the nitriles is shown in Table 9.7 as the CH_3/sulfolane interaction only for 1-heptyne.

Tables 9.3-9.6 and Figures 9.2-9.6 show numerical and graphical comparisons, respectively, between our and literature experimental data and predictions. The equimolar G^E and H^E values calculated using the new coefficients are presented in Tables 9.3 and 9.4. Generally, the agreement is satisfactory except for the sinusoidal shape of the H^E data. The relative r.m.s deviation of pressure $\sigma_r(P)$ calculated for the entire curve for isothermal P-x or P-x-y data, is less than 7 %. See Figs. 9.2 and 9.3 for 1-heptyne (1) + sulfolane (3), 1,1,1-trichloroethane (1) + sulfolane (3) as well as the following ethers: tetrahydrofuran (1) + sulfolane (3) at 353.15 K and 338.15 K, and 1,4-dioxane (1) + sulfolane (3) at 353.15 K, mixtures. The G^E values of benzene + sulfolane at 303.15 K[158] are worse than the results of Karvo[91]. This is probably due to experimental error. We expect that the G^E values predicted using the new coefficients are accurate to better than 7 % for the following four classes of solvents; I alkanes/sulfolane, II alkynes/sulfolane; II chlorohydrocarbons/suloflane; IV crown ethers/sulfolane. Good comparison of the theory with experimental data for the molar excess Gibbs energy G^E is shown in Fig. 9.4 for the mixtures of toluene (1) + sulfolane (3) at 313.15 K.[126]. It should be considered as a success, that the dependence on temperature of G^E is as usual well represented by the model, as G^E increases with temperature (Table 9.3).Caution should be exercised in the case of alcohol or nitriles + sulfolane mixtures because of the lack of experimental data (H^E and SLE only).

The results for H^E are shown in Table 9.4. Here, there is fairly good agreement (Fig. 9.5) for a toluene (1) + sulfolane (3) mixture. However, limitations of DISQUAC are related to the sinusoidal shape of the H^E, which is noted for a large number of systems in this work: benzene or 1,4-dioxane or acetonitrile. The excess enthalpies for benzene (1) + sulfolane (3) mixtures measured by Karvo[91] are more accurate than those of Pansini and Jannelli[159]. The r.m.s. deviation, σ_H (for the entire curve) is 13-18 $J \cdot mol^{-1}$. On the other hand the prediction of G^E is very good and the r.m.s. deviation is between 20-50 $J \cdot mol^{-1}$. In the case of the mixture with tetrachloromethane (1) + sulfolane (3) the difference of the maximum is about 54 $J \cdot mol^{-1}$ (experimental value H^E = 220 $J \cdot mol^{-1}$ at x_2 = 0.22, calculated value of H^E = 166 at x_2 = 0.46) and is strongly shifted to the low concentration region of the sulfolane. With such a shape it is difficult to attribute the difference between experimental and theory entirely to inadequacies of the model.As a matter of fact one value of coordination number z=10 for all systems cannot represent especially H^E over the entire concentration range. This behaviour is quite general for (polar + nonpolar) mixtures[156]. The predicted values of H^E of 1-heptyne(1) + sulfolane(2) mixture are much larger than the corresponding experimental results at 303.15 K. This difference may be explained by short-range orientational changes, termed "Patterson effect", when 1-alkynes are mixed with globular molecules or the parameters are not adequately optimized. This discrepancies between experiment and theory are not observed for VLE and SLE data (see Figs.9.2 and 9.6). The results of H^E for nitriles show r.m.s deviation from 21 to 42 $J \cdot mol^{-1}$ and underline a problem of optimizing parameters for CH_2CN group for two different shape of equilibrium curves: sinusoidal for acetonitrile and endothermic for n-nitriles; also only H^E data were available at one temperature.

Sulfolane, because of the steric hindrance of its globular molecule, may play

the role of an almost inert diluent and limits its action to a disturbing effect on the structure of the other component. Solid-liquid equilibrium measurements show weak interactions or only dipole-dipole interaction between sulfolane and different solvents[15-17] The largest interaction is observed with cyclic ethers and chlorohydrocarbons, the lowest with 1-heptyne and 2-methyl-2-propanol. Using the available interaction parameters for the surface type *a* and *c*/ type *t* contacts, the ability of the DISQUAC model on the prediction of the SLE has been successful. The r.m.s deviations, σ_T and relative r.m.s deviations, σ_{rT}, described by general eqns. (3) and (4) for the SLE equilibrium temperatures are from 0.9 to 5.5 K and from 0.3 to 2.2 % for all the mixtures investigated. The SLE T-x_2 curves are usually well represented by the model, even at rather low temperatures (see Fig.9.6).The DISQUAC prediction is somewhat poorer for solubility curve of sulfolane in tetrahydrofuran, where the experimental curve is shifted to the region of high sulfolane concentration in liquid component and is higher than the ideal solubility. Probably, these discrepancies may be due to some experimental inaccuracies, but also due to the stronger interaction between unlike molecules.

In Table 9.6 the natural logarithms of the activity coefficients at infinite dilution: $\ln \gamma_i^\infty = \mu_i^{E\infty}/RT$ have been listed. The result show, that structure- and temperature- dependent conformational effects and inaccuracies in accounting for non-randomness with the quasichemical equations, equally affect the quality of γ_i^∞ predictions. The $\ln \gamma_i^\infty$ predictions as a function of temperature may be considered satisfactory for n-alkanes, 1-alkynes and toluene. We were disappointed to see the disagreement between the calculated values in function of temperature and the experimental $\ln\gamma_i^\infty$ data given in Chapter 4. It seems difficult to explain other than by lack of the experimental data at different temperatures (especially ΔC_p) and not perfect values of our optimized interaction parameters. On the other hand, the observed

disagreement between the calculated and experimental $\ln\gamma_i^\infty$ values for solutions of c-hydrocarbons or crown ethers + sulfolane is probably due to free-volume effects and to the inadequacy of the Flory-Huggins combinatorial term used in the model. Moreover, we considered the application of DISQUAC to polar or associated systems as an empirical extension.

There have been several attempts in the literature to correlate and predict thermodynamic excess functions using either theoretical lattice-type or other ,more empirical, group-contribution models. In our opinion, the Modified Unifac[8] group contribution method based on the local composition concept may give G^E and H^E results comparable to DISQUAC. This method covers, in principle, all the classes of solvents considered in this study.

The Modified UNIFAC model

The Modified UNIFAC model has the same expression for the temperature dependence of the parameters as DISQUAC, needs four parameters per contact (two for Gibbs energy and two for enthalpy) to reproduce G^E and H^E; two heat capacity parameters have been considered also. However, a difference exists between the definition of the individual groups and values of the relative group increments for molecular volumes r_Q and areas q_Q. There is also no correlation between the interchange contact parameters and the structure of particular groups.

Although the Modified UNIFAC method is used world-wide, and the parameter matrix[160] is of similar size to that of UNIFAC, the possibility of new parameters for different solvents + sulfolane mixtures was taken into consideration. The results for mixtures with sulfolane have been used to fit the group interaction parameters for the new main group *n* (sulfolane) and solvents divided into various subgroups m, which

have been used by Modified UNIFAC (Dortmund). The temperature dependent parameters were obtained as far as the required experimental data for the different thermodynamic properties were available by fitting the parameters simultaneously to VLE, H^E, and SLE data using fitting procedure according to the equations 9.155 and 9.156. For VLE, no consistency test was performed and ideal gas phase was assumed. The van der Waals properties of the different subgroups were taken from Gmehling.[160] Sulfolane molecule was described, as before, by the parameters shown in the Table 9.1.[130] Table 9.8 shows the modified UNIFAC group interaction parameters between main group n (sulfolane) and different m subgroups existing in the tested solvents. The prediction of G^E and H^E is quite satisfactory. The difference between G^E (experimental) and G^E (calculated) rarely exceeds 40 $J \cdot mol^{-1}$ (Table 9.3), and this may be well within the limits of experimental error of certain measurements. There is excellent agreement between the VLE measurements (Chapter 7) and predicted values for chlorohydrocarbons, where the difference is less than 10 $J \cdot mol^{-1}$ (see Fig. 9.7). A comparsion of Modified UNIFAC with the experimental work of Karvo[91] is shown for benzene (1) + sulfolane (3) at four temperatures in Fig. 9.9. The weakest results were obtained for the prediction of VLE of THF (1) or propan-1-ol (1) + sulfolane (3), where the relative r.m.s. deviation ($\sigma_r(P)$) is 9.85 % or11-14%. The calculated excess enthalpies agree for most of the systems to within 15 $J \cdot mol^{-1}$ with the available measurements (Table 9.4), except for mixtures containing 1-heptyne + (TMS) where the experimental values, H^E, are much higher. Figure 9.8 shows the comparison of the predicted by Modified UNIFAC excess enthalpy for the tetrachloromethane (1) + sulfolane (3) mixture at 303.15 K. It is worth pointing out, that even the maximum is strongly shifted to the sulfolane low concentration region, the prediction is very good.

As expected the largest deviations appear in the case of the SLE predictions. For example, the solubility of sulfolane in benzene predicted by Modified UNIFAC is

much worse than the prediction by DISQUAC. The r.m.s. increased from 4.2 K to 7.2 K. For 1-heptyne the r.m.s increased from 2.0 K to 3.7 K from DISQUAC to Modified UNIFAC. The predicition of sulfolane solubility in chlorohydrocarbons is satisfactory; r.m.s. is less than 2 K.

The logarithms of the activity coefficients at infinite dilution $\ln\gamma_i^\infty$, have been determined for sulfolane in various solvents, and are listed in Table 9.6. The predictions are compared to literature values taken from various authors using a wide range of experimental techniques. The calculated ln γ_i^∞ for n-hydrocarbons and c-hydrocarbons are much lower than the experimentaly determined values. Unlike DISQUAC, the proper trend of the change of ln γ_i^∞ with temperature is noted in all systems. Nevertheless, the predicted values are similar to the measured values eg. benzene + TMS at 303.15 K, the predicted value of ln γ_i^∞ is 0.823, while the measured value by g.l.c is 0.770 (Chapter 4).

9.5.1. Conclusions

This work, following the series of comperative studies of the thermodynamic properties and molecular interactions in hundreds of mixtures by DISQUAC and Modified UNIFAC (Dortmund), illustrates the possibility of applying group contribution models to prediction of thermodynamic fuctions and phase equilibrium of certain polar mixtures invloving sulfolane.

Concidering the excess thermodynamic functions, the excess Gibbs energy, G^E and the excess molar enthalpy, H^E were mainly better represented by the Modified UNIFAC model. The optimization by the Modified UNIFAC model is consistently worse than the DISQUAC model in the prediction of the solid liquid equilibria. The prediction of activity coefficents at infinite dilution for both the straight chain and cyclic alkanes by the Modified UNIFAC model does not compare favourably with the

experimentally determined values. However the DISQUAC model has reasonable success with the alkanes, cycloalkanes and the aromatic compounds. Modified UNIFAC predicts the value $\ln\gamma_i^\infty$ accurately for the chloroalkanes.

TABLE 9.1. Relative group increments for molecular volumes, $r_G = V_G/V_{CH_4}$ and areas and for $q_G = A_G/A_{CH_4}$, calculated using Bondi's method[157], unless stated otherwise ($V_{CH_4} = 17.12 \times 10^{-6}$ m^3·mol^{-1}; $A_{CH_4} = 2.90 \times 10^5$ m^2·mol^{-1})

Group	r_G	q_G
$-CH_3$	0.79848	0.73103
$-CH_2-$	0.59755	0.46552
$HC\equiv C$	1.29200	1.08801
C_6H_6	2.82181	2.07212
$A\text{-}C_6H_5$	2.67752	1.83791
C	0.19451	0.00000
Cl[a]	0.71495	0.62759
$-CCl_3$	2.33936	1.88277
$CH_2<$[b]	0.59755	0.59482
O	0.21612	0.20690
$c\text{-}CH_2$	0.58645	$0.66377-0.0385m$ $4\leq m\leq 8$
OH(s,t)[c]	0.46951	0.50280
$CH_3\text{-}C\equiv N$	1.76761	1.60700
$CH_2\text{-}C\equiv N$	1.56667	1.34147
sulfolane[d]	4.03580	3.20000

[a] in CCl_3 and CCl_4 and in CH_2Cl_2
[b] in CH_2Cl_2
[c] deduced from OH(p) according to UNIFAC tables[130]
[d] Taken from UNIFAC tables[130]

TABLE 9.2. Volumes r_i, total surfaces q_i, and molecular surface fractions α_{si} (s = *a*, *c*, *e* or *t*), calculated from the group increments, r_G and q_G given in Table 9.1

Component	r_i	q_i	α_{ai}	α_{ci}	α_{ei}
1-Heptyne *a* = (CH_3,CH_2); *c* = (C≡CH)	4.4806	3.6811	0.7044	0.2955	0
Benzene *a* = (C_6H_6)	2.8218	2.0721	1.0000	0.0000	0
Toluene *a* = CH_3, *c* = (A-C_6H_5)	3.4760	2.5690	0.2846	0.7154	0
Tetracholomethane *a* = CCl_4	3.0543	2.5104	1.000	0.0000	0
1,1,1-Trichloroethane *a* = CH_3, *c* = CCl_3	3.1378	2.6138	0.2797	0.7203	0
Dichloromethane *a* = $CH_2<$, *c* = Cl	2.0275	1.8500	0.3215	0.6785	0
THF *a* = c-CH_2, *c* = O	2.5619	2.0920	0.9010	0.0989	0
1,4-Dioxane *a* = c-CH_2, *c* = O	2.7780	2.1449	0.8071	0.1929	0
Propan-2-ol *a* = CH_3, *c*= OH(s)	2.4625*	2.16141*	0.7674	0.2326	0
2-Methyl-2-propanol *a* = CH_3, *c* = OH(t), *e* = C	3.0595	2.6958	0.81349	0.1865	0
Acetonitrile *a* = CH_3, *c* = $CH_3C{\equiv}N$	1.7676	1.6070	0.0000	1.0000	0

Table 9.2 continued

Component	r_i	q_i	α_{ai}	α_{ci}	α_{ei}
Propionitrile $a = CH_3$, $c = CH_2C{\equiv}N$	2.36515	2.0725	0.2441	0.7558	0
Butyronitrile $a = CH_3$, $c = CH_2C{\equiv}N$	2.9627	2.5380	0.3827	0.61722	0
Valeronitrile $a = CH_3$, $b = CH_2C{\equiv}N$	3.56025	3.0035	0.4784	0.52155	0
Sulfolane $a = C_4H_8SO_2$	4.0358	3.2000	1.0000	0.0000	0

* deduced from OH(p) according to UNIFAC Tables[130]

TABLE 9.3. Molar excess Gibbs energies, G^E (T, x_1 = 0.5) of solvent (1) + sulfolane (3) mixtures at various temperatures T and equimolar compostions (x_1 = 0.5): comparison of direct experimental results with values calculated using the DISQUAC coefficients from Tables 9.1,9.2 and 9.7 and the Modified UNIFAC coefficients from Table 9.8, and realtive r.m.s deviations σ_r(P) (for the entire curve) of P/bar

Solvent(1)	T(K)	G^E(T, x_1=0.5)/ J·mol^{-1}		σ_r(P)/%	Source of experimental data
		Calc.	Exp.		
1-Heptyne	353.15	1495[a]	1540	5.63	
		1500[b]		6.50	
Benzene	303.15	645[a]	680	4.13	Karvo (1980)
		680[b]		2.26	
	303.15	645[a]	691	6.97	Benoit and Charbonneau
		678[b]		1.17	(1969)
	313.15	666[a]	701	4.39	Karvo (1980)
		701[b]		1.29	
	323.15	688[a]	723	4.62	Karvo (1980)
		720[b]		0.99	
	333.15	710[a]	744	4.70	Karvo (1980)
		744[b]		0.96	
Toluene	303.15	925[a]	930	5.72	Ashcroft et al. (1979)
		953[b]		2.85	
	303.15	925[a]	973	6.91	Karvo (1980)
		956[b]		4.94	
	313.15	947[a]	927	5.83	Ashcroft et al. (1979)
		973[b]		3.56	
	313.15	947[a]	994	6.72	Karvo (1980)
		976[b]		4.18	
	323.15	973[a]	1016	6.64	Karvo (1980)
		995[b]		3.97	
	333.15	1001[a]	1038	6.47	Karvo (1980)
		1014[b]		4.09	

Table 9.3 continued

Solvent(1)	T(K)	$G^E(T, x_1=0.5)$/ J·mol^{-1} Calc.	Exp.	$\sigma_r(P)$/%	Source of experimental data
Tetrahydrofuran					
	338.15	804[a]	745	1.65	
		785[b]		2.51	
	353.15	895[a]	1430	6.75	
		600[b]		9.85	
1,4-Dioxane	353.15	649[a]	448	3.84	
		780[b]		6.43	
Tetrachloromethane					
	338.15	1580[a]	1310	1.80	
		1298[b]		1.07	
1,1,1-Trichloroethane					
	338.15	1110[a]	1010	1.03	
		1017[b]		0.47	
Dichloromethane					
	303.15	-123[a]	-131	0.38	Benoit and Charbonneau
		-144[b]		2.06	(1969)
Propan-2-ol	303.15	1535[a]	1580	4.12	Ashcroft et al. (1978)
		1200[b]		11.52	
	313.15	1622[a]	1665	5.62	Ashcroft et al. (1978)
		1201[b]		14.24	

[a] Obtained by DISQUAC
[b] Obtained by Modified UNIFAC
where no reference is given implies experimental work present here.

Table 9.4. Molar excess enthalpies, H^E (T; x=0.5) of solvents (1) + sulfolane (3) mixtures at various temperatures (T) and equimolar composition (x_1 = 0.5): comparison of direct experimental results with values calculated using the DISQUAC coefficients from Tables 9.1, 9.2 and 9.7 and the UNIFAC coefficients from Table 9.8 and r.m.s deviations $\sigma_r(H)$ for the entire curve

Solvent(1)	T(K)	$H^E(T, x_1=0.5)$/ J·mol^{-1} Calc.	Exp.	σ_H/ J·mol^{-1}	Source of experimental data
1-Heptyne	303.15	911[a]	342	153.0	
		255[b]		73.05	
Benzene	303.15	11.6[a]	28.1	13.15	Karvo (1980)
		30.0[b]		13.29	
	303.15	11.6[a]	45	18.20	Pansini and Jannelli
		30.0[b]		10.29	(1986)
Toluene	303.15	318[a]	325	24.29	Karvo (1980)
		315[b]		31.62	
1,4-Dioxane	303.15	11.0[a]	38.3	7.63	Pansini and Jannelli
		17.2[b]		10.82	(1986)
Tetrachloromethane					
	303.15	165[a]	148	62.00	Pansini and Jannelli
		132[b]		15.00	(1986)
Acetonitrile	303.15	-20.1[a]	-15.5	23.03	Lopez et al. (1983)
Propionitrile	303.15	130[a]	173	34.43	Lopez et al. (1983)
Butyronitrile	303.15	338[a]	328	21.43	Lopez et al. (1983)
Valeronitrile	303.15	518[a]	463	43.78	Lopez et al. (1983)

[a] Obtained by DISQUAC [b] Obtained by Modified UNIFAC
where no reference is given implies experimental work present here.

TABLE 9.5. Values of the r.m.s. deviations σ and relative r.m.s. dviations $\sigma_r(\%)$ of solid-liquid equilibrium temperature (T) of solvent (1) + sulfolane (3) mixtures obtained using the DISQUAC and UNIFAC models

Solvent(1)	σ_T(K)[1]	σ_{rT}(%)[2]	Source of experimental data
1-Heptyne	2.04[a]	0.70	
	3.74[b]	1.33	
Benzene	4.23[a]	1.60	Jannelli and Sacco (1972)
	7.16[b]	2.81	
Tetrahydrofuran	5.49[a]	2.18	
	3.39[b]	1.19	
1,4-Dioxane	1.55[a]	0.56	Jannelli et al. (1975)
	3.20[b]	1.19	
	2.08[a]	0.74	
	1.23[b]	0.43	
Tetrachloromethane			
	2.51[a]	0.86	Sacco et al. (1976)
	2.89[b]	1.00	
1,1,1-Trichloroethane			
	0.94[a]	0.33	
	1.67[b]	0.61	
2-Methyl-2-propanol			
	3.43[a]	1.19	Inglese and Jannelli (1978)
	3.92[b]	1.37	

[1] calculated using Eqn. 3
[2] calculated using Eqn. 4
[a] Obtained by DISQUAC
[b] Obtained by Modified UNIFAC
where no reference is given implies experimental work present here.

TABLE 9.6. Logarithm of activity coefficients at infinite dilution, $\ln \gamma_i^\infty$ in solvent (1) + sulfolane (3) mixtures at various temperature (T). Comparison of direct experimental results with values calculated using the DISQUAC coefficients given in Tables 9.1, 9.2 and 9.7 and the UNIFAC coefficients given in Table 9.8

Solvent (1)	T(K)	$\ln \gamma_1^\infty$		$\ln \gamma_3^\infty$	
		Calc.	Exp.	Calc.	Exp.
Pentane	303.15	5.005[a]	4.063[1,c]	5.603	-
		1.509[b]		1.547	
Hexane	303.15	5.837[a]	4.317[1,c]	5.619	-
		1.499[b]		1.263	
Heptane	303.15	6.646[a]	4.585[1,c]	5.611	-
		1.488[b]		1.055	
Cyclopentane					
	303.15	1.771[a]	3.785[1,c]	2.410	-
		1.802[b]		3.296	
Cyclohexane					
	303.15	2.171[a]	3.531[1,c]	2.458	-
		2.166[b]		3.401	
Cycloheptane					
	303.15	2.544[a]	3.740[2,c]	2.467	-
		2.515[b]		3.611	
	313.15	2.552[a]	3.569[2,c]	2.475	-
		2.446[b]		3.583	
Cyclooctane	303.15	2.895[a]	3.940[2,c]	2.457	-
		2.852[b]		3.496	
	313.15	2.905[a]	3.780[2,c]	2.465	
		2.779[b]		3.490	

Table 9.6 (continued)

Solvent (1)	T(K)	$\ln \gamma_1^\infty$		$\ln \gamma_2^\infty$	
		Calc.	Exp.	Calc.	Exp.
1-Hexyne	303.15	1.233[a]	1.749[2,c]	1.178	-
		2.268[b]		2.373	
	313.15	1.267[a]	1.732[2,c]	1.220	-
		2.256[b]		2.359	
1-Heptyne	303.15	2.046[a]	2.118[2,c]	1.732	-
		2.267[b]		1.988	
	313.15	2.073[a]	2.050[2,c]	1.764	-
		2.254[b]		1.974	
	353.15	2.774[a]	1.820[3,d]	2.410	2.531
		2.208[b]		1.927	
1-Octyne	303.15	2.840[a]	2.476[2,c]	2.146	-
		2.261[b]		1.698	
	313.15	2.802[a]	2.420[2,c]	2.171	-
		2.247[b]		1.685	
Benzene	303.15	1.156[a]	0.770[1,c]	1.800	1.739
		0.823[b]	0.908[4,e]	1.582	
	313.15	1.154[a]	0.903[4,e]	1.797	1.735
		0.822[b]		1.580	
	323.15	1.152[a]	0.899[4,e]	1.795	1.732
		0.821[b]		1.578	
	333.15	1.152[a]	0.894[4,e]	1.794	1.729
		0.810[b]		1.576	
Toluene	303.15	1.527[a]	1.582[4,e]	1.407	2.815
		1.373[b]		1.736	
	313.15	1.503[a]	1.567[4,e]	1.399	2.786
		1.355[b]		1.718	
	323.15	1.480[a]	1.553[4,e]	1.406	2.759
		1.337[b]		1.699	
	333.15	1.458[a]	1.540[4,e]	1.426	2.734
		1.319[b]		1.681	

Table 9.6 (continued)

Solvent (1)	T(K)	$\ln \gamma_1^\infty$ Calc.	$\ln \gamma_1^\infty$ Exp.	$\ln \gamma_2^\infty$ Calc.	$\ln \gamma_2^\infty$ Exp.
Tetrahydrofuran					
	303.15	1.269[a]	0.806[1,c]	1.318	-
		1.093[b]		1.539	
	338.15	1.285[a]	0.830[3,d]	1.327	1.506
		1.024[b]		1.775	
	353.15	1.297[a]	1.330[3,d]	1.336	4.682
		0.800[b]		0.865	
Tetrahydropyran					
	303.15	1.692[a]	0.104[1,c]	1.576	-
		1.466[b]		1.953	
1,4-Dioxane	298.15	1.080[a]	1.20[5,c]	0.596	
		0.806[b]		0.890	
	353.15	1.090[a]	0.40[3,d]	0.567	1.280
		0.993[b]		1.159	
Tetrachloromethane					
	338.15	2.848[a]	1.319[3,d]	3.633	3.658
		1.423[a]		3.114	
1,1,1-Trichloroethane					
	338.15	1.763[a]	1.049[3,d]	2.148	2.216
		1.218[b]		1.863	
Dichloromethane					
	303.15	-0.118[a]	-0.139[6,e]	-0.265	-0.357
		-0.207[b]		-0.276	
Propan-2-ol	303.15	2.521[a]	2.578[7,d]	3.692	3.781
	313.15	2.623[b]		3.815	

[1] This work, [2]Unpublished, [3]This work, [4]Karvo (1980a), [5]Gmehling et al. (1994), [6]Benoit and Charbonneau (1969).[7] Ashcroft et al. (1979). [a] Obtained by DISQUAC,[b] Obtained by UNIFAC, [c] Obtained by gas-liquid chromatography (corrected for vapour-phase nonideality), [d] calculated from isothermal P-x-y data, extrapolated to x_i = o, [e] calculated from isothermal P-x data, extrapolated to $x_i = 0$.

TABLE 9.7. Interchange coefficients, dispersive $C^{dis}_{st,l}$ (l=1,2,3) and quasichemical $C^{quac}_{st,l}$(l=1,2,3), for the contacts between type s = *a*, or *c* or *e* and sulfolane (type *t*). The coordination number used for the quac part is z = 10

Component	$C^{dis}_{st,1}$	$C^{dis}_{st,2}$	$C^{dis}_{st,3}$	$C^{quac}_{st,1}$	$C^{quac}_{st,2}$	$C^{quac}_{st,3}$
1-Heptyne						
CH_3	0.0952	2.5345	-29.5327	1.6656	-2.2714	33.8022
$HC\equiv C$	-3.2159	3.2655	-48.6210	0.9177	-2.5730	-25.1276
Benzene						
C_6H_6	-1.0172	-0.1341	0.1031	1.6030	0.1811	-0.4980
Toluene						
A-C_5H_6	1.0889	2.9625	11.1932	-0.9461	-2.6574	-12.7009
Tetrachloromethane, 1,1,1-Trichloroethane, Dichloromethane						
CCl_4	0.8430	31.6700	-225.1871	-0.4660	-29.2605	86.1980
$-CCl_3$	-0.1522	7.9909	-10.2312	0.3331	-8.7742	7.9081
$CH_2<$ [a]	-0.2708	0.9301	-186.520	-0.3724	-9.7010	-27.1010
Cl	-0.8063	-18.3905	53.7153	0.4479	-20.5366	-32.0036
THF/1,4-Dioxane						
c-CH_2	-0.8879	-0.0225	-0.8512	1.6582	-0.01124	-0.5670
O	1.6064	-0.1297	2.4201	-2.0706	0.27203	1.6336
Propan-2-ol and 2-Methyl-2-propanol						
OH (s), (t)	-3.1022	1.1175	-17.129	2.4195	-7.5439	-24.6445
C	-373930	-4705.30	13935.8	-7711.84	119.543	15.1837
Acetonitrile and n-Nitriles						
CH_2CN	18049.4	-208.235	12360.6	2.7690	131.817	-7806.51

[a] in CH_2Cl_2

TABLE 9.8. Modified UNIFAC (Dortmund) group interaction parameters where n=sulfolane

m	a_{nm}(K)	b_{nm}	$c_{nm}(K^{-1})$	a_{mn}(K)	b_{mn}	$c_{mn}(K^{-1})$
CH_3	4.8559	-0.5691	0.0	17.957	0.3355	0.0
$HC\equiv C$	20.034	-0.4075	$-0.28\cdot10^{-3}$	15.074	2.4345	0.0008
A-CH	1.8533	-0.5074	0.0	2.8210	0.7809	0.0
A-CCH_3	12.245	0.6666	$-0.139\cdot10^{-2}$	2.6869	0.3974	0.0004
CH_2Cl_2	3.3360	-0.9443	$0.845\cdot10^{-3}$	-6.2341	0.3936	-0.00124
CCl_3	10.427	-0.3916	$0.07\cdot10^{-3}$	52.747	1.1948	-0.000415
CCl_4	9.2135	-0.9091	$0.49\cdot10^{-3}$	12.892	2.1653	-0.00207
c-CH_2	0.5878	-0.6335	$-0.112\cdot10^{-2}$	-0.5401	0.0665	0.2695
c-CH_2OCH_2	0.3340	-0.7474	$0.107\cdot10^{-2}$	0.2121	1.0228	-0.00174
$OH_{(s,t)}$	195.729	2.4758	$-0.733\cdot10^{-2}$	161.67	-111.11	0.53226
CH_3CN						

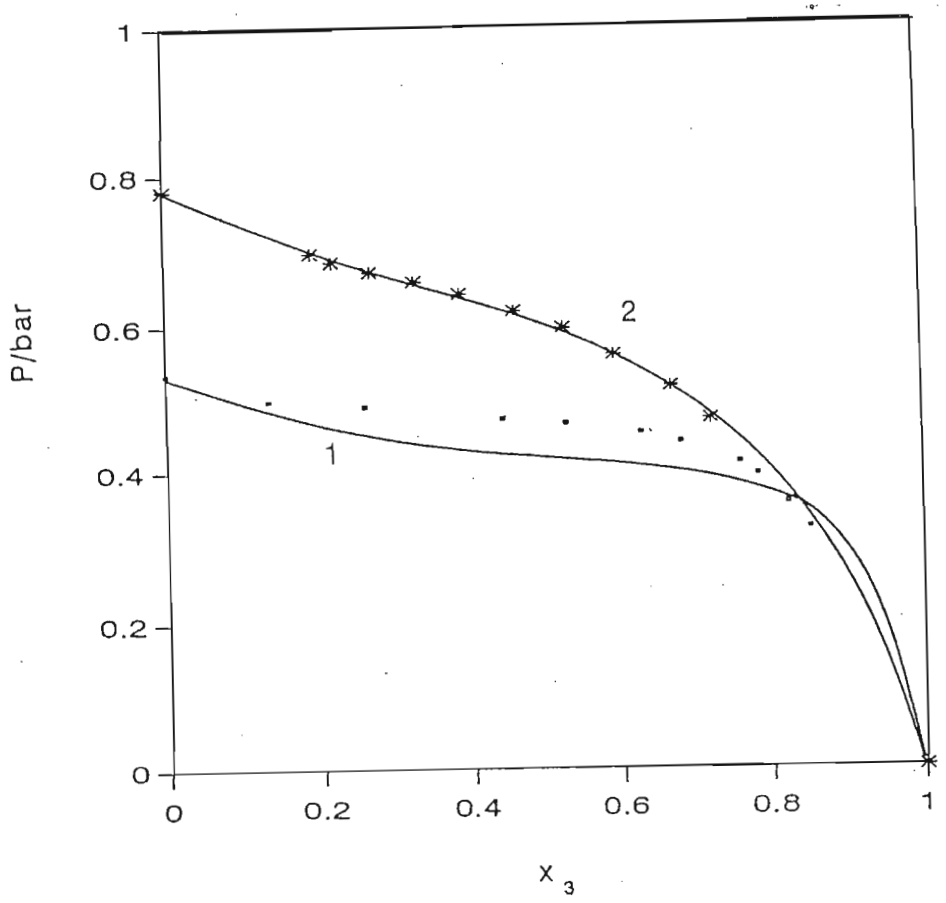

FIGURE 9.2. Comparison of theory with experiment for the isothermal vapour-liquid phase equilibrium diagram for 1-heptyne (1) + sulfolane (3) at 353.15 K, (1) and for 1,1,1-trichloroethane (1) + sulfolane (3) at 338.15 K (2).Total pressure, P, versus, x_2, the mole fraction of sulfolane in the liquid phase. Lines, DISQUAC predicted values, points, experimental results

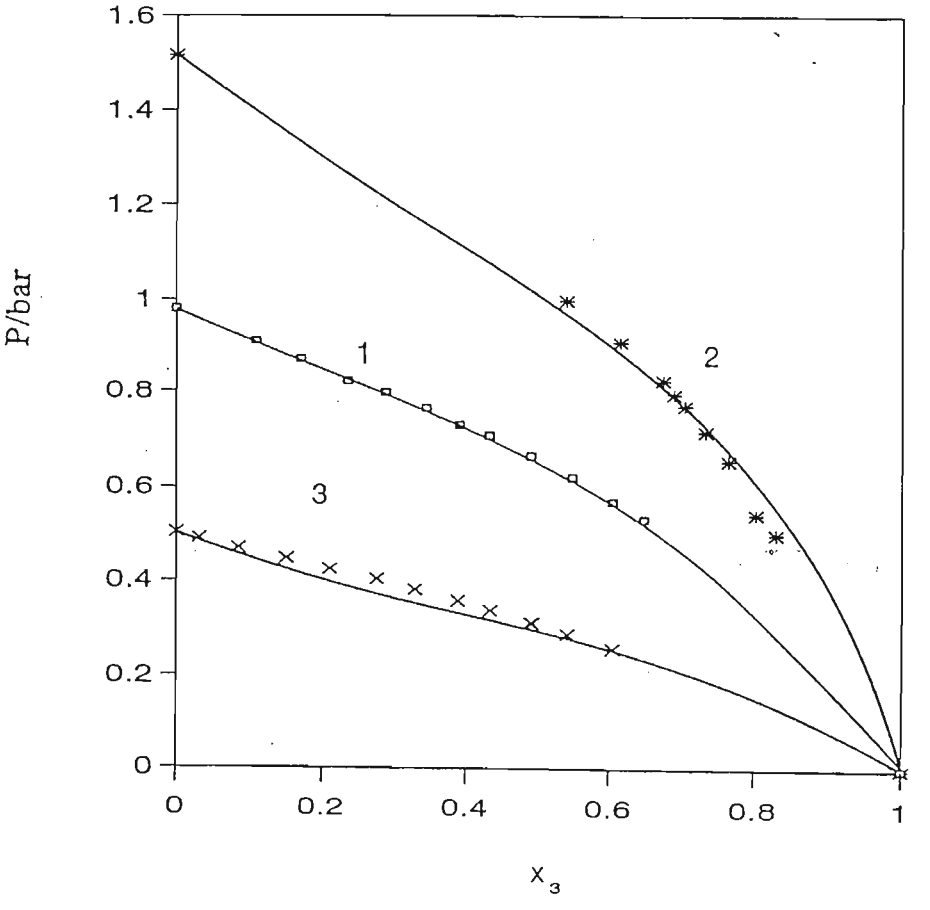

FIGURE 9.3. Comparison of theory with experiment for the isothermal vapour-liquid phase equilibrium diagram for tetrahydrofuran (1) + sulfolane (3) at 353.15 K (1) and 338.15 K (3) and for 1,4-dioxane (1) + sulfolane (3) at 353.15 (3). Lines, DISQUAC predicted values, points experimental results

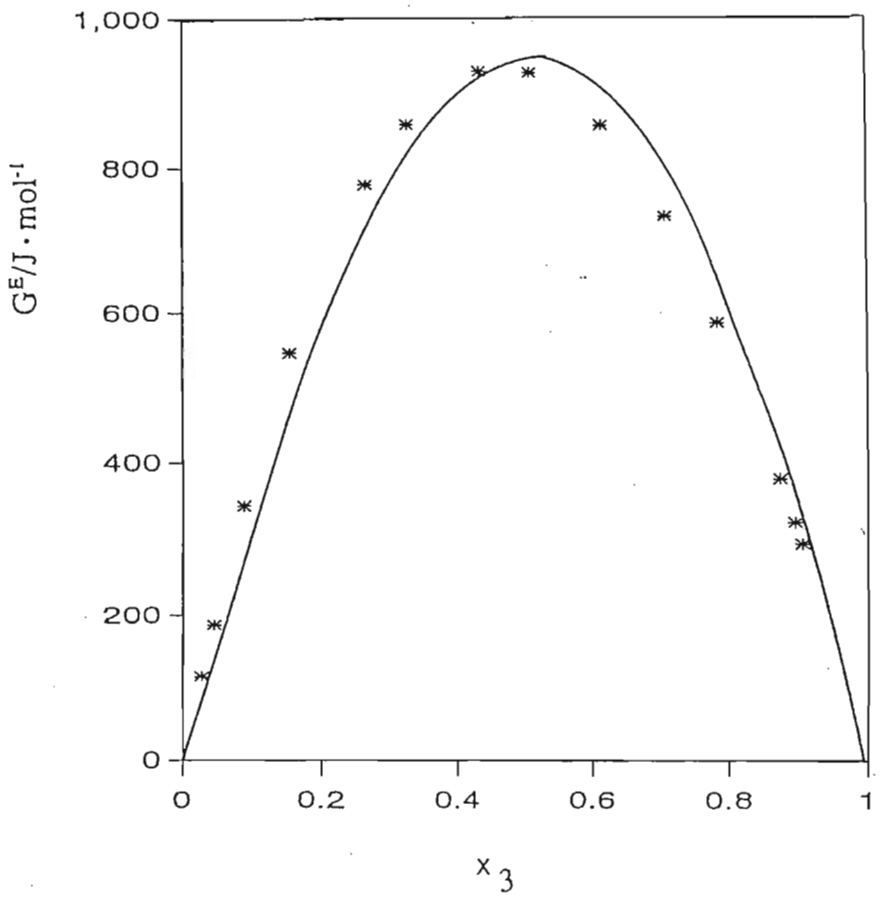

FIGURE 9.4. Comparison of theory with experiment for the molar excess Gibbs energy, G^E at 313.15 K (2) of toluene (1) + sulfolane (3) mixtures. Lines, DISQUAC predicted values, points, experimental results (Ashcroft et al., 1979).

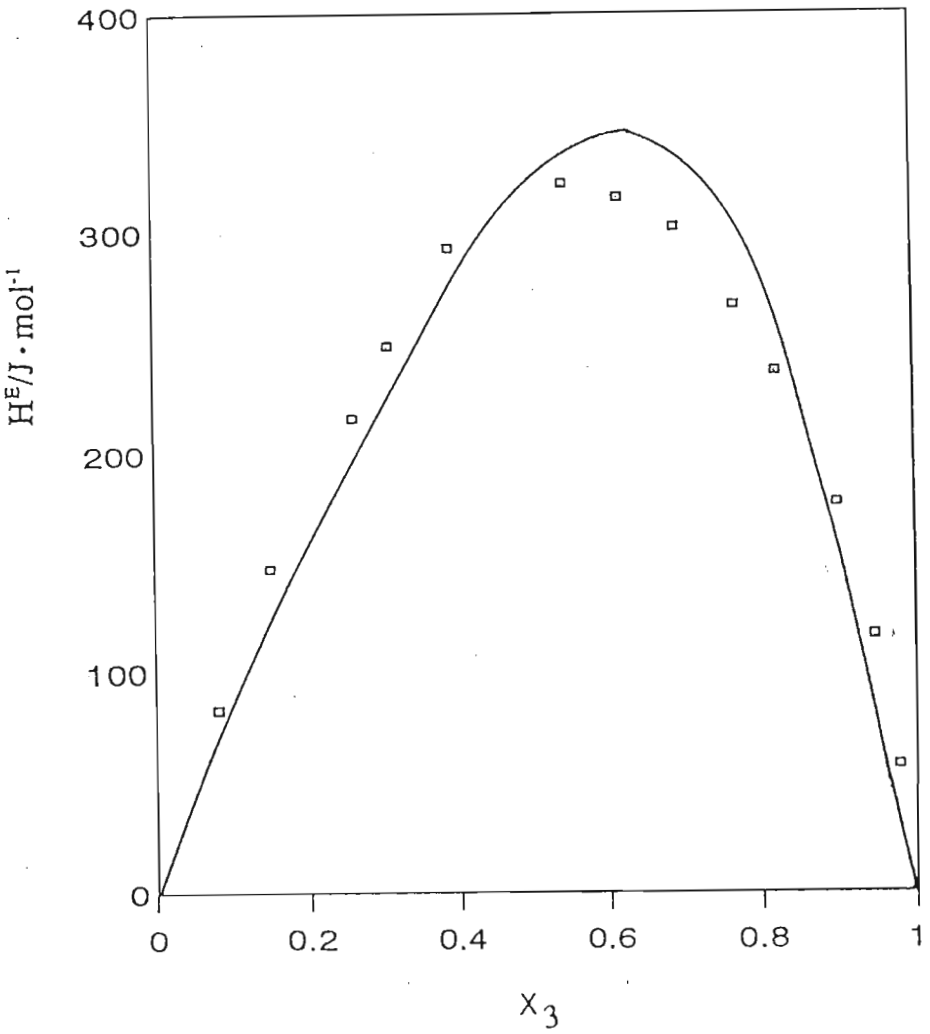

FIGURE 9.5. Comparison of theory with experiment for the excess enthalpies, H^E of toluene (1) + sulfolane (3) mixtures at 303.15 K. Lines, DISQUAC predicted values; points, experimental results (Karvo).

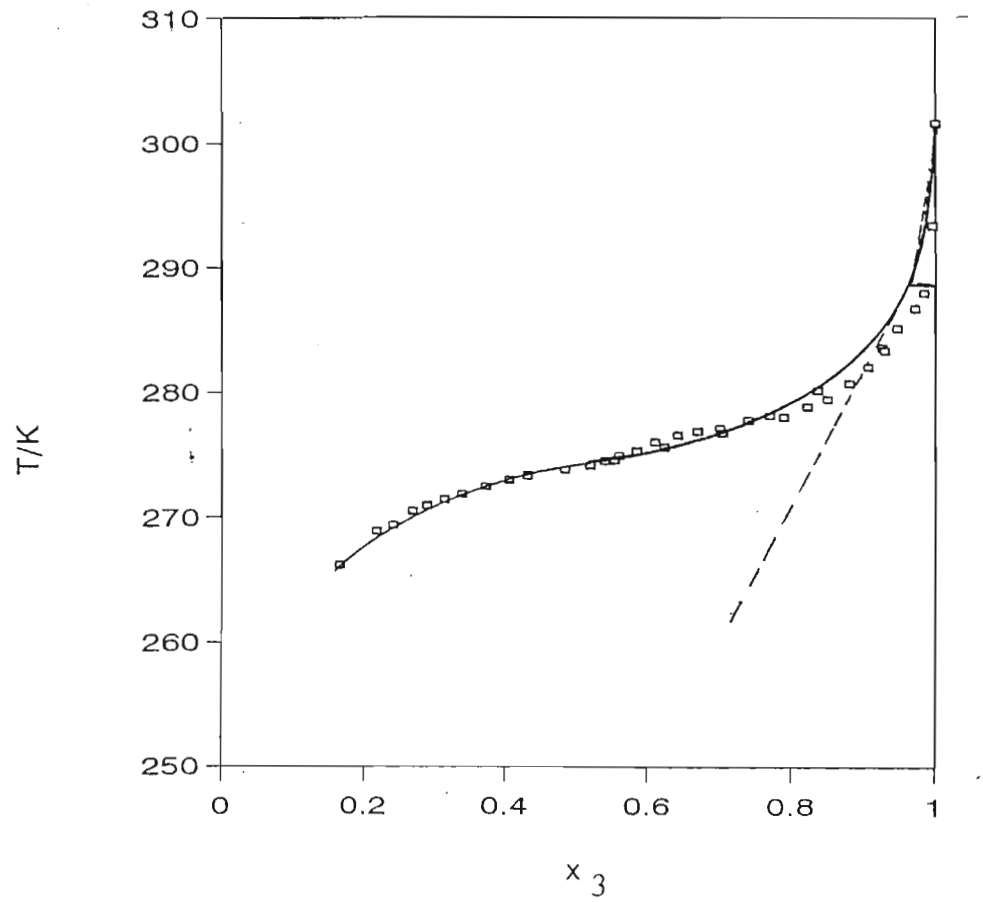

FIGURE 9.6 Solubility of sulfolane (3) in 1-heptyne (1). Solid curve, DISQUAC prediction, dashed lines, ideal solubility curve; points, experimental results

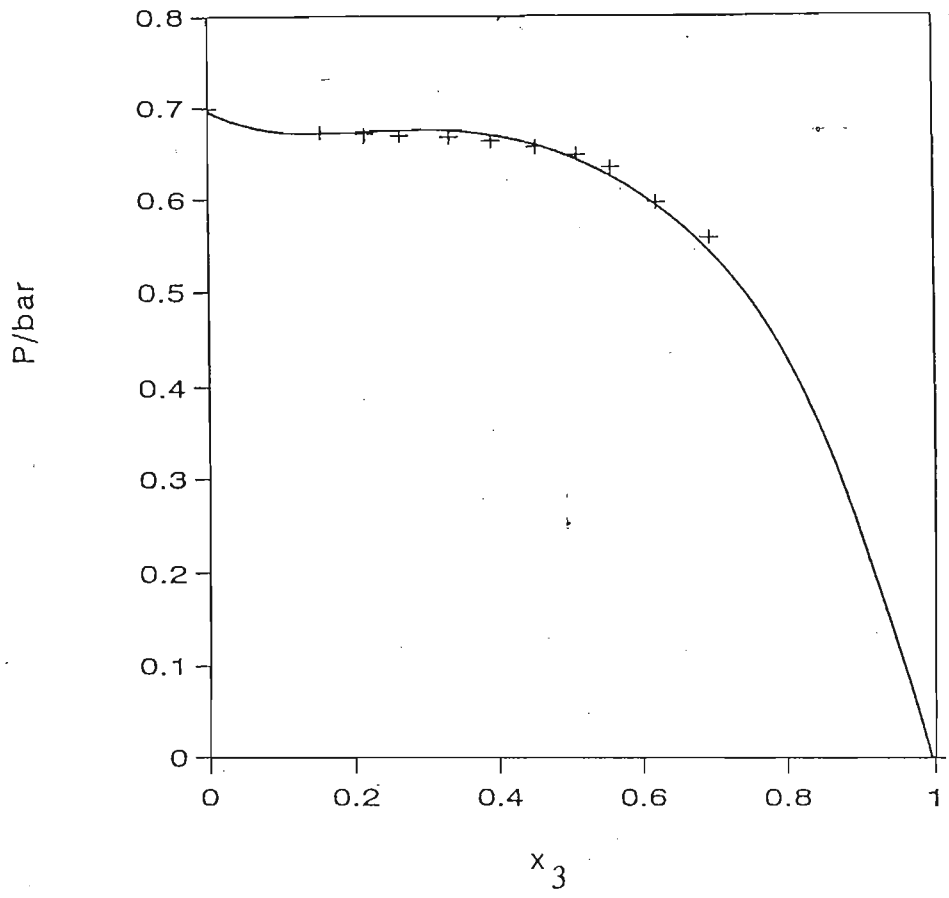

FIGURE 9.7. Comparison of theory with experiment for the isothermal vapour-liquid phase equilibrium diagram for tetrachloromethane (1) + sulfolane (3) at 338.15 K. Total pressure, P, versus, x_2, the mole fraction of sulfolane in the liquid phase. Lines, Modified UNIFAC predicted values, points, experimental results

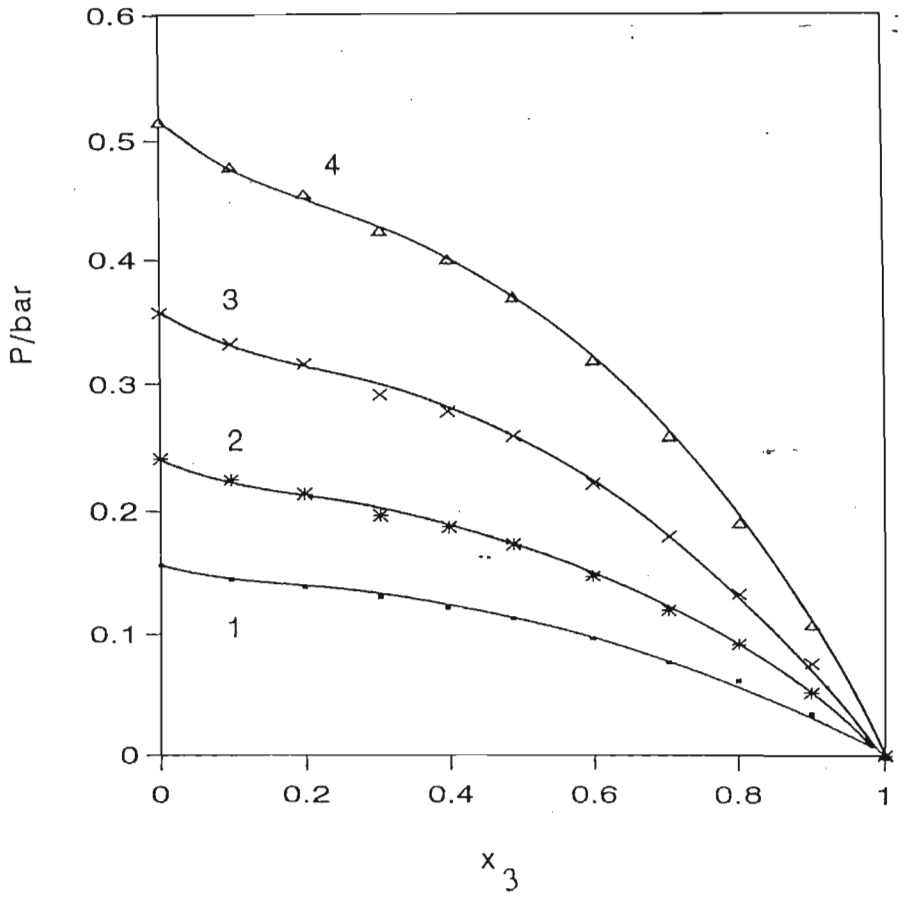

FIGURE 9.8. Comparison of theory with experiment for the isothermal vapour-liquid phase equilibrium diagram for benzene (1) + sulfolane (3) at 303.15 K (1), 313.15 K (2), 323.15 K (3) and 333.15 K (4).Total pressure, P, versus,x_2, the mole fraction of sulfolane in the liquid phase. Lines, Modified UNIFAC predicted values, points, experimental results (Karvo)

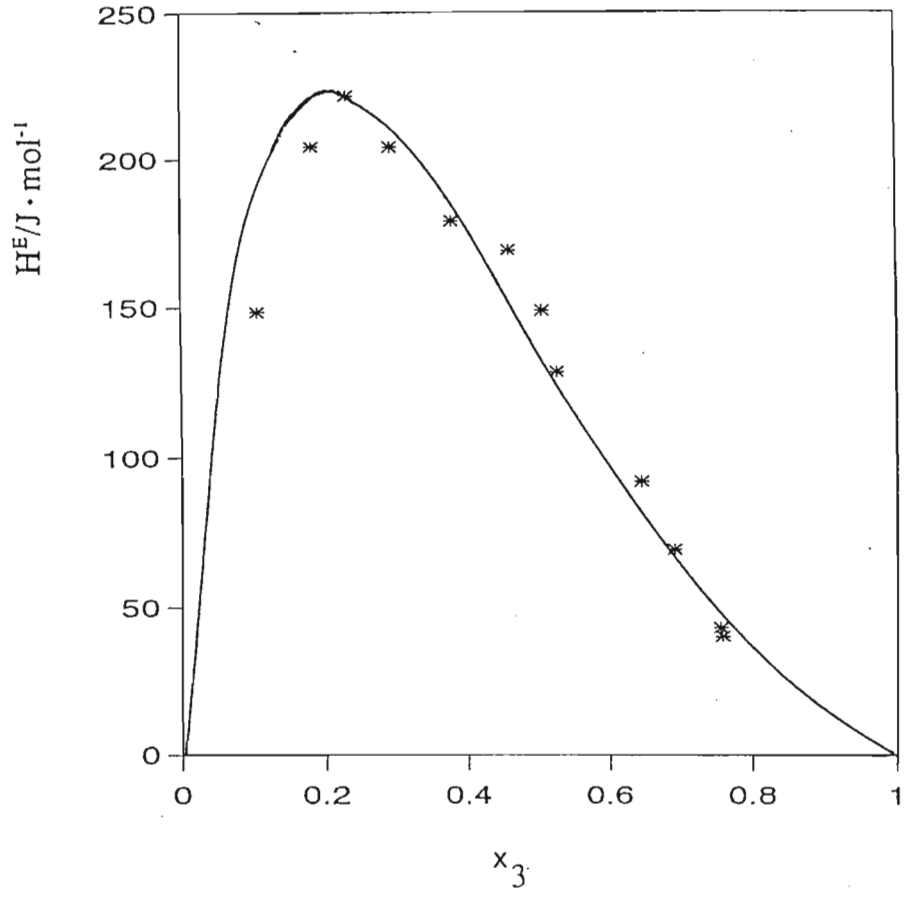

FIGURE 9.9. Comparison of theory with experiment for the excess enthalpies, H^E of tetrachloromethane (1) + sulfolane (3) mixture at 303.15 K. Lines, Modified UNIFAC predicted values; points, experimental results (Pansini and Jannelli)

CHAPTER 10
CONCLUSIONS

The aims of this work, given in Chapter 1, have been successfully carried out.

The extension to the Cruickshank and Everett method, for the determination of γ_{13}^{∞} of moderately volatile solvents, has been tested and new data of γ_{13}^{∞} for n-dodecane + various hydrocarbon mixtures have been obtained. These results fill a gap in the literature. The technique is also used to investigate the possibility of determining the solvent vapour pressure. The results for the vapour pressure obtained from the modified technique compare favourably with the published results. The results are an indication that this new techique may open up a large field of systems which can be investigated.

New γ_{13}^{∞} for sulfolane and various solutes have been obtained using G.L.C. One of the reasons for using sulfolane was because of its polar nature. The results indicate that polar solvents may also be used in the determination of γ_{13}^{∞} by G.L.C., without any modification to the existing theory. This is another advance in the applications that may be investigated by G.L.C. It is important to stress, that γ_{13}^{∞} of sulfolane and many of the systems studied here could not be obtained by other methods (exept static cell method), because of the limited solubility in the polar solvent sulfolane. This once again extends the field of study of γ_{13}^{∞} to a variety of solutes which are immiscible in partially involatile polar solvents.

New excess volume (V^E) data have been obtained for an alkyne + sulfolane. Other hydrocarbons + sulfolane mixtures could not be investigated because of their limited miscibility. The results indicate a significant interaction between the alkynes and sulfolane. This supports the evidence obtained from VLE and SLE.

The excess enthalpy (H^E) was determined for 1-heptyne and 1-octyne + sulfolane. Other mixtures were not investigated because of the limited solubility of most hydrocarbons and sulfolane. The results indicate a significant interaction between the alkynes + sulfolane and support the V^E results. The interaction is most likely between the acidic a proton in the 1-alkynes and the available oxygen atoms in sulfolane. The H^E is positive over the whole curve. This is most likely a result of the dissociation of sulfolane and of the alkyne molecules, which has masked the association between sulfolane and the alkyne. The association between sulfolane and the alkynes appears to be stronger than between sulfolane and benzene and smaller than between sulfolane and the nitriles. The obtained results are used in the "multi-optimization" procedure conducted in chapter 9. Both DISQUAC and UNIFAC is used to fit the curve. The obtained parameters are given in chapter 9.

Isothermal vapour-liquid equilibria at 338.15 K or 353.15 K for 1-heptyne, or tetrahydrofuran, or 1,4-dioxane, or tetrachloromethane, or 1,1,1-trichloroethane + sulfolane binary mixtures have been determined using an ebulliometric method. The data reported have been successfully described using the Margules, van Laar, WILSON, NRTL and UNIQUAC equations. The obtained parameters may be used to predict and correlate phase equilibria in ternary mixtures involving sulfolane.

The experimental data has allowed us to obtain new interaction parameters for the above mentioned groups with sulfolane (as an individual group) in the DISQUAC and Modified UNIFAC models.

The Margules, van Laar, WILSON, NRTL and UNIQUAC equations for the molar excess Gibbs energy, were chosen for the reduction of the VLE data as representatives of local composition equations and semi-empirical enthalpic expressions. The VLE data are the excess molar Gibbs energies, (G^E), calculated from the total pressure data.

The activity coefficients and the excess molar Gibbs energies were correlated with the same theories. Calculations done using the van Laar, Margules or Wilson equations were found to be inferior to the NRTL and UNIQUAC equations.

Each of the five mixtures studied in this work, showed significant positive deviations from ideality. The largest deviation was found for the mixture 1-heptyne + sulfolane. All systems studied exhibit zeotropic behaviour.

The maximum values of G^E are obtained for tetrahydrofuran + sulfolane at 353.15 K, and 1,4-dioxane + sulfolane at 353.15 K. A comparison of the excess molar Gibbs energies for the tetrachloromethane + sulfolane mixture and the trichloroethane + sulfolane mixture with the excess molar Gibbs energy, obtained for the related mixture of dichloromethane + sulfolane, at 303.15 K), suggests complex-forming interaction between the dichloromethane and sulfolane molecules. This indicates a different type of interaction between tetrachloromethane and sulfolane on the one hand, and between trichloroethane and sulfolane on the other. The asymmetric molecule trichloroethane shows weaker interactions with sulfolane than does dichloromethane.

The experimental values of the excess molar enthalpies H^E for two of the systems studied here have been reported in the literature. The H^E_m versus mole fraction for 1,4-dioxane + sulfolane mixture (also at 303.15 K) was found to be sinusoidal with a H^E_{min} in the sulfolane rich region, and H^E_{max} in the 1,4-dioxane rich region.[161] The excess enthalpy of mixing for the 1-heptyne + sulfolane system has also been measured at 303.15 K (Chapter 6), and shows endothermic deviations from ideality. These enthalpic results reflect the same interactions we have interpreted from the Gibbs energy results above.

For the mixtures studied in this work, strong nonideal behaviour is evident from the magnitude of the activity coefficients. The 1,4-dioxane + sulfolane mixture (with small values for both G^E_{max} and H^E_{max}) is the least non-ideal mixture.

The activity coefficient at infinite dilution, γ_1^∞, for each of the solvents in sulfolane was calculated using Margules, van Laar, WILSON, NRTL and UNIQUAC parameters obtained from VLE data. The calculated results for the mixtures 1-Heptyne + sulfolane at 313.15 K, and 303.15 K, and tetrahydrofuran + sulfolane at

303.15 K compare well with the published data.

The solubilities of sulfolane, have been determined experimentally in six solvents: 1-heptyne, tetrahydrofuran, 1,4-dioxane, 1,1,1-trichloroethane, benzene and cyclohexane - by a dynamic method in the temperature range 250 - 301 K. The results have been correlated by the WILSON, NRTL and UNIQUAC equations, utilizing parameters taken from solid-liquid equilibrium for the simple eutectic mixtures only. The correlations have been done using the data reported here as well as the data published earlier.

The solute, sulfolane is most soluble in tetrahydrofuran and least soluble in 1-heptyne. The order of solubility of sulfolane is tetrahydrofuran > 1,4-dioxane > trichloroethane > benzene > tetrachloromethane > cyclohexane > 1-heptyne. These results indicate that no hydrogen bonds exist between sulfolane and 1-heptyne, or 2-methyl-2-propanol. This is supported by work done by M. D. Monica *et al.*[4], that no hydrogen bonds exists between benzoic acid and sulfolane.

In all the solvents used in this work, with the exception of tetrahydrofuran over a small concentration range, the solubility of sulfolane is lower than ideal. The effect of the interactions between sulfolane and the solvents observed in vapour-liquid equilibria measurements, was similar to that observed in this SLE work. The solubility of sulfolane in 1-heptyne is much lower than ideal. The solubility of sulfolane in 1,4-dioxane for $x_2 > 0.84$ is close to ideal with experimental activity coefficients $\gamma_2 \approx 1.0$. This corresponds to the liquidus curve related to the sulfolane crystal phases I and II.

For 1,4-dioxane + sulfolane evidence for the formation of a solid molecular compound which largely decomposes on melting was observed. This indicates the possibility of strong interactions between sulfolane and 1,4-dioxane. Two eutectic points, were observed. The latter eutectic refers to the metastable crystalline phase II.

In this study, three methods that describe the Gibbs excess free energy of mixing (G^E) were used to represent the solute activity coefficient (γ_2): the WILSON equation, the nonrandom two-liquid theory (NRTL) and the UNIQUAC equation.

Calculations were performed on the data obtained from this work and also for mixtures of sulfolane in benzene, 1,4-dioxane, tetrachloromethane and cyclohexane, from literature data in the sulfolane rich region, for liquidus curves giving simple eutectic points.

The solubility of sulfolane in cyclohexane was only measured in the sulfolane rich region as a result the non-miscibility gap in the lower sulfolane concentrations.

For the nine solubility curves, the results obtained from the WILSON equation are slightly better than those derived from the NRTL and UNIQUAC equations.

The experimental data of SLE obtained in this work and the VLE data (Chapter 7) have been used to obtain new interaction parameters for the specific solvent groups with sulfolane using the DISQUAC and Modified UNIFAC models.

APPENDIX I

Calibration of the Hewlett-Packard 2804 A Quartz Thermometer

The thermometer was calibrated against a Tinsley Platinium resistance thermometer, which had been previously calibrated by the CSIR-South Africa. The platinum resistance thermometer, T, was measured with an FE Smith difference bridge. The offbalance current was amplified using a PYE Galvanometer Photocell preamplifier, and was fed to a PYE Scalamp galvanometer. A 2 V emf source was used to drive the circuit.

To eliminate stray emf,s it was necessary to take resistance readings of both themometers, with the current flowing in both directions in turn.
The resistance, R_T, is given by

$$R_T = [x_3 + x_4)/2 - (x_1 - x_2)/2]$$

where x refers to the number of readings. The first term in the equation corresponds to the average of the resistance of the standard resister, R, with current flowing, while the second term is with respect to the platinum thermometer.

Resistance reading were converted to temperature values using the iterative relationship.

$$T = [(R_T - R_o)/\alpha R_o + \delta[(T/100) - 1)](T/100)$$

where R, α, δ are constants of the platinum thermometer.

APPENDIX II
COMPUTER PROGRAM VLE

```
C ***********************************************************************
C  SUBROUTINE SETUP
C ***********************************************************************
C
      SUBROUTINE SETUP (NPARM,NPTS,NVARS,NCONST,SIGMA,Z)
      IMPLICIT REAL*8 (A-H,O-Z), INTEGER*4(I-N)
      DIMENSION DATA(35,4),EST(35,4),V(4,4),PROD1(4,2),B(2,4),
     *  PROD2(2,2),AINV(2,2),WORK(100),THETA(5),SIGMA(4),C(2),XI(4),
     *  PASS(6),GRAD(3),PROD4(2),PROD5(4),DIFF(4),PROD3(2)
      COMMON /AREA1/ DATA,EST
      COMMON /AREA3/ PASS
      DATA MAXEVM/7/
      DO 5 I=1,NVARS
        DO 5 J=1,NVARS
      WRITE(*,*)
          IF (I.EQ.J) THEN
            V(I,I)=SIGMA(I)**2
          ELSE
            V(I,J)=0.0D00
          END IF
5     CONTINUE
      RETURN
C
C ***********************************************************************
C  ENTRY POINT FOR OPTIMIZATION ROUTINE ZXMIN
C ***********************************************************************
C
      ENTRY FUNCT(NPARM,THETA,Q,GRAD,WORK,IFG)
C
C  INITIALIZE OBJECTIVE FUNCTION AND FLAG FOR NONCONVERGENCE
C  OF EVM LINEARIZATION
C
      Q=0.0D00
      Z=0.0D00
      SUMF=0.D0
C
C  FOR EACH DATA POINT CALCULATE VALUE OF QI. WITHIN THIS LOOP
C  IS THE LOOP THAT CALCULATES THE STATISTICAL TRUE VALUES OF
C  THE MEASURED VARIABLES
C
      DO 10 I=1,NPTS
C
C     INITIALIZE OLD VALUE OF OBJECTIVE FUNCTION FOR ONE
C     DATA POINT TO CHECK FOR EVM LINEARIZATION CONVERGENCE
C
        QOLD=0.0D00
C
C     INITIALIZE LOOP COUNTER FOR EVM LINEARIZATION
C
        IEVM=0
C
```

```
C     BEGIN LOOP FOR EVM LINEARIZATION
C
50     CONTINUE
C
C     ADD ONE TO EVM LINEARIZATION COUNTER
C
      IEVM=IEVM+1
C
C     SETUP XI-VECTOR FOR PASS TO USERS MODEL SUBPROGRAM
C
      DO 30 J=1,4
        XI(J)=EST(I,J)
30     CONTINUE
31    FORMAT(' XI:',4F10.3)
C
C     CALL MODEL EQUATION TO CALCULATE JACOBIAN OF THE CONSTRAINT
C     EQUATIONS WITH RESPECT TO THE VARIABLES MEASURED. THE
C     VALUES OF THE CONSTRAINT EQUATIONS ARE RETURNED IN THE
C     VECTOR C.
C
     IF(PASS(4).LT.7..OR.PASS(4).EQ.9.)
    *   CALL ACTMOD(XI,THETA,B,C)
     IF(PASS(4).GT.6..AND.PASS(4).LT.9.)
    *   CALL EOSMOD(XI,THETA,B,C)
C
C     CALCULATE   VB-TRANSPOSE
C
      CALL MULABT(V,B,NVARS,NVARS,NCONST,4,2,PROD1,4)
C
C     CALCULATE BVB-TRANSPOSE
C
      CALL MULAB (B,PROD1,NCONST,NVARS,NCONST,2,4,PROD2,2)
C
C     CALCULATE INVERSE OF BVB-T
C
      IF (NCONST.EQ.1) THEN
        AINV(1,1)=1.0D00/PROD2(1,1)
      ELSE
        IDGT=0
        CALL SYMINV(PROD2,NCONST,2,AINV,IER)
      END IF
      IOPT=0
      IF(IOPT.EQ.1) THEN
C
C     CALCULATE DIFFERENCE BETWEEN MEASURED VARIABLES AND
C     CURRENT ESTIMATES OF TRUE VALUES
C
      DO 20 J=1,NVARS
        DIFF(J)=DATA(I,J)-EST(I,J)
20     CONTINUE
C
C     CALCULATE BD, WHERE D IS DIFFERENCE VECTOR
C
      CALL MULAB  (B,DIFF,NCONST,NVARS,1,2,4,PROD3,2)
C
C     ADD TO VALUE OF CONSTRAINT VECTOR THE VECTOR BD
```

```
C
      DO 25 J=1,NCONST
        PROD3(J)=C(J)+PROD3(J)
25     CONTINUE
      ELSE
        DO 26 J=1,NCONST
          PROD3(J)=C(J)
26       CONTINUE
      END IF


C  DIPPR ROUTINE NAME - NRTL3
C
C ***********************************************************************
C
C
C  PURPOSE       - CALCULATION OF ACTIVITY COEFFICIENTS OF COMPONETNS
C                 IN A DEFINED LIQUID MIXTURE USING THE
C                 NRTL MODEL
C
C  USAGE         - CALL NRTL3 (NCOMP,PARM,T,X,ACT,IDV,IER,DT1,DT2,
C                 DX1,DX2)
C
C  ARGUMENTS
C    INPUT: NCOMP - NUMBER OF COMPONENTS IN THE MIXTURE
C         PARM  - VECTOR OF LENGTH NCOMP*NCOMP OF MODEL PARAMETERS:
C                 FOR EACH BINARY PAIR:
C                   PARM(3*N-2) =G(I,J)-G(J,J) (J/MOLE)
C                   PARM(3*N-1) =G(J,I)-G(I,I) (J/MOLE)
C                   PARM(3*N)   =NONRANDOMNESS PARAMETER (I,J)
C                 THE FOLLOWING SEQUENCE IS USED FOR N,I,J
C                   N=1         I=1, J=2
C                   N=2         I=1, J=3
C                   N=3         I=2, J=3
C                   N=4         I=1, J=4
C                   N=C*(C-1)/2  I=NCOMP-1, J=NCOMP  (C=NCOMP)
C         T     - TEMPERATURE OF THE SYSTEM (KELVINS).
C         X     - VECTOR OF LENGTH TWO OF MOLE FRACTIONS OF THE
C                 LIQUID PHASE.
C         IDV   - OPTION PARAMETER. WHEN IDV IS:
C                 0: DERIVATIVES OF THE ACTIVITY COEFFICIENTS WITH
C                   RESPECT TO THE MEASURED VARIABLES ARE NOT
C                   CALCULATED.
C                 1: DERIVATIVES OF THE ACTIVITY COEFFICIENTS WITH
C                   RESPECT TO THE MEASURED VARIABLES ARE
C                   CALCULATED.
C    OUTPUT: ACT   - VECTOR OF LENGTH TWO OF LIQUID PHASE ACTITIVTY
C                 COEFFICIENTS.
C         DT1   - DERIVATIVE OF ACT(1) WITH RESPECT TO TEMPERATURE
C                 (1/KELVINS).
C         DT2   - DERIVATIVE OF ACT(2) WITH RESPECT TO TEMPERATURE
C                 (1/KELVINS).
C         DX1   - DERIVATIVE OF ACT(1) WITH RESPECT TO LIQUID PHASE
C                 CONCENTRATION OF COMPONENT 1.
C         DX2   - DERIVATIVE OF ACT(2) WITH RESPECT TO LIQUID PHASE
C                 CONCENTRATION OF COMPONENT 1.
```

```
C
C LIMITATIONS:
C
C
C REFERENCES:    - RENON, H. AND PRAUSNITZ, J., "LOCAL COMPOSISTIONS
C                IN THERMODYNAMIC EXCESS FUNCTIONS FOR LIQUID
C                MIXTURES", AICHE J., 14 135 (1968).
C
C
C
C EXAMPLE:
C
C   IMPLICIT INTEGER*4 (I-N), REAL*8 (A-H, O-Z)
C   DIMENSION PARM(3),X(2),ACT(2)
C   NCOMP=2
C   PARM(1)= 360.0
C   PARM(2)=1320.0
C   PARM(3)= 0.3010E04
C   T=323.15
C   X(1)=0.290
C   X(2)=0.710
C   IDV=1
C   CALL NRTL3 (NCOMP,PARM,T,X,ACT,IDV,IER,DT1,DT2,DX1,DX2)
C   WRITE(*,*) ACT,DT1,DT2,DX1,DX2
C   STOP
C   END
C
C            - USING THESE VALUES, THE CALCULATED VALUES ARE:
C              ACT(1) =  1.3400
C              ACT(2) =  1.0559
C              DT1    = -0.1119E-02
C              DT2    = -0.1833E-03
C              DX1    = -1.1899
C              DX2    =  0.3830
C
C
C ***************************************************************************
C
      SUBROUTINE NRTL3 (NCOMP,PARM,T,X,ACT,IDV,IER,DTA1,DTA2,DXA1,DXA2)
      IMPLICIT INTEGER*4 (I-N), REAL*8 (A-H, O-Z)
      DIMENSION PARM(5),X(10),ACT(10),TAU(10,10),G(10,10)
      RJ=8.31429
C
      IF(NCOMP.GT.2) GOTO 500
C
      ALPHA=PARM(3)/10000.
C
C NOTE: NONRANDOMNESS PARAMETER IS MULTIPLIED BY A FACTOR OF 1E04 IN
C       THE SUBROUTINE EVM TO MAKE EACH PARAMETER IN THE REGRESSION
C       THE SAME ORDER OF MAGNITUDE
C
C
      TAU12  = PARM(1)/(RJ*T)
      TAU21  = PARM(2)/(RJ*T)
C
      G12 = DEXP(-ALPHA*TAU12)
```

```
      G21 = DEXP(-ALPHA*TAU21)
C
      TG21=TAU21*G21
      D21=X(1)+G21*X(2)
      C1 = TG21/D21
C
      TG12=TAU12*G12
      D12=X(2)+G12*X(1)
      C2 = TG12/D12
C
      X1SQD=X(1)*X(1)
      X2SQD=X(2)*X(2)
C
      ACT(1)=DEXP(X2SQD*(C1**2/TAU21 + C2**2/TG12))
      ACT(2)=DEXP(X1SQD*(C2**2/TAU12 + C1**2/TG21))
C
C  DERIVATIVES OF THE EXPRESSIONS
C
      IF(IDV.EQ.0) RETURN
      IF(IDV.NE.1) GOTO 51
       DTAU  = -1./T
       DTAU12  = TAU12*DTAU
       DTAU21  = TAU21*DTAU
C
       DELG12 = -ALPHA*DTAU12
       DELG21 = -ALPHA*DTAU21
C
       DTTG12 = TG12*(DTAU+DELG12)
       DTTG21 = TG21*(DTAU+DELG21)
C
       DXD12 = G12-1
       DXD21 = 1-G21
       DTD12 = X(1)*G12*DELG12
       DTD21 = X(2)*G21*DELG21
C
       DXC1= -C1*DXD21/D21
       DTC1= (D21*DTTG21-TG21*DTD21)/D21/D21
C
       DXC2= -C2*DXD12/D12
       DTC2= (D12*DTTG12-TG12*DTD12)/D12/D12
C
C
       DXA1 = ACT(1)*(-2.*X(2)*(C1*C1/TAU21+C2*C2/TG12) +
     *               X2SQD*(2.*C1*DXC1/TAU21 + 2.*C2*DXC2/TG12))
       DTA1 = ACT(1)*(X2SQD*
     *          ((2.*C1*DTC1-C1*C1*DTAU)/TAU21 +
     *           (2.*C2*DTC2-C2*C2*(DELG12+DTAU))/TG12))
C
       DXA2 = ACT(2)*( 2.*X(1)*(C2*C2/TAU12+C1*C1/TG21) +
     *               X1SQD*(2.*C2*DXC2/TAU12 + 2.*C1*DXC1/TG21))
       DTA2 = ACT(2)*(X1SQD*
     *          ((2.*C2*DTC2-C2*C2*DTAU)/TAU12 +
     *           (2.*C1*DTC1-C1*C1*(DELG21+DTAU))/TG21))
       RETURN
C
C
```

```
500  N=-2
     DO 10 I=1,NCOMP
       DO 20 J=I,NCOMP
          IF(I.EQ.J) THEN
             TAU(I,J)=0.0
             G(I,J)=1.
          ELSE
             N=N+3
             TAU(I,J)=PARM(N)/RJ/T
             TAU(J,I)=PARM(N+1)/RJ/T
             G(I,J)=DEXP(-PARM(N+2)/10000*TAU(I,J))
             G(J,I)=DEXP(-PARM(N+2)/10000*TAU(J,I))


C  NOTE: NONRANDOMNESS PARAMETER IS MULTIPLIED BY A FACTOR OF 1E04 IN
C        THE SUBROUTINE EVM TO MAKE EACH PARAMETER IN THE REGRESSION
C        THE SAME ORDER OF MAGNITUDE
C
          ENDIF
  20    CONTINUE
  10  CONTINUE
C
     DO 50 I=1,NCOMP
       SUM1=0.0
       SUM2=0.0
       SUM3=0.0
       DO 60 J=1,NCOMP
          SUM1=SUM1+TAU(J,I)*G(J,I)*X(J)
          SUM2=SUM2+G(J,I)*X(J)
          SUM3A=0.0
          SUM3B=0.0
          DO 70 L=1,NCOMP
             SUM3A=SUM3A+TAU(L,J)*G(L,J)*X(L)
  70          SUM3B=SUM3B+G(L,J)*X(L)
  60       SUM3=SUM3+X(J)*G(I,J)/SUM3B*(TAU(I,J)-SUM3A/SUM3B)
  50    ACT(I)=DEXP(SUM1/SUM2+SUM3)
C
     RETURN
C
  51  IER=51
     RETURN
     END
```

```
C  DIPPR ROUTINE NAME - VANLAR
C
C  ********************************************************************
C
C
C  PURPOSE       - CALCULATION OF ACTIVITY COEFFICIENTS OF COMPONETNS
C                  IN A DEFINED LIQUID MIXTURE USING THE
C                  VAN LAAR MODEL
C
C  USAGE         - CALL VANLAR (PARM,X,ACT,IDV,IER,DT1,DT2,DX1,DX2)
C
C  ARGUMENTS
C    INPUT: PARM  - VECTOR OF LENGTH TWO OF VALUES OF THE MARGULES
C                  CONSTANTS A12 AND A21.
C           X     - VECTOR OF LENGTH TWO OF MOLE FRACTIONS OF THE
C                  LIQUID PHASE.
C           IDV   - OPTION PARAMETER. WHEN IDV IS:
C                  0: DERIVATIVES OF THE ACTIVITY COEFFICIENTS WITH
C                    RESPECT TO THE MEASURED VARIABLES ARE NOT
C                    CALCULATED.
C                  1: DERIVATIVES OF THE ACTIVITY COEFFICIENTS WITH
C                    RESPECT TO THE MEASURED VARIABLES ARE
C                    CALCULATED.
C    OUTPUT: ACT   - VECTOR OF LENGTH TWO OF LIQUID PHASE ACTITIVTY
C                  COEFFICIENTS.
C           DT1   - DERIVATIVE OF ACT(1) WITH RESPECT TO TEMPERATURE
C                  (1/KELVINS).
C           DT2   - DERIVATIVE OF ACT(2) WITH RESPECT TO TEMPERATURE
C                  (1/KELVINS).
C           DX1   - DERIVATIVE OF ACT(1) WITH RESPECT TO LIQUID PHASE
C                  CONCENTRATION OF COMPONENT 1.
C           DX2   - DERIVATIVE OF ACT(2) WITH RESPECT TO LIQUID PHASE
C                  CONCENTRATION OF COMPONENT 1.
C
C  LIMITATIONS:    - THIS PROCEDURE CAN BE USED ONLY FOR BINARY SYSTEMS.
C                  FOR THE CALCULATION OF ACTIVITY COEFFICIENTS FOR
C                  MULTICOMPONENT SYSTEMS, USE ONE OF THE FOLLOWING
C                  MODELS: WILSON, NRTL, OR UNIQUAC.
C
C
C
C
C  EXAMPLE:
C
C    IMPLICIT INTEGER*4 (I-N), REAL*8 (A-H, O-Z)
C    DIMENSION PARM(2),X(2),ACT(2)
C    PARM(1)=0.604
C    PARM(2)=0.534
C    X(1)=0.290
C    X(2)=0.710
C    IDV=1
C    CALL VANLAR (PARM,X,ACT,IDV,IER,DT1,DT2,DX1,DX2)
C    WRITE(*,*) ACT,DT1,DT2,DX1,DX2
C    STOP
C    END
```

```
C
C             - USING THESE VALUES, THE CALCULATED VALUES ARE:
C                ACT(1) = 1.3266
C                ACT(2) = 1.0548
C                DT1    = 0.00
C                DT2    = 0.00
C                DX1    =-1.1506
C                DX2    = 0.3737
C
C
C ***************************************************************
C
C
      SUBROUTINE VANLAR (PARM,X,ACT,IDV,IER,DTACT1,DTACT2,DXACT1,DXACT2)
      IMPLICIT INTEGER*4 (I-N), REAL*8 (A-H, O-Z)
      DIMENSION PARM(5),X(10),ACT(10)
      IER=0
      A12=PARM(1)
      A21=PARM(2)
      DENOM=A12*X(1)+A21*X(2)
      IF(DABS(DENOM).LT.1.D-06) GOTO 920
      TERM1 = A21*X(2)/DENOM
      EXPO1= A12*TERM1**2
      IF(DABS(EXPO1).GT.170) GOTO 921
      ACT(1) = DEXP(EXPO1)
      TERM2 =A12*X(1)/DENOM
      EXPO2= A21*TERM2**2
      IF(DABS(EXPO2).GT.170) GOTO 921
      ACT(2) = DEXP(EXPO2)
      IF(IDV.EQ.0) RETURN
      IF(IDV.NE.1) GOTO 51
       DXACT1 = ACT(1)*(-2.*(A12*A21)**2*X(2)/DENOM**3)
       DTACT1 = 0.D0

       DXACT2 = ACT(2)*(2.*(A12*A21)**2*X(1)/DENOM**3)
       DTACT2 = 0.D0
      RETURN
  920 IER=920
      GOTO 925
  921 IER=921
  925 ACT(1)=1.0
      ACT(2)=1.0
      DXACT1=0.0
      DXACT2=0.0
      DTACT1=0.0
      DTACT2=0.0
      RETURN
   51 IER=51
      RETURN
      END


C     CALCULATE   INV(BVB-T)(C+BD)
C
      CALL MULAB  (AINV,PROD3,NCONST,NCONST,1,2,2,PROD4,2)
C
```

```
C     CALCULATE   QI=(C+BD)-T INV(BVB-T) (C+BD)
C
      CALL MULATB(PROD3,PROD4,1,NCONST,1,2,2,QI,1)
27     FORMAT(' VALUE OF THE Q:  ',F20.6,/)
      IF (IOPT.EQ.1) THEN
C
C     IF THE EVM LINEARIZATION HAD PREVIOUSLY FAILED, THEN
C     THE QI JUST CALCULATED WAS BASED ON THE TRUE VALUE BEING
C     THE MEASURED DATA POINT. GO ON TO THE NEXT POINT
C
      IF (IEVM.GT.MAXEVM) GOTO 60
C
C CALCULATE NEW DATA VECTOR
C
      CALL MULAB  (PROD1,PROD4,NVARS,NCONST,1,4,2,PROD5,4)
      DO 40 J=1,NVARS
        EST(I,J)=DATA(I,J)-PROD5(J)
40     CONTINUE
      IF (QI.EQ.0.0D00) GOTO 60
      IF (DABS(QOLD-QI)/QI.LT.1.0D-07) GOTO 60
      IF (EST(I,3).LT.0.D0.OR.EST(I,3).GT.1.D0) IEVM=MAXEVM
      IF (EST(I,4).LT.0.D0.OR.EST(I,4).GT.1.D0) IEVM=MAXEVM
C
C     SAVE RECENTLY CALCULATED QI FOR COMPARISON ON NEXT
C     LINEARIZATION
C
  49 FORMAT(' Q AND XI:',F15.6,2F10.3,2F15.5)
      QOLD=QI
C
C     EVM LINEARIZATION CONVERGES IN FOUR TO FIVE ITERATIONS
C     (IEVM) USUALLY. HOWEVER, SOMETIMES THE LINEARIZATION
C     FAILS WHEN THETA IS NOT CLOSE TO THE MAXIMUM
C     LIKELIHOOD ESTIMATES. IN THIS CASE, SET VARIABLE ESTIMATES
C     TO THE MEASURED DATA AND CALCULATED QI. THIS
C     IS USUALLY A CLOSE ENOUGH APPROXIMATION TO ALLOW ZXMIN
C     TO GET CLOSER TO THE CORRECT VALUE OF THETA. WHEN THE
C     TRUE VALUE OF THETA IS APPROACHED, THE EVM LINEARIZATION
C     CONVERGES.
C
      IF (IEVM.LT.MAXEVM) GOTO 50
      WRITE (6,*) ' EVM DID NOT CONVERGE POINT ',I
      DO 70 J=1,NVARS
        EST(I,J)=DATA(I,J)
70     CONTINUE
      GOTO 50
60     CONTINUE
      END IF
      SUMF=SUMF+C(1)+C(2)
      Q=Q+QI
      Z=Z+DSQRT(QI)
10   CONTINUE
2000  FORMAT(' TH,QI,Q,F1,F2,SF',F8.3,5F10.0)
    RETURN
     END
```

```
C  DIPPR ROUTINE NAME - UNIQUA
C
C  ***************************************************************************
C
C
C  PURPOSE       - CALCULATION OF ACTIVITY COEFFICIENTS OF COMPONETNS
C                  IN A DEFINED LIQUID MIXTURE USING THE
C                  UNIQUAC MODEL
C
C  USAGE         - CALL UNIQUA (NCOMP,PARM,R,QQ,QP,T,X,ACT,IDV,IER,
C                  DT1,DT2,DX1,DX2)
C
C  ARGUMENTS
C    INPUT: NCOMP - NUMBER OF COMPONENTS IN THE MIXTURE
C           PARM  - VECTOR OF LENGTH NCOMP*(NCOMP-1) OF PARAMETERS:
C                   FOR EACH BINARY PAIR:
C                     PARM(2*N-1) =U(I,J) (J/MOLE)
C                     PARM(2*N)   =U(J,I) (J/MOLE)
C                   WHERE N IS THE BINARY PAIR NUMBER.  THE FOLLOWING
C                   SYSTEM IS USED TO NUMBER BINARY PAIRS: PAIR
C                   NUMBER ONE IS I=1, J=2.  PAIRS ARE NUMBERED
C                   SUCCESIVELY UNTIL I=1,J=NCOMP.  THE NEXT PAIR IS
C                   I=2,J=3, AND PAIRS ARE NUMBERED SUCCESSIVELY
C                   UNTIL I=2,J=NCOMP.  THE NUMBERING CONTINUES UNTIL
C                   I=NCOMP-1 AND J=NCOMP.
C           R     - VOLUME PARAMETER FOR UNIQUAC MODEL.
C           QQ    - SURFACE AREA PARAMETER FOR UNIQUAC MODEL.
C           QP    - SURFACE AREA PARAMETER FOR UNIQUAC MODEL ADJUSTED
C                   FOR ALCOHOLS AND WATER.
C           T     - TEMPERATURE OF THE SYSTEM (KELVINS).
C           X     - VECTOR OF LENGTH TWO OF MOLE FRACTIONS OF THE
C                   LIQUID PHASE.
C           IDV   - OPTION PARAMETER. WHEN IDV IS:
C                   0: DERIVATIVES OF THE ACTIVITY COEFFICIENTS WITH
C                     RESPECT TO THE MEASURED VARIABLES ARE NOT
C                     CALCULATED.
C                   1: DERIVATIVES OF THE ACTIVITY COEFFICIENTS WITH
C                     RESPECT TO THE MEASURED VARIABLES ARE
C                     CALCULATED.
C    OUTPUT: ACT   - VECTOR OF LENGTH TWO OF LIQUID PHASE ACTITIVTY
C                   COEFFICIENTS.
C           DT1   - DERIVATIVE OF ACT(1) WITH RESPECT TO TEMPERATURE
C                   (1/KELVINS).
C           DT2   - DERIVATIVE OF ACT(2) WITH RESPECT TO TEMPERATURE
C                   (1/KELVINS).
C           DX1   - DERIVATIVE OF ACT(1) WITH RESPECT TO LIQUID PHASE
C                   CONCENTRATION OF COMPONENT 1.
C           DX2   - DERIVATIVE OF ACT(2) WITH RESPECT TO LIQUID PHASE
C                   CONCENTRATION OF COMPONENT 1.
C
C  LIMITATIONS:  -
C
C
C  REFERENCES:    - ABRAMS, D. AND PRAUSNITZ, J., "STATISTICAL
C                  THERMODYNAMICS OF LIQUID MIXTURES: A NEW
C                  EXPRESSION FOR THE EXCESS GIBBS ENERGY OF
```

```
C               PARTIALLY OR COMPLETELY MISCIBLE SYSTEMS", AICHE
C               J., 21 116 (1975).
C
C
C
C  EXAMPLE:
C
C    IMPLICIT INTEGER*4 (I-N), REAL*8 (A-H, O-Z)
C    DIMENSION PARM(2),X(2),ACT(2),R(2),QQ(2),QP(2)
C    NCOMP=2
C    PARM(1)=1448.0
C    PARM(2)=1188.0
C    T=323.15
C    X(1)=0.290
C    X(2)=0.710
C    R(1)=2.5735
C    R(2)=1.4311
C    QQ(1)=2.336
C    QQ(2)=1.432
C    QP(1)=2.336
C    QP(2)=0.96
C    IDV=1
C    CALL UNIQUA (NCOMP,PARM,R,QQ,QP,T,X,ACT,IDV,IER,DT1,DT2,DX1,DX2)
C    WRITE(*,*) ACT,DT1,DT2,DX1,DX2
C    STOP
C    END
C
C             - USING THESE VALUES, THE CALCULATED VALUES ARE:
C                 ACT(1) =  1.5746
C                 ACT(2) =  1.2051
C                 DT1    = -0.2210E-02
C                 DT2    = -0.6366E-03
C                 DX1    = -3.4384
C                 DX2    =  1.1543
C

C ***********************************************************************
C
      SUBROUTINE UNIQUA (NCOMP,PARM,R,QQ,QP,T,X,
     *                   ACT,IDV,IER,DT1,DT2,DX1,DX2)
      IMPLICIT INTEGER*4 (I-N), REAL*8 (A-H, O-Z)
      REAL*8 L,L1,L2
      DIMENSION ACT(10),PARM(5),X(10),R(10),
     *        QQ(10),QP(10),THP(10),
     *        L(10),TAU(10,10)
C
      X1SQ=X(1)*X(1)
      X2SQ=X(2)*X(2)
      RJ=8.31439
      Z=10.D00
      DX1=0.D0
      DX2=0.D0
      DT1=0.D0
      DT2=0.D0
C
```

```
      IF(NCOMP.GT.2) GOTO 500
C
      SUMXR  = X(1)*R(1)+X(2)*R(2)
      SUMXQ  = X(1)*QQ(1)+X(2)*QQ(2)
      SUMXQP = X(1)*QP(1)+X(2)*QP(2)
      SUMXR2 = SUMXR*SUMXR
      SUMXQ2 = SUMXQ*SUMXQ
      SMXQP2 = SUMXQP*SUMXQP
C
      PHI1 = X(1)*R(1)/SUMXR
      PHI2 = X(2)*R(2)/SUMXR
      TH1  = X(1)*QQ(1)/SUMXQ
      TH2  = X(2)*QQ(2)/SUMXQ
      TH1P = X(1)*QP(1)/SUMXQP
      TH2P = X(2)*QP(2)/SUMXQP
      TAU12  = DEXP(-PARM(1)/(RJ*T))
      TAU21  = DEXP(-PARM(2)/(RJ*T))
C
      DPHI1 =  R(1)*R(2)/SUMXR2
      DPHI2 = -R(1)*R(2)/SUMXR2
      DTH1  =  QQ(1)*QQ(2)/SUMXQ2
      DTH2  = -QQ(1)*QQ(2)/SUMXQ2
      DTH1P =  QP(1)*QP(2)/SMXQP2
      DTH2P = -QP(1)*QP(2)/SMXQP2
      DTAU12 = TAU12*PARM(1)/(RJ*T*T)
      DTAU21 = TAU21*PARM(2)/(RJ*T*T)
C
      W11= TH1P + TH2P*TAU21
      W22= TH1P*TAU12 + TH2P
      L1 = Z/2.*(R(1)-QQ(1))-(R(1)-1.D0)
      L2 = Z/2.*(R(2)-QQ(2))-(R(2)-1.D0)
C
      IF(X(1).LE.1.D-08) THEN
        ACT(1)=1.D0
        ACT(2)=1.D0
        GOTO 5
        ENDIF
      IF(X(2).LE.1.D-08) THEN
        ACT(1)=1.D0
        ACT(2)=1.D0
        GOTO 5
        ENDIF
      GOTO 6
    5 RETURN
C
    6 A1 = PHI1/X(1)
      B1 = (TH1/PHI1)**(Z/2.*QQ(1))
      D1 = PHI2*(L1-R(1)/R(2)*L2)
      C1 = W11**(-QP(1))
      E1 = TH2P*QP(1)/W11
      F1 = TH2P*QP(1)/W22
C
      A2 = PHI2/X(2)
      B2 = (TH2/PHI2)**(Z/2.*QQ(2))
      D2 = PHI1*(L2-R(2)/R(1)*L1)
      C2 = W22**(-QP(2))
```

```
      E2 = TH1P*QP(2)/W22
      F2 = TH1P*QP(2)/W11
C
      ACT(1) = A1 * B1 * C1 * DEXP(D1 + TAU21*E1 - TAU12*F1)
      ACT(2) = A2 * B2 * C2 * DEXP(D2 + TAU12*E2 - TAU21*F2)
C
      IF(IDV.EQ.0) RETURN
      IF(IDV.NE.1) GOTO 51
C     WRITE(*,*)'THE VALUES OF ACT1,2:',ACT1,ACT2
C
      DXA1 = (X(1)*DPHI1-PHI1)/X1SQ
      DXB1 = Z/2.*QQ(1)*(TH1/PHI1)**(Z/2.*QQ(1)-1.D0)
     *                    *(PHI1*DTH1-DPHI1*TH1)/PHI1/PHI1
      DXC1 = -QP(1)*W11**(-QP(1)-1.D0)*(DTH1P+DTH2P*TAU21)
      DXD1 = DPHI2*(L1-R(1)/R(2)*L2)
      DXE1 = QP(1)*(W11*DTH2P-(DTH1P+DTH2P*TAU21)*TH2P)/W11/W11
      DXF1 = QP(1)*(W22*DTH2P-(DTH1P*TAU12+DTH2P)*TH2P)/W22/W22
C
      DXA2 = (X(2)*DPHI2+PHI2)/X2SQ
      DXB2 = Z/2.*QQ(2)*(TH2/PHI2)**(Z/2.*QQ(2)-1.D0)
     *                    *(PHI2*DTH2-DPHI2*TH2)/PHI2/PHI2
      DXC2 = -QP(2)*W22**(-QP(2)-1.D0)*(DTH1P*TAU12+DTH2P)
      DXD2 = DPHI1*(L2-R(2)/R(1)*L1)
      DXE2 = QP(2)*(W22*DTH1P-(DTH1P*TAU12+DTH2P)*TH1P)/W22/W22
      DXF2 = QP(2)*(W11*DTH1P-(DTH1P+DTH2P*TAU21)*TH1P)/W11/W11
C
      DX1=ACT(1)*
     *     (DXA1/A1+DXB1/B1+DXC1/C1+(DXD1+TAU21*DXE1-TAU12*DXF1))
      DX2=ACT(2)*
     *     (DXA2/A2+DXB2/B2+DXC2/C2+(DXD2+TAU12*DXE2-TAU12*DXF2))
C
      DTC1 = -QP(1)*W11**(-QP(1)-1.D0)*(TH2P*DTAU21)
      DTE1 = -E1/W11*(TH2P*DTAU21)
      DTF1 = -F1/W22*(TH1P*DTAU12)
C
      DTC2 = -QP(2)*W22**(-QP(2)-1.D0)*(TH1P*DTAU12)
      DTE2 = -E2/W22*(TH1P*DTAU12)
      DTF2 = -F2/W11*(TH1P*DTAU21)
C
      DT1=ACT(1)*
     *     (DTC1/C1+TAU21*DTE1+DTAU21*E1-(TAU12*DTF1+DTAU12*F1))
      DT2=ACT(2)*
     *     (DTC2/C2+TAU12*DTE2+DTAU12*E2-(TAU21*DTF2+DTAU21*F2))
C
      RETURN
C
  500 N=-1
      SUMXR= 0.D0
      SUMXQ= 0.D0
      SUMXQP=0.D0
      DO 10 I=1,NCOMP
        DO 20 J=I,NCOMP
          IF(I.EQ.J) THEN
            TAU(I,J)=1.D0
          ELSE
            N=N+2
```

```
            TAU(I,J)=DEXP(-PARM(N)/RJ/T)
            TAU(J,I)=DEXP(-PARM(N+1)/RJ/T)
          ENDIF
 20     CONTINUE
        SUMXR= SUMXR + X(I)*R(I)
        SUMXQ= SUMXQ + X(I)*QQ(I)
        SUMXQP=SUMXQP+ X(I)*QP(I)
        L(I)=Z/2.*(R(I)-QQ(I))-(R(I)-1.)
 10   CONTINUE
C
      SUM1=0.D0
      DO 50 I=1,NCOMP
        SUM1=SUM1+X(I)*L(I)
 50     THP(I)=X(I)*QP(I)/SUMXQP

C
      DO 100 I=1,NCOMP
        PHI=X(I)*R(I)/SUMXR
        THETA=X(I)*QQ(I)/SUMXQ
        A=PHI/X(I)
        B=THETA/PHI
        SUM2=0.D0
        SUM3=0.D0
        DO 110 J=1,NCOMP
          SUM2=SUM2+THP(I)*TAU(J,I)
          SUM3A=0.D0
          DO 120 K=1,NCOMP
 120        SUM3A=SUM3A+THP(K)*TAU(K,J)
 110      SUM3=SUM3+THP(J)*TAU(I,J)/SUM3A
 100    ACT(I)=A*DEXP(Z/2.*QQ(I)*DLOG(B)+L(I)-A*SUM1
     *       -QP(I)*DLOG(SUM2)+QP(I)-QP(I)*SUM3)
C
      RETURN
 51   IER=51
      RETURN
      END


C  DIPPR ROUTINE NAME - DELIJ
C
C **********************************************************************
C
C
C  PURPOSE        - CALCULATION OF ENERGY PARAMETER A(I,J) AND BINARY
C                   INTERACTION PARAMETER DEL(I,J) USING THE
C                   GEOMETRIC MEAN MIXING RULE OR COMPOSITION
C                   DEPENDENT INTERACTION PARAMETER MIXING RULE.
C
C  USAGE          - CALL DELIJ (NCOMP,MIX,THETA,XY,K,AIJ,DEL,DXDEL)
C
C  ARGUMENTS
C    INPUT: NCOMP - NUMBER OF COMPONENTS IN THE MIXTURE
C           MIX   - INDICATOR FOR MIXING RULES.  WHEN MIX IS:
C                   1: GEOMETRIC MEAN MIXING RULES (REFERENCE #1)
C                   2: COMPOSITION DEPENDENT INTERACTION PARAMETER
C                      (REFERENCE #2)
```

```
C       THETA - VECTOR OF LENGTH 2*NPARM OF PARAMETERS
C             FOR MIX=1:
C               THETA(N)= DEL(I,J)
C             FOR MIX=2:
C               THETA(2*N-1)= K(I,J)
C               THETA(2*N)  = K(J,I)
C             WHERE N IS THE BINARY PAIR NUMBER.  THE FOLLOWING
C              SYSTEM IS USED TO NUMBER BINARY PAIRS: PAIR
C              NUMBER ONE IS I=1, J=2.  PAIRS ARE NUMBERED
C              SUCCESIVELY UNTIL I=1,J=NCOMP.  THE NEXT PAIR IS
C              I=2,J=3, AND PAIRS ARE NUMBERED SUCCESSIVELY
C              UNTIL I=2,J=NCOMP.  THE NUMBERING CONTINUES IN
C              THIS MANNER UNTIL I=NCOMP-1 AND J=NCOMP.
C       XY    - VECTOR OF LENGTH NCOMP OF MOLE FRACTIONS, EITHER
C              VAPOR OR LIQUID.
C  OUTPUT: K     - MATRIX OF DIMENSION (NPARM,NPARM) OF BINARY
C              INTERACTION PARAMETERS.
C       AIJ   - MATRIX OF DIMENSION (NPARM,NPARM) OF ENERGY
C              PARAMETERS USED IN THE CALCULATION OF THE ENERGY
C              PARAMETER A OF THE MIXTURE.
C       DEL   - MATRIX OF DIMENSION (NPARM,NPARM) OF BINARY
C              INTERACTION PARAMETERS.
C       DXDEL - DERIVATIVE OF THE BINARY INTERACTION PARAMETER
C              DEL(I,J) WITH RESPECT TO COMPOSITION.  USED ONLY
C              BINARY SYSTEMS.
C
C
C LIMITATIONS:    - THE SOAVE EQUATION OF STATE WORKS BEST FOR HIGH
C              PRESSURE SYSTEMS (REGIONS NEAR THE CRITICAL).
C              FOR LOW PRESSURE SYSTEMS, ACTIVITY COEFFICIENT
C              MODELS PERFORM BETTER.  THE MATHIAS-COPEMAN
C              MIXING RULES (MIX=4) WORK BEST, BUT GREATLY
C              INCREASE COMPUTATION TIMES.  THE HURON-VIDAL
C              MIXING RULES (MIX=3) ARE THE NEXT BEST AVAILABLE
C              MIXING RULE.  A COMPARISON OF THE MIXING RULES
C              FOR LOW PRESSURE SYSTEMS CAN BE FOUND IN CHAPTER
C              8 OF GESS AND DANNER (1988).
C
C
C REFERENCES:     - SOAVE, G., "EQUILIBRIUM CONSTANTS FROM A MODIFIED
C              REDLICH-KWONG EQUATION OF STATE," CHEM. ENG.
C              SCI., 27, 1197 (1972).
C
C           - PANAGIOTOPOLOUS, A. Z. AND REID, R. C., "NEW MIXING
C              RULES FOR CUBIC EQUATIONS OF STATE FOR HIGHLY
C              POLAR, ASYMMETRIC SYSTEMS," EQUATIONS OF STATE-
C              THEORIES AND APPLICATIONS, ACS SYMPOSIUM SERIES,
C              NO. 300, 571 (1986).
C
C
      SUBROUTINE DELIJ (NCOMP,MIX,PARM,XY,K,AIJ,DEL,DXDEL)
      IMPLICIT INTEGER*4 (I-N), REAL*8 (A-H, O-Z)
      REAL*8 K
      DIMENSION PARM(5),XY(10),K(10,10),AIJ(10,10),
     *          DEL(10,10)
      N=1
```

```
      DO 10 I=1,NCOMP
       DO 20 J=I,NCOMP
        IF(I.EQ.J) GOTO 25
        IF(MIX.EQ.1) GOTO 30
          K(I,J)=PARM(2*N-1)/10.
          K(J,I)=PARM(2*N)/10.
          DEL(I,J)= K(I,J)-(K(I,J)-K(J,I))*XY(I)
          DEL(J,I)= K(J,I)-(K(J,I)-K(I,J))*XY(J)
          GOTO 40
   30      K(I,J)=0.0
          K(J,I)=0.0
          DEL(I,J)=PARM(N)/10.
          DEL(J,I)=DEL(I,J)
   40      N=N+1
         AIJ(I,J)=DSQRT(AIJ(I,I)*AIJ(J,J))*(1-DEL(I,J))
         AIJ(J,I)=DSQRT(AIJ(I,I)*AIJ(J,J))*(1-DEL(J,I))
C      WRITE(*,*) 'I,J,AIJ,DELIJ',I,J,AIJ(I,J),DEL(I,J)
          GOTO 20
   25     K(I,J)=0.D0
         DEL(I,J)=0.0
   20    CONTINUE
   10  CONTINUE
C
C     WRITE(*,7)  AIJ(1,1),AIJ(2,2),AIJ(1,2),XY(1)
C   7  FORMAT(' APX:',4D15.5)
      DXDEL=-K(1,2)+K(2,1)
C
      RETURN
      END


      SUBROUTINE DATMOD
      IMPLICIT REAL*8 (A-H,O-Z), INTEGER*4 (I-N)
      REAL*8 LMV
      INTEGER*4 VLEID
      DIMENSION VAP(5),UNIQ(8),IDREC(500)
      CHARACTER VLENAM*30,VLEFOR*10,FMSRCH*10,RC*3,YON*1
      CHARACTER DISPL1*11,DISPL2*10
      CHARACTER ENDH
      CHARACTER*3 BEG
      CHARACTER BEGX(3)
      EQUIVALENCE (BEG,BEGX)
      DATA UNIQ /0.96, 0.92, 0.89, 0.88, 1.15, 1.78, 2.71, 1.00/
      BEGX(1)=CHAR(19)
      BEGX(2)=CHAR(255)
      BEGX(3)=CHAR(1)
      ENDH=CHAR(1)
C
      OPEN (20,FILE='PUREDAT',ACCESS='DIRECT',FORM='FORMATTED',RECL=80)
      OPEN (25,FILE='PURELST',ACCESS='DIRECT',FORM='FORMATTED',RECL=80)
      READ (20,1,REC=1) NTOT
    1 FORMAT(I4,76X)
C
    2 WRITE(*,*) BEG,'USE,MAI102.AID',ENDH
      WRITE(*,*) BEG,'MENU',ENDH
```

```
      READ(*,5) IOPT
    5 FORMAT(I2)
      IF (IOPT.EQ.4) GO TO 1000
C
      IF (IOPT.EQ.1) THEN
  102   WRITE(*,*) BEG,'USE,DAT001.AID',ENDH
        WRITE(*,*) BEG,'MENU',ENDH
        READ(*,5) IOPT1
        IF (IOPT1.EQ.4) GO TO 2
        IC=0
        IF (IOPT1.EQ.1) THEN
          IC=NTOT
          DO 104 I=1,IC
            IDREC(I)=I+1
  104     CONTINUE
        ELSE IF (IOPT1.EQ.2) THEN
          WRITE(*,*) BEG,'OPEN,DAT003.AID,16,25',ENDH
          WRITE(*,*) BEG,'INPUT,IDSRCH',ENDH
          READ(*,105) IDSRCH
  105     FORMAT(I4)
          IF ((IDSRCH.LE.0).OR.(IDSRCH.GT.NTOT)) THEN
            DO 108 I=1,80
              WRITE(*,*) BEG,'MERGE,DAT008.AID,22,25',ENDH
  108       CONTINUE
            GO TO 102
          END IF
          IC=1
          IDREC(IC)=IDSRCH+1
        ELSE IF (IOPT1.EQ.3) THEN
          WRITE(*,*) BEG,'OPEN,DAT004.AID,16,25',ENDH
          WRITE(*,*) BEG,'INPUT,FMSRCH',ENDH
          READ(*,110) FMSRCH
  110     FORMAT(A10)
          IF (FMSRCH.EQ.' ') GO TO 112
          CALL FORM (FMSRCH,IDREC,IC)
          IF (IC.EQ.0) THEN
  112       DO 113 I=1,80
              WRITE(*,*) BEG,'MERGE,DAT008.AID,22,25',ENDH
  113       CONTINUE
            GO TO 102
          END IF
        END IF
C
        IK=IC/16
        IF(IC.GT.(IK*16)) IK=IK+1
        JJ=0
  120   WRITE(*,*) BEG,'USE,DAT002.AID',ENDH
        IF(JJ.EQ.0) WRITE(*,*) BEG,'MERGE,DAT009.AID,24,12',ENDH
        IF(JJ.EQ.(IK-1)) WRITE(*,*) BEG,'MERGE,DAT009.AID,24,51',ENDH
        JJ16=JJ*16
        DO 130 I=1,16
          II=I+JJ16
          IF(II.LE.IC) THEN
            READ(25,125,REC=IDREC(II))VLEID,VLENAM,VLEFOR
  125       FORMAT(I4,5X,A30,A10,31X)
            WRITE(*,*) BEG,'DISPLAY,VLEID,',I,',=',VLEID,ENDH
```

```
          WRITE(*,*) BEG,'DISPLAY,VLEFOR,',I,',=',VLEFOR,ENDH
          WRITE(*,*) BEG,'DISPLAY,VLENAM,',I,',=',VLENAM,ENDH
        END IF
130    CONTINUE
      WRITE(*,*) BEG,'MENU',ENDH
      READ(*,5) IOPTL
      IF ((JJ.EQ.0).AND.(JJ.EQ.(IK-1))) GO TO 102
      IF (JJ.EQ.0) THEN
        IF (IOPTL.EQ.1) THEN
          GO TO 102
        ELSE IF (IOPTL.EQ.2) THEN
          JJ=JJ+1
          GO TO 120
        END IF
      END IF
      IF (JJ.EQ.(IK-1)) THEN
        IF (IOPTL.EQ.1) THEN
          JJ=JJ-1
          GO TO 120
        ELSE IF (IOPTL.EQ.2) THEN
          GO TO 102
        END IF
      END IF
      IF (IOPTL.EQ.1) THEN
        JJ=JJ-1
        GO TO 120
      ELSE IF (IOPTL.EQ.2) THEN
        GO TO 102
      ELSE IF (IOPTL.EQ.3) THEN
        JJ=JJ+1
        GO TO 120
      END IF
    END IF
C
    IF (IOPT.EQ.3) THEN
      WRITE(*,*) BEG,'USE,DAT007.AID,17,23',ENDH
      WRITE(*,*) BEG,'INPUT,IDEDIT',ENDH
      READ(*,105) IDEDIT
      IF ((IDEDIT.LE.0).OR.(IDEDIT.GT.NTOT)) THEN
        DO 308 I=1,80
          WRITE(*,*) BEG,'MERGE,DAT008.AID,22,25',ENDH
308      CONTINUE
        GO TO 2
      END IF
      READ(25,125,REC=IDEDIT+1)VLEID,VLENAM,VLEFOR
      READ(20,320,REC=2*IDEDIT)VLEID,(VAP(I),I=1,5),LMV,TC,PC,
     *       DPM,RG,ASSOC,UNIQ1,UNIQ2,UNIQ3,ACEN
320    FORMAT(I4,1X,5(1PE11.4,1X),0PF8.6,1X,F6.2,/,
     *       F8.2,3X,F6.4,3X,F6.4,3X,F4.2,3X,4(F7.4,3X),4X)
      YON='N'
      IF (UNIQ3.NE.UNIQ2) YON='Y'
C
      WRITE(*,*) BEG,'VERTICAL,YES',ENDH
      WRITE(*,*) BEG,'EXIT,RET=D,TAB=D,BAT=U,FK1=H,FK3=V,FK0=V',ENDH
      WRITE(*,*) BEG,'USE,DAT005.AID',ENDH
      WRITE(*,*) BEG,'DISPLAY,VLEID,=',VLEID,ENDH
```

```
      WRITE(*,*) BEG,'DISPLAY,VLENAM,=',VLENAM,ENDH
      WRITE(*,*) BEG,'DISPLAY,VLEFOR,=',VLEFOR,ENDH
      WRITE(*,*) BEG,'DISPLAY,TC,=',TC,ENDH
      WRITE(DISPL2,330)PC*1000.0
330    FORMAT(1PE10.4)
      WRITE(*,*) BEG,'DISPLAY,PC,=',DISPL2,ENDH
      WRITE(*,*) BEG,'DISPLAY,LMV,=',LMV,ENDH
      WRITE(*,*) BEG,'DISPLAY,ACEN,=',ACEN,ENDH
      WRITE(DISPL2,330)RG*1.0E-10
      WRITE(*,*) BEG,'DISPLAY,RG,=',DISPL2,ENDH
      WRITE(DISPL2,330)DPM*3.33564E-30
      WRITE(*,*) BEG,'DISPLAY,DPM,=',DISPL2,ENDH
      WRITE(*,*) BEG,'DISPLAY,ASSOC,=',ASSOC,ENDH
      WRITE(*,*) BEG,'DISPLAY,UNIQ1,=',UNIQ1,ENDH
      WRITE(*,*) BEG,'DISPLAY,UNIQ2,=',UNIQ2,ENDH
      WRITE(*,*) BEG,'DISPLAY,YON,=',YON,ENDH
      DO 340 I=1,5
        WRITE(DISPL1,335)VAP(I)
335      FORMAT(1PE11.4)
        WRITE(*,*) BEG,'DISPLAY,VAP,',I,',=',DISPL1,ENDH
340    CONTINUE
      GO TO 440
    END IF
C
    VLEID=NTOT+1
    WRITE(*,*) BEG,'VERTICAL,YES',ENDH
    WRITE(*,*) BEG,'EXIT,RET=D,TAB=D,BAT=U,FK1=H,FK3=V,FK0=V',ENDH
    WRITE(*,*) BEG,'USE,DAT005.AID',ENDH
    WRITE(*,*) BEG,'DISPLAY,VLEID,=',VLEID,ENDH
C
440  WRITE(*,*) BEG,'SCREEN,VERIFY,RC',ENDH
    READ(*,450) RC
450  FORMAT(A3)
    IF (RC.EQ.'XXX') THEN
      WRITE(*,*) BEG,'FIRST,VAP,1,',ENDH
      GO TO 440
    END IF
    WRITE(*,*) BEG,'EXIT',ENDH
    WRITE(*,*) BEG,'VERTICAL,NO',ENDH
    IF(RC.EQ.'FK3') GO TO 2
C
    WRITE(*,*) BEG,'RECOVER,VLENAM',ENDH
    READ(*,205) VLENAM
205  FORMAT(A30)
    WRITE(*,*) BEG,'RECOVER,VLEFOR',ENDH
    READ(*,210) VLEFOR
210  FORMAT(A10)
    CALL FORM (VLEFOR,IDREC,-1)
    WRITE(*,*) BEG,'RECOVER,TC',ENDH
    READ(*,215) TC
215  FORMAT(F6.2)
    WRITE(*,*) BEG,'RECOVER,PC',ENDH
    READ(*,220) PC
220  FORMAT(G10.4)
    PC=PC/1000.0
    WRITE(*,*) BEG,'RECOVER,LMV',ENDH
```

```
      READ(*,225) LMV
  225 FORMAT(F8.6)
      WRITE(*,*) BEG,'RECOVER,ACEN',ENDH
      READ(*,230) ACEN
  230 FORMAT(F6.4)
      WRITE(*,*) BEG,'RECOVER,RG',ENDH
      READ(*,220) RG
      RG=RG/1.0E-10
      WRITE(*,*) BEG,'RECOVER,DPM',ENDH
      READ(*,220) DPM
      DPM=DPM/3.33564E-30
      WRITE(*,*) BEG,'RECOVER,ASSOC',ENDH
      READ(*,235) ASSOC
  235 FORMAT(F4.2)
      WRITE(*,*) BEG,'RECOVER,UNIQ1',ENDH
      READ(*,240) UNIQ1
  240 FORMAT(F7.4)
      WRITE(*,*) BEG,'RECOVER,UNIQ2',ENDH
      READ(*,240) UNIQ2
      WRITE(*,*) BEG,'RECOVER,YON',ENDH
      READ(*,245) YON
  245 FORMAT(A1)
      DO 255 I=1,5
        WRITE(*,*) BEG,'RECOVER,VAP,',I,ENDH
        READ(*,250) VAP(I)
  250   FORMAT(G11.4)
  255 CONTINUE
C
      IF (YON.EQ.'Y') THEN
        WRITE(*,*) BEG,'VERTICAL,YES',ENDH
        WRITE(*,*) BEG,'USE,DAT006.AID,17,39',ENDH
        WRITE(*,*) BEG,'MENU',ENDH
        READ(*,5) IOPTM
        IF (IOPTM.EQ.9) THEN
          UNIQ3=UNIQ2
        ELSE
          UNIQ3=UNIQ(IOPTM)
        END IF
        WRITE(*,*) BEG,'VERTICAL,NO',ENDH
      ELSE
        UNIQ3=UNIQ2
      END IF
C
      IF (IOPT.EQ.2) NTOT=NTOT+1
      WRITE (20,1,REC=1) NTOT
      WRITE (20,320,REC=2*VLEID)VLEID,(VAP(I),I=1,5),LMV,TC,PC,DPM,
     *       RG,ASSOC,UNIQ1,UNIQ2,UNIQ3,ACEN
      WRITE (25,1,REC=1) NTOT
      WRITE (25,125,REC=VLEID+1)VLEID,VLENAM,VLEFOR
      GO TO 2
C
 1000 CLOSE(20)
      CLOSE(25)
      RETURN
      END
```

```
C  DIPPR ROUTINE NAME - MARG
C
C ***********************************************************************
C
C
C  PURPOSE       - CALCULATION OF ACTIVITY COEFFICIENTS OF COMPONETNS
C                  IN A DEFINED LIQUID MIXTURE USING THE
C                  THREE-SUFFIX MARGULES MODEL
C
C  USAGE         - CALL MARG (PARM,X,ACT,IDV,IER,DT1,DT2,DX1,DX2)
C
C  ARGUMENTS
C    INPUT: PARM  - VECTOR OF LENGTH TWO OF VALUES OF THE MARGULES
C                   CONSTANTS A12 AND A21.
C           T     - TEMPERATURE OF THE SYSTEM (KELVINS).
C           X     - VECTOR OF LENGTH TWO OF MOLE FRACTIONS OF THE
C                   LIQUID PHASE.
C           IDV   - OPTION PARAMETER. WHEN IDV IS:
C                   0: DERIVATIVES OF THE ACTIVITY COEFFICIENTS WITH
C                     RESPECT TO THE MEASURED VARIABLES ARE NOT
C                     CALCULATED.
C                   1: DERIVATIVES OF THE ACTIVITY COEFFICIENTS WITH
C                     RESPECT TO THE MEASURED VARIABLES ARE
C                     CALCULATED.
C    OUTPUT: ACT  - VECTOR OF LENGTH TWO OF LIQUID PHASE ACTITIVTY
C                   COEFFICIENTS.
C           DT1- DERIVATIVE OF ACT(1) WITH RESPECT TO TEMPERATURE
C                   (1/KELVINS).
C           DT2   - DERIVATIVE OF ACT(2) WITH RESPECT TO TEMPERATURE
C                   (1/KELVINS).
C           DX1   - DERIVATIVE OF ACT(1) WITH RESPECT TO LIQUID PHASE
C                   CONCENTRATION OF COMPONENT 1.
C           DX2   - DERIVATIVE OF ACT(2) WITH RESPECT TO LIQUID PHASE
C                   CONCENTRATION OF COMPONENT 1.
C
C  LIMITATIONS:    - THIS PROCEDURE CAN ONLY BE USED FOR BINARY SYSTEMS.
C                   FOR THE CALCULATION OF ACTIVITY COEFFICIENTS FOR
C                   MULTICOMPONENT SYSTEMS, USE ONE OF THE FOLLOWING
C                   MODELS: WILSON, NRTL, OR UNIQUAC.
C
C  REFERENCES:     -
C
C
C
C  EXAMPLE:
C
C     IMPLICIT INTEGER*4 (I-N), REAL*8 (A-H, O-Z)
C     DIMENSION PARM(2),X(2),ACT(2)
C     PARM(1)=0.600
C     PARM(2)=0.534
C     X(1)=0.290
C     X(2)=0.710
C     IDV=1
C     CALL MARG (PARM,X,ACT,IDV,IER,DT1,DT2,DX1,DX2)
```

```
C     WRITE(*,*) ACT,DT1,DT2,DX1,DX2
C     STOP
C     END
C
C              - USING THESE VALUES, THE CALCULATED VALUES ARE:
C                 ACT(1) =  1.3273
C                 ACT(2) =  1.0542
C                 DT1    =  0.00
C                 DT2    =  0.00
C                 DX1    = -1.1405
C                 DX2    =  0.3721
C
C

C ***********************************************************************
C
      SUBROUTINE MARG (PARM,X,ACT,IDV,IER,DTACT1,DTACT2,DXACT1,DXACT2)
      IMPLICIT INTEGER*4 (I-N), REAL*8 (A-H, O-Z)
      DIMENSION PARM(5),X(10),ACT(10)
C
      IER=0
      A12=PARM(1)
      A21=PARM(2)
C
      ACT(1) = DEXP((A12+2.*(A21-A12)*X(1))*X(2)**2.)
      ACT(2) = DEXP((A21+2.*(A12-A21)*X(2))*X(1)**2.)
C
      IF(IDV.EQ.0) RETURN
      IF(IDV.NE.1) GOTO 51
       DXACT1 = ACT(1)*2*X(2)*((A21-A12)*X(2)-(A12+2*(A21-A12)*X(1)))
       DTACT1 = 0.D0
C
       DXACT2 = ACT(2)*2*X(1)*(-(A12-A21)*X(1)+(A21+2*(A12-A21)*X(2)))
       DTACT2 = 0.D0
C
      RETURN
   51 IER=51
      RETURN
      END

C
C  SUBROUTINE FUGC2
C     B(I,J) ARE IN UNITS OF CUBIC METERS / KMOL
C
      SUBROUTINE FUGC2 (NCOMP,T,P,Y,TC,PC,RG,DM,NU,PSAT,FUGC,
     *                  FUGCST,IER,IDV,DPSAT,DFUGC,DFUGST)
      IMPLICIT INTEGER*4 (I-N), REAL*8 (A-H,O-Z)
      REAL*8 NU
      DIMENSION Y(10),TC(10),PC(10),RG(10),DM(10),NU(2,2),PSAT(10),
     *          FUGC(10),FUGCST(10),B(10,10),DB(2,2),DPSAT(2),DFUGST(2),
     *          BF(10,10),BD(10,10),DBF(2,2),DBD(2,2),DFUGC(3,2)
C
C     CHECK FOR FATAL ERRORS AND WARNINGS.
C
      IER=0
      DO 4 I=1,NCOMP
```

```
      FUGC(I)=0.0
      FUGCST(I)=0.0
4   CONTINUE
    IF (NCOMP.LE.0) THEN
      IER=100
      RETURN
    ELSE IF (T.LE.0.0) THEN
      IER=101
      RETURN
    ELSE IF (P.LE.0.0) THEN
      IER=102
      RETURN
    END IF
    TOT=0.0
    ICHEM=0
    DO 5 I=1,NCOMP
      IF (Y(I).LT.0.0 .OR. Y(I).GT.1.0) THEN
        IER=610
        RETURN
      ELSE IF (TC(I).LE.0.0) THEN
        IER=110
        RETURN
      ELSE IF (PC(I).LE.0.0) THEN
        IER=111
        RETURN
      ELSE IF (RG(I).LE.0.0) THEN
        IER=231
        RETURN
      ELSE IF (DM(I).LT.0.0) THEN
        IER=720
        RETURN
      ELSE IF (PSAT(I).LE.0.0) THEN
        IER=230
        RETURN
      END IF
      DO 6 J=I,NCOMP
        IF (NU(I,J).LT.0.0) THEN
          IER=740
          RETURN
        END IF
        IF (NU(I,J).GE.4.5) ICHEM=1
6   CONTINUE
      FUGC(I)=0.0
      TOT=TOT+Y(I)
5 CONTINUE
    IF (ABS(TOT-1.0).GT.0.0001) THEN
      IER=1
    END IF
C
C   INITIALIZE PARAMETER TO BE USED IN CALCULATIONS.
C
    BMIX=0.
    DO 10 I=1,NCOMP
      DO 20 J=1,NCOMP
C
C   CALCULATE ACENTRIC FACTOR (ACENI), PARAMETERS C1 AND C2, SIGMA'
```

```
C  (SIGMA1), AND E/K'(EOK1) FROM EQUATIONS 6C-18, 6C-24, 6C-23, 6C-22,
C  AND 6C-21 RESPECTIVELY OF COMPONENT I.
C
      ACENI=0.006026*RG(I)+0.02096*RG(I)**2-0.001366*RG(I)**3
      C1=(16.+400.*ACENI)/(10.+400.*ACENI)
      C2=3./(10.+400.*ACENI)
      SIGMA1=(2.44-ACENI)*(101.33*TC(I)/(PC(I)/1000.))**(1./3.)
      EOK1=TC(I)*(0.748+0.91*ACENI-0.4*NU(I,I)/(2.+20.*ACENI))
C
C  CALCULATE PARAMETER XI FROM EQUATION 6C-23 OR SET EQUAL TO ZERO,
C  DEPENDING ON THE VALUE OF THE DIPOLE MOMENT FOR COMPONENT I.
C
      IF (DM(I).LT.1.45) THEN
        XI=0.0
      ELSE
        XI=1.7941E07*DM(I)**4/((2.822-1.882*ACENI/(0.03+ACENI))*
     *     TC(I)*SIGMA1**6*EOK1)
      END IF
C
C  CALCULATE MOLECULAR SIZE (SIGMAI) AND CHARACTERISTIC ENERGY (EOKI)
C  FOR COMPONENT I FROM EQUATIONS 6C-20 AND 6C-19.
C
      SIGMAI=SIGMA1*(1.+XI*C2)**(1./3.)
      EOKI=EOK1*(1.-XI*C1*(1.-XI*(1.+C1)/2.))
C
C  IF I IS NOT EQUAL TO J, CALCULATE ACENTRIC FACTOR (ACENJ), AND
C  PARAMETERS C1, C2, SIGMA1, EOK1, XI, SIGMAJ, AND EOKJ FOR COMPONENT
C  J FROM SAME EQUATIONS USED FOR COMPONENT I.
C
      IF (I.NE.J) THEN
        ACENJ=0.006026*RG(J)+0.02096*RG(J)**2-0.001366*RG(J)**3
        C1=(16.+400.*ACENJ)/(10.+400.*ACENJ)
        C2=3./(10.+400.*ACENJ)
        SIGMA1=(2.44-ACENJ)*(101.33*TC(J)/(PC(J)/1000.))**(1./3.)
        EOK1=TC(J)*(0.748+0.91*ACENJ-0.4*NU(J,J)/(2.+20.*ACENJ))
        IF (DM(J).LT.1.45) THEN
          XI=0.0
        ELSE
          XI=1.7941E07*DM(J)**4/((2.822-1.882*ACENJ/(0.03+ACENJ))
     *       *TC(J)*SIGMA1**6*EOK1)
        END IF
        SIGMAJ=SIGMA1*(1.+XI*C2)**(1./3.)
        EOKJ=EOK1*(1.-XI*C1*(1.-XI*(1.+C1)/2.))
C
C  IF I IS NOT EQUAL TO J, CALCULATE CROSS PARAMETER ACENTRIC FACTOR
C  (ACEN), CROSS PARAMETERS C1, C2, SIGMA1, EOK1, AND XI1, CHARACTER-
C  ISTIC ENERGY FOR THE I-J INTERACTION (EOK), AND CROSS PARAMETER
C  MOLECULAR SIZE FROM EQUATIONS 6C-26, 6C-32, 6C-33, 6C-30, 6C-29,
C  6C-31, 6C-27, AND 6C-28 RESPECTIVELY.
C
        ACEN=0.5*(ACENI+ACENJ)
        C1=(16.+400.*ACEN)/(10.+400.*ACEN)
        C2=3./(10.+400.*ACEN)
        SIGMA1=SQRT(SIGMAI*SIGMAJ)
        EOK1=0.7*SQRT(EOKI*EOKJ)+0.6/(1./EOKI+1./EOKJ)
        IF (DM(I).GE.2. .AND. DM(J).EQ.0.) THEN
```

```
          XI1=DM(I)**2*EOKJ**(2./3.)*SIGMAJ**4/(EOK1*SIGMA1**6)
        ELSE IF (DM(J).GE.2. .AND. DM(I).EQ.0.) THEN
          XI1=DM(J)**2*EOKI**(2./3.)*SIGMAI**4/(EOK1*SIGMA1**6)
        ELSE
          XI1=0.0
        END IF
        SIGMA=SIGMA1*(1.-XI1*C2)
        EOK=EOK1*(1.+XI1*C1)
      ELSE
C
C  IF I EQUALS J, SET ACENTRIC FACTOR (ACEN), MOLECULAR SIZE (SIGMA),
C  AND CHARACTERISTIC ENERGY FOR THE I-J INTERACTION (EOK) EQUAL TO
C  PURE COMPONENT PROPERTIES OF COMPONENT I.
C
        ACEN=ACENI
        SIGMA=SIGMAI
        EOK=EOKI
      END IF
C
C  CALCULATE PARAMETER E FROM EQUATION 6C-17 DEPENDING ON THE VALUE OF
C  THE ASSOCIATION OR SOLVATION PARAMETER.
C
      IF (NU(I,J).LT.4.5) THEN
        E=EXP(NU(I,J)*(650./(EOK+300.)-4.27))
      ELSE
        E=EXP(NU(I,J)*(42800./(EOK+22400.)-4.27))
      END IF
C
C  CALCULATE PARAMETERS DM* (DMSTAR), DELTAH, AND A FROM EQUATIONS
C  6C-16, 6C-15, AND 6C-14 RESPECTIVELY.
C
      DMSTAR=7243.8*DM(I)*DM(J)/(EOK*SIGMA**3)
      DELTAH=1.99+0.2*DMSTAR**2
      A=-0.3-0.05*DMSTAR
C
C  CALCULATE PARAMETER DM*' (DMSTR1) FROM EQUATION 6C-13 DEPENDING ON
C  THE VALUE OF DM*.
C
      IF (DMSTAR.LT.0.04) THEN
        DMSTR1=DMSTAR
      ELSE IF (DMSTAR.GE.0.04 .AND. DMSTAR.LT.0.25) THEN
        DMSTR1=0.0
      ELSE
        DMSTR1=DMSTAR-0.25
      END IF
C
C  CALCULATE PARAMETERS BO, T* (TSTAR), AND T*' (TSTAR1) FROM EQUATIONS
C  6C-12, 6C-11, AND 6C-10 RESPECTIVELY.
C
      BO=0.00126*SIGMA**3
      TSTAR=T/EOK
      TSTAR1=1./(1./TSTAR-1.6*ACEN)

C
C  CALCULATE CHEMICAL (BCHEM), METASTABLE + BOUND (BMETBB), POLAR
C  (BPOLAR), AND NONPOLAR (BNPOLR) CONTRIBUTIONS TO THE SECOND VIRIAL
```

```
C   COEFFICIENT FROM EQUATIONS 6C-9, 6C-8, 6C-7, AND 6C-6 RESPECTIVELY.
C
      BCHEM =B0*E*(1.-EXP(1500.*NU(I,J)/T))
      BMETBB=B0*A*EXP(DELTAH/TSTAR)
      BPOLAR=-B0*DMSTR1*(0.74-3./TSTAR1+2.1/TSTAR1**2+2.1/TSTAR1**3)
      BNPOLR=B0*(0.94-1.47/TSTAR1-0.85/TSTAR1**2-1.015/TSTAR1**3)
C
C   CALCULATION OF DERIVATIVES
C
      IF(IDV.EQ.0) GOTO 9
      DTSTAR=1/EOK
      DTST1 =-1./(TSTAR**2.*(1/TSTAR-1.6*ACEN)**2.)*DTSTAR
      DBCHEM=-B0*E*EXP(1500.*NU(I,J)/T)*(-1500.*NU(I,J)/T**2)
      DBMTBB=BMETBB*(-DELTAH/TSTAR**2.)*DTSTAR
      DBPOLR=-B0*DMSTR1*(3./TSTAR1**2.-2.1/TSTAR1**3-2.1/TSTAR1**4)
     *       *DTST1
      DBNPLR=B0*(1.47/TSTAR1**2.+0.85/TSTAR1**3+1.015/TSTAR1**4)
     *       *DTST1
C
  9   IF (ICHEM.EQ.1) GOTO 40
C
      B(I,J) =BNPOLR+BPOLAR+BMETBB+BCHEM
      DB(I,J)=DBNPLR+DBPOLR+DBMTBB+DBCHEM
C
C   CALCULATE MIXTURE SECOND VIRIAL COEFFICIENT FROM EQUATION 6C-2.
C
      BMIX=BMIX+Y(I)*Y(J)*B(I,J)
      FUGC(I)=FUGC(I)+Y(J)*B(I,J)
C
C   CALCULATE FUGACITY COEFFICIENT FOR PURE SATURATED COMPONENT I
C   (FUGCST) FROM EQUATION 6C-34.
C
      IF (I.EQ.J) THEN
       FUGCST(I)=EXP(B(I,J)*PSAT(I)/(8314*T))
       IF(IDV.EQ.0) GOTO 20
       DFUGST(I)=FUGCST(I)*(T*(DB(I,I)*PSAT(I)-B(I,J)*DPSAT(I))-
     *                B(I,J)*PSAT(I))/T/T/8314.
      END IF
      GOTO 20
C
  40  BF(I,J)=BPOLAR+BNPOLR
      DBF(I,J)=DBNPLR+DBPOLR
      BD(I,J)=BCHEM+BMETBB
      DBD(I,J)=DBMTBB+DBCHEM
C
  20  CONTINUE
  10 CONTINUE
C
C   CALCULATE FUGACITY COEFFICIENT OF COMPONENT I IN THE VAPOR PHASE
C   (FUCG) FROM EQUATION 6C-1 AND RETURN TO CALLING PROGRAM.
C
    IF (ICHEM.EQ.1) GOTO 50
    DO 30 I=1,NCOMP
     ARG    =(2.*FUGC(I)-BMIX)*P/(8314*T)
     FUGC(I)=EXP(ARG)
     DFUGC(1,I)=FUGC(I)*ARG/P
```

```
  30 CONTINUE
C
     IF(IDV.EQ.0) GOTO 60
     DFUGC(2,1) = FUGC(1)*(P/8314/T*
     *       (Y(1)*(2-Y(1))*DB(1,1)+2*Y(2)**2*DB(1,2)-Y(2)**2*DB(2,2))
     *       -DLOG(FUGC(1))/T)
     DFUGC(2,2) = FUGC(2)*(P/8314/T*
     *       (-Y(1)**2*DB(1,1)+2*Y(1)**2*DB(1,2)+Y(2)*(2-Y(2))*DB(2,2))
     *       -DLOG(FUGC(2))/T)
C
     DFUGC(3,1)=FUGC(1)*2*P/8314/T*Y(2)*(-2*B(1,2)+B(1,1)+B(2,2))
     DFUGC(3,2)=FUGC(2)*2*P/8314/T*Y(1)*( 2*B(1,2)-B(1,1)-B(2,2))
C
  60 RETURN
C
  50 CALL CHEM (NCOMP,T,P,PSAT,Y,BF,BD,FUGC,FUGCST,IER,
     *                  IDV,DBF,DBD,DPSAT,DFUGC,DFUGST)
     RETURN
     END


C
C  DIPPR ROUTINE NAME - ACTMOD
C
C ***************************************************************************
C
C
C  PURPOSE       - CALCULATION OF THE CONSTRAINTS AND DERIVATIVES OF
C                  THE CONSTRAINTS FOR USE IN THE ERROR-IN-VARIABLES
C                  REGRESSION TECHNIQUE OF ACTIVITY COEFFICIENT
C                  PARAMETERS.
C
C  USAGE         - CALL ACTMOD (XI,THETA,C,F)
C
C  ARGUMENTS
C    INPUT: XI    - VECTOR OF LENGTH 4 OF ESTIMATES OF THE TRUE VALUES
C                  OF THE MEASURED QUANTITIES. FOR THE APPROXIMATE
C                  EVM METHOD, THE EXPERIMENTAL VALUES ARE USED.
C                  XI(1) = PRESSURE (PA)
C                  XI(2) = TEMPERATURE (KELVINS)
C                  XI(3) = LIQUID MOLE FRACTION OF COMPONENT 1
C                  XI(4) = VAPOR MOLE FRACTION OF COMPONENT 1
C          THETA - VECTOR OF LENGTH 3 OF PARAMETERS TO BE REGRESSED.
C     COMMON
C     STATEMENTS:
C          COMMON/AREA2/PD
C          PD    - MATRIX OF DIMENSION (15,2) OF PARAMETERS. FOR THIS
C                  SUBROUTINE, THE ABOVE COMMON STATEMENT MUST BE
C                  INCLUDED IN THE CALLING ROUTINE OR ANY PREVIOUSLY
C                  CALLED ROUTINE AND THE FOLLOWING VARIABLES MUST
C                  BE DEFINED:
C                 PD(1,I) TO PD(5,I) - DIPPR VAPOR PRESSURE
C                  CONSTANTS, A THROUGH E, FOR EACH COMPONENT.
C                 THE FOLLOWING IS NEEDED ONLY FOR THE WILSON MODEL:
C                  PD(6,I) - LIQUID MOLAR VOLUME OF EACH COMPONENT
C                        (M**3/MOL).
```

```
C               THE FOLLOWING ARE NEEDED ONLY IF FUGACITY
C               COEFFICIENTS ARE CALCULATED WITH THE METHOD OF
C               HAYDEN-O'CONNELL:
C                 PD(7,I) - CRITICAL TEMPERATURES OF EACH COMPONENT
C                       (KELVINS).
C                 PD(8,I) - CRITICAL PRESSURES OF EACH COMPONENT
C                       (KILOPASCALS).
C                 PD(9,I) - DIPOLE MOMENTS OF EACH COMPONENT
C                       (DEBYE).
C                 PD(10,I)- RADIUS OF GYRATION OF EACH COMPONENT
C                       (ANGSTROMS).
C                 PD(11,I)- ASSOCIATION PARAMETERS OF EACH
C                       COMPONENT (DIMENSIONLESS).
C               THE FOLLOWING ARE NEEDED ONLY IF THE UNIQUAC MODEL
C               IS CHOSEN:
C                 PD(12,I)- UNIQUAC VOLUME PARAMETER, R, FOR EACH
C                       COMPONENT
C                 PD(13,I)- UNIQUAC AREA PARAMETER, Q, FOR EACH
C                       COMPONENT.
C                 PD(14,I)- UNIQUAC AREA PARAMETER, Q, ADJUSTED FOR
C                       ALCOHOLS AND WATER, FOR EACH COMPONENT.
C
C         COMMON/AREA3/EOFS
C         EOFS  - VECTOR OF LENGHT 6 OF PARAMETERS. FOR THIS
C                 SUBROUTINE, THE ABOVE COMMON STATEMENT MUST BE
C                 INCLUDED IN THE CALLING ROUTINE OR ANY PREVIOUSLY
C                 CALLED ROUTINE AND THE FOLLOWING VARIABLES MUST
C                 BE DEFINED:
C               EOS(3) - INDICATOR FOR THE INCLUSION OF PURE
C                 COMPONENT ENDPOINTS IN THE DATA SET:
C                   EOS(3) = 1 FOR INCLUSION OF ENDPOINTS
C                   EOS(3) = 0 FOR EXCLUSION OF ENDPOINTS
C               EOS(1) - PRESSURE OF SYSTEM AT X(1)=0.0. (NEEDED
C                       ONLY IF EOS(3)=1).
C               EOS(2) - PRESSURE OF SYSTEM AT X(1)=1.0. (NEEDED
C                       ONLY IF EOS(3)=1).
C               EOS(4) - INDICATOR FOR ACTIVITY COEFFICIENT MODEL
C                       1: THREE-SUFFIX MARGULES
C                       2: VAN LAAR
C                       3: WILSON (TWO-PARAMETER)
C                       4: UNIQUAC
C                       5: NRTL
C                       6: WILSON (THREE-PARAMETER)
C               THE FOLLOWING ARE NEEDED ONLY IF FUGACITY
C                 COEFFICIENTS ARE CALCULATED WITH THE METHOD OF
C                 HAYDEN-O'CONNELL:
C               EOS(5) - SOLVATION PARAMETER BETWEEN COMPONENTS ONE
C                       AND TWO (DIMENSIONLESS).
C
C   OUTPUT: C    - MATRIX OF DIMENSION (2,4) OF DERIVATIVES OF THE
C                 CONSTRAINTS WITH RESPECT TO THE MEASURED
C                 VARIABLES.
C           F    - VECTOR OF LENGTH 2 OF CONSTRAINTS
C
C
C  SUBROUTINES REQ.- MARG   (THREE-SUFFIX MARGULES MODEL)
```

```
C               VANLAR (VAN LAAR MODEL)
C               WILSON (TWO-PARAMETER WILSON MODEL)
C               UNIQUA (UNIQUAC MODEL)
C               NRTL   (NRTL MODEL)
C               WIL3   (THREE-PARAMETER WILSON MODEL)
C               FUGC   (HAYDEN-O'CONNELL FUGACITY COEFF ROUTINE)
C
C
C LIMITATIONS:    - THE ACTIVITY COEFFICIENT APPROACH SHOULD ONLY BE
C                   USED FOR LOW PRESSURE SYSTEMS.  THE REGRESSION
C                   METHOD CAN ONLY BE USED FOR BINARY SYSTEMS.
C
C
C REFERENCES:     - WILSON, G. M., "VAPOR-LIQUID EQUILIBRIUM. XI. A NEW
C                   EXPRESSION FOR THE EXCESS FREE ENERGY OF MIXING,"
C                   J. AMER. CHEM. SOC. 86, 127 (1964).
C
C                 - ABRAMS, D. S. AND PRAUSNITZ, J. M., "STATISTICAL
C                   THERMODYNAMICS OF LIQUID MIXTURES: A NEW
C                   EXPRESSION FOR THE EXCESS GIBBS ENERGY OF
C                   PARTIALLY OR COMPLETELY MISCIBLE SYSTEMS," AICHE
C                   J., 21, 116 (1975).
C
C                 - RENON, H. AND PRAUSNITZ, J. M., "LOCAL COMPOSITIONS
C                   IN THERMODYNAMIC EXCESS FUNCTIONS FOR LIQUID
C                   MIXTURES," AICHE J., 14, 135 (1968).
C
C
C EXAMPLE:
C
C    IMPLICIT INTEGER*4 (I-N), REAL*8 (A-H, O-Z)
C    DIMENSION XI(4),THETA(3),C(2,4),F(2),PD(15,2),
C   *          FUGC(2,2),DPFC(2,2),DTFC(2,2),DXFC(2,2),EOFS(6)
C    COMMON /AREA2/ PD
C    COMMON /AREA3/ EOFS
C    XI(1) = 90.446E03
C    XI(2) = 323.15
C    XI(3) = 0.290
C    XI(4) = 0.423
C    EOFS(4) = 5
C    THETA(1) = 1000.0
C    THETA(2) = 700.0
C    THETA(3) = 0.3
C    CALL EOSMOD (XI,THETA,C,F)
C    WRITE(*,10) F,C
C 10 FORMAT(' F:', 2D15.5,/,' C1:',4E15.5,/,' C2:',4E15.5)
C    STOP
C    END
C
C                 - USING THESE VALUES, THE CALCULATED VALUES ARE:
C                   F(1) =              F(2) =
C                   C(1,1) =            C(2,1) =
C                   C(1,2) =            C(2,2) =
C                   C(1,3) =            C(2,3) =
C                   C(1,4) =            C(2,4) =
C
```

```
C
C ***********************************************************************
C
      SUBROUTINE ACTMOD(XI,THETA,B,F)
      IMPLICIT INTEGER*4 (I-N), REAL*8 (A-H, O-Z)
      REAL*8 NU
      DIMENSION XI(4),THETA(5),B(2,4),F(2),R(10),QQ(10),VOL(10),
     *          X(10),Y(10),DM(10),RG(10),TC(10),PD(15,10),PC(10),
     *          NU(2,2),FUGC(10),FUGCST(10),PSAT(10),GAMMA(10),
     *          QP(10),AM(6),DPSAT(2),DFUGC(3,2),DFUGST(2)
      COMMON /AREA2/ PD
      COMMON /AREA3/ AM
C
      IDV=1
      IER=0
      NCOMP=2
      RPA=8.31439
      RKMOL=8314.39
      P= XI(1)
      T= XI(2)
      X(1)=XI(3)
        X(2)=1.-X(1)
      Y(1)=XI(4)
        Y(2)=1.-Y(1)
C
      DO 15 N=1,2
        VOL(N)=PD(6,N)
        TC(N)=PD(7,N)
        PC(N)=PD(8,N)*1.D03
        DM(N)=PD(9,N)
        RG(N)=PD(10,N)
        NU(N,N)=PD(11,N)
   15 CONTINUE
C
C  ASSIGNMENT OF VAPOR PRESSURES
C   OPTION TO USE EXPERMENTAL DATA POINTS FOR VAPOR PRESSURES
C   **  AM(3)=1 FOR AN ISOTHERMAL SYSTEM WITH ENDPOINTS  **
C
      IF (AM(3).EQ.1.D0) THEN
       PSAT(1)=AM(1)
       PSAT(2)=AM(2)
      ELSE
       DO 100 J=1,2
  100   PSAT(J)=DEXP(PD(1,J)+PD(2,J)/T+PD(3,J)*DLOG(T)+
     *          PD(4,J)*T**PD(5,J))
      ENDIF
C
      IF(X(1).EQ.0.0) PSAT(2)=AM(2)
      IF(X(1).EQ.1.0) PSAT(1)=AM(1)
C
       DTVP1 = -PD(2,1)/T**2+PD(3,1)/T+PD(4,1)*PD(5,1)*T**(PD(5,1)-1)
       DTVP2 = -PD(2,2)/T**2+PD(3,2)/T+PD(4,2)*PD(5,2)*T**(PD(5,2)-1)
        DPSAT(1) = PSAT(1)*DTVP1
        DPSAT(2) = PSAT(2)*DTVP2
C
C  CALCULATION OF THE OBJECTIVE FUNCTIONS F(1) AND F(2)
```

```
C
C  CALLING OF ACTIVITY COEFFICIENT ROUTINES
C
     IF(AM(4).EQ.1.)
    * CALL MARG (THETA,X,GAMMA,IDV,IER,DTACT1,DTACT2,DXACT1,DXACT2)
     IF(AM(4).EQ.2.)
    * CALL VANLAR (THETA,X,GAMMA,IDV,IER,DTACT1,DTACT2,DXACT1,DXACT2)
     IF(AM(4).EQ.3.)
    * CALL WILSON (NCOMP,THETA,VOL,T,X,
    *                  GAMMA,IDV,DTACT1,DTACT2,DXACT1,DXACT2)
     IF(AM(4).EQ.4.) THEN
       DO 30 J=1,2
        R(J)=PD(12,J)
        QQ(J)=PD(13,J)
 30      QP(J)=PD(14,J)
 31    FORMAT(6F10.3)
      CALL UNIQUA (NCOMP,THETA,R,QQ,QP,T,X,
    *                  GAMMA,IDV,IER,DTACT1,DTACT2,DXACT1,DXACT2)
       ENDIF
     IF(AM(4).EQ.5.)
    *CALL NRTL3 (NCOMP,THETA,T,X,GAMMA,IDV,IER,
    *                          DTACT1,DTACT2,DXACT1,DXACT2)
     IF(AM(4).EQ.6.)
    *CALL WIL3 (THETA,PD(6,1),PD(6,2),T,X,
    *                  ACT1,ACT2,DTACT1,DTACT2,DXACT1,DXACT2)
     IF(AM(4).EQ.9.)
    *CALL MARGUL (THETA, X, ACT1, ACT2, DXACT1, DXACT2, DTACT1,DTACT2)
     IF(AM(4).LT.6.) THEN
       ACT1=GAMMA(1)
       ACT2=GAMMA(2)
     ENDIF
C
C  CALLING OF FUGACITY COEFFICIENT ROUTINE
C
     NU(1,2)=AM(5)
     NU(2,1)=NU(1,2)
     POYNT1= (P-PSAT(1))*PD(6,1)/RKMOL/T
     POYNT2= (P-PSAT(2))*PD(6,2)/RKMOL/T
      DTPYN1 = 1/T*(-PD(6,1)*DPSAT(1)/RKMOL-POYNT1)
      DTPYN2 = 1/T*(-PD(6,2)*DPSAT(2)/RKMOL-POYNT2)
C
     IF(AM(4).EQ.9.) GOTO 1000
     CALL FUGC2(NCOMP,T,P,Y,TC,PC,RG,DM,NU,PSAT,FUGC,FUGCST,IER,
    *                  IDV,DPSAT,DFUGC,DFUGST)
     SSFUG1=FUGCST(1)*PSAT(1)*DEXP(POYNT1)
     SSFUG2=FUGCST(2)*PSAT(2)*DEXP(POYNT2)
C
  89  FORMAT(' X,PHI1,PHI2,PHI1S,PHI2S:',F8.3,4F10.4)
  91  FORMAT(' X1',F10.3)
     IF(FUGC(1).LE.0.0) WRITE(*,*) 'ERROR CODE:',IER
     IF(FUGC(2).LE.0.0) WRITE(*,*) 'ERROR CODE:',IER
C
C  THE OBJECTIVE FUNCTIONS
C
     F(1) = Y(1)*P*FUGC(1) - ACT1*X(1)*SSFUG1
     F(2) = Y(2)*P*FUGC(2) - ACT2*X(2)*SSFUG2
```

```
 510  FORMAT('      FUGC 1,2: ',2F15.5,/,
     *       ' SSFUG 1/PSAT1: ',2F15.5,/,
     *       ' SSFUG 2/PSAT2: ',2F15.5,/,
     *       ' ACT 1  /ACT 2: ',2F15.5)
C
C  CALCULATION OF DERIVATIVES WITH RESPECT TO PRESSURE
C
      DPSSF1 = SSFUG1*PD(6,1)/RKMOL/T
      DPSSF2 = SSFUG2*PD(6,2)/RKMOL/T
C
      B(1,1) = DFUGC(1,1)*Y(1)*P + FUGC(1)*Y(1) - ACT1*X(1)*DPSSF1
      B(2,1) = DFUGC(1,2)*Y(2)*P + FUGC(2)*Y(2) - ACT2*X(2)*DPSSF2
C
C  CALCULATION OF DERIVATIVES WITH RESPECT TO TEMPERATURE
C
      DTSSF1 = SSFUG1*(DTPYN1 + DTVP1) + PSAT(1)*DEXP(POYNT1)*DFUGST(1)
      DTSSF2 = SSFUG2*(DTPYN2 + DTVP2) + PSAT(2)*DEXP(POYNT2)*DFUGST(2)
C
      B(1,2) = DFUGC(2,1)*Y(1)*P - DTACT1*X(1)*SSFUG1 - ACT1*X(1)*DTSSF1
      B(2,2) = DFUGC(2,2)*Y(2)*P - DTACT2*X(2)*SSFUG2 - ACT2*X(2)*DTSSF2
C
C  CALCULATION OF DERIVATIVES WITH RESPECT TO X1
C
      B(1,3) = (-DXACT1*X(1)*SSFUG1 - ACT1*SSFUG1)
      B(2,3) = (-DXACT2*X(2)*SSFUG2 + ACT2*SSFUG2)
C
C  CALCULATION OF DERIVATIVES WITH RESPECT TO Y1
C
      B(1,4) = (DFUGC(3,1)*Y(1)*P + FUGC(1)*P)
      B(2,4) = (DFUGC(3,2)*Y(2)*P - FUGC(2)*P)
C
  500 FORMAT(' F(1) AND F(2)     :', 2F15.6)
  502 FORMAT(' F(1) AND F(2)     :', 2F15.6,/,
     *'       LEFT & RIGHT TERMS :', 4F15.2,/,
     *'FUG1,FUGSAT1 - FUG2,FUGSAT2:', 4F10.6,/,
     *'         B(1,1) AND B(2,1) :', 2F15.6,/,
     *'         B(1,2) AND B(2,2) :', 2F15.6,/,
     *'         B(1,3) AND B(2,3) :', 2F15.6,/,
     *'         B(1,4) AND B(2,4) :', 2F15.6)
  501 FORMAT (/,' COMP1: X1  Y1  ACT1EXP  ACT1:',4F12.4,
     *      /,' COMP2: X2  Y2  ACT2EXP  ACT2:',4F12.4,/)
      RETURN
C
C  ENTRY POINT FOR CALCULATION OF CONSTRAINTS FOR CONSISTENCY TEST
C
 1000 CALL FUGC2(NCOMP,T,P,Y,TC,PC,RG,DM,NU,PSAT,FUGC,FUGCST,IER,
     *                    IDV,DPSAT,DFUGC,DFUGST)
  345 FORMAT(' T,Y1,PHI1,PHI2 -REG-',F10.2,3F12.4)
      IF(IER.GT.0) WRITE(*,*) 'IER=',IER
  115 SSFUG1=FUGCST(1)*PSAT(1)*DEXP(POYNT1)
      SSFUG2=FUGCST(2)*PSAT(2)*DEXP(POYNT2)
C
C  THE OBJECTIVE FUNCTIONS
C
      PCALC = X(1)*ACT1*SSFUG1/FUGC(1) + X(2)*ACT2*SSFUG2/FUGC(2)
      F(1) = P - PCALC
```

```
C
 120  FC1SQ=FUGC(1)*FUGC(1)
      FC2SQ=FUGC(2)*FUGC(2)
C
C  CALCULATION OF DERIVATIVES WITH RESPECT TO PRESSURE
C
      B(1,1) = 1.
C
C  CALCULATION OF DERIVATIVES WITH RESPECT TO TEMPERATURE
C
      DTSSF1 = SSFUG1*(DTPYN1 + DTVP1 + DFUGST(1)/FUGCST(1))
      DTSSF2 = SSFUG2*(DTPYN2 + DTVP2 + DFUGST(2)/FUGCST(2))
C
      B(1,2)= -X(1)*ACT1*(FUGC(1)*DTSSF1 - SSFUG1*DFUGC(2,1))/FC1SQ
     *        -X(2)*ACT2*(FUGC(2)*DTSSF2 - SSFUG2*DFUGC(2,2))/FC2SQ
C
C  CALCULATION OF DERIVATIVES WITH RESPECT TO X1
C
      B(1,3) = -SSFUG1/FUGC(1)*(X(1)*DXACT1 + ACT1)
     *         -SSFUG2/FUGC(2)*(X(2)*DXACT2 - ACT2)
C
      RETURN
      END

C
C ***********************************************************************
C  SUBROUTINE MARGUL (MARGULES MODEL PARAMETERS)
C ***********************************************************************
C
      SUBROUTINE MARGUL (THETA,X,ACT1,ACT2,LACT1,LACT2,DXACT1,DXACT2)
      IMPLICIT INTEGER*4 (I-N), REAL*8 (A-H, O-Z)
      REAL*8 LACT1,LACT2
      DIMENSION X(2),THETA(5)
C
      X1SQ=X(1)*X(1)
      X2SQ=X(2)*X(2)
      A = THETA(1)
      B = THETA(2)
      D = THETA(3)
C
      LACT1 = X2SQ*(A + 2*(B-A-D)*X(1) + 3*D*X1SQ)
      LACT2 = X1SQ*(B + 2*(A-B-D)*X(2) + 3*D*X2SQ)
C
C     WRITE(*,9) THETA,LACT1,LACT2
   9  FORMAT(' TH,LACT1,2:',3F10.5,2F15.5)
      ACT1 = DEXP(LACT1)
      ACT2 = DEXP(LACT2)
      DXACT1 = (-2*A*X(2) + 2*(B-A-D)*(X2SQ - 2*X(2)*X(1)) + 3*D
     *  *(-2*X1SQ*X(2) + 2*X2SQ*X(1)))*ACT1
      DXACT2 = ( 2*B*X(1) + 2*(A-B-D)*(2*X(1)*X(2) - X1SQ) + 3*D
     *  *( 2*X2SQ*X(1) - 2*X1SQ*X(2)))*ACT2
      RETURN      END
```

REFERENCES

1. Cruickshank, A. J. B.; Gainey, B. W.; Hicks, C. P.; Letcher, T. M.; Woods, R.W. Young, C. L. Trans. Faraday Soc.; 1969, 65, 1014

2. Everett, D. H. Trans. Faraday Soc.; 1965, 61, 1637

3. Young, C. L. PhD. Thesis, Bristol, 1967

4. Shell Technical Bulletine, Sulfolane, Shell Chemical Co. 1964

5. Wilson, G. M. J. Am. Chem. Soc. 1964, 86, 127.

6. Renon, H.; Prausnitz, J. M. AIChE J. 1968, 14, 135.

7. Abrams, D. S.; Prausnitz, J. M. AIChE J. 1975, 21, 116.

8.Fredenslund, A.; Jones, R. L.; Prausnitz, J. M., AIChE J. 21, 1086-1098, 1975

9.Kehiaian, H. V.; Grolier, J-P.; Benson, G. C. J de Chemie Physique, 1978, 75, 44

10. Rogalski, M.; Malanowski, S. Fluid Phase Equilibria 1980, 5, 97

11. Rogalski, M.; Rybaklewicz, K.; Malanowski, S. Ber. Bunsenges Phys. Chem. 1977, 81, 1070

12. Zemansky, M. W.; Heat and Thermodynamics. Fifth Edition. Ney York: McGraw-Hill Book Company. 1968

13. van Laar, J. J. Z. Physik Chem. 1910, 18, 57

14. Della Monica, M.; Janelli, L.; Lamanna, U. J. Phys. Chem. 1968, 72, 1068.

15. Jannelli, L.; Sacco, A. J. Chem. Thermodynamics, 1972, 4, 715.

16. Jannelli, L.; Inglese, A.; Sacco, A.; Ciani, P. Z. Naturforsch, 1975, 30a, 87.

17. Sacco, A.; Inglese, A.; Ciani, P.; Dell'Atti, A.; Rakshit, A. K. Thermochim. Acta, 1976, 15, 71.

18. Dallinger, L.; Schiller, M.; Gmehling, J.; J. Chem. Eng. Data.1993, 38, 147

19. Thomas, E.; Newman, B. A.; Lang, T. C.; Wood, D. A.; Eckert, C. A.; J. Chem. Eng.Data 1982, 27, 399

20. Eckert, C. A.; Newman, B. A.; Nicolades G. L.; Long, T. C. AIChE J. 1981, 27, 33

21. Schreiber, L. B.; Eckert, C. A.; Ind. Eng. Chem. Proc. Des. Dev. 1971, 10, 572

22. Tassios, D. AIChE J. 1971, 17, 1367

23. Smith, J. M.; Van Ness, H. C.; Intro. Chem. Engineering Thermodynamics, McGraw Hill, NY, 1975

24. Wong, K. F.; Eckert, C. A.; Ind. Eng. Chem. Fund. 1971, 10, 20

25. Chemical Thermodynamics, Vol I. A Specialist Thermodynamic Report. Ed.: McGlashan M. London, 1973

26. Activity Coefficients at Infinite Dilution. Chemistry Data Series Vol 9. DECHEMA, Germany 1993

27. Barker, J. A. Aust. J. Chem. 1953, 6, 207

28. Letcher T.M. Chemical Thermodynamics Vol 2. A Specialist Report, Editor: McGlashan M. L.; The Chemical Society London. 1978

29. Leroi, J. C.; Masson, J. C.; Renon, H.; Fabries, J.F.; Sannier, H. Ind. Eng. Chem. Process. Des. Dev. vol 16, no. 1. 1977

30. Surovy, J.; Oveckova, J.; Graczova, E. Collect. Czesc. Chem. Commun. 1990, vol 55

31. Privdal, K. A.; Britigh, A.; Sandler, S. J. Chem. Eng. Data, 1992, 37, 484

32. Tramp, D. B.; Eckert, C. A.; AIChE J. 1993, 39, 6

33. Null, H. R.; Phase Equilibrium in Process Design, Wiley, NY, 1970

34. Gautreaux, M. F.; Coates, J. AIChE J. 1955, 1, 496

35. Hala, E.; Pick, J.; Fried, V.; Vilim, O. Vapour Liquid Equilibrium, Pergomaon Press, London, 1967

36. Hayden, J. G.; O'Connell, J. P.; AIChE J. 1975, 1, 496

37. Li, J. J.; Dallas, A. J.; Eigens, D. I.; Carr, P. W.; Bergman, D. K.; Hait, M. J.; Eckert, C. A.; Anal. Chem. 1993, 65, 3212

38. Shaffer, D. L.; Daubert, T. E. Anal. Chem. 1966, 3, 1661

39. Golubkok, Y. V.; Pepneva, T. G.; Raginskaya, L. M.; Promst. Sint. Kauch. Ref. SB. 1975, 7, 1

40. Hussam, A.; Carr, P. W.; Anal. Chem, 1985, 793, 57

41. Ray, A. K.; Venkatraman, S.; AIChE J. 1995, 41, 4

42. Conder, J. R.; Young, C. L. Physicochemical measurements by Gas Chromatography, John Wiley and Sons Ltd.; 1979

43. Purnell, H. Gas Chromatography, John Wiley and Sons Ltd. U.S.A.; 1962
44. Martin, A. J. P.; Purnell, R. L.; Biochem. J.; 1941, 35, 1358
45. James, A. T.; Martin, A. J. P. Biochem. J.; 1952, 50, 679
46. Porter, P. E; Deal, C. H.; Stross, F. H. J. Am. Chem. Soc.; 1956, 78, 2999
47. Everett, D. H.; Stoddart, C. T. H.; Trans. Faraday Soc. 1961, 57, 746
48. Desty, D. H.; Goldup, A.; Luckhurst, G. R.; Swanton, W. T. Gas Chromatography, 1962, Butterworth, 1962
49. Laub R.J.; Pesock R.L. Physicochemical Application of Gas Chromatography, John Wiley and Sons Ltd. U.S.A. 1978
50. Kwantes, A.; Rijnders, G. W. A. Gas Chromatography, 1958 Editor: D. Desty, Butterworth, London, 1958
51. Kurkchi, G. A.; Iogansen, A. V. Proc. Acad. Sci.; USSR, 145, 571, 1962
52. Langer, S. H.; Iogansen, A. V.; Conder, J. R. J. Phys. Chem. 72, 4020, 1968
53. Letcher, T. M.; Baxter, R. C.; J. Solution Chem.; 18, 65, 1989
54. Marsicano, F. Ph. D. Thesis, South Africa, 1989
55. McGlashan, M.L.; Potter, D.J.B. Proc. Roy. Soc. A, 1962, 267, 478
56. Hudson, G.H.; McCoubrey, J.C. Trans. Faraday Soc. 1960, 56, 761
57. Cruickshank, A.J.B.; Windsor, M.L.; Young, C.L. Trans. Faraday Soc. 1966, 2341.
58. Letcher, T.M.; Baxter, R.C,; Bean, A.; Sewry, J.D. J. Chem. Thermodynamics 1988, 20, 581
59. Baonza, V. G.; Cáceres, M.; Núñez, J.; Fluid Phase Equilibria. 1992, 78, 43
60. Selected Values of Properties of Hydrocarbons and Related Compounds. American Petroleum Institute, Research Project 44, Thermodynamics Research Centre. Texas A&M University, College Station, Texas. Tables 6k, 20k, and 21k, 1953
61. Selected Values of Properties of Hydrocarbons and Related Compounds. American Petroleum Institute, Research Project 44, Thermodynamics Research Centre. Texas A&M University, College Station, Texas. Tables 20d, and 21d, 1975
62. Bayles, J.W.; Letcher, T.M.; Moollan, W.C. J. Chem. Thermodynamics 1993, 27, 781

63. Bayles, J.W.; Letcher, T.M.; Moollan, W.C. J. Chem. Thermodynamics 1994, 26, 571

64. Karol, A. N., Ukr. Khim. Zh. 1966, 32, 198

65. Karol, A. N.; Neftkhimiya 1963, 5, 635

66. Kikic, I; Renon, H.; Sep. Sci. 1076, 11, 45

67. Kwantes, A. Rjinders, G. W. A.; Gas Chromatography, ed. Desty , D. H. Butterworths, London 1958

68. Young, C. L. Trans. Faraday Soc. 1968, 64, 349

69. Martire, D. E.; Piedle, P.; J. Phys. Chem. 1968, 72, 3473

70. Letcher, T. M.; Marsicano, F.; J. Chem. Thermodynamics 1974, 6, 501

71. Letcher, T. M.; Jerman, P.; J. Chem. Thermodynamics 1976, 8, 127

72. Janini, G. M.; Martire, D. E.; J. Phys. Chem. 1974, 78, 1644

73. Letcher, T. M.; J. Chem. Thermodynamics 1975, 7, 969

74. Gainey, B. W.; Young, C. L.; Trans. Faraday Soc. 1968, 64, 348

75. Martire, D. E.; Opllara, L. Z.; J. Chem. Eng. Data 1965, 40, 10

76. Hicks, C. P.; Young, C. L.; Trans. Faraday Soc. 1968, 64, 2675

77. Parcher, J. F.; Yun, K. S.; J. Chromatog. 1975, 105, 257

78 Tewari, J. B.; Martire, D. E.; Sheridan, J. P.; J. Phys. Chem. 1970, 3263, 74

79. Chen, S. S.; Zwolinski, B.; J. Chem. Thermodynamics 1973, 1133

80. Bowden, W. W.; Ataton, J. C.; Smith, B. D.; J. C. Eng. Data 1966, 3, 296

81. Meyer, H. S.; Petrol. Ref. 1957, 13, 175

82. Cummins, L. W. T.; Stones, F. W.; Volante, M. A.; Ind. Eng. Chem. 1933, 25, 728

83. Smith, V. C.; Robinson Jr. R. L; J. Chem. Eng. Data 1970, 3, 391

84. Smyth, C. P.; Engel, E. W.; J. Am. Chem. Soc. 1929, 15, 2646

85. Ott, J. B.; Marsh, K. N.; Stocks R. H.; J. Chem. Thermodynamics 1981, 13, 371

86. Gómez-Ibanez, J. D.; Sheih, J. J. C.; Thorsteinson, E. M.; J. Phys. Chem. 1966, 70, 1998

87. Messow, U.; Quitzsch, K.; Z Phy. Chem. (Leipzig) 1976, 257, 121

88. Keistler, J.; Winkler, R. Ind. Eng. Chem. 1952, 44, 622

89. C.R.C. Handbook of Chemistry and Physics. 64th edition. Editor; Weast, R.C. C.R.C Press Inc.: Boca Raton. 1994

90. Gajle, A. A.; Pariževa, N. V.; Proskurjokov, V. A.; Zh. Prik. Khim. 1974, 47, 191

91. Karvo, M.; J. Chem. Thermodynamics 1980, 12, 1175

92. Prausnitz, J. M.; Lichtenthaler, R. N.; Gomes de Azevedo, E. Molecular Thermodynamics of Fluid-Phase equilibria, Prentice-Hall Inc.; Englewood Cliffs, N. J. 1986

93. Batinno, R. Chem. Reviews, 1971, 5, 71.

94. Letcher, T. M.; Chem. South Africa, 1975, 1, 226.

95. Handa, Y. P.; Benson, G. C.; Fluid Phase Equilibria , 1976, 185, 3

96. Stokes, R. H.; Marsh, K. N. Ann. Rev. Phy. Chem. 1972, 65, 23

97. Marsh, K. N. Ann. Rev. RSC, Sect, C, 1980, 77, 101

98. Marsh, K. N. Ann. Rev. RSC, Sect, C, 1984, 209, 81

99. Scatchard, G.; Wood, S. E.; Muchel, J. M. J. Am. Che, Soc. 1946, 68, 1957

100. Hepler, L. J. Phys. Chem. 1957, 61, 1426

101. Battino, R. J. Phys. Chem. 1966, 3408, 70

102. Kimura, T.; Takagi, S. J. Chem. Thermo. 1979, 11, 119

103. Leopold, H. Electronik, 1970, 19, 297

104. Keyes, D. B.; Hildebrand, J. H. J. Am. Chem. Soc. 1917, 39, 2126

105. Geffcken, W.; Kruis, A.; Salana, Z.; Z. Phys. Chem. 1937, 35, 317

106. Battino, R. J. Phys. Chem. 1966, 3408, 70

107. Flory J. A.; J. Am. Chem. Soc. 1965, 87, 1833

108. Heintz, A.; Dolch, E.; Lichtenthaler, R. N.; Fluid Phase Equilib. 1986, 27, 61

109. Treszezanowicz, G. C.; Benson, G. C., J. Chem. Thermos. 1977, 4, 1189

110. Redlich, O.; Kister, A. T. Ind. Eng. Chemistry, 40, 345, 1948.

111. Ross, P. D. Biochemica et Biophysica Acta, 1973, 106, 313.

112. Letcher, T. M., Bayles, J. W. J. Chem. Eng. Data 1971, 16, 266

113. Govender, U. P. Masters Thesis, University of Natal, South Africa, 1993.

114. Letcher, T. M.; Schoonmbaert, F. E. Z.; Bean, B. Fluid Phase Equilibria, 1990, 61, 111

115. Świętosławski, W. Ebulliometric Measurements, Reinhold, New York, 1945

116. Marsh, K. N. Chemical Thermodynamics, Specialist Reports, Vol II. Editor McGlashen, M. L. Chemicial Society, London. 1978

117. Allen, P. W.; Everett, D. H.; Penney, M. F. Proc. Roy. Soc. 1952, A212, 149

118. Baxendale, J. H.; Enustun, B. V.; Stein, J. Phil. Trans. 1951, A243, 169

119. McGlashen, M.L.; Williamson, A. G. Trans. Faraday Soc. 1961, 57, 588

120. Brown, I. Austral. J. of Sci. Research, 1952, 5A, 530

121. Malanowski, S., Rõwnowaga Ciecz-Para, PWN, Warsaw, 1974

122. Rogalski, M., PhD Thesis, Institute of Physical Chemistry, Warsaw, 1974.

123. Prausnitz, J.; Anderson, T.; Grens, E.; Eckert, C.; Hsieh, R.; O'Connell, J. Computer Calculations for Multicomponent Vapour-Liquid and Liquid-Liquid Equilibria, Prentice-Hall International Series, Englewood Clifts, NJ, 1980

124. Benoit, R.L.; Charbonneau, J. Can. J. Chem. 1969, 47, 4195

125. De Fré, R. M.; Verhoeye, L. A. J. Appl. Chem. Biotechnol. 1976, 26, 469

126. Ashcroft, S. J.; Clayton, A. D.; Shearn, R. B. J. Chem. Eng. Data 1979, 24, 195

127. Riddick, J. A.; Bunger, W. B.; Sakano, T. K.; Organic Solvents Physical Properties and Methods of Purification, Fourth Edition; Wiley-Interscience Publication, 1986

128. Inglese, A.; Jannelli, L. Thermoch. Acta, 1978, 23, 263.16

129. Gess, M. A.; Danner, R.P.; Nagvekar, Thermodynamic Analysis of Vapour-Liquid Equilibria: Recommended Models and Standard Data Base Am. Inst. Chem. Eng.:PA, 1991

130. Walas, S. M. Phase Equilibria in Chemical Engineering, Butterworth Publishers, Boston: 1985

131. Gmehling, J.; Onken, U. Vapor-Liquid Equilibrium Data Collection; Chemistry Data Series, DECHEMA: Frankfurt, 1977; vol 1, Part 1

132. Letcher, T. M.; Moollan, W. C. J. Chem. Thermodynamics 1995, 27, 867 132.

133. Domańska, U.; Sporzyński, A.; Moollan, W. C.; Letcher T. M., J. Chem. Eng. Data, 1995 - submitted.

134. Neu, E.; Peneloux, A., Fluid Phase Equilibria, 1981, 6, 1

135. Patino-Leal, H.; Reilly, P. AIChE, 1982, 28, 580

136. Jannelli, L.; Lopez, A.; Jalent, R.; Silvestri, L. J. Chem. Eng. Data, 1982, 27, 28.

137. Hildebrand, J. J. Chem. Phys. 1947, 15, 225

138. Nagata, J.; Nakamiya, Y.; Kotoh, K.; Kogabu, J. Themochim. Acta 1981, 45, 153

139. Nagata, J. Fluid Phase Equilibrium, 1985, 19, 153

140. Domańska, U.; Rolińska, J.; Fluid Phase Equilibria, 1989, 45, 25

141. Domańska, U.; Rolińska, J.; Fluid Phase Equilibria, 1993, 86, 233

142. Domańska, U.; Hofman , T.; Fluid Phase Equilibria, 1991, 68, 103

143. Domańska, U. Fluid Phase Equilibria, 1986, 26, 201

144. Vera, J. H.; Sayegh, G. S.; Ratcliff, G. M.; Fluid Phase Equilibria, 1977, 1, 113.

145. Guggenheim, E. A., Mixtures. Oxford: Oxford Press. 1952

146. Alesi, P. Activity coefficients at Infinte Dilution. Determination and Retrieval. Experimental Thermodynamics measurements ans Correlations. Editors: Malanowski, S.; and Anderko, A. Institute of Physical Chemistry of the Polish Acadamy of Science. Warsaw. 1990.

147. Scatchard, G.; Hamer, W. J.; J. Am. Chem. Soc. 57, 1805, 1935.

148 Wohl, K. Tran. AIChE. 42, 215, 1946

149. Orye, R. V.; and Prausnitz, J. M. Ind. Eng. Chem. 57, 18, 1965

150. Anderson, T. F.; and Prausnitz, J. M. Ind. Eng. Chem. 17, 552, 1978.

151. Kehiaian, H. V.; Fluid Phase Equilibrium, 13, 243-253, 1983

152. Christensen, J. J.; Hanks, R. W.; Izatt, M. R. Handbook of Heat of Mixing, Wiley-Interscience Publication, Ney York, 1988

153. González, J. A., Garcia de la Fuente, I., Cobos, J.C. and Casanova, C., Ber. Bunsenges. Phys. Chem., 1994, 95, 1658

154. González, J. A., Garcia de la Fuente, I., Cobos, J.C., Casanova, C. and Domańska, U., Ber. Bunsenges. Phys. Chem., 1994, 98, 955

155. Kehiaian, H. V. and Marongiu, B. Fluid Phase Equilibria, 1988, 40, 23

156. Kehiaian, H. V., Fluid Phase Equilibria, 1983, 13, 243

157. Bondi, A., 1968. Physical Properties of Molecular Crystals, Liquids and Glasses, Wiley, NY, 502 pp.

158. Benoit, R. L. and Charbonneau, J. Can. J. Chem. 1969, 47, 4195

159. Lopez, A., Pansini, M. and Jannelli, L., J.Chem. Eng. Data, 1983, 28, 173-175

160. Gmehling, J . Results of a modified UNIFAC method for alkane - alcohol systems. In: H.V. Kehiaian and H. Renon (Editors), Measurements, Evaluation and Prediction of Phase Equilibria, Elsevier, Amsterdam.

161. Pansini, M. and Jannelli, L., 1986. J.Chem. Eng. Data, 1986, 31, 157